Role of Epac2 in high glucose-mediated cardiac calcium mishandling.

Magali Samia El Hayek

université PARIS-SACLAY

Role of Epac2 in high glucose-mediated cardiac calcium mishandling

Thèse de doctorat de l'université Paris-Saclay

École doctorale n°569 : Innovation thérapeutique : du fondamental à l'appliqué (ITFA)
Spécialité de doctorat: Physiologie, physiopathologie
Unité de recherche : Université Paris-Saclay, Inserm, UMR-S 1180, 92296, Châtenay-Malabry, France
Référent : Faculté de Pharmacie

Thèse présentée et soutenue à Châtenay-Malabry, le 2 décembre 2020, par

Magali SAMIA EL HAYEK

Composition du Jury

Christian POÜS Professeur, Université Paris-Saclay, Paris	Président
Bruno ALLARD Professeur, Université Claude Bernard, Lyon	Rapporteur & Examinateur
Gema RUIZ-HURTADO Chargée de recherche, HDR, Hospital Universitario 12 de Octubre, Madrid	Rapporteur & Examinatrice
Geneviève DERUMEAUX PUPH, Inserm, Université Paris-Est Créteil	Examinatrice
Pierre JOANNE MCU, Sorbonne Université, Paris	Examinateur
Ana-Maria GOMEZ DR, Inserm, Université Paris-Saclay, Paris	Directrice de thèse
Laetitia PEREIRA MCU, Université Paris-Saclay, Paris	Co-Encadrante de thèse

Thèse de doctorat

NNT : 2020UPASQ019

université PARIS-SACLAY

ECOLE DOCTORALE N°569

Innovation thérapeutique, du fondamental à l'appliqué (ITFA)

Titre : Rôle de l'Epac2 dans l'altération de la signalisation calcique cardiaque induite par les fortes concentrations de glucose

Mots clés : Epac2, calcium, glucose, récepteur à la ryanodine, O-GlcNacylation, cardiomyocyte.

Résumé : Epac2 (protéine d'échange directement activée par l'AMPc) est un acteur essentiel dans la régulation de l'homéostasie calcique cardiaque, jouant un rôle dans les cardiomyopathies, telles que l'insuffisance cardiaque et l'arythmie. Récemment, nous avons découvert que les fortes concentrations de glucose induisent une fuite calcique du réticulum sarcoplasmique (RS) dépendante de la calmoduline kinase de type II (CaMKII), un effecteur d'Epac2. Cependant, le rôle d'Epac2 dans ce mécanisme était encore inconnu. De ce fait, l'objectif de ma thèse était d'étudier l'implication d'Epac2 dans l'altération de la signalisation calcique cardiaque induite par les fortes concentrations de glucose. Mes travaux de thèse, montrent que les cardiomyocytes adultes de souris exposés à des concentrations élevées de glucose (300 et 500 mg/dl) présentent une augmentation de la fuite calcique diastolique du RS, qui est pro-arythmogène, sans altérer la libération calcique globale nécessaire à la contraction cellulaire. La fréquence de ces libérations spontanées de calcium est réduite par l'inhibition pharmacologique ou génétique de l'Epac2. Cette fuite calcique est reliée à une augmentation de la probabilité d'ouverture du canal de libération du calcium, le récepteur à la ryanodine (RyR), qui est prévenue par l'inhibition d'Epac2. De façon intéressante, l'hyperactivation du RyR par les fortes concentrations de glucose est prévenue aussi par l'inhibition de l'O-GlcNacylation. L'O-GlcNacylation est une modification post-traductionnelle sur les résidus sérines et thréonines des protéines modifiant leur activité, et qui est hyperactivée par les fortes concentrations de glucose. Comme Epac2 est une protéine à multidomaines possédant plusieurs sérines et thréonines qui peuvent potentiellement être O-GlcNacylées, nous avons mis en évidence pour la première fois l'activation d'Epac par O-GlcNAcylation sous concentrations hyperglycémiques. Afin d'étudier la relevance de ce mécanisme dans un contexte humain, nous avons utilisé des cellules humaines souches pluripotentes différenciées en cardiomyocytes (h-iPSC-CM), et traitées par de fortes concentrations de glucose. Comme dans les cellules de souris nous n'observons aucune diminution de la libération calcique en fortes concentrations aigues de glucose. Cependant une exposition chronique de 7 jours à des concentrations hyperglycémiques diminue la libération calcique nécessaire pour la contraction, qui est prévenue par l'inhibition pharmacologique d'Epac2. Pour conclure, Epac2 est activée par O-GlcNacylation sous fortes concentrations de glucose, induisant une fuite calcique anormale du RS. A long terme, cette fuite calcique peut participer à la diminution de la libération calcique nécessaire pour la contraction, pouvant participer à l'altération de la contraction cardiaque observée dans les pathologies caractérisées par une hyperglycémie, comme le diabète.

Title : Role of Epac2 in high glucose-mediated cardiac calcium mishandling

Keywords : Epac2, calcium, glucose, ryanodine receptor, O-GlcNacylation, cardiomyocyte.

Abstract : Epac2 (an exchange protein directly activated by cAMP) is a key player in the regulation of cardiac calcium homeostasis, playing a role in cardiomyopathies, such as heart failure and arrhythmia. Recently, we have discovered that high glucose concentrations induce calcium leak from the sarcoplasmic reticulum (SR) mediated by calmodulin kinase type II (CaMKII), an effector of Epac2. However, the role of Epac2 in this mechanism was unknown. Therefore, the objective of my thesis was to study the involvement of Epac2 in the alteration of cardiac calcium signaling induced by high glucose concentrations. My thesis work shows that adult mouse cardiomyocytes exposed to high glucose concentrations (300 and 500 mg/dl) exhibit an increase of diastolic SR calcium leak, which is pro-arrhythmogenic, without altering the calcium released needed for cell contraction. The frequency of these spontaneous calcium releases is reduced by pharmacological or genetic inhibition of Epac2. This calcium leak is related to an increase of the open probability of the calcium release channel, the ryanodine receptor (RyR), which is prevented by Epac2 inhibition. Interestingly, the rise in RyR activity by high glucose concentrations is also prevented by O-GlcNacylation inhibition. O-GlcNacylation is a post-translational modification on the serine and threonine residues of proteins modifying their activities, which is upregulated by high glucose concentrations. Since Epac2 is a multidomain protein with several serine and threonine residues that can potentially be O-GlcNacylated, we demonstrated for the first time the activation of Epac by O-GlcNAcylation under hyperglycemic concentrations. In order to study the relevance of this mechanism in a human context, we used human induced pluripotent stem cells derived into cardiomyocytes (h-iPSC-CM) treated with high glucose concentrations. As in murine cardiomyocytes, we didn't observe a decrease of calcium release for contraction in acute high glucose concentrations. However, chronic exposure for 7 days to hyperglycemic concentrations decreases the calcium release for contraction, prevented by pharmacological inhibition of Epac2. To conclude, Epac2 is activated by O-GlcNacylation under high glucose concentrations, inducing a diastolic calcium leak from the SR. During chronic exposure of high glucose, this calcium leak can decrease the calcium release for contraction, which may participate in the cardiac contraction alteration observed in pathologies characterized by hyperglycemia, such as diabetes.

Acknowledgements

This journey has come to an end and it wouldn't be that fruitful without the presence of several people that gave it a special taste.

First of all, I want to thank the jury for evaluating my work. I want to thank ***Pr. POUS*** *who accepted to preside the jury,* ***Pr. ALLARD*** *and* ***Dr. RUIZ-HURTADO*** *for their reports on my work, as well as* ***Dr. JOANNE*** *and* ***Pr. DERUMEAUX*** *for being part of the committee.*

I want to thank ***Ana Maria GOMEZ*** *that welcomed me in her lab and offered me an internship in her team for my master's degree, and a thesis project afterwards. Thank you Ana for your constructive remarks that helped me become a little expert in calcium signaling, and for being always available despite your busy schedule.*

Thank you ***Laetitia*** *for coaching me on a daily basis over these 4 years. Thank you for all the scientific discussions, all the time spent on my oral/written work in order to make me progress. Thank you for trusting me to present our work many times in various national and international congresses. Thank you for mentoring me to become a professional scientist.*

Thank you ***Jean-Pierre*** *for all your scientific advices and statistics mentoring, and for welcoming me into your office.*
Special thanks to ***Jean-Jacques*** *without whom I wouldn't have enrolled in the Biocoeur master and wouldn't be in this lab.*
I want to thank all the members of the team 3 who participated in the evolution of this project by their advices and comments.

A big thank to all the people who gave me their technical help throughout my journey in the laboratory and especially ***Flo*** *for teaching me the art of dissos', and* ***Deborah*** *for teaching me all the biochemistry and biomol experiments.*
Thank you ***Jessica*** *for teaching me the principles and techniques of the confocal microscopy.*
Thank you ***Pascale*** *for preparing my iPSC-CM and saving my Co-IPs experiments.*
Thank you ***Almu*** *for your remarks on iPSC-CM confocal experiments.*
Thank you princess ***Gladys*** *for making our lives easier and thanks to* ***Sophie*** *without whom*

everything would be more complicated.
*A big thank to **Ayma** for your work on Epac mice lines all these years and thank you **Valérie** for helping me in the diabetic rats project.*
*Thanks to **Claudine** for your help at the qPCR platform, and **Valérie** for your expertise in cell imaging.*

*Thank you **Anne** for accepting me in the physiology mentoring team and thank you **Jérôme** for your small tips on how to handle a class. Thank you **Véro** and **Boris** for trusting me to help you in the pharmacology courses.*

*I want also to thank **Dr.Carmen VALDIVIA** for her technical help in this project and **Dr. Hector VALDIVIA** for his course on the Heart that was definitely the best and funniest physiology course I've ever had.*
*Thank you **Dr. Aniella ABI-GERGES** for trusting me and enrolling me in your diabetes project.*

*I am very grateful to **Dr. Rania AZAR** and **Dr. Racha KARAKI**, my mentors during my Pharma studies who encouraged me to take on this adventure.*

*And THANK YOU, THANK YOU, THANK YOU "**les copains du Coeur**" (BurEx, JPEx, MartEx and AnnEx). It's the part where I feel so overwhelmed, where words can't describe my gratitude. Thanks for being here when things were tough, where nothing was okay and I was about "de péter les câbles", where I felt homesick with "des valises sous les yeux" and you let me feel home. You're not friends you're my French family!*

*Thank you **Rima** for who you are! Thank you for always being there for me, for letting me feel home, for all our talks, our shared meals, our English courses, our Friends episodes :P Thanks for your patience, your faith, your positivity, your care, your craziness, your kindness and more and more…*

*Thanks **Carole** for being the one who let me directly feel welcomed. Your kindness and graciousness touch the soul. Thank you for all the RER rides we took together, all the long discussions and crazy trips. Thank you for letting me discover the French language and culture and letting me fall in love more and more with this country. Thanks for your interest*

in Lebanon, your questions, your Lebanese learning…. Thank you for letting me discover the love of my life AKA "crème de marron":P and sharing with me the endless Haribo passion. Thank you for being who you are, a blessing in my life!

*Thank you Ma Mikette (AKA **Delphine**) for your folyee (folie), removing a lot of soucye (souci) and adding lots of "paillettes" and laughter to my long lab days. You're one of a kind, this lab wouldn't be "labo de Coeur" without la Mika touch.*

*Thank you Gandoun Gandounette Marinette (AKA **Marine**) for helping me discover the bench work when I first came. Yes, you literally taught me how to pipet! Thank you for helping us every time we're lost since you know everything! Thank you for all your care when things go bad.*

*Thank you Rom (AKA **Romain**) for helping me in my genotyping struggling, for saving my life every time I messed up in the lab and for handling my virgin Ricard "à la canelle" during winter. I hope I will always be your best "princesse libanaise" :P*

*Thank you Beyonce (AKA **Anne-So**) for letting me mess your hair these 3 years!*
*Thank you Mama (AKA **Marion**) for awaking in me the Celine Dion love :D*
*Thank you **Estelle** for all the laughs at the JPEx and sharing together all the endless statistics lessons of JP ;P*
*Thank you **Anissa** for all the car rides to the RER, for the ADIT work and most of all for all the funny struggles we shared for Epac genotyping and WB ;P*
*Thank you coach **Matthieu** for all your fitness advices!*
*Thank you Féfé (AKA **Félix**) for all the Carrefour rides and all the water packs you lifted to the 5th floor when the lift was out of service!*
*Thank you Aureillette (AKA **Aurelia**) for all the laughs at the congresses where we shared the hotel room :P*
*Thank you **Kaouter, Marta, Walma**, **Audrey and Fiona** for your friendship and kindness.*
"On est géniaux!"

*A big thank to all my friends in Paris and abroad that made all these years exciting and full of funny adventures: my "Maison du Liban" friend **Aya**, my travel buddies **Musab** and **Oliver**, my shopping girl **Walaa**, my crazy friend **Essraa**, my fitness mate **Doaa**, my chill buddy*

***Bahaa**, my foodie lover **Naji**, my classy girl **Nay**, my sweet friend **Rana**, my swimming champion **Maria**, my jumelle **Karen**, my hermana **Nada**, my roomie **Marilyn**.*
*Thank you **Karim** for all the dishes you cooked for me and all the times you had my back when I was about to quit during my masters. I wouldn't be here without your encouragement.*

*My warmest thanks go to my family, no words can describe my gratitude. **Mum and Dad**, I am the luckiest person to have you as my parents. You always believed in me and supported me in my projects and made the impossible become possible with your unconditional love. Thank you for letting me grow and dream …and thank you mum for all the recipes by whatsApp voice notes!*
***Melissa**, my hedgehog piglet, my sista, my interviews coach and my wardrobe sponsor in Lebanon; **Marilyn**, my Dr, my Em Rhea, my Big Sista; thank you both for being my backbones, my spiritual mentors, my psychologists, my therapists, my advisors… how blessed am I to have you as my sisters.*
*Thank you **Elie** for being that brother my sister chose for us!*
*Thank you **Rayoucha**, my attouta chouquette, for all your funny videos that made Tata laugh during her lonely moments. Tata can't wait to see you!*
Thanks to all my cousins and big family who always supported me and were there for me.

*And last thanks to the one who never stopped loving me, cherishing me, believing in me, supporting me, being proud of me, listening to me, caring for me, being there for me…my dance partner, my cooking assistant, my evening date, **My T-Rex**.*

Table of contents

Table of contents

Abbreviations list

$[Ca^{2+}]_i$: cytosolic Ca^{2+} concentration

$[Ca^{2+}]_l$: luminal Ca^{2+} concentration

$[Ca^{2+}]_n$: nuclear Ca^{2+} concentration

4-AP : 4-aminopyridine

AC: adenylate cyclase

AGE: advanced glycation end-products

AKAP: A kinase anchoring protein

AKT: protein kinase B

AM: acetyl-methyl

ANF: atrial natriuretic peptide

AP: action potential

ATP: adenosine triphosphate

AV node: auriculo-ventricular node

BCA: bicinchoninic acid

Bpm: beats per min

BS3: bis(sulfosuccinimidyl)suberate

BSA: bovine serum albumin

Ca^{+}: calcium

CaM: calmoduline

CaMKII: calmoduline kinase II

cAMP: cyclic adenosine monophosphate

Cav1.2 : alpha subunit of the ventricular L-Type Calcium channel

CDC25HD: CDC25-homology domain

cDNA: complementary desoxyribonucleic acid

CFP: cyan fluorescent protein

CICR: calcium induced-calcium release

Cn: calcineurin

CNBD: cAMP high-affinity binding domain

Co-IP: Co-immunoprecipitation

Cs^+: Cesium

DAD: delayed after depolarization

DAG: diacylglycerol

DAPI: 4',6-diamidino-2-phenylindole

DEP: disheveled-Egl-10-pleckstrin

DHP: dihydropyridine

DNA: desoxyribonucleic acid

DOC: sodium deoxycolate acid

DTT: Dithiothreitol

EAD: early after depolarization

ECC: Excitation contraction coupling

EDTA: Ethylenediaminetetraacetic acid

EPAC: exchange protein directly activated by cAMP

ESC: embryonic stem cells

ETC: excitation transcription coupling

FA: fatty acid

FKBP 12.6: FK506 binding protein

FRET: Förster (or fluorescence) resonance energy transfer

GDP: guanosine diphosphate

GEF: Guanine exchange

GFAT: L-glutamine-fructose-6-phosphate amidotransferase

GLP-1: glucagon like peptide

GTP: guanosine triphosphate

GTPase: guanosine triphosphatase

HbA1c: glycated hemoglobin

HBP: hexosamine biosynthesis pathway

HCN4: hyperpolarization-activated cyclic nucleotide-gated channels type 4

HDAC: histone deacetylase

HF: heart failure

h-iPSC-CM: human induced pluripotent stem cells derived into cardiomyocytes

HRP: horseradish peroxidase

IC50: half maximal inhibitory concentration

ICa_L: inward calcium current

I_f: funny current

IF: immunofluorescence

Ik_1: inward rectifying potassium current

Ik_r: rapid delayed rectifier K^+ currents

I_{Ks}: slow delayed rectifier K^+ current

INa^+: inward sodium current

IP: immunoprecipitation

IP3: 1,4,5 trisphosphate

IP_3R:Inositol triphosphate receptor

Ito: transient outward potassium current

Ito_1 / Ito_f: fast transient outward potassium current

Ito_2 / Ito_s: slow transient outward potassium current

K^+: potassium

K_d :constant of dissociation

KO: Knocked out

KV1.4: voltage-dependent K^+ channels

KV4.3: voltage-dependent K^+ channels

LDS: lithium dodecyl sulfate

LTCC: L-type Calcium Channel

MI: myocardial infarction

mRNA : messenger ribose nucleic acid

MyBP-C: myosine binding protein C

Na^+/K^+ ATPase : sodium potassium ATP pump

Na^+: sodium

NaCl: sodium chloride

NADPH: Nicotinamide adenine dinucleotide phosphate

NaV1.5 : voltage-dependent sodium channels NaV1.5

NCX: sodium calcium exchanger channel

NFAT: nuclear factor activated by T cells

NOS: nitric oxide synthase

OGA: O-GlcNAc-ase or β-N-acetylglucosaminidase

OGT: O-GlcNAc transferase

PA: action potential

PAGE: polyacrylamide gel electrophoresis

PBS: phosphate-buffered saline

PCR: polymerase chain reaction

PDE: phosphodiesterases

PI3K: phosphoinositide 3- protein kinase B

PKA: proteine kinase A

PLB: phospholamban

PLC: phospjolipase C

PVDF: PolyVinyliDene Fluoride

RA : Ras association domain

RA: Ras association

RAGE: receptor for advanced glycation end products

REM: Ras-exchange motif

RIPA: Radioimmunoprecipitation assay

RNA: ribose nucleic acid

ROS: reactive oxygen species

RT-qPCR: retrotranscription-quantitative polymerase chain reaction

RyR: ryanodine receptor

SAN: Sinoatrial node

SDS: sodium dodecyl sulfate

Ser: serine

SERCA : Sarco-endoplasmic reticulum calcium ATPase

SOCE: store operated calcium entry

SR: sarcoplasmic reticulum

TAC: thoracic aortic constriction

TAE: tris-acetate EDTA

Thr: threonine

Tm : tropomyosin

TnC: Ca^{2+} binding toponin C

TnI: inhibitory troponin I

TnT: tropomyosin binding troponin

TRPC: transient receptor potential canonical channels

T-tubules: transverse tubules

UDP-GlcNac: Uridine 5′-diphospho-N-acetylglucosamine sodium salt

VDCC: voltage dependent calcium channel

WB: western blot

WT: wild type

RT-qPCR: Retrotranscription quantitative polymerase chain reaction

YFP: yellow fluorescent protein

α-AR: alpha adrenergic receptors

β-AR: beta adrenergic receptors

Figures list

Tables list

Preamble

Preamble

Greeks, Egyptians, Indians and most of the ancient time people have considered the heart as an extraordinary organ, object of myth or at least mystery. Nothing is more omniscient than the heart: it constantly beats; its rhythm accelerates and slows down with each effort, rest, anxiety or tranquillity.

Thus, the heart has been since a long time a study subject in science to better unravel its mystery and better understand its electromechanical activity and related diseases. At a simple level, the heart may be considered as a blood pump insuring nutrient and oxygen distribution to the organs and carbon dioxide and waste products elimination. However, at a cellular level, it is more complex, and the calcium plays a key role in the transduction of the electrical activity of the heart into its mechanical contractile one. The alteration of the calcium homeostasis can affect the cardiac function and participates in the development of cardiac diseases.

Since the heart possesses a constant activity, it requires a constant fuel supply, such as glucose. However, excess glucose, as seen in some pathologies such as diabetes, is harmful for cardiac function, since it can alter calcium homeostasis. Yet, the underlying mechanisms are not well elucidated. Epac2 has emerged as a key player in calcium mishandling as seen with high glucose concentrations. Thus, in this study we aimed to gain knowledge of the high glucose-mediated cardiac calcium mishandling, deciphering a new mechanism featuring Epac2.

First, we described the basics of the electro-mechanical activity of the heart and the role of calcium in this mechanism, the role of Epac2 in the regulation of the calcium homeostasis and the calcium-related alterations observed under high glucose.

Second, we will present and discuss our obtained data and the role of Epac2 in the high glucose-mediated calcium mishandling

Introduction

Introduction

I. Overview of cardiac physiology

1) Ventricular action potential

The heart pumps the blood throughout the body continuously resulting in around 2 billion beats in a lifetime (Opthof 2000). For each beat, the heart undergoes a relaxation phase, named diastole, during which the ventricles and the atrium are filled with blood, followed by a contraction phase, systole, where the blood is propelled throughout the body. In heart failure (HF) cardiac contraction and relaxation are reduced resulting in a decrease of the cardiac activity (Lohse, Engelhardt, and Eschenhagen 2003). The cardiac contractile function is mediated by the electrical activity of the heart, where each heart beat is initiated by an electrical impulse, called action potential (AP). The AP is generated in specialized cells, the Sinoatrial Node (SAN), located in the right atrium. The SAN is characterized by its automatic electrical activity mediated by a delicate interplay between the calcium (Ca^{2+}) clock and the voltage clock (Lakatta, Maltsev, and Vinogradova 2010). The AP generated in the SAN propagates into both atriums, the auriculo-ventricular node (AV node), the Purkinje fibres along the ventricles and finally to the ventricular cardiomyocytes, that contract from the apex toward the base of the heart (Figure 1).

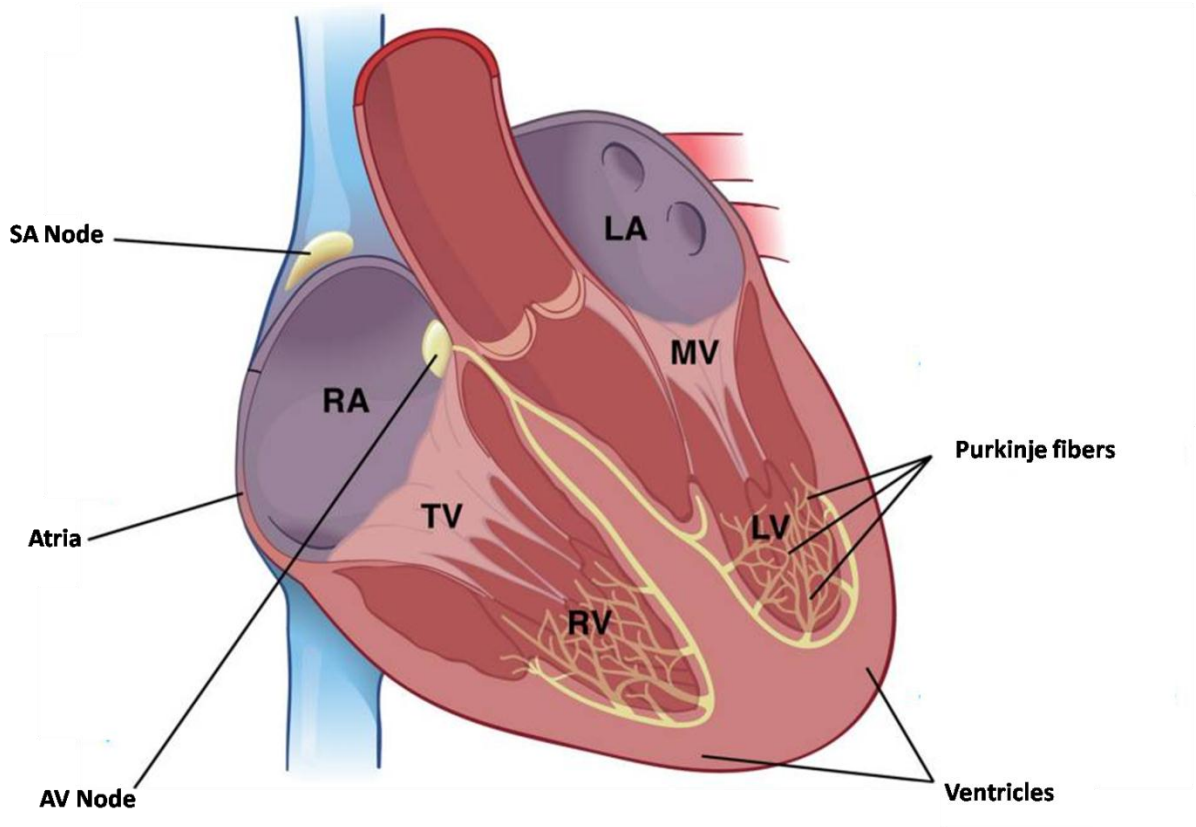

Figure 1: Cardiac conduction system, modified from (Munshi 2012). The heart rhythm generates in the sinoatrial node (SA node) located in the right atrium. The generated action potential propagates then into both atriums, the auriculo-ventricular node, the Purkinje fibres along the ventricles that contract from the apex toward the base of the heart. (RA: right atrium, LA: left atrium, SA node: sinoatrial node, AV node: auriculo-ventricular node, TV: tricuspid valve, MV: mitral valve).

The AP is the result of different ionic movements through the cardiac cell membrane. Ions mouvements depend on their concentration and electrical gradients through the membrane, as well as on the membrane potential. This transport is done through ion channels in a passive manner that does not require energy. The ventricular AP was first recorded by Coraboeuf and Weidmann (Coraboeuf and Weidmann 1954) in a canine Pukinje fiber, and consists of 5 phases (Figure 2). First, the excitation of ventricular myocytes by adjacent cells, results in membrane depolarization and activation of a rapid inward[1] Na^+ current (INa) through the voltage-dependent sodium channels (NaV1.5). The entry of Na^+ into the cell depolarizes the membrane potential to +30 mV which corresponds to the overshoot of the AP (end of phase

[1]Current that depolarizes the cell (makes the voltage more positive or less negative)

0). At this potential, NaV1.5 channels are rapidly inactivated (Colatsky 1980; DeMarco and Clancy 2016; Marban, Yamagishi, and Tomaselli 1998) and voltage-dependent K^+ channels (KV4.3 and KV1.4) are activated generating a rapid outward[2] repolarizating current, known as the transient outward potassium current (Ito) (phase 1). Ito is responsible for the early rapid repolarization and the "notch" shape of the ventricular AP. This transient outward potassium current has two components (Coraboeuf and Carmeliet 1982; Tseng and Hoffman 1989): Ito_1 or Ito_f (for fast) which activates and inactivates rapidly in a voltage-dependent manner. It is blocked by 4-aminopyridine (4-AP) and independent of Ca^{2+} concentrations. Ito_2 or Ito_s (for slow) which inactivates in a slower rate than Ito_f, is not blocked by 4-AP but is Ca^{2+}-dependent (Jeevaratnam et al. 2018; Kenyon and Gibbons 1979a, 1979b; Nerbonne and Kass 2005; Snyders 1999).

The phase 2, also known as the plateau phase, results from a fine balance between K^+ efflux, (or outward K^+ current), and Ca^{2+} influx (or inward Ca^{2+} current) into the cell. The Ca^{2+} enters through the L-type Ca^{2+} voltage sensitive channel (LTCC). The inward Ca^{2+} current (ICa_L) is activated at membrane potentials above −40 mV with a peak between 0 to +10 mV (Benitah, Alvarez, and Gómez 2010; Isenberg and Klöckner 1982; Linz and Meyer 1998; Orkand and Niedergerke 1964) driving Ca^{2+} entry. During phase 2, the Na^+/Ca^{2+} exchanger channel (NCX), which extrudes the Na^+ entered through INa participates in Ca^{2+} entry but to a lesser extent than the LTCC. This NCX-dependent Ca^{2+} entry is responsible for the influx of 1 Ca^{2+} for the extrusion of 3 Na^+ , which is electrogenic, participating in this reverse mode (Ca^{2+} entry) to membrane repolarization (Fujioka, Komeda, and Matsuoka 2000; Weber et al. 2002). The entry of Ca^{2+} in phase 2 is counterbalanced by K^+ exit (Noble and Tsien 1969) which explains the plateau shape of AP phase 2. The K^+ efflux is driven by 2 outward K^+ currents, known as rapid delayed rectifier K^+ currents (Ik_r) and slow delayed rectifier K^+

[2]Current that repolarizes the cell (makes the membrane potential more negative)

currents (Iks) (Li et al. 1996; Salata et al. 1996). The Ikr is carried out by the ERG K^+ channel, encoded by the KCNH2 gene (Jones et al. 2004; Sanguinetti et al. 1995), that activates and inactivates rapidly (Li et al. 1996; Salata et al. 1996). However, the Iks is carried out by the KCNQ1 channel (Lundby, Tseng, and Schmitt 2010; Sanguinetti et al. 1996) that activates and inactivates more slowly (Li et al. 1996; Salata et al. 1996). At the end of the plateau phase 2, the LTCC closes whereas the K^+ channels remain open allowing the cell repolarization in phase 3. In addition to these 2 outward rectifying K^+ current, the inward rectifying potassium current (Ik1) is also activated and contributes to the terminal repolarization of phase 3 (Lopatin and Nichols 2001). The Ik1 stays active during phase 4 allowing the return to the resting membrane potential that is close to the resting potential of the K^+ (-70 mV) (Jan and Jan 1997; Tourneur et al. 1987). It is important to note that K^+ channels expression depends on both cardiac cells type and cardiac regions and differs between species resulting in different AP shape and duration (Liu, Gintant, and Antzelevitch 1993; Näbauer 1998; Nerbonne and Guo 2002; Soltysinska et al. 2009; Wettwer et al. 1994). Furthermore, alterations of K^+ channel expression or activity in the different cardiac regions are involved in several pathologies such as cardiac hypertrophy, whereas genetic mutations of these channels result in inherited arrhythmias (Amin, Tan, and Wilde 2010; Schmitt, Grunnet, and Olesen 2014). The Na^+ and K^+ gradients through the cell membrane are restored by the Na^+/K^+ ATP-ase extruding 3 Na^+ for the entry of 2 K^+, an energy consuming process requiring ATP hydrolysis and being also electrogenic (Bers 2002; Marbán 2002; Shattock et al. 2015).

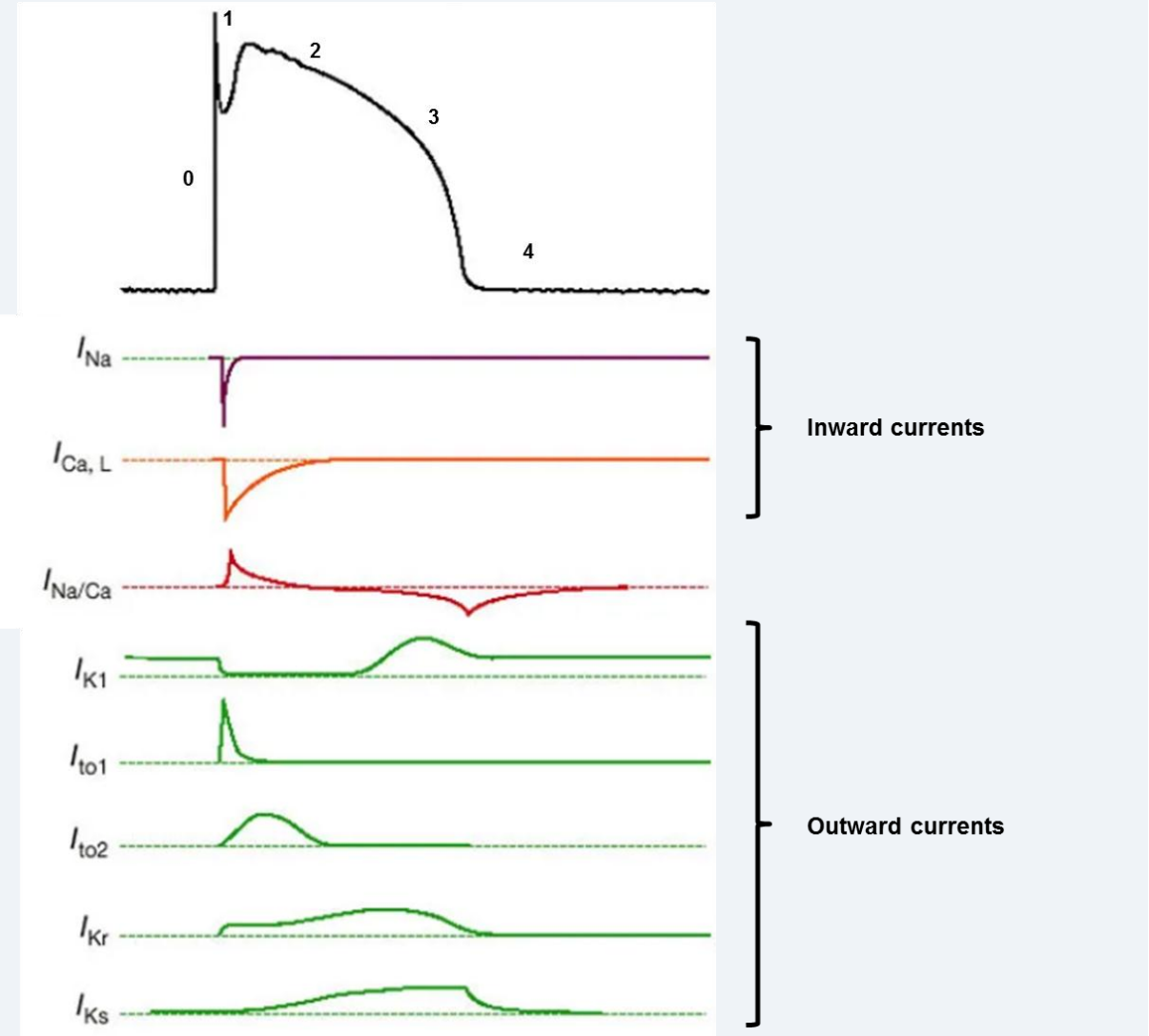

Figure 2: Ventricular action potential (AP) with its respective ionic currents, adapted from (Marbán 2002). The excitation of the ventricular cell induces an inward sodium current (INa) that depolarizes the membrane to +30 mV, which corresponds to phase 0. At this potential, sodium channels are inactivated and transient inward potassium current (Ito) is activated inducing a rapid transient repolarization of the cell, known as phase 1. Phase 2 is characterized by a plateau resulting from inward calcium current (ICaL) counterbalanced by a rapid (IKr) and a slow (IKs) outward rectifying potassium currents. The repolarization phase 3 is ensured by these potassium currents with the involvement of the inward rectifying potassium channel (IK1) at the late repolarization phase toward the resting potential (phase 4).

2) The excitation-contraction coupling

a. The dyad functional structure

Cardiac contraction is initiated by the electrical activity of the heart. The opening of the LTCC during the AP phase 2 drives the Ca^{2+} into the ventricular cardiomyocyte leading to

ventricular cardiomyocyte contraction. This mechanism is known as excitation-contraction coupling (Fabiato and Fabiato 1979) which is due to a specific structure of the sarcolemma and a tight communication between the various elements of the ECC detailed below.

Ventricular cardiomyocyte membrane presents several invaginations of 150 to 300 nm wide (Soeller and Cannell 1999). Those invaginations form into the cytosol a wide interconnected network, called transverse tubules (T-tubules) (Huxley 1971).

The junctional SR cisterna contain the ryanodine receptors (RyR) allowing Ca^{2+} release, and longitudinal SR contain the sarco-endoplasmic reticulum Ca^{2+} ATP-ase (SERCA) which pumps back the Ca^{2+} into the SR (Fawcett and McNutt 1969; Page and Surdyk-Droske 1979). The closeness between the T-tubule and the SR, of about 15 nm (Fawcett and McNutt 1969), permits a functional and essential communication to allow ECC between the LTCC cluster on the T-tubules and RyR cluster on the SR, forming the dyad (Louch et al. 2004; Scriven, Asghari, and Moore 2013) (Figure 3 and Figure 4). Each junction between the T-tubule and the SR, where 10-25 LTCC and 100-200 RyR are clustered, constitutes a Ca^{2+} signaling complex, or couplon, the functional unit of the dyad. The AP induces the simultaneous activation of over 20 000 couplons which results into a synchronous massive release of Ca^{2+} from the SR into the cell (Bers 2008).

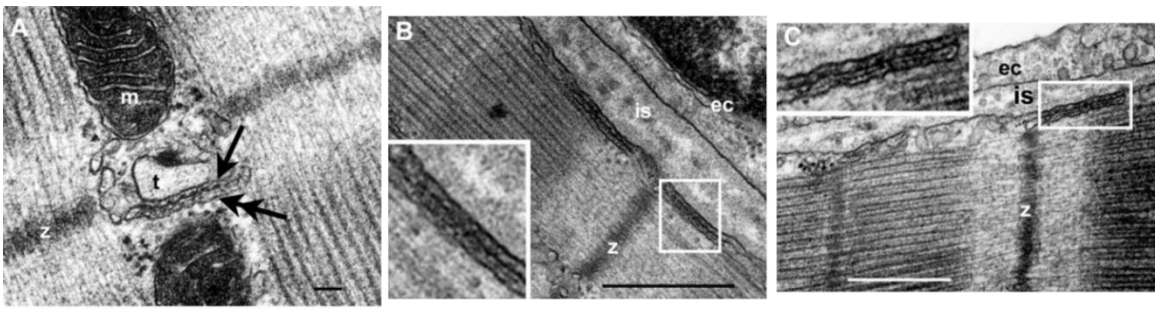

Figure 3: Dyad structure adapted from (Asghari et al. 2009). Transmission electron micrographs of junctions in the rat ventricle. (A) A dyad on the T-tubule: ryanodine receptors (single arrow), SR (double arrow), mitochondria (m), Z-line (z). Scale bar = 100 nm. (B) and (C) Surface junctions. Insets of the indicated regions are magnified 2.5×: endothelial cell (ec), interstitial space (is). Scale bars = 500 nm.

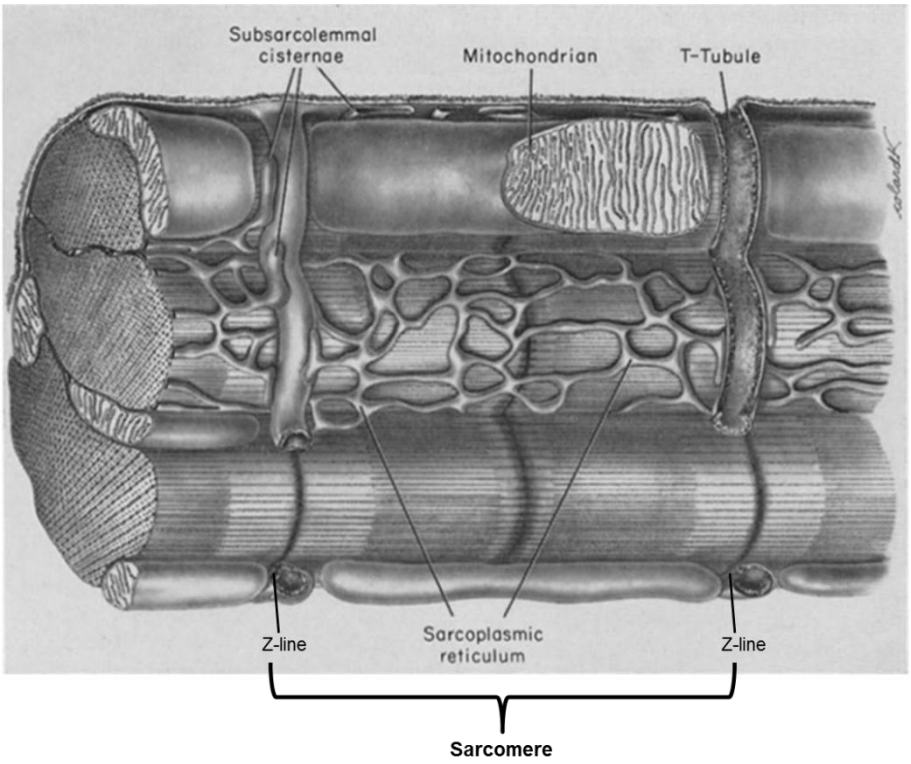

Figure 4: The ultrastructure of cat myocardium ventricular papillary muscle adapted from (Fawcett and McNutt 1969). Junctional sarcoplasmic reticulum (sub-sarcolemmal cisternae) faces the T-tubule. The sarcomere delimited by 2 Z-lines is in close contact with the dyad structure for an effective ECC.

Indeed, the membrane depolarisation during the AP induces the opening of the LTCC cluster, which are concentrated on the T-tubules (phase 2). As a result, a small amount of Ca^{2+} enters into the cell. Although this Ca^{2+} entry is insufficient to induce cell contraction, it activates the RyR cluster on the SR facing this LTCC cluster and induces a massive release of the Ca^{2+} stored into the SR, called Ca^{2+} transient. Then, cytosolic Ca^{2+} concentration ($[Ca^{2+}]_i$) rises from 100 nM at rest to 1 µm. This Ca^{2+} release induced by the Ca^{2+} entry is known as the calcium induced-calcium release (CICR), firstly described by Fabiato and Fabiato in 1979 (Fabiato and Fabiato 1979). Therefore, the CICR is an amplification process inducing a great increase of the $[Ca^{2+}]_i$ mandatory for myofibrils contraction (Figure 5).

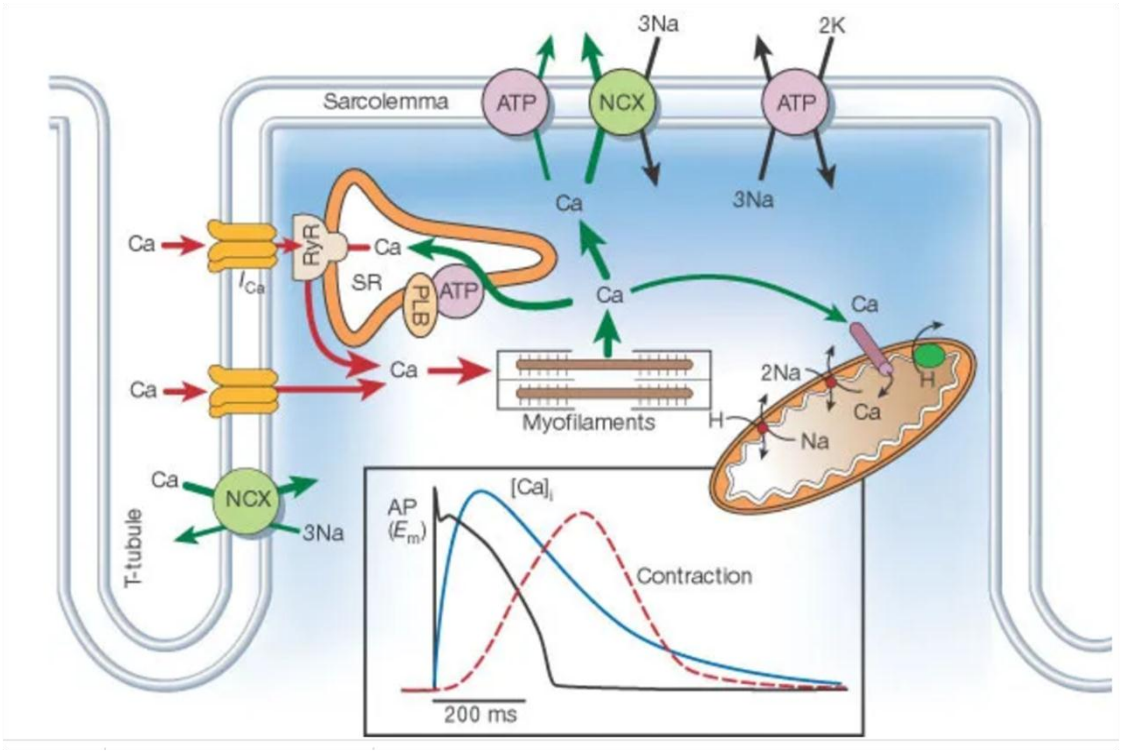

Figure 5: ECC mechanism, modified from (Bers 2002). The depolarization of the membrane by the AP (black curve) induces the opening of the LTCC for a Ca^{2+} entry in the cell. This Ca^{2+} entry activates the RyR allowing a massive release of Ca^{2+} in the cell (Ca^{2+} transient, blue curve) which induces cell contraction (red curve). The major part of the Ca^{2+} is pumped back into the SR by SERCA or extruded by NCX allowing cell relaxation, and a slight part is removed by the mitochondria.

The functional unit of the myofilament is called sarcomere, and is delimited by 2 Z-lines (Figure 6). The Z-lines are close to the T-tubules (Figure 3 and Figure 4) for a maximum coordination between CICR and contraction.

Cardiac sarcomeres, are composed of repeating units of thin (actin) and thick (myosin) filaments. Titin, an intracellular anchor protein, works as a spring both at rest and during contraction. It helps to keep the alignment of the filaments during contraction, and contributes to the return to the resting length of the cardiomyocyte during relaxation. Thin filaments consist of actin and the regulatory proteins tropomyosin (Tm) and troponin (Tn). Thick filaments are myosin chains with globular heads called cross-bridges. Troponin is composed of inhibitory troponin I (TnI), Ca^{2+} binding toponin C (TnC) and tropomyosin binding troponin (TnT). Tn binds to Tm through TnT to form the troponin-tropomyosin complex (Stehle and Iorga 2010). The contraction-relaxation mechanism was described for

the first time by Huxley *et al.* (Huxley and Hanson 1954) in 1954: at rest, TnI of the tropomyosine-troponin complex binds to actin avoiding its interaction with myosin (steric inhibition). When Ca^{2+} is released from the SR during CICR, it binds to TnC which removes the Tn-Tm complex from its steric blocking position, allowing myosin to interact with actin for contraction, called cross-bridging of the actin and myosin filaments (Stehle and Iorga 2010) (Figure 6).

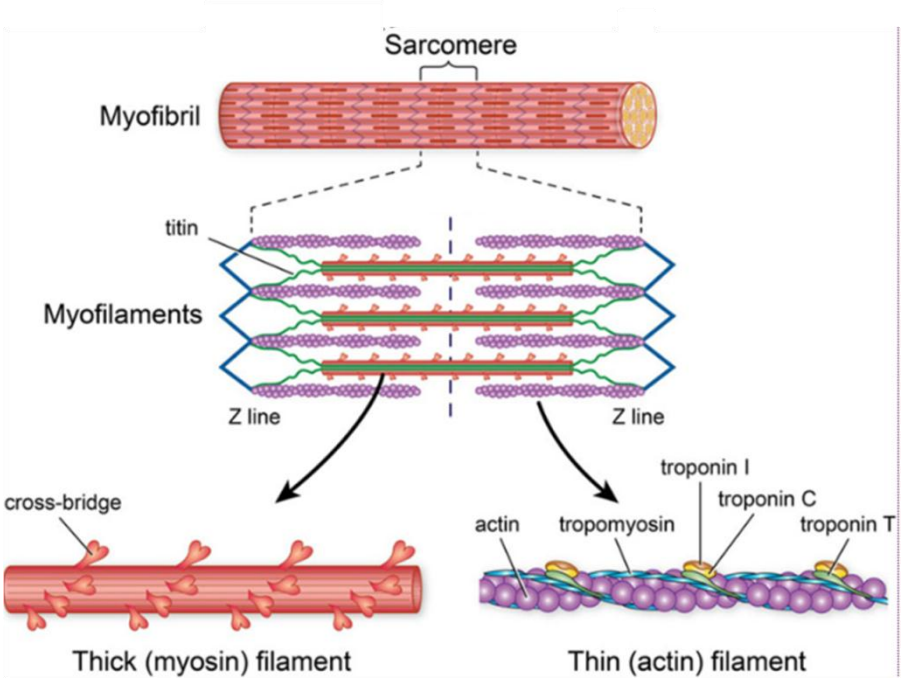

Figure 6: Sarcomere structure adapted from (Golob, Moss, and Chesler 2014). Cardiac myofibrils are constituted of several sarcomeres, the contraction unit, which are delimited by 2 Z-lines. Sarcomeres are composed of titin that insures the alignment of the filaments during contraction, and contributes to the return to the resting length of the cardiomyocyte during relaxation. Sarcomeres contain also repeating units of thin and thick filaments. The thin filaments consist of actin and the regulatory proteins tropomyosin, inhibitory troponin I, Ca^{2+} binding troponin C and tropomyosin binding troponin T. Thick filaments are composed of myosin with globular heads called cross-bridges that allow the interaction with actin filaments for cell contraction.

Then $[Ca^{2+}]_i$ decreases due mainly to its pumping back into the SR, inducing Ca^{2+} dissociation from the troponin allowing relaxation. Two main proteins are responsible for the $[Ca^{2+}]_i$ decrease. First, the SERCA pump located at the longitudinal SR pumps back the Ca^{2+} into the SR. The activity of this pump is constitutively inhibited by its regulatory protein,

phospholamban (PLB) (Simmerman and Jones 1998). When $[Ca^{2+}]_i$ increases, Ca^{2+} binds to SERCA inducing a partial dissociation of the PLB and therefore the release of its inhibition. Next, the NCX extrudes a lower amount of Ca^{2+} outside the cell. The mitochondria also integrate a slight part of Ca^{2+} by its uniporter (Figure 5). The contribution of these different mechanisms differs depending on the species. Indeed, in rabbits, dogs and humans, the SERCA pump recaptures 70% of cytosolic Ca^{2+}, the NCX expels 28% of Ca^{2+} while the remaining 2% is removed by the mitochondria and plasmalemmal Ca^{2+} ATPase. However, in mouse or rat, the SERCA pump has a preponderant role by pumping 92% of cytosolic Ca^{2+} into the SR. In those rodents, the NCX only participates in relaxation up to 7%, while mitochondria and plasmalemmal Ca^{2+} ATPase only remove 1% in the expulsion of cytosolic Ca^{2+} (Bassani, Bassani, and Bers 1994).

b. ECC components

LTCC

LTCC are hetero-tetrameric proteins composed of a pore-forming α_{1C} subunit ($Ca_v1.2$) and several accessory proteins: an intracellular β subunit, an extracellular $\alpha_2\delta$ subunit and a γ subunit. Both β and $\alpha_2\delta$ subunits modulate the biophysical properties and trafficking of the α_{1C} subunit to the membrane. The ventricular LTCC α_{1C} subunit ($Ca_v1.2$) is encoded by CACNA1C gene and is dihydropyridine (DHP)-sensitive, which is referred by extension in ventricles as $Ca_v1.2$ channel or DHP receptor (Benitah, Alvarez, and Gómez 2010; Bodi et al. 2005; Catterall 2011). LTCC activation is voltage dependent for potentials above −40 mV with a peak between 0 to +10 mV, and tends to reverse at +60 to +70 mV (Isenberg and Klöckner 1982; Linz and Meyer 1998; Orkand and Niedergerke 1964), whereas its inactivation is Ca^{2+}- and voltage-dependent. The Ca^{2+}-dependent inactivation of the LTCC is mediated by the calmodulin (CaM) (Pitt et al. 2001; Zühlke et al. 1999). This Ca^{2+}-dependent

inactivation of the channel acts as a negative feedback loop to avoid Ca^{2+} overload. Ca^{2+} also mediates ICaL facilitation which is an acceleration of the activation of ICaL resulting in a moderate increase of the ICaL amplitude and slowing of its inactivation (Richard et al. 2006). The ICaL facilitation is dependent on the SR Ca^{2+} released (Delgado et al. 1999), and mediated by the Ca^{2+} calmodulin kinase type 2 (CaMKII) (Anderson et al. 1994; Xiao et al. 1994) that is activated by Ca^{2+}-CaM, to phosphorylate the α_{1C} and β subunits (Hudmon et al. 2005; Pitt 2007).

NCX

The Na^+/Ca^{2+} exchanger (NCX) is widely distributed on the cell membrane, including the T-tubules and the dyad. NCX participates to the relaxation by extruding Ca^{2+} entered into the cell *via* the LTCC during the AP (Acsai et al. 2011; Despa et al. 2003; Frank et al. 1992; Jayasinghe, Cannell, and Soeller 2009; Thomas et al. 2003). In forward mode, NCX extrudes 1 Ca^{2+} for the entry of 3 Na^+ (Reeves and Hale 1984) resulting in 1 positive net charge which confers the channel an electrogenic property. The NCX can also act in the reverse mode where it extrudes Na^+ for the entry of Ca^{2+} depending on Na^+ and Ca^{2+} concentrations (Armoundas et al. 2003). Throughout the AP the I_{NCX} driven current is an inward current that favours Na^+ entry and Ca^{2+} extrusion. However, during the upstroke phase of the AP (phase 0), the membrane potential reaches +30 mV favouring an outward I_{NCX} with the extrusion of Na^+ and entry of Ca^{2+} participating to the Ca^{2+} influx along with the LTCC and further Ca^{2+} release from the SR (Larbig et al. 2010; Neco et al. 2010; Weber et al. 2002). However, this outward I_{NCX} is very brief since the massive release of Ca^{2+} from the SR reverse the NCX activity, and the I_{NCX} becomes inward again (Weber et al. 2002). The direct regulation of the NCX by Ca^{2+} and Na^+ is not fully understood yet. Very high Na^+ concentration (non-physiological > 20 mM) inactivates the NCX probably to avoid a large extrusion of Na^+ and

Ca^{2+} overload (Hilgemann, Collins, and Matsuoka 1992; Hilgemann et al. 1992). On the other hand, the high concentration of Ca^{2+} activates the NCX inducing Ca^{2+} extrusion to prevent Ca^{2+} overload and favours cardiomyocytes relaxation (Weber et al. 2001; Weber et al. 2002). As mentioned above, the percentage of Ca^{2+} removed through NCX during cell relaxation is highly dependent on animal species.

SERCA pump

SERCA plays a major role in the reduction of the $[Ca^{2+}]_i$ besides NCX allowing cell relaxation. SERCA is a SR protein with different isoforms such as the SERCA2a being the major adult ventricular cardiomyocyte isoform (Wuytack et al. 1998). SERCA is localized on the longitudinal SR (Greene et al. 2000; Vangheluwe et al. 2003) as well as on the SR close to the Z-lines (Drago, Colyer, and Lederer 1998; Greene et al. 2000; Vangheluwe et al. 2003) to modulate $[Ca^{2+}]_i$. The activity of SERCA is inhibited by a phosphoprotein, the phospholamban (PLB) (Katz, Tada, and Kirchberger 1975; Tada, Kirchberger, and Katz 1975; Tada, Yamamoto, and Tonomura 1978) whose phosphorylation by the protein kinase A (PKA) at the Serine (Ser) 16 and by CaMKII at the Threonine (Thr) 17 lifts its inhibitory action on SERCA accelerating Ca^{2+} reuptake and thus cell relaxation (Kranias, Schwartz, and Jungmann 1982; Kuschel, Karczewski, et al. 1999; Simmerman et al. 1986).

Ryanodine receptor (RyR)

Structure and distribution

The ryanodine receptors (RyR) are Ca^{2+} channels located at the junctional SR. Their name is referred to the ryanodine, an alkaloid which can modify their activity. Indeed, upon its binding to the activated RyR, low concentration of ryanodine blocks the channel at its subconductance state (half-open), whereas at high concentration ryanodine inhibits RyR

opening (Alderson and Feher 1987; Anderson et al. 1989; Meissner and Henderson 1987; Rousseau et al. 1986).

Three mammalian RyR isoforms have been identified: RyR_1 is found in the SR membrane of skeletal muscle, while RyR_2 is present in heart muscle. RyR_3 is coexpressed at low level with the other RyR isoforms in the smooth muscle (Neylon et al. 1995) and the brain (Furuichi et al. 1994).

The cardiac RyR_2 is a large homo-tetramer complex of 2.2 MDa constituted of 4 monomeres of 565 kDa each (Bers 2004; Otsu et al. 1990). RyR interacts with several proteins (e.g. sorcin, calstabin or FKBP, junctin, triadin, and calsequestrin) forming a huge macromolecular complex (Figure 7). This macromolecular complex is also connected to PKA, phosphatases (e.g. phosphatase 1 and 2A) and phosphodiesterase (PDE4D) which are tethered to the channel and held near their target sites by anchoring proteins (Bers 2004; Meissner 2017) (Figure 7).

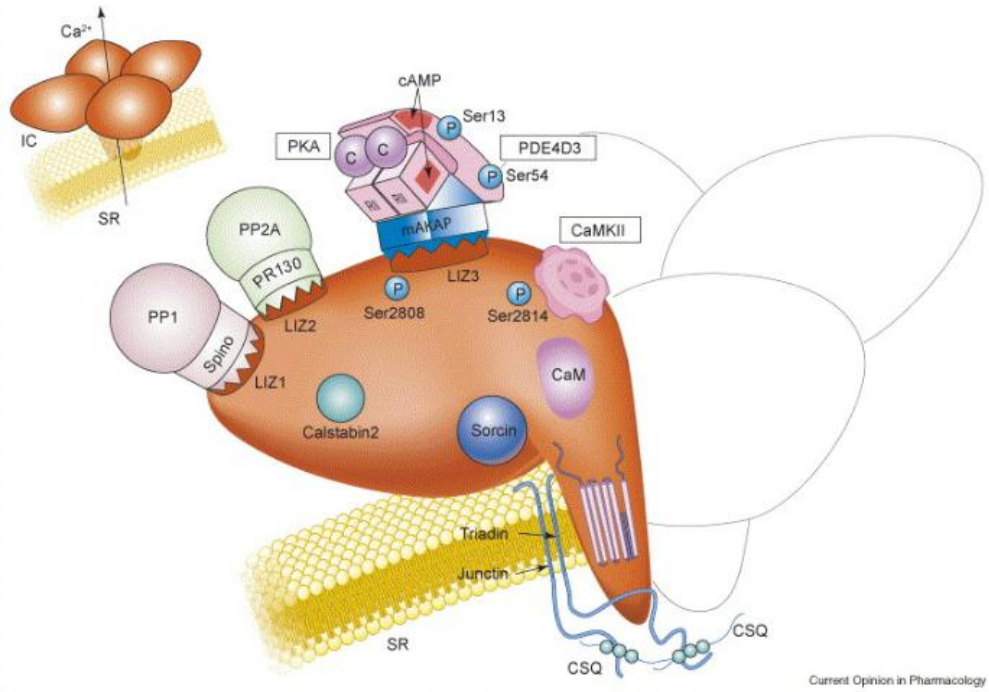

Figure 7: RyR supercomplex from (Lehnart 2007), Top left: The cardiac RyR_2 is a large homo-tetramer constituted of 4 monomeres forming a large "foot-like" structure on the SR membrane. Lower right: RyR interacts with several proteins such as CaM, CaMKII, sorcin, calstabin, triadin, junction and calsequestrin, forming a huge macromolecular complex. This macromolecular complex is also connected to protein kinase A (PKA), phosphatases (PP1 and PP2A) and phosphodiesterase (PDE4D) which are tethered to the channel and held near their target sites by anchoring proteins (AKAP).

RyR Ca^{2+} release

2 major forms of RyR Ca^{2+} release are described: the single unit Ca^{2+} release called Ca^{2+} sparks that is observed at rest (diastole), and the Ca^{2+} transient, that is the summation of several Ca^{2+} sparks during the CICR (systole). These 2 forms of Ca^{2+} release are described below.

Ca^{2+} spark, the RyR Ca^{2+} release unit

The mechanism of Ca^{2+} release from the SR has taken several years to be elucidated. First Stern (Stern 1992) proposed that the Ca^{2+} release from the SR follows a "local-control" model: either the local Ca^{2+} from one LTCC directly stimulates a single highly conductant RyR for Ca^{2+} release, or one LTCC triggers a cluster of RyRs on the SR. This "local-control" theory (Stern 1992) opposes a "Common-pool" model where the CICR mechanism follows an all-or-none Ca^{2+} release from the SR upon AP. The “local-control” theory was lately confirmed with the development of the confocal microscopy, where the RyR Ca^{2+} release was described as a Ca^{2+} spark (Cheng, Lederer, and Cannell 1993). Ca^{2+} spark is defined as a spontaneous and local (around 2 μm) increase in the concentration of $[Ca^{2+}]_i$ (200 nM) (around 10 ms time to peak) with a moderate decay time (20 ms decay time at half peak) (Guatimosim et al. 2002). Ca^{2+} spark generates from the synchronous opening of a cluster of RyR, process called “coupled-gating” (Marx et al. 2001) where the RyRs (between 10 to 200) of a cluster tend to open and close together.

Ca^{2+} transient

During an AP, the opening of several clusters of LTCC activates several clusters of RyR that open “together”. The Ca^{2+} transient is thus defined as the summation of a large amount of Ca^{2+} sparks released in the cardiomyocyte upon AP (Cannell, Cheng, and Lederer 1995).

Although the Ca^{2+} release mechanism is now well defined, the termination of RyR Ca^{2+} release is still not totally elucidated. At least 3 theories have been proposed:

- First, upon CICR, the RyR is inactivated over time by the increased cytosolic $[Ca^{2+}]_i$ (Sham et al. 1998) and thus requires larger stimulus to stay open (Györke and Fill 1993; Valdivia et al. 1995). Actually, RyR activity is regulated by cytosolic $[Ca^{2+}]_i$ (Meissner 1994; Rousseau et al. 1986; Xu, Mann, and Meissner 1996): at resting Ca^{2+} levels (0.1 μM), the RyR is closed. Then, during ECC, cytosolic Ca^{2+} concentration increases to micromolar concentrations (1 to 10 μM) which fully activate RyR that get adapted and inactivated (Bers 2008).
- The second theory is known as the stochastic attrition where the probability that all the RyRs from one cluster close altogether, dropping the $[Ca^{2+}]_i$ to a level that cannot further activate the RyRs (Baddeley et al. 2009).
- The third and maybe the most probable mechanism of Ca^{2+} release termination is the induction decay mechanism: the massive Ca^{2+} release upon AP (25 to 50 % of Ca^{2+} remain in the SR, around 0.4 mM after CICR (Shannon, Guo, and Bers 2003)) decreases the SR luminal Ca^{2+} concentration ($[Ca^{2+}]_l$) which becomes insufficient to induce more Ca^{2+} release from the SR (Bassani, Yuan, and Bers 1995; Santana et al. 1997; Shannon, Ginsburg, and Bers 2000). This suggests that RyR activity is modulated by the luminal SR $[Ca^{2+}]_l$ (Györke and Györke 1998; Shannon, Guo, and Bers 2003; Sitsapesan and Williams 1994; Xu and Meissner 1998). Furthermore, the drop in $[Ca^{2+}]_l$ decreases the Ca^{2+} release from the SR to a level where the cytosolic $[Ca^{2+}]_i$ is not able to further activate RyR, which is called the induction decay (Cannell et al. 2013; Laver et al. 2013). This theory based on SR luminal $[Ca^{2+}]_l$ modulating RyR activity assumes that the Ca^{2+} transient amplitude does not only depend on the ICaL, but also on the SR Ca^{2+} load. The smaller SR Ca^{2+} load, the less

Ca^{2+} released upon CICR, thus a smaller Ca^{2+} transient is produced which can affect cell contraction (Bassani, Yuan, and Bers 1995; Hüser, Bers, and Blatter 1998; Negretti, O'Neill, and Eisner 1993; Santana et al. 1997; Shannon, Ginsburg, and Bers 2000; Spencer and Berlin 1995).

RyR Ca^{2+} leak

During diastole, SR Ca^{2+} release normally shuts off almost completely (~99%), however there is still a finite level of SR Ca^{2+} release, known as SR Ca^{2+} leak. Indeed, in the absence of triggering I_{CaL}, Ca^{2+} sparks can still occur in the cardiomyocyte (Satoh, Blatter, and Bers 1997) reflecting a diastolic SR Ca^{2+} leak. This SR Ca^{2+} leak can be due to the increase of the SR Ca^{2+} load that regulates, as we already mentioned, RyR activity and increases its open probability (Bers and Shannon 2013; Cheng, Lederer, and Cannell 1993; Eisner et al. 2017; Györke and Györke 1998; Santana, Kranias, and Lederer 1997; Satoh, Blatter, and Bers 1997; Shannon, Ginsburg, and Bers 2002). A Ca^{2+} spark is usually restricted to the opening of one cluster of RyR such that due to brief duration and fast buffering, the local cytosolic $[Ca^{2+}]_i$ around the neighbouring RyR cluster is not increased as to activate it. However, when the luminal $[Ca^{2+}]_l$ is very high or the RyRs are sensitized, a spark in one cluster can activate Ca^{2+} spark at neighbouring clusters producing a cell-wide Ca^{2+} wave (Bers 2014; Cheng et al. 1996; Izu, Wier, and Balke 2001; Keizer and Smith 1998). These Ca^{2+} waves are of particular interest since they can be the substrate of arrhythmic events in the ventricular cells such as delayed after depolarization (DAD). Indeed, the Ca^{2+} wave activates an electrogenic current through NCX to extrude this release of Ca^{2+}. In return, the corresponding Na^+ entry depolarizes the cell leading to a DAD, which if of enough amplitude to reach threshold, can generate an AP (triggered activity) (Berlin, Cannell, and Lederer 1989; Ferrier, Saunders, and Mendez 1973; Kass et al. 1978; Lederer and Tsien 1976). Furthermore, the increase of SR Ca^{2+} leak can decrease the SR Ca^{2+} content, thus decreasing the Ca^{2+} availability for the next

cardiac beat. This can result in a decrease of Ca^{2+} transient amplitude that can affect cell contraction as observed for example in some HF models (Belevych et al. 2007; Bers 2014; Eisner et al. 2017; Shannon TR1 2003).

SR Ca^{2+} leak is not only related to the SR Ca^{2+} store, as mentioned above, but is also related to the RyR open probability which depends on several proteins, as discussed below (Bers 2004).

RyR regulating proteins

FKBP

FK-506-binding proteins (FKBP) are proteins of 12 kDa that bind to the RyR on its cytosolic side. Two isoforms are expressed in the heart, FKBP 12 and 12.6. Whereas FKBP12 is more expressed in the heart than FKBP12.6, it exhibits around 200-fold lower affinity to RyR_2 (Jeyakumar et al. 2001; Timerman et al. 1996). FKBP12.6 stabilizes the RyR in its closed state and thus decreases SR Ca^{2+} leak and Ca^{2+} sparks frequency (Brillantes et al. 1994; Gellen et al. 2008; Gómez et al. 2004; Guo et al. 2010; Loughrey et al. 2004; Prestle et al. 2001; Wehrens et al. 2003) which increases the SR Ca^{2+} content and the CICR gain (Loughrey et al. 2004; McCall et al. 1996; Prestle et al. 2001). Marx *et al.* (Marx et al. 2001) have also proposed the role of FKBP12.6 in the RyR coupled gating, allowing RyRs to open and close together which participates in the CICR regulation. Several reviews describe in more details the regulation of RyR by FKBP12.6 (Chelu et al. 2004; Gonano and Jones 2017).

Sorcin

Sorcin is another regulatory protein of 22 kDa that interacts with both RyR and LTCC (Meyers et al. 1995). In lipid bilayers, sorcin reduces the open probability of the RyR (Lokuta et al. 1997) and decreases Ca^{2+} sparks frequency in mouse cardiomyocytes (Farrell et al.

2003). However, the effect of sorcin overexpression on the SR Ca^{2+} load and Ca^{2+} transients remains controversial. Indeed, overexpression of sorcin in rats ventricular cardiomyocytes is associated to an increase of cell contraction (Frank et al. 2005), whereas cardiomyocytes from mice (Farrell et al. 2003; Meyers et al. 2003) or from rabbits (Seidler et al. 2003) with sorcin overexpression have a decrease of Ca^{2+} transient amplitude associated with an increase of NCX activity and Ca^{2+} extrusion (Seidler et al. 2003). Recently, Chen *et al.*(Chen et al. 2018) have shown that sorcin KO mice present an increase susceptibility to ventricular arrhythmias and death under sympathetic stimulation. Even though further studies are needed to understand the exact role of sorcin on RyR activity, it is for sure implicated in the regulation of the ECC.

Calmodulin (CaM)

CaM is another cytosolic protein regulating RyR. CaM is ubiquitously expressed, highly conserved, 17 kDa protein that upon binding to the RyR decreases its open probability (Yamaguchi et al. 2003). Thereby CaM can regulate RyR closure and the termination of the SR Ca^{2+} release in CICR (Xu and Meissner 2004).

RyR luminal side proteins

From its luminal side, RyR interacts with Calsequestrin, a 45 kDa protein that presents a low-affinity, high-capacity Ca^{2+}-binding, sequestering Ca^{2+} in the SR (Mitchell, Simmerman, and Jones 1988). Junctin and triadin are two other luminal proteins that couple the calsequestrin to the RyR (Zhang et al. 1997) inhibiting its opening under low $[Ca^{2+}]_l$ (20 μM) (Györke et al. 2004). However this inhibition is lifted at high $[Ca^{2+}]_l$ (5 mM) (Györke et al. 2004) suggesting that RyR regulation by luminal Ca^{2+} may be mediated by calsequestrin (Györke et al. 2004; Györke and Terentyev 2008).

RyR post-translational modifications

RyR can undergo post-translational modifications that regulate its activity such as oxidation, nitrosylation, and phosphorylation (Niggli et al. 2013).

RyR oxidation and nitrosylation

Oxidative stress is gaining importance in the development of cardiac diseases such as HF, cardiac remodeling and arrhythmias (Maack and Böhm 2011; Münzel et al. 2017; Münzel et al. 2010). RyR is susceptible to redox reactions with a higher activation under oxidation (Boraso and Williams 1994; Sun et al. 2008; Xu et al. 1998). Taking this into consideration, long term activation of the RyR by oxidation increases SR Ca^{2+} leak, decreases the SR Ca^{2+} content and thus impairs Ca^{2+} transient participating in ECC mishandling as seen in cardiomyopathies (Jung et al. 2008; Lim et al. 2008; Terentyev et al. 2008). RyR is also a substrate for nitrosylation upon the activation of the nitric oxide synthase (NOS) (Lim et al. 2008). However the effect of RyR nitrosylation on the open probability of the channel (Stoyanovsky et al. 1997; Zahradníková et al. 1997) and thus on Ca^{2+} signaling remains controversial (Carnicer et al. 2012). Cardiomyocytes from NOS-KO mice show a decrease of RyR open probability with a decrease of Ca^{2+} sparks frequency and an increase of SR Ca^{2+} load (Wang et al. 2010). In line with these findings, cardiomyocytes with upregulated NOS activity present an increase of RyR nitrosylation accompanied by an increase in SR Ca^{2+} leak (Carnicer et al. 2012).

RyR phosphorylation

Two major proteins are involved in the regulation of RyR activity by phosphorylation: the protein kinase A (PKA) and the calmodulin kinase type II (CaMKII).

Marks group has shown that PKA phosphorylates the RyR on its Ser2808 residue enhancing its open probability which leads to an increase of SR Ca^{2+} leak, a mechanism involved in the

development of HF (Marx et al. 2000; Wehrens et al. 2006). This effect was attributed to FKBP12.6 dissociation from RyR. Since FKBP12.6 stabilizes RyR in its closed state (Brillantes et al. 1994), its displacement by PKA phosphorylation increases RyR open probability and subsequent Ca^{2+} leak (Marx et al. 2000; Wehrens et al. 2006). The ablation of Ser2808 site protects mice from the development of HF after myocardial infarction (MI) (Wehrens et al. 2006). However, later studies conducted by Houser and Valdivia groups (Benkusky et al. 2007; MacDonnell et al. 2008; Xiao et al. 2004; Zhang et al. 2012) have shown totally opposite results. First, Xiao *et al.* (Xiao et al. 2004) have shown that PKA phosphorylation of the RyR does not affect FKBP12.6 binding to RyR. Next, the ablation of the Ser2808 RyR residue didn't protect mice from HF induced neither by transverse aortic constriction (TAC) (Benkusky et al. 2007) nor by MI (Zhang et al. 2012). These opposite results between Marks group and Houser-Valdivia groups may be attributed to different mice lines used by these groups, and to that the phosphorylation of the RyR by PKA, even though increases the channel sensitivity, it accelerates its adaptation, decreasing its activity (Valdivia et al. 1995). Besides the basal state of RyR phosphorylation at Ser2808 is already high (Huke and Bers 2008) and thus may limit its potential increase in HF models (Jiang et al. 2002; Xiao et al. 2005). Another PKA phosphorylation site has been also described at the Ser2030 (Xiao et al. 2005). Cardiomyocytes with RyR S2030 ablation site present a decrease in SR spontaneous Ca^{2+} release under β-adrenergic stimulation, placing S2030 as a novel site of the PKA modulation of the RyR (Potenza et al. 2019).

Although there are lots of controversies regarding PKA phosphorylation effect on RyR, the effect of CaMKII-dependent RyR phosphorylation seems to be clearer. RyR open probability is increased (Wehrens et al. 2004) as well as the Ca^{2+} sparks frequency (Guo et al. 2006) upon CaMKII activation. Since then, CaMKII activation and subsequent RyR phosphorylation have been described as a major player in Ca^{2+} signaling alteration as well as

in HF development and arrhythmias generation (Ai et al. 2005; Huke et al. 2011; Kohlhaas et al. 2006; van Oort et al. 2010).

3) β-adrenergic regulation of the ECC

a. The adrenergic system

The ECC is finely regulated by the sympathetic nervous system, also called adrenergic system. The adrenergic system corresponds to the autonomic nervous system that coordinates the "fight or flight" response during stress conditions. In the heart, sympathetic stimulation results in a chronotropic (heart rate), and dromotropic (conduction velocity) positive effects by innerving the SAN and the AV node. It also presents an inotropic (contraction force for a specific systolic volume), and lusitropic (relaxation) positive effects on the ventricular cardiomyocytes. Acute sympathetic stimulation is necessary to fulfil the organism needs under stress or physical activities. However, a chronic activation of this system induces long term cardiac remodelling participating in the development of HF (Lohse, Engelhardt, and Eschenhagen 2003). The parasympathetic system, the second component of the autonomic nervous system, mainly innerves the SAN and the AV node (sparse in the ventricles) and presents only a chronotropic and dromotropic negative effects (Gordan, Gwathmey, and Xie 2015).

In the heart, two types of adrenergic receptors are expressed, the alpha and beta adrenergic receptors (α-ARs and β-ARs respectively), as firstly proposed by Aliquist in 1948 (Ahlquist 1948), with a predominance of the β-ARs (90%) compared to the α-ARs (10%) (Brodde et al. 2001).

These adrenergic receptors belong to the superfamily of receptors with seven transmembrane domains coupled to G proteins (RCPGs). There are 2 types of α-ARs, α_1-ARs and α_2-ARs,

that are still not well described in the heart. α_1-ARs are coupled to a Gαq protein and are implicated in the development of an adaptive hypertrophy to counteract the deleterious effects of the activation of the β-ARs in HF (Cotecchia et al. 2015; Jensen, O'Connell, and Simpson 2014). The α_2-ARs are less known and are mainly classified as pre-synaptic receptors inhibiting norepinephrine secretion during upregulation of the sympathetic system (Ahles and Engelhardt 2014).

The β-ARs are preponderant and widely regulate the ECC. Three types of β-ARs are expressed in the heart: β_1-ARs, β_2-ARs and β_3-ARs, with around 80% of β_1-ARs, 20% of β_2-ARs and β_3-ARs much less expressed at basal conditions (Brodde et al. 2001; Gauthier et al. 1996; Lohse, Engelhardt, and Eschenhagen 2003).

The β_1-ARs and β_2-ARs are coupled to $G_{\alpha s}$ (although β_2-ARs are also coupled to $G_{\alpha i}$ (Kuschel, Zhou, et al. 1999)), and regulate the ECC with an inotropic and lusitropic positive effects by activating the cyclic adenosine monophosphate (cAMP) pathway that we will discuss later in this chapter (Brodde et al. 2001; Lohse, Engelhardt, and Eschenhagen 2003). However the β_3-ARs are coupled to a $G_{\alpha i}$ that inhibits the cAMP pathway, and are activated under high adrenergic stimulation in order to limit the positive inotropic and hypertrophic effects of β_1-ARs and β_2-ARs (Gauthier et al. 1996).

b. cAMP pathway

The activation of the β_1-ARs and β_2-ARs by their agonists (epinephrine and norepinephrine) activates the $G_{\alpha s}$ subunit and the subsequent adenylate cyclase (AC) which catalyses the local conversion of the adenosine triphosphate (ATP) to cAMP (Brodde et al. 2001). cAMP is a predominant second messenger in the cells which activates both PKA and exchange protein directly activated by cAMP (EPAC), both involved in the regulation of the ECC.

The cAMP signaling is well compartmentalized in the cell due to isoform specific subcellular

localization of phosphodiesterases (PDE) (Weishaar et al. 1987; Berisha and Nikolaev 2017; Mika et al. 2012). PDE hydrolyses cAMP to inactive AMP (Jurevicius and Fischmeister 1996). At least eleven PDE families including 20 genes and about 50 isoforms have been identified in the organism (Conti and Beavo 2007). Four of these eleven PDE families are responsible for cAMP degradation in the heart: PDE1, PDE2, PDE3 and PDE4 (Mika et al. 2012).

Furthermore, the β_1-ARs and the β_2-ARs are distributed differently on the cell membrane participating in the compartmentalization of the cAMP actions. While the β_1-ARs are localized at the entire surface of the cardiomyocytes including the T-tubules, the β_2-ARs are mainly distributed in the T-tubules and the lipid rafts including the caveolea, where they interact with LTCC (Nikolaev et al. 2006; Nikolaev et al. 2010). Thereby, β_1-ARs stimulation leads to the phosphorylation of LTCC, RyR, PLB, and TnI to regulate cardiac contraction and relaxation *via* downstream mediators such as PKA and Epac as described below.

c. PKA

Upon the activation of the β-ARs, the elevation of the cAMP levels in cardiomyocytes activates the PKA that mediates the positive inotropic and lusitropic effects of the sympathetic system (Figure 8).The subcellular localization of PKA is regulated by anchoring proteins, A-kinase-anchoring protein (AKAP). AKAP address PKA to its individual subcellular substrates, which spatially regulates protein phosphorylation and participates in the compartmentalization of cAMP signaling (Berisha and Nikolaev 2017; Diviani et al. 2011; Diviani et al. 2016; Pidoux and Taskén 2010).

PKA phosphorylates several components of the ECC to regulate the Ca^{2+} cycling. First, PKA phosphorylates the LTCC leading to an increase of the Ca^{2+} current amplitude and shifts the channel activation to more negative potential (facilitation of the channel activation)

(Niedergerke and Page 1977; Osterrieder et al. 1982; Tsien et al. 1986; Yatani and Brown 1989; Yue, Herzig, and Marban 1990). This will lead to more Ca^{2+} entry into the cell and thus participates to the β-adrenergic stimulation-mediated positive inotropic effect. However a higher Ca^{2+} entry induces also a more rapid inactivation of the channel (Cens et al. 2006; Tsien et al. 1986; Yatani and Brown 1989), as we described above in the LTCC section, which participates in the lusitropic effect of PKA. The specific PKA-mediated LTCC phosphorylation site is still controversial. The Serine 1928 (Ser1928) of the α-channel subunit was the first site proposed by Hulme *et al.* (Hulme et al. 2006) as the PKA target. Since then, other distal serine and threonine residues, such as Ser1700 and Thr1704, have been identified on the α-channel subunit (Ganesan et al. 2006) or even on the β-subunit (Bünemann et al. 1999) as PKA targets on LTCC.

PKA also exhibits a positive lusitropic effect by acting on the PLB and the TnI. PKA phosphorylates the PLB on the Ser16 dissociating it from SERCA. This lifts the PLB inhibitory effect on SERCA, enhancing SR Ca^{2+} storage, and thus Ca^{2+} release at the next ECC cycle, supporting the positive inotropic effect of PKA (Li et al. 2000; Luo et al. 1994; MacLennan and Kranias 2003). Enhancing the SR Ca^{2+} storage also increases SR Ca^{2+} leak observed by PKA activation (Li et al. 2002). At last, PKA phosphorylates the TnI (Li et al. 2000) decreasing its sensitivity to Ca^{2+} and thus accelerating cardiac relaxation.

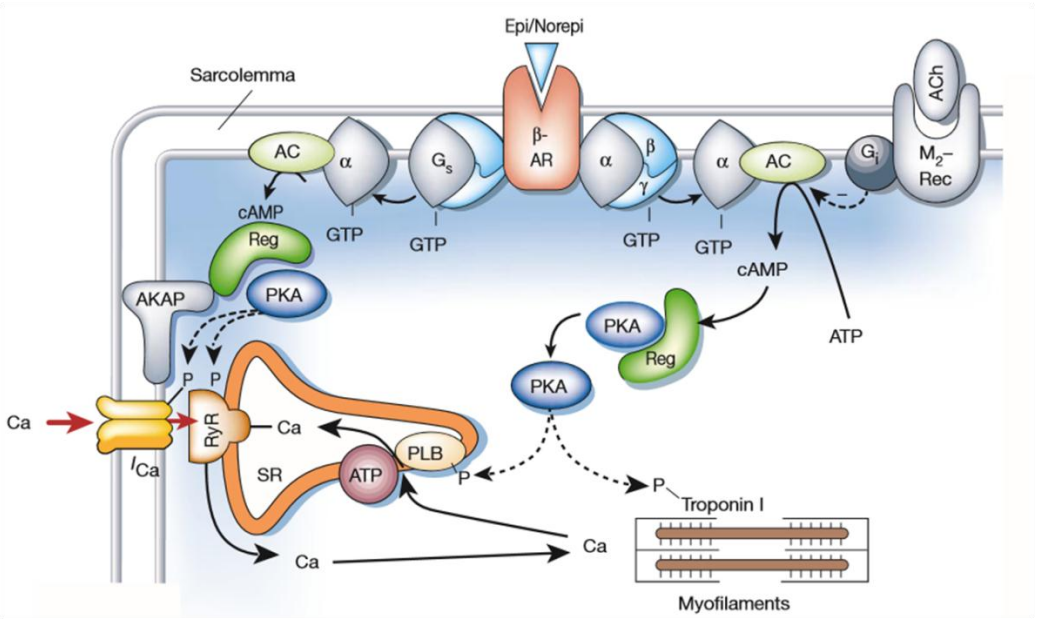

Figure 8: PKA regulation of ECC, adapted from (Bers 2002). PKA phosphorylates the LTCC participating in the inotropic effect of the β-adrenergic stimulation. It also phosphorylates the RyR on the SR with a mild effect on SR Ca^{2+} leak. PKA participates in the β-adrenergic lusitropic effect by phosphorylating the PLB thus increasing the Ca^{2+} pumping into the SR. It also phosphorylates the TnI reducing its affinity to Ca^{2+} and favouring myofibrils relaxation.

II. Epac

PKA was considered as the only downstream effector of cAMP, until 1998 when DeRooj *et al.* (de Rooij et al. 1998) and Kawaski *et al.* (Kawasaki et al. 1998), two independent groups, discovered a new exchange protein directly activated by cAMP, the Epac.

1) Isoforms and distribution

Two Epac isoforms have been identified, Epac1 and Epac2 which are respectively encoded by two different genes, Rapgef3 and Rapgef4 (de Rooij et al. 1998; Kawasaki et al. 1998).

The Epac isoforms exhibit a wide expression profile (Niimura et al. 2009) with distinct expression level depending on the developmental stage (Ulucan et al. 2007). For instance, in mice, Epac1 reaches its maximal levels at 3 weeks in brain, heart, lungs and kidneys (de Rooij et al. 1998; Kawasaki et al. 1998; Ulucan et al. 2007), whereas Epac2 expression decreases in the lungs and is almost not expressed in the kidneys at the adult stage. In the

adult heart mice, Epac2 expression increases with a decrease in Epac1/Epac2 ratio during cardiac development (Ulucan et al. 2007).

Epac1 is ubiquitously expressed, whereas Epac2 presents several splice variants with different organ distribution (Hoivik et al. 2013; Niimura et al. 2009): Epac2A which is broadly expressed notably in the central nervous system and the heart, Epac2B which is expressed in the adrenal glands and the pancreas, and finally, Epac2C expressed in the liver.

In the ventricular cardiomyocyte, Pereira *et al.* (Pereira et al. 2015) have shown that Epac1 and Epac2 exhibit specific subcellular localization with Epac1 located at the perinuclear region to regulate hypertrophic mechanisms. Epac2 is located at the T-tubules region, and is implicated in the SR Ca^{2+}leak and ventricular arrhythmia (Pereira et al. 2013; Pereira et al. 2015).

Epac isoforms expression also depends on the diseases stages (Metrich et al. 2008; Ulucan et al. 2007; Yokoyama et al. 2008). Both Epac1 and Epac2 expression are increased in isoproterenol-induced left ventricular hypertrophy in mice (Ulucan et al. 2007), whereas only Epac1 is increased in pressure overload-induced hypertrophy in mice and rats as well as in human failing heart samples (Metrich et al. 2008; Ulucan et al. 2007).

2) Structure and activation

Epac proteins exert a guanine exchange factor (GEF) activity allowing the activation of the small GTPase (guanosine triphosphatase), such as Rap1 and Rap2, their effectors, by exchanging the guanosine diphosphate (GDP) into guanosine triphosphate (GTP) (de Rooij et al. 1998; Kawasaki et al. 1998).

Epac are multidomain proteins with a C-terminal catalytic region and a N-terminal regulatory region (Figure 9) (de Rooij et al. 2000; Rehmann et al. 2008; Rehmann et al. 2006; Rehmann, Prakash, et al. 2003; Rehmann, Rueppel, et al. 2003; Rehmann, Schwede, et al. 2003;

Rehmann, Wittinghofer, and Bos 2007). The catalytic function resides in the CDC25-homology domain (CDC25HD) that exhibits the GEF activity of Rap1 and Rap2. This domain is stabilized by the Ras-exchange motif (REM). The CDC25HD and REM domains are separated by a Ras association (RA) domain. The RA domain allows Epac2 interaction with Ras which is required for Epac2 relocation to the plasma membrane and subsequent Rap1 activation (Li et al. 2006; Liu et al. 2008). The N-terminal domain contains a membrane-anchoring disheveled-Egl-10-pleckstrin (DEP) important for subcellular Epac localization (Consonni et al. 2012; Ponsioen et al. 2009). This domain is followed by a cAMP high-affinity binding domain (CNBD-B) which is common to both isoforms (de Rooij et al. 1998). Epac2 possess an additional cAMP low-affinity binding domain (CNBD-A) not required for Epac activation, but necessary for intracellular localization of Epac2 (de Rooij et al. 1998; Niimura et al. 2009).

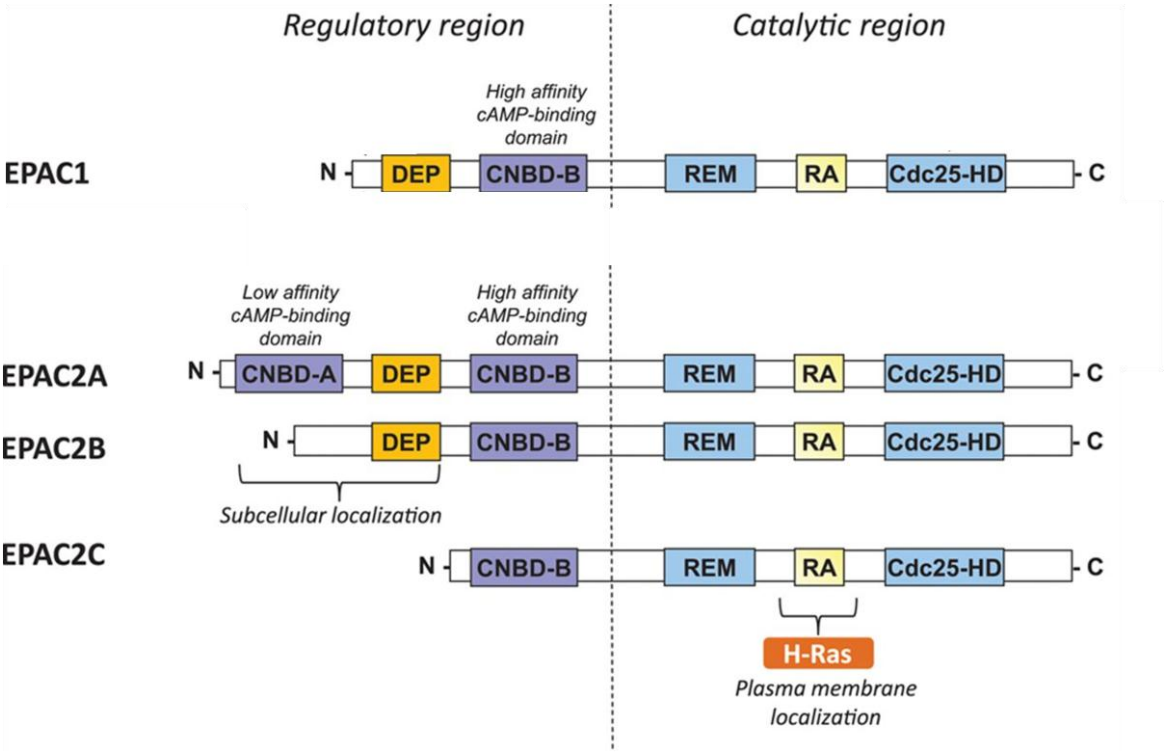

Figure 9: Epac structure, adapted from (Lezoualc'h et al. 2016). Epac are multidomain proteins containing a N-regulatory and a C-catalytic region. The N-regulatory region consists of a cyclic nucleotide–binding domain (CNBD-B) that binds cAMP with high affinity. Epac2 presents an additional CNBD domain (CNBD-A) that binds cAMP with a lower affinity. The N-regulatory region also contains a Dishevelled, Egl-10, Pleckstrin (DEP) region, which is involved in Epac subcellular localization. The catalytic domain is composed of a catalytic CDC25 homology domain (CDC25-HD) stabilized by a Ras-exchange motif (REM). Ras binds to the Epac2 Ras association (RA) domain to regulate Epac2 membrane localization and its biological function.

In the absence of cAMP, the N-regulatory region sterically inhibits the C-catalytic region. The binding of cAMP to its CNBD-B domain induces a conformational modification of Epac lifting the auto-inhibition of the N-region on the C-region. This allows binding of Rap to the GEF domain and its activation by exchange of GDP by GTP (Figure 10) (de Rooij et al. 2000; Rehmann et al. 2008; Rehmann et al. 2006; Rehmann, Prakash, et al. 2003; Rehmann, Rueppel, et al. 2003; Rehmann, Schwede, et al. 2003). To date, cAMP is the only known effector to activate Epac.

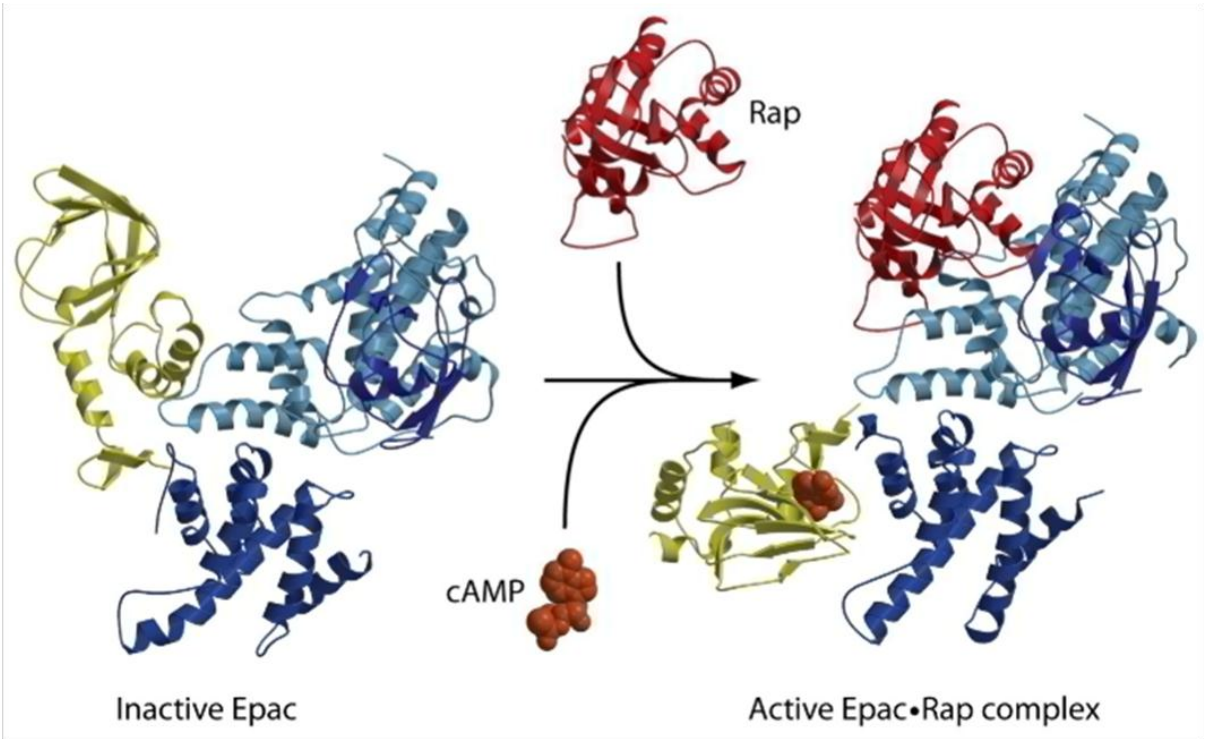

Figure 10: Epac activation, adapted from (Gloerich and Bos 2010). In the absence of cAMP, the N-regulatory region sterically inhibits the C-catalytic region of Epac. The binding of cAMP to the CNBD-B domain induces a conformational modification of Epac lifting up the auto-inhibition of the N-region on the C-region. This allows binding of Rap to the GEF domain and its activation by exchange of GDP by GTP.

3) Epac modulation of the ECC

Acute and chronic Epac activation modulate ECC by distinct mechanisms resulting in different outcomes that will be discussed in this paragraph. Briefly, acute Epac activation modulates ECC mainly by its downstream effector, CaMKII, that phosphorylates its targets (RyR, PLB, and contractile myofilaments proteins) resulting in an increase of Ca^{2+} leak with

or without affecting the Ca^{2+} transient and cell contraction. However chronic Epac activation modulates ECC mainly by CaM overexpression that affects ECC players' activity.

Morel *et al.* (Morel et al. 2005) were the first to describe spontaneous Ca^{2+} bursts in neonatal rat cardiomyocytes treated with Epac agonist 8-CPT (a cAMP analog). Later, Pereira *et al.* (Pereira et al. 2007) have demonstrated the involvement of Epac in the regulation of the cardiac ECC. In their work, an acute treatment (2-5 minutes) of adult rat ventricular cardiomyocytes with 8-CPT, increases Ca^{2+} sparks frequency with a subsequent decrease of the Ca^{2+} transient amplitude (Pereira et al. 2007). Neither the LTCC, nor the NCX functions were affected by 8-CPT (Pereira et al. 2007). This 8-CPT effect on the SR Ca^{2+} leak was CaMKII-dependent (Pereira et al. 2007), suggesting that 8-CPT-mediated effects on SR Ca^{2+} leak is induced by CaMKII phosphorylation of the RyR at the Ser2814 (Pereira et al. 2007). Interestingly, Oestreich *et al.* (Oestreich et al. 2009) found that a brief treatment (less than 1 minute) with 8-CPT increases the Ca^{2+} transient amplitude in mice ventricular cardiomyocytes. This Epac effect was mediated by the phospholipase Cε (PLCε), downstream to Epac (Oestreich et al. 2009). However, Hothi *et al.* (Hothi et al. 2008), didn't detect any alteration of the Ca^{2+} transient amplitude although they found aberrant Ca^{2+} release, as Ca^{2+} waves and triggered activities[3], in mice isolated ventricular cardiomyocytes after 1 to 3 minutes of 8-CPT application. Those distinct 8-CPT-mediated effects on the Ca^{2+} transient amplitude (decrease, increase or no modification) may be due, in part, to the animal model used (mice or rats), and in a second part, to the 8-CPT application duration. Besides, 8-CPT effect on the Ca^{2+} transient amplitude depends also on the Ca^{2+} concentration (Lezcano et al. 2018). For instance, Lezcano *et al.* (Lezcano et al. 2018) have shown that at low Ca^{2+} concentration (0.5 mM), 8-CPT increases the Ca^{2+} transient amplitude in rat ventricular cardiomyocytes, and decreases it at 1.8 mM of $[Ca^{2+}]$ as observed by Pereira *et al.* (Pereira et

[3]A spontaneous action potential in quiescent cardioymocyte.

al. 2007) as well as Cazorla *et al.* (Cazorla et al. 2009). However, 1.8 mM of [Ca^{2+}] increases the Ca^{2+} transient amplitude in mice cardiomyocytes as observed by Oestrich *et al.* (Oestreich et al. 2009) that was not observed in ventricular cardiomyocytes from transgenic mice lacking the PLB's CaMKII phosphorylation site (Lezcano et al. 2018). Taking this into consideration, it should be noted that acute 8-CPT effects on Ca^{2+} transient, even though are independent of NCX and LTCC activity (Pereira et al. 2007), depends on CaMKII SR targets, the RyR and the PLB (Lezcano et al. 2018).

The involvement of both CaMKII and PLCε in Epac-mediated regulation of ECC independently of PKA have been confirmed in several papers (Oestreich et al. 2007; Pereira et al. 2007; Hothi et al. 2008; Cazorla et al. 2009; Oestreich et al. 2009; Pereira et al. 2012; Pereira et al. 2015) even though the detailed mechanism is not well elucidated yet. The 8-CPT-mediated increase of the Ca^{2+} sparks frequency and the diastolic Ca^{2+} concentration in rats cardiomyocytes observed by Pereira *et al.* (Pereira et al. 2012) were prevented by inhibition of phospholipase C (PLC), CaMKII and inositol trisphosphate receptors (IP3Rs). Knowing that PLC activation produces diacylglycerol (DAG) and inositol trisphosphate (IP3), the authors suggested that IP3 production via the Epac/PLC pathway might activate the surrounding IP3Rs on the SR leading to Ca^{2+} release (Pereira et al. 2012). This Ca^{2+} can then activate the neighbouring CaMKII which phosphorylates the RyR resulting into further SR Ca^{2+} leak (Pereira et al. 2007). Beside the PLC/IP3/Ca^{2+} pathway, Pereira *et al*. (Pereira et al. 2017a) have shown that 8-CPT-mediated SR Ca^{2+} leak following CaMKII activation and RyR phosphorylation were prevented by nitric oxide synthase 1 (NOS1) and phosphoinositide 3-kinase (PI3K) inhibition in mice and rabbit cardiomyocytes (Pereira et al. 2017a). This study (Pereira et al. 2017a) unravels a new mechanism of Epac-mediated CaMKII activation through PI3K, protein kinase B (AKT) and NOS1 (PI3K/AKT/NOS/CaMKII) pathway (Pereira et al. 2017a).

Epac also regulates myofilaments Ca^{2+} sensitivity (Cazorla et al. 2009). Indeed, acute 8-CPT treatment increases cell shortening in rats cardiomyocytes even though the Ca^{2+} transient amplitude is reduced (Cazorla et al. 2009). This effect is due to an increase in myofilaments Ca^{2+} sensitivity by TnI and myosine binding protein C (MyBP-C) phosphorylation depending on PLC, PKC and CaMKII (Cazorla et al. 2009). The 8-CPT-mediated CaMKII activation v*ia* the PLC/PKC pathway has already been described by Oestreich *et al.* (Oestreich et al. 2009) in mice cardiomyocytes. Taking these into consideration, we can assume that Epac regulates ECC by enhancing myofilaments Ca^{2+} sensitivity *via* a PLC/PKC/CaMKII pathway to compensate the reduction of the Ca^{2+} transient amplitude seen by Pereira *et al.* (Pereira et al. 2007) and preserve cardiomyocytes shortening (Pereira et al. 2007).

While Epac is chronically activated (e.g. for over 4 weeks) with 8-CPT, using osmotic minipumps, Ca^{2+} transient amplitude and the SR Ca^{2+} load are increased (Gema Ruiz-Hurtado 2012). The same effect was also observed in rat cardiomyocytes treated for 5 hours with 8-CPT (Gema Ruiz-Hurtado 2012). Contrarily to the acute effect, chronic 8-CPT shifts LTCC activation toward more negative potentials without affecting its inactivation kinetics, therefore increasing the window current that explains the observed positive inotropic effect (more entry of Ca^{2+} by the LTCC, greater Ca^{2+} release from the SR (Gema Ruiz-Hurtado 2012)). This effect is CaM-dependent which expression is increased by chronic 8-CPT application (Ruiz-Hurtado et al. 2012). Furthermore, chronic treatment with 8-CPT slows down Ca^{2+} extrusion by NCX and accelerates SERCA activity leading to higher SR Ca^{2+} load (Ruiz-Hurtado et al. 2012). This increase of SERCA activity is due to the phosphorylation of the PLB by CaMKII at the Thr17 residue (Ruiz-Hurtado et al. 2012). Even though chronic 8-CPT activates CaMKII, the Ca^{2+} sparks frequency is not increased (Ruiz-Hurtado et al. 2012), due to the CaM overexpression (Gema Ruiz-Hurtado 2012) that inhibits RyR activity (Gong et al. 2019; Smith, Rousseau, and Meissner 1989) counteracting CaMKII action. To conclude,

this study (Ruiz-Hurtado et al. 2012) showed that a chronic activation of Epac2 modulates protein expression, CaM for instance, that affects ECC.

4) Epac and arrhythmia

Epac also participates in the regulation of the ventricular electrical activity and seems to play a role in the generation of cardiac arrhythmia through several mechanisms: by increasing the SR Ca^{2+} leak, by modulating the activity and/or expression of K^{+} and Ca^{2+} channels, and by affecting the GAP junctions' function.

Hothi *et al.* (Hothi et al. 2008) were the first to demonstrate ventricular arrhythmia in perfused mice hearts treated with 8-CPT. In this study (Hothi et al. 2008), the action potential duration or the ventricular refractory period were not affected after 8-CPT perfusion which could explain the observed arrhythmia. Instead, ectopic Ca^{2+} transients in isolated paced cardiomyocytes and Ca^{2+} waves in quiescent cells were observed 1 to 3 minutes after 8-CPT application and prevented by CaMKII inhibition (Hothi et al. 2008) as already described by Pereira *et al.* (Pereira et al. 2007). Therefore the 8-CPT-CaMKII-dependent arrhythmogenic events observed by Hothi *et al*. correlate with what was observed by Pereira *et al.* (Pereira et al. 2007) which attributes it to RyR phosphorylation by CaMKII and subsequent Ca^{2+} leak induced by Epac activation.

Besides affecting RyR activity, Epac participates in Ca^{2+}-related arrhythmias by increasing the store operated calcium entry (SOCE) (Dominguez-Rodriguez et al. 2015). Indeed, 4 to 6 hours of 8-CPT treatment increases the transient receptor potential canonical channels type 3 and 4 (TRPC3 and TRPC4) protein expression in rat ventricular myocytes with a subsequent increase of the Ca^{2+} influx *via* these channels, SOCE, blunted by Epac inhibition. This SOCE is associated with arrhythmogenic Ca^{2+} waves that are prevented by either Epac or TRPC inhibition, yet the underlying arrhythmogenic mechanism is still not elucidated (Dominguez-

Rodriguez et al. 2015). However, it is to note that SOCE are an emerging mechanism in the development of ventricular arrhythmia and HF (Eder 2017; Wu et al. 2010).

In addition to Ca^{2+}-related arrhythmias, Epac activation alters ionic channels activity and/or expression affecting AP duration, known to be an arrhythmia substrate (Amin, Tan, and Wilde 2010). For instance, Brette *et al.* (Brette et al. 2013) have observed an increase of the AP duration in rat ventricular cardiomyocytes under 8-CPT due to a decrease of the repolarizing K^+ current steady state. In line with these results, chronic Epac activation (30 hours) downregulates KCNE expression *via* calcineurin (Cn) and its downstream effector nuclear factor activated by T-cells (NFAT) pathway, subsequently decreasing the repolarizing current I_{Ks} in guinea pig ventricular cardiomyocytes (Aflaki et al. 2014). The alteration of the repolarizing K^+ currents affects AP duration, a substrate to arrhythmia (Schmitt, Grunnet, and Olesen 2014). Furthermore, chronic Epac activation enhances the Ca^{2+} influx *via* the LTCC as described above with subsequent arrhythmogenic early-after depolarization (EAD) (Ruiz-Hurtado et al. 2012). Indeed, increase of the Ca^{2+} current can affect membrane potential with a prolongation of AP phase 2, a substrate for EAD that are abnormal secondary depolarizations taking place during the repolarization phase of the AP (Benitah, Alvarez, and Gómez 2010).

Finally, Epac signaling could trigger cardiac arrhythmia through Gap junctions. Neonatal (Duquesnes et al. 2010; Somekawa et al. 2005) and adult rat ventricular cardiomyocytes (Duquesnes et al. 2010) treated with 8-CPT present an increase of connexin 43 (the main ventricular gap junction protein (Vozzi et al. 1999)) phosphorylation and activity in a Rap1 (Somekawa et al. 2005) and/or PKCε (Duquesnes et al. 2010) dependent manner which can affect the cardiac electrical activity (Beauchamp et al. 2012).

5) Epac and excitation-transcription coupling

Pereira *et al.* (Pereira et al. 2012) have shown that Epac affects nuclear Ca^{2+} concentration ($[Ca^{2+}]_n$) as well as cytosolic Ca^{2+} one, playing a role in the excitation-transcription coupling (ETC) and a subsequent activation of translational hypertrophic pathways. For instance, paced adult rat cardiomyocytes treated with 8-CPT present an increase of $[Ca^{2+}]_n$ with a subsequent activation of the hypertrophic transcription machinery of histone deacetylase/myocyte enhancer factor 2/nuclear factor activated by T-cells (HDAC/ MEF2 /NFAT) which is prevented by CaMKII, IP3R and PLC pharmacological inhibition (Pereira et al. 2012). This study (Pereira et al. 2012) shows for the first time the implication of Epac in the nuclear Ca^{2+} modulation and its subsequent hypertrophic effect which highlights the role of Epac in the cardiac ETC. The ETC can be defined as the implication of the Ca^{2+} fluctuation during ECC in the Ca^{2+}-dependent gene transcription mechanism (Anderson 2000). Indeed, the increase of $[Ca^{2+}]_n$ by Epac is IP3-dependent (Pereira et al. 2012), known to have abundant receptors on the nuclear membrane and to participate in ETC (Wu et al. 2006), pointing out the implication of Epac in this process, although the underlying molecular mechanism is not established yet. In line with these results, Morel *et al.* (Morel et al. 2005) have shown that Ca^{2+} chelation prevents the increase of hypertrophic gene markers expression, such as the atrial natriuretic peptide (ANF) and the skeletal muscle α-actin in neonatal rat ventricular cardiomyocytes infected two hours with Epac adenovirus. In this study, the Epac-Ca^{2+}-mediated hypertrophic mechanism depends on the Rac/Cn/NFAT cell pathway (Morel et al. 2005).

Metrich *et al.* (Metrich et al. 2010; Metrich et al. 2008) have also deciphered the molecular pathway underlying Epac-mediated hypertrophy: 8-CPT promotes HDAC4 transport in COS cells transfected with Epac adenovirus (Metrich et al. 2010). In addition, neonatal rat ventricular cardiomyocytes transfected with Epac adenovirus present an increase of the

NFAT and MEF2 transcription factors activation prevented by CaMKII and RAS inhibition, pointing out that Ras and CaMKII are downstream effectors of Epac hypertrophic mechanism (Metrich et al. 2010), later confirmed in adult rat cardiomyocytes by Pereira *et al.* (Pereira et al. 2012). Furthermore, Ras, CaMKII and Cn inhibition prevent 8-CPT-mediated hypertrophy in adult rat cardiomyocytes transfected with Epac adenovirus (Metrich et al. 2008).

Taken all these studies into consideration, Epac plays a role in the ETC-mediated hypertrophy, by altering cytosolic and nuclear Ca^{2+} signaling activating Ca^{2+}-dependent hypertrophic pathways such as the PLC/IP3/Ca^{2+}/CaMKII/HDAC5/MEF2 (Metrich et al. 2010; Pereira et al. 2015; Pereira et al. 2012) and the Rac/calcineurin/NFAT (Morel et al. 2005 ; Metrich et al. 2008).

To summarize the role of Epac in Ca^{2+} signaling and its hypertrophic effect (Figure 11) : Epac stimulation modulates $[Ca^{2+}]_i$ release in cardiomyocytes (Gema Ruiz-Hurtado 2012; Morel et al. 2005; Oestreich et al. 2009; Oestreich et al. 2007; Pereira et al. 2007; Pereira et al. 2012); it increases RyR phosphorylation through the activation of CaMKII that leads to SR Ca^{2+} leak (Pereira et al. 2017b; Pereira et al. 2007; Pereira et al. 2015); this SR Ca^{2+} leak is pro-arrhythmogenic (Gema Ruiz-Hurtado 2012; Hothi et al. 2008) and increases diastolic Ca^{2+} concentration (Pereira et al. 2012); these alterations of cytosolic Ca^{2+} with the activation of CaMKII can alter nuclear Ca^{2+} signaling (Pereira et al. 2012) and activate pro-hypertrophic Ca^{2+} signaling pathways (Metrich et al. 2010; Metrich et al. 2008; Morel et al. 2005; Pereira et al. 2015; Pereira et al. 2012).

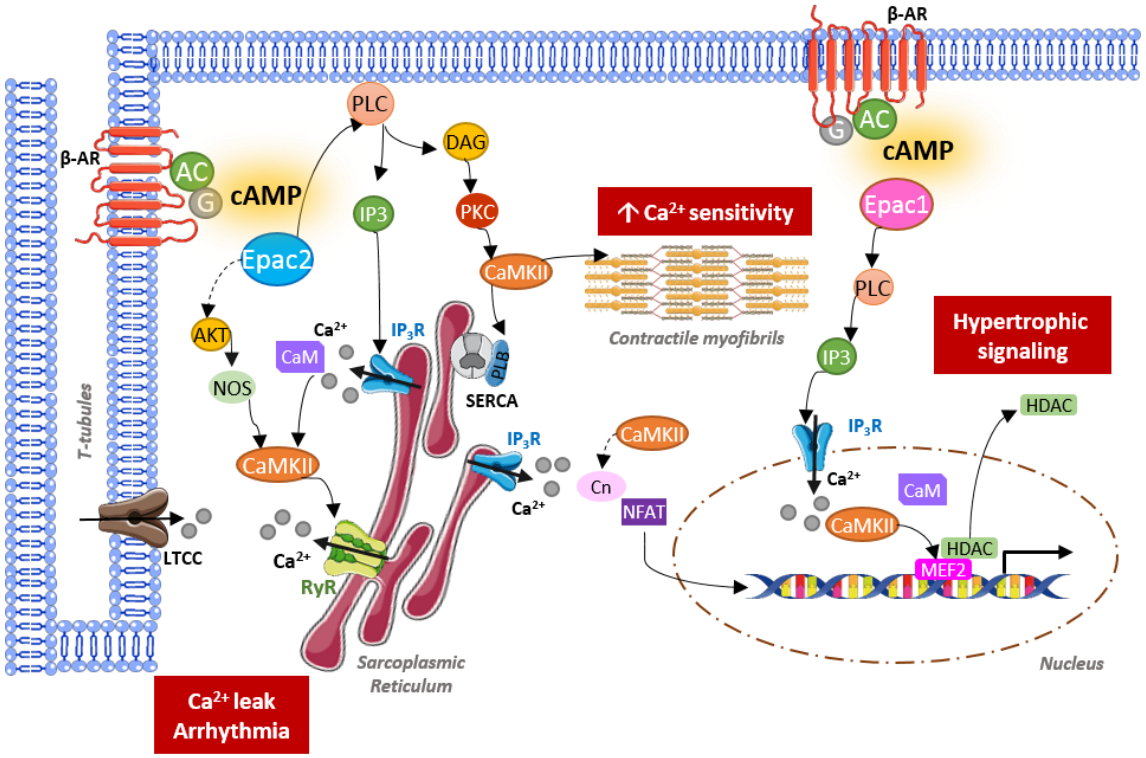

Figure 11: Epac signaling pathway in ventricular cardiomyocyte. Upon cAMP production, Epac2 activation at the T-tubules stimulates PLC with a subsequent activation of CaMKII *via* DAG/PKC and IP3/Ca^{2+}/CaM pathways. CaMKII phosphorylates myofilaments binding proteins increasing myofibrils Ca^{2+} sensitivity, PLB favouring Ca^{2+} reuptake in the sarcoplasmic reticulum (SR), and RyR leading to SR Ca^{2+} leak and subsequent arrhythmias. Epac2 also activates CaMKII by an AKT/NOS pathway participating in the SR Ca^{2+} leak. On the other hand, Epac1 activation at the perinuclear region induces IP3 production and subsequent pro-hypertrophic mechanisms involving CaMKII/MEF2 and subsequent HDAC nuclear export, and CaMKII/Cn/NFAT.

III. High glucose and ECC

1) Glucose and cardiac function

The heart is a non-stop working organ that requires a permanent energy supply. Fatty acids (FA) constitute the essential fuel utilized by adult healthy heart (70 %) while glucose constitutes 20 % and lactate the remaining 10 %. However the heart is characterized by a highly flexible energy metabolism, and can use either substrate depending on its plasma availability (Pascual and Coleman 2016). Insulin plays a major role in this metabolic

flexibility and favors glucose uptake and utilization, thus insulin and glucose disturbances affect cardiac metabolism with subsequent results on its activity (Bertrand et al. 2008).

Upon entering the cell, glucose is phosphorylated to glucose-6-phosphate, then metabolized to fructose-6-phosphate to undergo several metabolism pathways: glycolysis followed by the krebs cycle, neoglucogenesis, pentose phosphate pathway, the polyol pathway or the hexosamine biosynthesis pathway (Kolwicz and Tian 2011) (Figure 12).

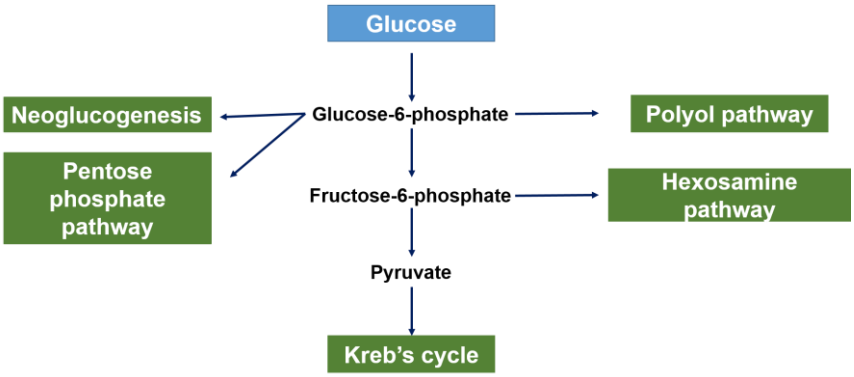

Figure 12: Glucose metabolism pathways, adapted from (Kolwicz and Tian 2011). Once in the cell, glucose is phosphorylated to glucose-6-phosphate, then metabolized to fructose-6-phosphate to undergo several metabolism pathways: glycolysis followed by the krebs cycle, neoglucogenesis, the pentose phosphate pathway, the polyol pathway or the hexosamine pathway.

Even though glucose is an essential cell nutrient, high glucose concentrations are harmful and cause tissue damage through five major mechanisms (Brahma, Pepin, and Wende 2017; Bugger and Abel 2014; Giacco and Brownlee 2010; Jia, Hill, and Sowers 2018; Singh et al. 2018) that are associated with oxidative stress and reactive oxygen species (ROS) production with a subsequent development of microvascular and cardiovascular complication through (Brownlee 2005; Giacco and Brownlee 2010):

1. Increasing flux of glucose and other sugars through the polyol pathway which is a reduction of carbonyl compounds to their respective sugar alcohols (polyol) using nicotinamide adenine dinucleotide phosphate (NADPH), a cofactor for ROS scavenger generation, subsequently exacerbating ROS production (Giacco and Brownlee 2010; Kolwicz and Tian 2011),

2. Increasing intracellular formation of advanced glycation end-products (AGEs) that are a non-enzymatic addition of a sugar moiety (fructose or glucose) to a protein leading to the formation of stable and irreversible AGEs compounds. AGEs formation is driven by oxidative stress and, in return, AGEs accelerate oxidation favouring their own formation and resulting in a vicious circle (Bodiga, Eda, and Bodiga 2014),
3. Increasing the expression of the receptor for advanced glycation end products (RAGEs) and its activating ligands,
4. Activation of PKC isoforms that are mainly involved in the vascular complications seen in diabetes (Geraldes and King 2010),
5. Upregulation of the hexosamine biosynthesis pathway that will be discussed in the following section.

The deleterious glucose effects have been widely associated with diabetes mellitus, a metabolic disorder with a chronic hyperglycemic state, which constitutes a major risk factor in cardiac diseases such as HF (Kannel and McGee 1979). Two major forms of diabetes are known and classified as diabetes type 1 with a deficiency of insulin secretion and diabetes type 2 with insulin resistance ('2. Classification and Diagnosis of Diabetes: Standards of Medical Care in Diabetes-2019' 2019). Even though diabetes is a multifactorial disease featuring inflammation, insulin resistance, hyperglycemia, lipotoxicity and others that can participate in cardiac dysfunction, hyperglycemia seems to play an important role in these disturbances (Bugger and Abel 2014), that have been highlighted on a clinical as well as on a fundamental bases.

2) Cardiac glucose toxicity

a. Clinical evidences of cardiac glucose toxicity

Clinical studies have highlighted a correlation between glycemic level and the prevalence of HF in diabetic patients (Elder et al. 2016; Erqou et al. 2013; Iribarren et al. 2001), pointing out the cardiac toxicity of high glucose. For instance, Irbarren *et al.* (Iribarren et al. 2001) have shown that 1% increase of glycated hemoglobin[4] (HbA1c), which is an indication that glucose levels have been maintained elevated, is associated with 8% rise of HF hospitalization in diabetic patients after excluding factors such as age, gender, race/ethnicity, education level, cigarette smoking, alcohol consumption, hypertension, obesity, medications, diabetes type and duration, and interim myocardial infarction. Furthermore, Montaigne *et al.* (Montaigne et al. 2014) found that *ex vivo* contractile dysfunction of atrial trabeculae is associated with mitochondrial dysfunction and related to HbA1c level regardless of insulin resistance or obesity in type 2 diabetic patients. These clinical data highlight the deleterious effects of high glucose on cardiac function seen in diabetes which could be in part explained by the high glucose-mediated disturbances on a cellular level.

b. Glucose and ECC

The deleterious effects of glucose on cardiac function could be related in part to ECC alterations, although few studies on direct high glucose effects on cardiac ECC have been conducted, with discordant results depending on glucose duration treatment and cell type.

Acute high glucose concentrations (30 mM) didn't affect Ca^{2+} transient in mice cardiomyocytes (Lu et al. 2020). However, a longer exposure, for instance of 48-72 hours to

[4] The average glycemic control over the past 2-3 months that accounts for both pre-prandial and post-prandial blood glucose levels.

high glucose concentration (25 mM), prolongs the Ca^{2+} transient duration by decreasing SERCA expression in neonatal rat cardiomyocytes (Clark et al. 2003). Ren *et al.* (Ren et al. 1997) have also observed an increase of the Ca^{2+} transient decay time, associated with an increase of the AP duration in adult rat cardiomyocytes treated 24 hours with high glucose concentration (25.5 mM). Furthermore, human induced pluripotent stem cells derived into cardiomyocytes (h-iPSC-CM) treated 7 days with high glucose concentrations (22 mM) show a decrease of the cell fractional shortening despite an increase of the Ca^{2+} transient amplitude (Ng et al. 2018).

Besides Ca^{2+} transient, high glucose exposure affects also the SR Ca^{2+} leak. Erickson *et al.* (Erickson et al. 2013) have shown that hyperglycemia increases the Ca^{2+} sparks frequency by activating CaMKII in adult rat cardiomyocytes with a subsequent arrhythmia propensity exacerbated under β-adrenergic stimulation of rats' hearts. Lu *et al*. (Lu et al. 2020) have also observed an increase of the Ca^{2+} sparks in mice cardiomyocytes as well as an increase of the spontaneous Ca^{2+} release events in h-iPSC-CM under high glucose (30 mM) which are CaMKII-dependent. This increase of the SR Ca^{2+} leak could be correlated with the findings of Federico *et al.* (Federico et al. 2017) where HEK293 cells treated with high glucose concentration (450 mg/dl = 25 mM) presented an increase of CaMKII-dependent RyR phosphorylation with an increase of the RyR activity.

These few *in vitro* studies have revealed some of high glucose-mediated alterations of ECC, notably an increase of the Ca^{2+} transient decay time which could participate in reduced cardiac relaxation observed in pathological model with a chronic exposure to high glucose such as diabetic type 1 animal models (Choi et al. 2002; Delucchi et al. 2012; Depre et al. 2000). Although diabetic type 2 animals also present an altered cardiac function (Belke, Swanson, and Dillmann 2004; Pereira et al. 2006), this model is characterized by other disturbances than hyperglycemia, such as insulin resistance, inflammation, and lipotoxicity

that could all participate in the cardiac alterations (Bugger and Abel 2014), making it more difficult to distinguish the implication of hyperglycemia in these cardiac alterations from the other causes.

Besides, the increase of the SR Ca^{2+} leak observed under high glucose exposure *in vitro* (Erickson et al. 2013; Lu et al. 2020) is also observed in some type 1 diabetic animal models (Yaras et al. 2007; Yaras et al. 2005) which could reduce overtime the SR Ca^{2+} store (Lacombe et al. 2007; LaRocca et al. 2012) and participate into the reduction of the Ca^{2+} transient amplitude (Delucchi et al. 2012; Kranstuber et al. 2012; Shao et al. 2007) and a subsequent reduction of the systolic function (Kranstuber et al. 2012; Lu et al. 2007; Shao et al. 2007).

3) Glucose and Epac2

Besides its role on the cardiac ECC, Epac2 plays a major role in glucose-mediated insulin secretion in the organism. Indeed, glucose induces the release of glucagon-like peptide (GLP-1) from the gastro-intestinal cells, which increases cAMP production in the β-pancreatic cells and subsequent insulin secretion. Epac2 participates in the GLP-1-mediated insulin secretion in several ways (Figure 13) as below:

- Targeting the RyR channels on the endoplasmic reticulum, increasing Ca^{2+} release necessary for insulin exocytosis (Kang, Chepurny, and Holz 2001; Kang et al. 2003),
- Inhibiting the K_{ATP} channels by interacting with their regulatory sulfonylurea receptor subunit (SUR1). The inhibition of the K_{ATP} depolarizes the cell membrane inducing voltage dependent calcium channel (VDCC) opening and a subsequent Ca^{2+} entry (Kang et al. 2006; Ozaki et al. 2000),

- Binding to several components of the exocytosis machinery, such as Rim2 and Piccolo localized at the cytosolic face of the insulin granules (Fujimoto et al. 2002; Ozaki et al. 2000).

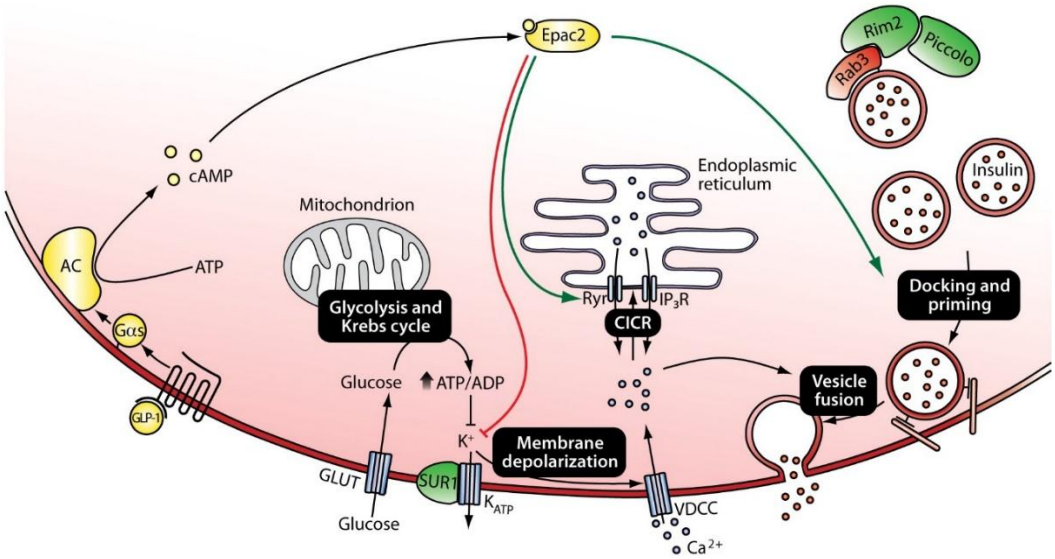

Figure 13: Role of Epac2 in insulin secretion, from (Gloerich and Bos 2010). Epac2 participates in the GLP-1-mediated insulin secretion by activating the endoplasmic reticulum RyR involved in Ca^{2+} release, inhibiting K_{ATP} channels, and interacting with Rim2, and Piccolo implicated in insulin granule secretion.

Since Epac2 participates in the GLP-1-mediated insulin secretion, pancreatic-specific Epac2-KO mice have been generated (Hwang et al. 2017; Shibasaki et al. 2007). The specific pancreatic β-cells Epac2-KO mice present a reduction of the glucose-induced insulin exocytosis (Shibasaki et al. 2007). These mice present a normal glucose and insulin sensitivity tolerance until 12 weeks of age (Hwang et al. 2017). However, they develop obesity under high-fat diet due to an impaired leptin signaling compared to their WT littermate (Hwang et al. 2017). Cardiac function was not assessed in these pancreatic β-cells KO mice to date. Therefore, it is important to take into consideration possible metabolic state modifications when generating constitutive Epac2-KO mice since Epac2 plays a critical role in glucose-mediated insulin secretion.

4) O-GlcNAcylation

a. Nutrient sensor

The hexosamine biosynthesis pathway (HBP) is, as mentioned above, one of the cellular metabolic pathways of glucose. The activation of the HBP results in a post translational modification of proteins by the addition of an N-acetylglucosamine (O-GlcNAc) moiety to serine and threonine residues resulting in a change in protein activity. In contrast to classical glycosylation process, O-GlcNAcylation affects nuclear as well as cytosolic proteins whereas glycosylated proteins are found in the cell membrane (Hart, Housley, and Slawson 2007). In addition, unlike extracellular complex glycans, which are static, O-GlcNAc rapidly cycles on and off proteins on a time scale similar to that of phosphorylation/dephosphorylation. However, protein phosphorylation involves a plethora of kinases and phosphatases, whereas O-GlcNAcylation is only regulated by 2 enzymes that we will discuss below (Slawson, Housley, and Hart 2006). It is now believed that there is a complex interplay between protein O-GlcNAcylation and phosphorylation, where both modifications can compete on the same serine or threonine of a protein regulating its activity (Leney et al. 2017; Zeidan and Hart 2010).

The HBP is constituted of four enzymatic reactions that convert fructose-6-phosphate to uridine diphosphate-N-acetylglucosamine (UDP-GlcNAc), the monosaccharide donor for O-GlcNAc protein modifications (Figure 14). The conversion of the fructose-6-phosphate to glucosamine-6-phosphate by L-glutamine-fructose-6-phosphate amidotransferase (GFAT) is the rate-limiting reaction of this process, with a concomitant conversion of glucosamine to glutamine then glutamate. The glucosamine-6-phosphate is then transformed by glucosamine-6-phosphate acetyl-transferase into N-acetylglucosamine-6-

phosphate, then to N-acetyleglucosamine-1-phosphate by a phosphoglucomutase. Finally, pyrophosphorylase catalyzes the conjugation of N-acetylglucosamine to a uridine nucleotide to generate UDP-GlcNAc, the donor for O-GlcNAcylation reaction. During this process, O-GlcNAc transferase (OGT) attaches O-GlcNAc moiety to serine and/or threonine residues of the protein; it's the protein O-GlcNAcylation. In contrast, β-N-acetylglucosaminidase (or 'O-GlcNAc-ase', OGA) removes O-GlcNAc residues (Hart, Housley, and Slawson 2007; Qin et al. 2017).

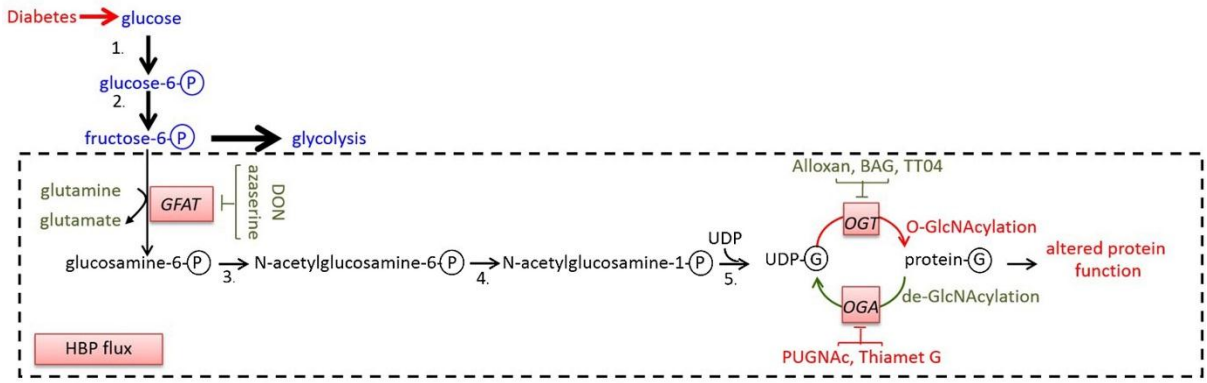

Figure 14: The hexosamine biosynthesis pathway, adapted from (Qin et al. 2017). Upon entering the cell, glucose is phosphorylated to glucose-6-phosphate, then metabolized to fructose-6-phosphate to undergo the HBP pathway. Fructose-6-phosphate is converted to glucosamine-6-phosphate by L-glutamine-fructose-6-phosphate amidotransferase (GFAT), the rate-limiting reaction of this process, with a concomitant conversion of glutamine to glutamate. The glucosamine-6-phosphate is then transformed by glucosamine-6-phosphate acetyl-transferase into N-acetylglucosamine-6-phosphate, then to N-acetyleglucosamine-1-phosphate by a phosphoglucomutase. Finally, pyrophosphorylase catalyzes the conjugation of N-acetylglucosamine to a uridine nucleotide to generate UDP-GlcNAc, the donor for O-GlcNAcylation reaction. During this process, O-GlcNAc transferase (OGT) attaches O-GlcNAc to serine and/or threonine residues of the protein altering their function. 1. hexokinase; 2. phospho-glucose-isomerase; 3. glucosamine-6-phosphate acetyltransferase; 4. N-acetylglucosamine-6-phospho mutase; 5. UDP-N-acetylglucosamine pyrophosphorylase.

The HBP flux does not only depend on glucose metabolism, but also on the glutamine amino acid availability, and can be modulated by the FA metabolism. Indeed, the increase of the FA oxidation, as seen in the diabetic heart, decreases glucose oxidation and favours glucose flux into the hexosamine or the polyol pathways (Hawkins et al. 1997). Besides substrate availability, O-GlcNAcylation seems to be modulated also by cellular stressors such as heat, ultraviolet radiation (Zachara et al. 2004) and superoxide (Du et al. 2000).

In adipocytes, it has been shown that HBP consumes 2–5% of cellular glucose under

physiological conditions (Marshall, Bacote, and Traxinger 1991). Recently, Olson *et al.* (Olson et al. 2020) have estimated the HBP in mice perfused heart under normal glucose concentration (5.5 mM) at approximately 2.5 nmol/g heart protein/min.

O-GlcNAcylation is now considered as a main important regulator of several physiological mechanisms such as gene transcription, circadian clock, protein migration, metabolism, and autophagy. Thus an alteration of the O-GlcNAcylation homeostasis is related to several pathological conditions such as cancer, Alzheimer's disease, glomerular sclerosis, retinopathy, insulin resistance, diabetes, cardiac hypertrophy, and ischemia. However the mechanism of chronic O-GlcNAcylation increase in these conditions is poorly understood and could be either a cause or a consequence of the disease state (Chatham, Zhang, and Wende 2020).

b. O-GlcNAcylation in cardiac pathologies: ECC alterations

Several studies are ongoing in order to decipher the growing role of O-GlcNacylation in the pathophysiology of cardiac diseases, where it can be protective or detrimental.

For instance, an acute increase of O-GlcNAcylation during ischemia-reperfusion is cardioprotective, with attenuation of Ca^{2+} overload, prevention of the loss of the mitochondrial membrane potential and prevention of the endoplasmic reticulum stress which participate in the ischemia-reperfusion injury (Jensen et al. 2019). O-GlcNacylation seems also to be implicated in cardiac hypertrophy. However, whether it is beneficial or detrimental for the hypertrophic heart, or if it plays a pro or anti-hypertrophic effect is still under debate (Mailleux et al. 2016).

Growing evidences about the role of O-GlcNacylation in ECC alteration, as seen in diabetes, have also been postulated. O-GlcNacylation targets several components of ECC notably SERCA, PLB affecting the Ca^{2+} transient duration, and CaMKII resulting in Ca^{2+} leak, which

both participate in high glucose-mediated ECC mishandling.

Clark *et al.* (Clark et al. 2003) have first reported that infection of neonatal rat ventricular cardiomyocytes with adenovirus encoding for OGA prevents the Ca^{2+} transient prolongation induced by 48-72 hours treatment with high glucose (25 mM) or with glucosamine (Clark et al. 2003). This effect was due to the O-GlcNacylation of the transcription factor specificity protein 1 (Sp1), with a subsequent downregulation of SERCA expression and activity (Clark et al. 2003; Fricovsky et al. 2012). PLB is also O-GlcNacylated at thr17 in rat cardiomyocytes treated with PUGNAC (an OGA inhibitor), with a concomitant reduction of its phosphorylation state at Ser16. Thus PLB O-GlcNacylation by high glucose inhibits its phosphorylation promoting his interaction with SERCA with a subsequent prolongation of Ca^{2+} transient (Yokoe et al. 2010).

CaMKII is also an O-GlcNacylation target. Erickson *et al.* (Erickson et al. 2013) have shown that CaMKII O-GlcNacylation in rat cardiomyocytes treated 24 hours with high glucose (500 mg/dl) is associated with an increase of the Ca^{2+} sparks frequency, prevented either by CaMKII or O-GlcNacylation inhibition. This spontaneous Ca^{2+} release contributes to ventricular arrhythmia generation in isolated rat hearts perfused with high glucose (Erickson et al. 2013). This is correlated with an increase of CaMKII O-GlcNacylation observed in diabetic rats and human hearts samples (Erickson et al. 2013).

Studies have also shown that O-GlcNacylation affects cardiac electrical activity through membrane channels. Indeed, Nav1.5 O-GlcNacylation in neonatal rat ventricular cardiomyocytes treated 48 hours with high glucose reduces its interaction with Nav1.5-binding proteins resulting in a decrease of its incorporation into the cytoplasmic membrane (Yu et al. 2018) and a subsequent reduction of Nav1.5 current density prevented by DON (GFAT inhibitor). The abnormal distribution and loss of function of Nav1.5 induced by hyperglycemia can explain in part the observed increase of susceptibility to ventricular

arrhythmias in diabetic type 1 rats after phenylephrine application (Yu et al. 2018).

The aforementioned O-GlcNacylation alterations of ECC and cardiac electrical activity participate in the high glucose/diabetes-related cardiac function reduction *in vivo* where O-GlcNAcylation is upregulated in diabetic type 1 (Akimoto et al. 2000; Kronlage et al. 2019; De Blasio et al. 2020; Hu et al. 2005) and type 2 (Fricovsky et al. 2012; Fülöp et al. 2007; Kronlage et al. 2019) animals. For instance, OGA overexpression prevents cardiac fractional shortening reduction in diabetic type 2 mice (Fricovsky et al. 2012) and improves diastolic function of perfused diabetic mice heart (Hu et al. 2005). This protective effect is associated with improvement of the cardiomyocytes' contractility (Hu et al. 2005). Furthermore, removal of O-GlcNac residues from diabetic type 1 rats myofilaments restores Ca^{2+} sensitivity of cardiac muscle (Ramirez-Correa et al. 2015).

These *in vitro* and *in vivo* evidences prove the growing role of O-GlcNacylation in affecting ECC and cardiac function.

Recently, it has been reported that in retinal cells, angiotensin 1-7 increases cAMP production which inhibits OGT activity with a subsequent reduction of O-GlcNacylation levels in an Epac and not PKA-dependent manner (Dierschke et al. 2020). This paper (Dierschke et al. 2020) shows a possible interaction between Epac and O-GlcNac in retinal cells, however not reported to date in the heart.

Objectives

Objectives

My thesis work has two main objectives:1) to study the role of Epac2 in high glucose-mediated cardiac Ca^{2+} mishandling and 2) to determine the Ca^{2+} signalling in Epac2 cardio-specific KO mice.

Part 1

High glucose induces cardiac Ca^{2+} mishandling by activating CaMKII, a downstream effector of Epac2 (Erickson et al. 2013), that is a key regulator of cardiac Ca^{2+} homeostasis. The inhibition of CaMKII or its genetic deletion prevented high glucose-mediated SR Ca^{2+} leak in rat ventricular cardiomyocytes and β-adrenergic-dependent cardiac arrhythmias, but can't reveal the role of Epac2 in this mechanism.

Thus my first objective was to study the implication of Epac2 in high glucose-mediated Ca^{2+} mishandling, deciphering a new mechanism of high glucose-dependent ECC alteration. Using selective pharmacological inhibitor of Epac2 and genetic deletion of Epac2 approaches, we studied *in vitro* the effect of high glucose on Ca^{2+} homeostasis, notably SR Ca^{2+} leak, in mice adult cardiomyocytes.

The second objective was to decipher the possible activation mechanism of Epac2 under high glucose concentration. O-GlcNacylation is a post-translational modification of proteins that modify their activity which is upregulated under high glucose concentration (Chatham, Zhang, and Wende 2020). Since Epac2 is a multidomain protein with several serine and threonine residue that could potentially undergo O-GlcNacylation (Rehmann et al. 2008; Rehmann et al. 2006), and since O-GlcNacylation is reported to participate in the high glucose-mediated Ca^{2+} alterations (Erickson et al. 2013), we postulated that O-GlcNacylation might activate Epac2 under high glucose to mediate SR Ca^{2+} leak.

Finally, to study the relevance of this mechanism in human, we used human induced

pluripotent stem cells derived into cardiomyoctes (h-iPSC-CM) treated acutely and chronically with high glucose concentration. We assess the effects of high glucose treatments on Ca^{2+} homeostasis in these cells and the possible role of Epac2 in this mechanism.

Part 2

The second part of my thesis was to characterize the ECC-Ca^{2+} dynamics of a newly generated cardio-specific Epac2-KO mice provided by Dr. Franck Lezoulc'h (Inserm UMR-1048, Institut des Maladies Métaboliques et Cardiovasculaires, Université Toulouse III). These mice have been generated by the excision of the exon 17 by the Cre-Lox technique under the control of cardiac specific promotor of the α-Myosin Heavy-Chain.

Even though constitutive (Pereira et al. 2013; Pereira et al. 2015) and pancreatic-specific Epac2-KO (Hwang et al. 2017; Shibasaki et al. 2007) mice have already been generated and documented, no studies have been performed so far on cardio-specific ones. Epac2 is a widely expressed protein in the organism and thus generation of cardio-specific Epac2-KO mice is interesting in order to avoid possible side effects or compensation mechanisms of constitutive Epac2-KO model in studying Epac2 role in cardiac diseases.

Material and methods

Material and methods

I. Animal and cellular model

In this project, we aimed to study the role of Epac2 in high glucose-mediated cardiac Ca^{2+} mishandling. To do so, we first used cardiomyocytes freshly isolated from control mice treated with Epac2 pharmacological inhibitor under different glucose concentrations. To overpass the possible off-target effects of pharmacological tools, we also used transgenic mice with constitutive Epac2 deletion. However, mice and human present several differences in cardiac function and feature. For example, the mice heart rate is approximately 10-fold higher (around 600 beats per minute (bpm)), than in humans (around 70 bpm). This implicates shorter action potentials, and different ionic current regulating cardiac electrical activity (Bassani, Bassani, and Bers 1994; Blechschmidt et al. 2008).

We also choose to work with human induced pluripotent stem cells derived into cardiomyocytes (h-iPSC-CM) since they are derived from human and present a novel model in studying cardiac diseases (Yoshida and Yamanaka 2017). We investigated the effect of acute and chronic high glucose treatments in the presence, or the absence of a pharmacological inhibitor of Epac2. However, this model presents some limitations, notably the immature development stage with a neonatal ventricular cardiomyocytes-like shape, a spontaneous beating activity, no or few T-tubules, even though the cells express the key structural and functional cardiomyocyte genes (Karakikes et al. 2015).

1) Murine model

a. C57Bl6

C57Bl6 strain mice from 8 to 12 weeks old were purchased from Janvier lab and used for experiments. Mice were used to study, *in vitro*, the effect of glucose on cardiac Ca^{2+} signaling and the possible role of Epac2 in this mechanism by using its pharmacological inhibitor. Then, we used transgenic Epac2 Knocked out (KO) mice, as described below, to overpass potential side effects of the pharmacological tools used in our experiments (cf. II.1).

b. Epac2 constitutive KO mice

The Epac2-KO transgenic mice were generously provided by Dr. Ju CHEN, University of California, San Diego. These mice have been generated by the deletion of the exon 7 of the Epac2 gene (Figure 15). Exon 7 was flanked by two loxP sites. These constitutive Epac2 KO mice were used at the age of 12 weeks for our experiments. The deletion of Epac2 does not affect the cardiac function nor the basal Ca^{2+} signaling (Pereira et al. 2013).

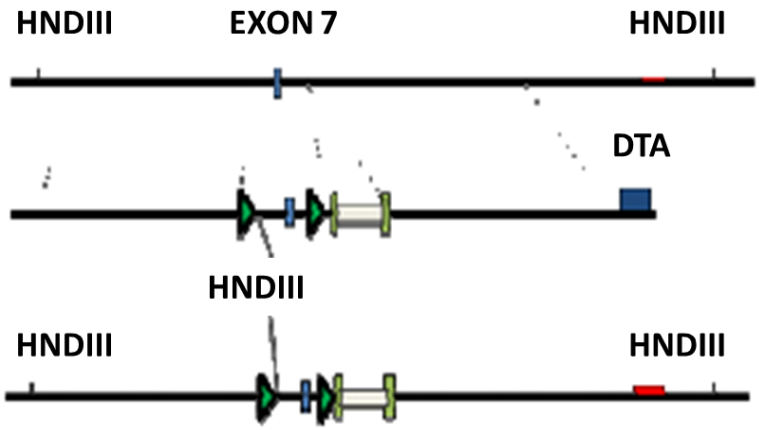

Figure 15: Generation of Epac2 KO mice, adapted from (Pereira et al. 2013). Exons 7 (blue rectangle) was flanked by two LoxP sites (triangle). A neomycin cassette (grey rectangle) flanked by two Frt sites (open rectangle) was inserted into intron 5. A DNA probe (red rectangle) upstream of the 5' arm was used as a probe for Southern blot analysis. A DTA (diphtheria toxin; black rectangle) cassette was used to assist in correct recombination.

c. Epac2 cardio-specific KO mice

Cardio-specific Epac2-KO mice were generated using a Mer-Cre-Mer-LoxP system. Exon 17, located in the catalytic domain at the REM, was flanked on both sides by LoxP sites, leading to a codon stop which ends the transcription. Cre is fused to the mutated oestrogen receptor binding domain making it insensitive to endogenous oestrogen, but can recognize a synthetic ligand for this receptor, tamoxifen. This Cre-receptor complex is under the control of the specific cardiac promoter α-Myosin Heavy-Chain (α-MHC), limiting its expression to cardiomyocytes, and is called α-MHC MerCreMer.

In the absence of ligand, the oestrogen receptor is sequestered in the inactive state by Heat Shock Protein 90 (HSP 90) in the cytoplasm. Following the injection of tamoxifen, a change in conformation releases the α-MHC MerCreMer fusion protein and allows its translocation to the nucleus. Cre can then excise exon 17 at the LoxP sites, thus allowing the generation of the KO model for Epac2 in a cardiac-specific and inducible manner.

The Epac2-KO mice were generated by crossing two lines of C57BL/6J genetic background: homozygous mice carrying the floxed gene of Epac2 (EPAC2flox / flox line) and mice heterozygous for the gene encoding the α-MHC MerCreMer fusion protein (α-MHC-MerCreMer line). The animals resulting from this cross, heterozygous for the floxed gene, were crossed with each other in order to obtain a line homozygous for Epac2 flox. Males expressing both floxed exon 17 and Cre recombinase were selected by genotyping. Their brothers expressing the floxed gene but not the Cre were used as controls.

2) Human induced pluripotent stem cells derived into cardiomocytes (h-iPSC-CM)

Induced pluripotent stem cells (iPSCs) were first reported in 2006 (Takahashi and Yamanaka 2006), but the principle of cell reprogramming have been described long before. Stem cells are defined as cells with self-renewal and multiple differentiation abilities (Wu et al. 2020). Two keys steps have preceded the establishment of iPSC: the first principle is that nuclei of somatic cells can be reprogrammed into pluripotent stem state. Indeed, in 1958 Gurdon *et al.* (Gurdon, Elsdale, and Fischberg 1958) produced a cloned frog by injecting the nucleus of somatic cells from a Xenopus tadpole into an enucleated oocyte. The second principle is that each cell type has its own master regulator genes, which specifically work to maintain the cellular identity, where skeletal fibroblast mice cells have been differentiated for the first time into skeletal muscle by the expression of a single gene, MyoD (Davis, Weintraub, and Lassar 1987). Taking these into consideration, Takahashi *et al.* (Takahashi and Yamanaka 2006) have established mouse iPSCs by retrovirally introducing into mouse fibroblasts 4 transcription factors (c-Myc, Oct3/4, Sox2, and Klf4) that lead to reprogramming somatic cells into pluripotency. Then, in 2001, Kehat *et al*. (Kehat et al. 2001) have generated cardiac myocytes from stem cells. Since then studies have multiplied in order to optimize cell differentiation efficiency.

In our study, h-iPSC were obtained from a Spanish family healthy donor's blood cells (Domingo et al. 2015). The de-differentiation of blood cells to h-iPSC was performed in the iPSC platform of Nantes, France. The h-iPSC culture and differentiation into cardiomyocytes had been carried out by the engineer of the team, Dr Pascale GERBAUD, using the protocol described below (Figure 16).

a. h-iPSC culture

Once rapidly defrosted, the h-iPSCs were transferred to a falcon tube and mTesR™ (STEMCELL) culture medium supplemented with Rho-Associated Coil Kinase (ROCK) inhibitor Y27632 (5 μM) (to increase h-iPSC survival). mTeSR™ is a highly defined, feeder-free medium suitable for h-iPSCs. It contains only the most critical components required for iPSCs culture (Chen et al. 2011). The h-iPSCs were then seeded on plates previously coated with Matrigel hESC-qualified Matrix (Corning 354277), which is a gelatinous protein mixture secreted by Engelbreth-Holm-Swarm (EHS) mouse sarcoma cells resembling the complex extracellular environment needed for cell culture. Aliquots of Matrigel were diluted in Dulbecco's Modified Eagle Medium/Nutrient Mixture F-12 (DMEM/F12 medium, ThermoFisher). It is a 1:1 mixture of DMEM and Ham's F-12 combining DMEM's high concentrations of glucose, amino acids, and vitamins with F-12's wide variety of components such as zinc, putrescine, hypoxanthine, and thymid, all needed for cell culture and growth.

b. h-iPSC passage

The passage was done when the cells grew into 80% confluence. The medium was completely removed and cells rinsed once with phosphate-buffered saline (PBS). 1 mL of passage PBS + EDTA (Ethylenediaminetetraacetic acid, FisherScientific, 11599686) was added to each well to separate cells clusters. EDTA is a chelating agent that sequesters metal ions such as Ca^{2+} and Fe^{3+}. Ca^{2+} is necessary for h-iPSCs adhesion to the bottom of well, thus when removed, h-iPSCs detached into clusters. Then, the small clusters were diluted in mTeSR™ culture medium and seeded on new plates. The plates were homogenized and incubated at 37°C, 5% CO_2 overnight. The medium was changed every day until the next

passage.

c. h-iPSC differentiation into cardiomyocytes

When h-iPSCs are at 80% confluence, they can be used to launch the differentiation protocol. The medium was completely removed and cells washed once with PBS. Then, the accutase enzyme (StemPRO accutase, Gibco ThermoFisher, 11568896) was added 5 minutes at 37°C to dissociate h-iPSCs along with 10 µM ROCK inhibitor Y27632 2HCl (Euromedex, S1049) to protect single cells from damage. Accutase was then discarded after centrifugation (200 g, 5 minutes) and the pellet suspended in mTesR^{TM} medium with Y27632. The cell density was counted on Mallasez chamber. Cells were then seeded on plates with a density between 100,000 and 200,000 cells/cm² in order to form an adequate monolayer for differentiation. The plates were then incubated at 37°C, 5% CO_2, which counted as Day (-2). Then following the protocol shown in (Figure 16), the medium was changed every 48 hours. Several components were added or removed depending on the differentiation stage. We first activated the Wnt pathway by 6 µM GSK3β inhibitor (CHIR9902, Euromedex, S1263) to induce meso-endodermal/mesodermal differentiation. Then, this pathway was inhibited by 5 µM IWP2 (Euromedex, S7085) to promote the cardiac/cardiomyocyte phenotype formation. We later added insulin to the medium which promotes cell survival and proliferation. It is to note that medium choice is detrimental for cell growth and viability, that's why we chose the RPMI 1640 (Fisher Scientific, 12004997) + B27 Medium (Fisher Scientific, 15285074). This medium contains the reducing agent glutathione and high concentrations of vitamins (such as biotin, vitamin B_{12}, inositol, choline) suitable for cell culture and growth. Between day 5 and day 7, cells start to spontaneously beat.

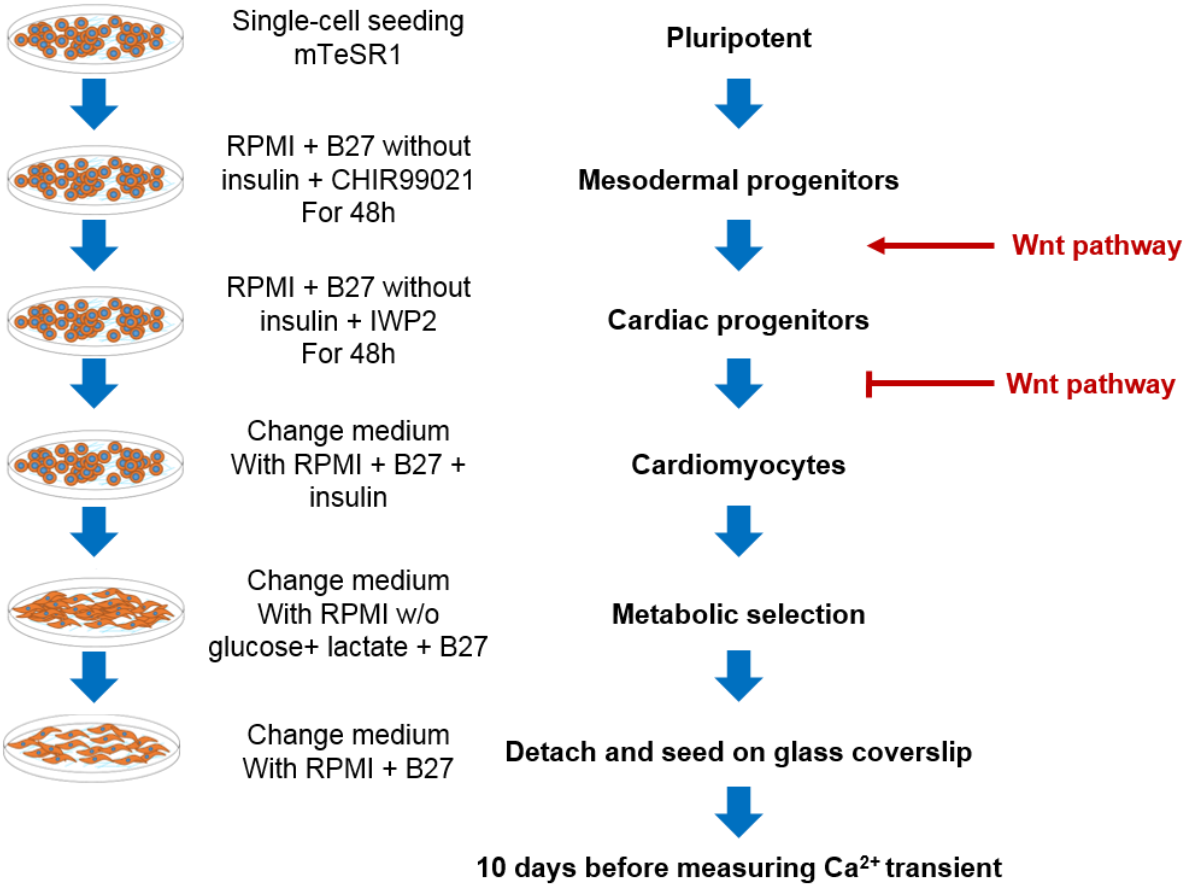

Figure 16: Schematic representation of the h-iPSCs differentiation protocol into cardiomyocytes.

d. h-iPSC-CM for experiments

On day 18, h-iPSC-CM were detached and seeded either on ibidi (Ibiditreat, 81176) dishes with small chambers for Ca^{2+} measurement and immunofluorescence labelling, or on plates for RNA extraction.

Culture medium was discarded and h-iPSC-CM were rinsed once with PBS. Cells were incubated 5 minutes at 37°C with TrypLE enzyme (Fisher Scientific, 11528856) twice which detaches and dissociates cells. TrypLE was then removed by centrifugation and the pellet resuspended in RPMI 1640 with B27. The medium was changed regularly until experiments were conducted at day 31 ± 1 day.

II. Pharmacological tools

1) Epac agonists/antagonists

Several pharmacological compounds have been developed to study Epac signaling. cAMP can activate both PKA and Epac and thus scientists tend to develop cAMP-like molecules selectively activating Epac rather than PKA. Epac proteins lack the glutamate residue required for PKA and HCN channels interaction with the 2' OH group of the cAMP ribose (Enserink et al. 2002). Thus cAMP analogs with a replacement of this 2'OH residue by an O-methyl residue on the ribose present a selectivity toward Epac proteins, such as 8-(4-chloro-phenylthio)-2'-O-methyladenosine-3',5'-cyclic monophosphate (8-CPT, or 8pCPT or 007) (Enserink et al. 2002). 8-CPT activates Epac with a constant of dissociation[5] (K_d) of 2.9 µM compared with 45 µM for cAMP (Rehmann, Schwede, et al. 2003). Although 8-CPT is 100-fold more effective in activating Epac1 than cAMP, it is a weaker agonist of Epac2 compared to cAMP (Courilleau et al. 2013). Later, Schwede *et al.* (Schwede et al. 2015) have characterised a cAMP analog, the Sp-8-BnT-cAMPS, with a benzyl group that activates Epac2 rather than Epac1, though with a slight activation of PKA. In our project, we used 8-pCPT at 10 µM (Sigma Aldrich, C8988) which is higher than the K_d value and thus ensure an activation of Epac.

Selective Epac antagonists have also been developed. ESI-05 and ESI-07 (Tsalkova et al. 2012) are 2 antagonists that preferentially inhibit Epac2 GEF activity with respectively 0.43 and 0.7 µM IC50[6] values. They bind allosterically to the interface formed by the 2 CNBD in Epac2 and stabilize Epac2 in its auto-inhibitory conformation (Chen et al. 2013; Tsalkova et

[5] K_d is the constant of dissociation of a ligand for its target. It's a pharmacological term that reflects the binding affinity of a ligand for its target. The smaller the K_d value, the greater the binding affinity of the ligand for its target.

[6] IC50 is the half maximal inhibitory concentration which is a measure of the needed concentration of a substance to inhibit 50% of a biological process. It reflects the potency of an inhibitor.

al. 2012). Since Epac1 presents only 1 CNBD residue, ESI-05 and ESI-07 inhibit preferentially Epac2. In our study we used ESI-05 (Sigma Aldrich, SML1907) at a concentration of 10 µM to pharmacologically inhibit Epac2 effects (Dominguez-Rodriguez et al. 2015).

2) O-GlcNacylation pharmacological tools

We assessed O-GlcNacylation levels in our preparations by using activators or inhibitors of this pathway. The 6-diazo-5-oxonorleucine (DON) was used to inhibit the O-GlcNacylation pathway. DON is an analogue of L-glutamine that irreversibly inhibits amido-transferases, such as GFAT, reducing glucose metabolism by the HBP, and thus protein O-GlcNAcylation modification. However, DON is not specific to GFAT and can also inhibit other amido-transferases and possess anti-neoplastic properties *in vivo* (Catane et al. 1979). In our study, we used DON (Sigma Aldrich, D2141) at 50 µM to inhibit GFAT (Erickson et al. 2013).

We used OGA inhibitor, the O-(2-acetamido-2-deoxy-d-glucopyranoseylidene) amino N-phenyl carbamate (PUGNAC) to inhibit O-GlcNac residues removal (Haltiwanger, Grove, and Philipsberg 1998), at a concentration of 10 µM (Sigma Aldrich, A7229). However, PUGNAC can also inhibit other hexoaminidases and is not specific to OGA (Macauley and Vocadlo 2010; Whitworth et al. 2007).

III. Ventricular cell isolation

1) Principle

The ventricular cell isolation was used to study cardiac Ca^{2+} signaling at the cellular level with no interaction with the extracellular matrix and the adjacent cells.

We used the Langendorff retrograde perfusion at 37°C with fixed pressure (around 60 cm of a perfusion column) to isolate the cardiomyocytes by enzymatic dissociation. This technique allows performing a retrograde perfusion of the heart down to the aorta, opposite to the normal physiologic flow. The closure of the aorta under pressure allows a perfusion through the coronary circulation and not through the ventricle chambers (Powell, Terrar, and Twist 1980). This technique is commonly used for over 100 years in the heart physiology studies such as contractile function, coronary blood flow regulation, cardiac metabolism and pathophysiology of ischemia/reperfusion (Bell, Mocanu, and Yellon 2011).

The ventricular cell isolation is performed as follow. First, the beating heart is removed out of the mice and placed in a cooled physiological solution (Table 2) deprived of Ca^{2+} to stop metabolic reactions and cardiac contractions. The heart was weighed and the aorta cannulated under the binocular microscope without perforating the aortic valve. The heart was then transferred to the Langendorff apparatus and blood washed away for few minutes with a physiological solution deprived of Ca^{2+} to avoid cardiac contraction (Table 1). Then, the extracellular matrix is digested by an enzymatic perfusion solution deprived of Ca^{2+} to help disrupt cellular junctions (Gopal, Multhaupt, and Couchman 2020; Maurer and Hohenester 1997) and isolate cardiomyocytes. The digestion time is estimated by the sudden increase in effluent flow reflecting the digestion of the aortic valve. At this point, the heart is removed and undergoes mechanical digestion with gentle scissors cuts. The cardiomyocytes are then suspended in a physiological solution with gradual increase of Ca^{2+} concentration (Table 2). This step is necessary to avoid the Ca^{2+} paradox damage. Indeed, when the heart is infused with the solution without Ca^{2+} (Table 2), the NCX extrudes the cytosolic Ca^{2+} for the entry of Na^{+}. However, when the cells that were deprived form Ca^{2+} are suddenly suspended in Ca^{2+}-containing solutions (Table 2), the NCX operates in reverse mode. This results in a massive entry of Ca^{2+} and an extrusion of Na^{+}, which can cause cell death. Thus it is important to

gradually increase the Ca^{2+} concentration to avoid Ca^{2+} overload in the cell. Bovine serum albumin (BSA) is added to the solution when the digestion is over in order to neutralize the digesting enzyme activity. Finally, the cardiomyocytes are kept in 1 mM Ca^{2+} solution at room temperature for experimental usage.

2) Protocol

Mice were anesthetized by intraperitoneal injection of sodium pentobarbital at 100 mg/kg. The absence of any motor reflexes proves the effectiveness of the anesthesia. The mice were then attached in dorsal decubitus position. After removing the skin, we performed a thoracotomy by lateral incision of the right and left costal grids. The beating heart was removed and placed in solution I, previously cooled at -20^{o}C for 10 minutes (Table 2). The heart was then canulated by its aorta and transferred to the Langendorff apparatus at 37^{o}C. The heart was washed for 2-4 minutes with solution I, then perfused by the solution II containing the Liberase enzyme (Roche®, 0540011271001) for 8 to 10 minutes. When digestion is finished, the heart was removed and placed in solution III. The aorta and atrium were discarded, the 2 ventricles separated and finely cut with scissors. The suspension was then filtered through a nylon filter (mesh diameter = 250 µm) and decanted for 10 minutes. The cell pellet is re-suspended in solution IV (0.5 mM Ca^{2+}) for 10 minutes and finally in solution V (1 mM Ca^{2+}). Once isolated, the cells are kept at room temperature (23^{o}C) for later experiments.

3) Cardiomyocytes isolation solutions

Solution I

Product	Concentration (mM)
NaCl	113
KCl	4,7
$MgSO_4$	1,2
KH_2PO_4	0,6
NaH_2PO_4	0,6
$NaHCO_3$	1,6
HEPES	10
Taurine	30
Glucose	20
pH=7,4 with NaOH (10 and 1 N)	

Table 1: Composition of the cardiomyocytes isolation solution I

Solution I to V

Then we prepared the following solutions from the solution I

Solution I (washing)	See Table 1
Solution II (enzymatic digestion)	Solution I Liberase 0.083 mg/ml
Solution III (enzyme neutralizing and Ca^{2+} increase)	Solution I [Ca^{2+}] 0.2 mM BSA 5 mg/ml
Solution IV (enzyme neutralizing and Ca^{2+} increase)	Solution I [Ca^{2+}] 0.5 mM BSA 5 mg/ml
Solution V (Ca^{2+} increase)	[Ca^{2+}] 1 mM

Table 2: Composition of the cardiomyocytes isolation solution II to V

Liberase enzyme

The Liberase (Roche®, cat # 0540011271001) was suspended in MilliQ water to obtain a final stock solution of 5 mg/ml. Aliquots of 250 µl were then made and stored at -20°C. For

heart's digestion, the liberase was used at a final concentration of 0.083 mg/ml (i.e. 250 µl in 15 ml solution II).

IV. Fluorescence techniques

We used three different fluorescent techniques in this project. First, we assessed Ca^{2+} signaling in adult ventricular cardiomyocytes and in h-iPSC-CM using confocal microscopy. We also perform h-iPSC-CM immunofluorescence as a routine control by confocal microscopy. Finally, we measured Epac activation state using the Förster (or fluorescence) resonance energy transfer (FRET) technique.

1) Fluorescence principle

Fluorescence is the light emission from fluorophores that have the property to absorb and emit energy in the form of photons as shown in the Jablonski diagram (Figure 17). This process includes 3 phases. First, the excitation phase, when the photon energy dispensed by a light energy source (such as a laser or a lamp) is absorbed by the fluorophore. Thus the electron of the fluorophore goes from its ground state to an excited electronic state (Phase 1, Figure 17-1). Once excited, the electron interacts with its environment and dissipates part of its energy; it's the energy dissipation phase (Phase 2, Figure 17-2). The electron then returns to its ground level by emitting photons with lower energy than that absorbed (and therefore of longer wavelength), known as the the emission phase (Phase 3, Figure 17-3).

Thereby the emitted fluorescence can be distinguished from the excitation light since they have different wavelengths, which is crucial to avoid signal overlap between the excitation energy and the emitted one.

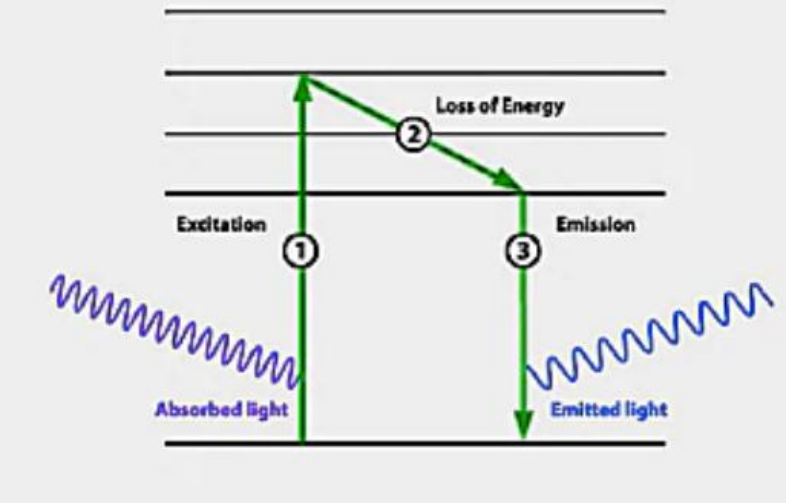

Figure 17: Jablonski diagram, adapted from www.thermofisher.com. This figure presents the process of excitation/emission of a fluorophore: 1) the excitation phase, 2) the energy dissipation phase, 3) the emission phase.

2) Confocal microscopy

a. Principle

Confocal microscopy is an imaging technique used to obtain optical sections of a given sample. It requires the use of a fluorescent probe excited by a light source, a laser. The energy of the light source is absorbed by the fluorescent probe (excitation phase) that emits photons of less energy than the one absorbed (emission phase). This photon emission is transmitted to the detector by the dichroic mirror (beam splitter). The diaphragm (confocal pinhole), placed in front of the detector, blocks the fluorescence emitted out of focus which considerably improves the images resolution by avoiding contamination by fluorescence outside the focal plane. The selected wavelength is detected by the system and transformed into an image, produced by the point-by-point scanning of the sample by the laser (Figure 18).

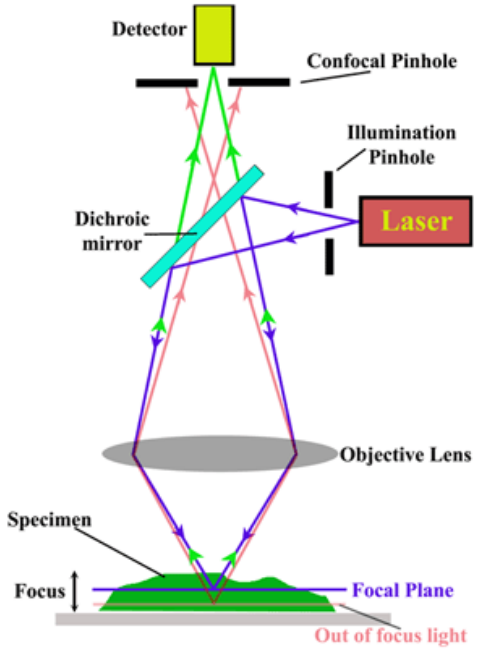

Figure 18: Principle of confocal microscopy. The laser of the light source passes through the specimen (sample) and stimulates the fluorophore which in turn emits fluorescence radiation in another wavelength. This photon emission is transmitted to the detector by the dichroic mirror. The confocal pinhole, placed in front of the detector, blocks the fluorescence emitted out of focus which considerably improves the images resolution by avoiding any contamination by fluorescence outside the focal plane.

b. Ca^{2+} signaling study protocol

Ca^{2+} fluorescent loading

Once isolated, the adult ventricular cells were incubated in a Tyrode solution (Table 3) with normal glucose concentration of 100 mg/dl (1 hour at room temperature).

Product	Concentration (mM)
NaCl	140
KCl	4
$MgCl_2$	1.1
$CaCl_2$	1.8
HEPES	10
pH=7.4 with NaOH (10 and 1 N)	

Table 3: Tyrode solution composition

Then, the cells were pre-incubated and loaded for 30 minutes with a fluorescent Ca^{2+} probe. For the mice ventricular cardiomyocytes, Fluo-4 AM (Invitrogen, F14201) was used in the

dark and diluted in pluronic DMSO (Biotium, 59004), at a final concentration of 5 µM. Fluo-4 AM has an acetyl-methyl ester (AM) which allows it to enter the cell. Fluo-4 AM is then degraded by esterases and the active form released. Once Fluo-4 AM binds to Ca^{2+}, its fluorescence increases over 100 times, which significantly increases sensitivity without causing cellular damage or significant auto-fluorescence phenomena. The Fluo-4 AM has an excitation wavelength of 488-500 nm in the visible spectrum and emits at 526 nm.

h-iPSC-CM were loaded with Calbryte™ 520 AM (AAT Bioquest, 20651) instead of Fluo-4 AM. Indeed, once seeded on ibidi dishes, h-iPSC-CM present a tissue-like shape that requires a higher concentration of Fluo-4 AM for loading to be able to get enough signal. However, we found that higher Fluo-4 AM concentrations alter cell shape and viability. That's why we shifted to Calbryte™ 520 AM that had good fluorescence signal without altering the cells. As Fluo-4 AM, the lipophilic blocking groups of Calbryte™ 520 AM are cleaved by esterases once inside the cell. It gives a negatively charged fluorescent dye that stays inside the cells, which fluorescence greatly increases upon binding to Ca^{2+}. The h-iPSC-CM were used for Ca^{2+} handling study at 31±1 days after differentiation. They were loaded by 10 µM of Calbryte™ 520 in pluronic DMSO for 1 hour at 37°C followed by 15 minutes at room temperature. The Calbryte™ 520 has an excitation wavelength of 493 nm in the visible spectrum and emits at 515 nm.

The ventricular mice cardiomyocytes loaded with the Fluo-4 AM and the h-iPSC-CM loaded with Calbryte™ 520 were scanned with the white light laser (λex = 500 nm) along a longitudinal axis, point by point to build a two-dimensional image (xt). The emission of these fluorophores was detected by emission filters which collect a wavelength greater than 510 nm. The Ca^{2+} signaling recordings were produced using the confocal Leica® TCS SP5X microscope, Solms, Germany, and were analyzed by an IDL 8.6 (Interactive Data Language) by homemade routine programs.

Ca^{2+} signaling measurements

Ca^{2+} transient

Ca^{2+} transients in mice ventricular cardiomyocytes were obtained under electric field stimulation at 1 Hz with platinum electrodes. The loaded cell with Fluo-4 AM were scanned along the longitudinal axis with the white light laser (Objective x40 with water immersion) at a 400 Hz frequency (Figure 19-A). The obtained line-scan image shows the fluorescence modification over time that reflects cytosolic Ca^{2+} concentration (Figure 19-B). For the h-iPSC-CM Ca^{2+} transient measurements, a two-dimension recording mode at 1000 Hz (bidirectional, format 512x250, 250 frames) was done. Then we performed a line scan at 700 Hz (zoom=2.5, 5000 lines). The recordings were conducted on spontaneously beating cells (without field stimulation).

Ca^{2+} sparks and Ca^{2+} waves

Ca^{2+} leak in diastole is observed as Ca^{2+} sparks which correspond to a spontaneous and brief local elevation of the cytosolic Ca^{2+} concentration (Stern 1992). This release reflects a spontaneous opening of a RyR cluster. Ca^{2+} sparks were measured in quiescent mice cardiomyocytes previously loaded with Fluo-4 AM and electrically paced (Objective x40 with water immersion, zoom=4, scanning frequency at 700 Hz). The frequency of sparks is reported as the number of sparks observed in 100 µm of cell per second. Sparks are normally sporadic and isolated. However, when Ca^{2+} release is significant from a RyR cluster, it can activate the neighbouring clusters and lead to signal propagation and the generation of pro-arrhythmogenic Ca^{2+} waves (Bers 2014; Cheng et al. 1996; Izu, Wier, and Balke 2001; Keizer and Smith 1998).

SR Ca^{2+} load

We evaluated the SR Ca^{2+} load of the mice ventricular cardiomyocytes by a rapid application of a caffeine solution (10 mM) with a scan speed of 400 Hz on paced cells. Caffeine has a fast and reversible action on RyR where it increases its sensitivity to Ca^{2+} and maintains the RyR in an open state. The opening of the RyR persists as long as the caffeine is present, which makes it possible to empty the SR of its Ca^{2+} content. It is important to assess SR Ca^{2+} load that is correlated to the SR Ca^{2+} leak (Bers and Shannon 2013; Cheng, Lederer, and Cannell 1993; Eisner et al. 2017; Györke and Györke 1998; Santana et al. 1997; Satoh, Blatter, and Bers 1997; Shannon, Ginsburg, and Bers 2002). The amplitude of the Ca^{2+} transient obtained upon caffeine application allows performing an estimation of the SR Ca^{2+} load. The cells were paced with the electrodes at 1Hz, until we reached a steady state. The caffeine is then applied and the stimulation stopped once the emptying of the SR begins.

Ca^{2+} signaling analysis

Ca^{2+} transient

The fluorescence obtained (F) was normalized by the fluorescence at rest (F_0) after subtracting the background noise (Figure 19-C). We thus measure the amplitude of the Ca^{2+} transient F/F_0 = [(F-background) / (F_0-background)] as well as the decrease kinetics of F/F_0 (τ in ms) by adjusting the descending part of the transient by a mono-exponential function. The τ measurement represents mostly the SERCA activity that pumps back the Ca^{2+} into the SR, and at a lesser extend the Ca^{2+} extrusion through the NCX (Figure 19-C).

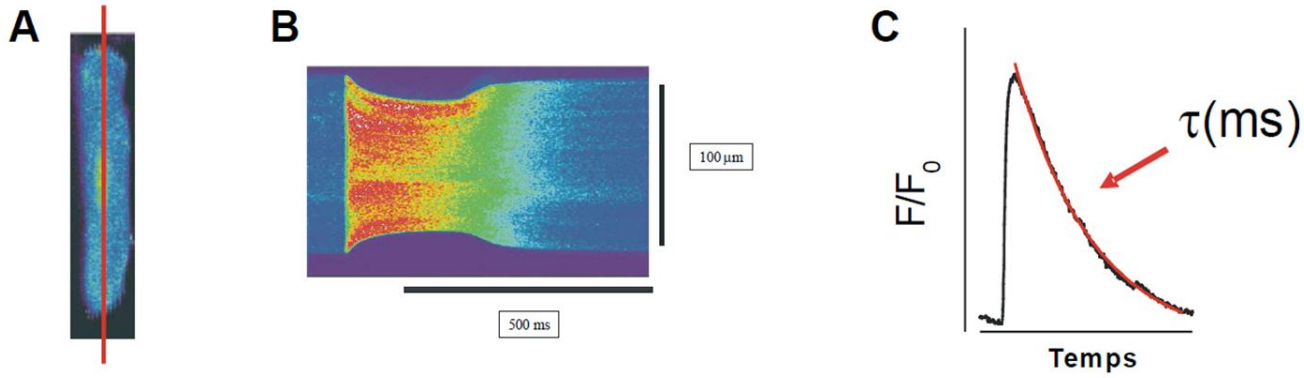

Figure 19: Analysis of a Ca^{2+} transient. (A) The cell (in blue) is scanned by the white light laser (red line) every 2.5 ms (400Hz). (B) Example of line-scan image of a cardiomyocyte. The depolarization leads to an increase in fluorescence which results in the transition from blue to red color. The length of the selected line is shown vertically and the sweep time horizontally. (C) Plot of the recorded fluorescence signal (F) normalized by basal fluorescence (F_0) with the adjustment of the decrease of the Ca^{2+} transient by a mono-exponential function (in red).

Ca^{2+} sparks and Ca^{2+} waves

Ca^{2+} waves were counted for each cell and expressed as number of waves/second. We also calculated the percentage of cells presenting waves for each condition. We performed the analysis of Ca^{2+} sparks as fellow: Ca^{2+} sparks are selected manually by a box in IDL program. The homemade analysis program will then measure the Ca^{2+} sparks frequency.

SR Ca^{2+} load

As for the Ca^{2+} transient, the fluorescence obtained (F) after the caffeine application is normalized by the fluorescence at rest (F_0) after subtracting the background noise [(F-background) / (F_0-background)]. The amplitude of the Ca^{2+} transient (F/F_0) obtained is an estimation of the SR Ca^{2+} load. The decrease kinetics of the caffeine-induced transient F/F_0 is adjusted by a mono-exponential function and represents mainly the NCX activity that extrudes the Ca^{2+} outside the cell.

3) Immunofluorescence of h-iPSC-CM

We performed this technique to validate a cardiac-like phenotype of the h-iPSC-CM, by labelling the nucleus and the Z-like sarcomere striation.

a. Principle

Immunofluorescence (IF) combines the use of antibodies with fluorescence imaging techniques to visualize target proteins and other biomolecules within fixed cell or tissue samples. The fluorophore attached to the bound antibody permits the detection of the antigen-antibody complex. This process can reveal the localization, relative expression, and even activation states of target proteins. Herein we used DAPI as a nucleus marker and α-actinin as a Z-like sarcomere striation marker in h-iPSC-CM.

Immunohistochemistry is used in case of a tissue preparation, whereas immunocytochemistry is referred to seeded or isolated cell preparation. The choice of the primary antibody is critical for IF success and directly affects data quality. Detection of a specific band on a western blot (WB) is not sufficient to guarantee a chosen antibody will perform in IF. Indeed, in WB experiment, proteins are denaturated which alter their structure (section VI.*Western blot*). An epitope of this protein recognized by an antibody approved for WB may be inaccessible for IF, where proteins remain in their native state.

There are two types of IF (Figure 20) depending on where the fluorescent dye is conjugated: either on the primary antibody that detects the desired target, and thus called direct IF (as for the DAPI), or on a secondary antibody that binds to the complex primary antibody-antigen, and is called in this case indirect IF (as for α-actinin).

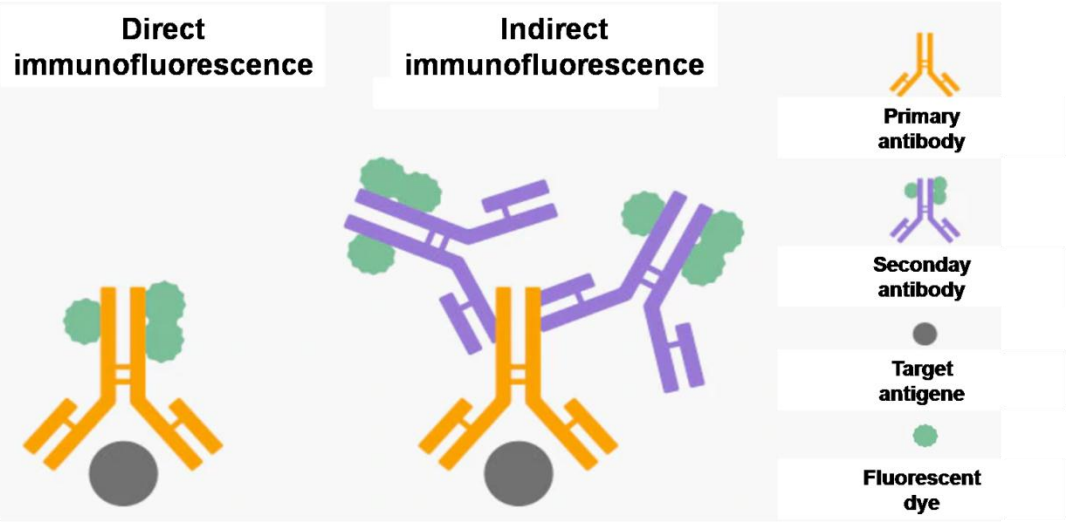

Figure 20: Immunofluorescence principle, adapted from www.thermofisher.com. For direct IF, the antibody binding to the target is labelled with fluorophore. For indirect IF, the primary antibody binds to the target and a fluorophore-labelled secondary antibody specific for the primary antibody binds to it.

Both direct and indirect methods of IF have advantages and disadvantages. The indirect IF is the most common and cost effective, since fluorescently labeled secondary antibodies are relatively inexpensive, come in a wide array of colors, and it can be used in conjunction with any same specie of the primary antibody. Furthermore, it offers greater sensitivity because more than one secondary antibody can bind to each primary antibody, resulting in signal amplification. However, secondary antibody may react with endogenous immunoglobulin in tissue samples, which can result in higher background fluorescence. It is also important to pay attention to possible secondary antibody cross-reactivity; when performing multi-labelled experiments (when an antibody raised against one specific antigen has a competing high affinity toward a different antigen). This is often the case when two antigens have similar structural regions that the antibody recognizes. To overpass this problem, primary antibodies used should be raised in different species. This problem is not observed in direct IF, where different primary antibodies raised in the same specie can be used, since this technique does not require a secondary antibody. Direct IF also requires shorter sample staining time than the

indirect IF, but is more expensive and demand commercial availability of labeled desired antibody. Furthermore, the fluorescence signal relies on the finite number of fluorophores in direct IF that can be attached to a single antibody, and consequently, can limit detection to high-abundance targets.

It is also important to minimize spectral overlap of different fluorophores used in case of multi-labeling. Otherwise, bleed-through fluorescence from the shorter wavelength channel into the longer wavelength channel is observed.

b. Protocol

Cell fixation

After confocal experiments, h-iPSC-CM dishes were washed 3 times with PBS and fixed with paraformaldheyde (PFA) 4% in PBS 20 minutes at room temperature. Then dishes were washed with PBS twice and kept at 4°C.

Cell immuno-labelling

h-iPSC-CM dishes were washed three times in PBS, and blocked in PBS + BSA 1% 1 hour at room temperature, which reduces the background signal caused by non-specific binding of primary and secondary antibodies. Then the h-iPSC-CM were incubated with primary anti-alpha-actinin monoclonal mouse antibody (Sigma Aldrich, A7811) 1/400 in PBS + BSA 1% + tripton 0.1% overnight at 4°C. Tripton is a permeabilizing buffer used to create pores in the cellular membrane to allow antibody access. After removal of primary antibodies, dishes were rinsed with PBS 3 times and once with PBS + BSA 1%. Cells were then incubated with secondary goat anti-mouse antibody coupled to AlexaFluor 488/500 (Thermo Scientific, A11029) in PBS + BSA 1% for 1 hour in the dark at room temperature. AlexaFluor 488/500 is a fluorophore with an excitation wavelength of 490 nm and signal emission wavelength at

520 nm. Dishes were then washed with PBS 3 times and coverslips were mounted on the cells incubated in a drop of Prolong gold antifade reagent containing DAPI (Thermo Scientific, P36962). Prolong gold antifade reagent is a glycerol-based liquid mountant applied directly to fluorescently labelled cells or tissue samples on microscope slides. The mounting agent helps stabilize the sample preparation and prevent fluorophores bleaching by exposure to high-energy light during image acquisition. It contains the DAPI (4',6-diamidino-2-phenylindole), a fluorochrome that binds strongly to the DNA adenine and tymine bases, used to stain the nucleus. Dishes were stored at 4°C in the dark. Images were acquired with an inverted Leica TCS SP8 microscope (oil immersion, objective 63, Leica, Germany). DAPI has an excitation wavelength of 350 nm in the visible spectrum and its signal emission is detected at 450 nm. Alexa-488 was excited at 490 nm and signal emission was detected for wavelength ≥ 500 nm. The two fluorophores spectra don't overlap (Figure 21) which makes the measurements possible.

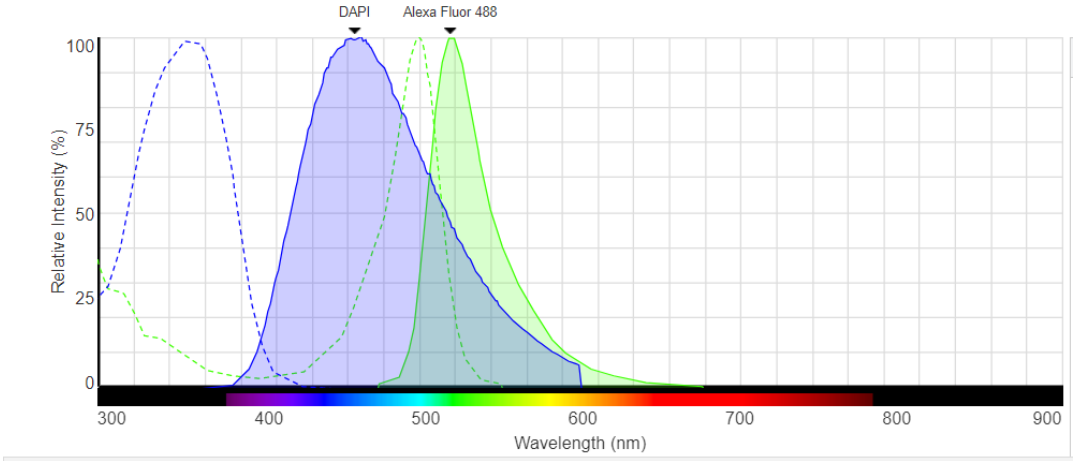

Figure 21: Fluorescence spectrum of DAPI and Alexa-488. DAPI has an excitation wavelength of 350 nm in the visible spectrum and an emission wavelength between 450-490 nm. Alexa-488 has an excitation wavelength at 490 nm and signal emission wavelength at 520 nm.

4) Förster (or fluorescence) resonance energy transfer (FRET)

This technique was used to asses Epac activation state in cardiomyocytes under glucose treatment.

a. Principle

The Förster (or fluorescence) resonance energy transfer (FRET) is a process by which energy is transferred from an excited fluorophore (the donor) to a second fluorophore (the acceptor). When the first fluorophore is excited by an energy source (a laser for example) it passes from its ground state to an excited one. Then it returns to its ground state by emitting photons of less energy than absorbed. This energy emitted by the donor will then be absorbed by the acceptor if it is sufficiently close to the donor (distance < 100 Å). Otherwise this photon emission is dissipated by emission of fluorescence from the donor. This transfer of fluorescence energy from the donor to the acceptor will therefore result in a decrease in the fluorescence signal from the donor and in an increase in the fluorescence emission from the acceptor. The overlap of the emission spectrum of the donor and the excitation spectrum of the acceptor is crucial for the transfer of energy from the donor to the acceptor (Figure 22). The methods for measuring the efficiency of this transfer are therefore particularly well suited to the study of interactions between macromolecules or protein conformational changes when sandwiched by a donor and an acceptor.

The FRET technique can be used to co-localize macromolecules: the first protein will be linked to a donor fluorophore and the second protein to an acceptor fluorophore. If these 2 proteins are co-localized (distance less than 100 Å), the distance between the 2 fluorophores will allow energy transfer. The FRET technique can also be used to visualize a change in

conformation reflecting an activation or inactivation of a protein, by merging on two different parts of a protein, two fluorophores. For example, if the protein is unfolded or lysed by proteolysis, the two fluorophores will be distant and there will be no FRET. If the protein folds, for example when it gets activated, the fluorophores couple will be closer and there will be energy transfer from the donor to the acceptor. However, these FRET protein sensors require first to be synthesized and then transfected into the studied cell. The transfection efficacy can vary a lot from a cell to another and may result in differences in sensor expression levels. Moreover, fluorophores are prone to photobleaching with long exposure time that can affect FRET signal.

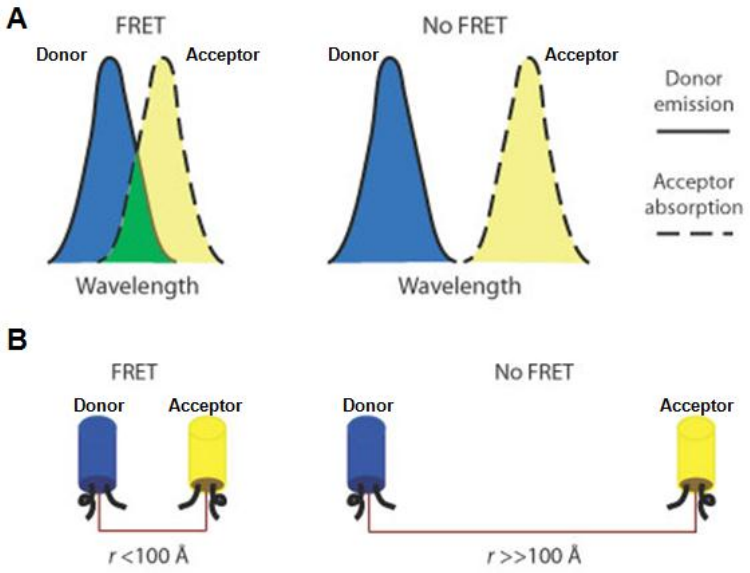

Figure 22: FRET principle adapted from (Vogel, Thaler, and Koushik 2006). (A) FRET requires an overlap of the emission spectrum of the donor (solid line) with the absorption spectrum of the acceptor (dashed line). The overlapping region is shown in green. (B) FRET is observed when the distance separating the two fluorophores (*r*) is less than 100 Å.

In this project we used the Epac-based FRET biosensor to assess the activation state of Epac. A fluorescent donor marker CFP (cyan fluorescent protein) is attached to the C-catalytic part and a fluorescent acceptor marker YFP (yellow fluorescent protein) is attached to the N-regulatory part of Epac (Figure 23). When Epac is inactive the 2 sensors are close enough so that once the donor is excited it transfers its energy to the acceptor, allowing a FRET signal

(decrease of the CFP/YFP ratio). However, when Epac is activated, its conformation changes which increases the distance between CFP and YFP, resulting in a decrease of the FRET signal (increase of the CFP/YFP ratio).

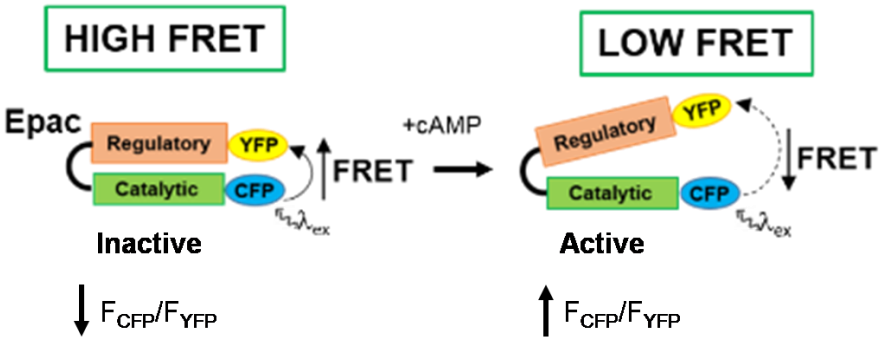

Figure 23: Epac-based FRET biosensor. When Epac is inactive the 2 sensors are close enough so that once the donor is excited it transfers its energy to the acceptor, allowing a FRET signal (decrease of the CFP/YFP ratio). However, when Epac is activated by cAMP, its endogenous activator, its tridimensional conformation changes which increases the distance between the 2 fluorophores, resulting in a decrease of the FRET signal (increase of the CFP/YFP ratio).

b. Protocol

Freshly isolated cardiomyocytes were transfected 3 to 4 hours with adenovirus encoding Epac-FRET biosensor. Experiments were performed 20 to 24 hours after transfection. Cells were treated 30 minutes with each condition. Emission ratio was measured between CFP and YFP using λex = 457 nm and appropriate emission filters (CFP ; 485/30 nm) and (YFP ; 545/40 nm).

V. Single channel recordings

This technique is used to study the activity of the single RyR incorporated into artificial lipid bilayer.

1) Principle

This technique is based on the incorporation of the RyR contained in the SR vesicles into an artificial lipid bilayer to measure the channel electrical activity. Artificially spontaneously produced, planar, bimolecular lipid membranes (bilayers) are formed from a mix of lipids in a hydrophobic solvent such as n-decane. Ion channel incorporations occur spontaneously and can be detected by conductance changes in the bilayer membrane. The side of the bilayer to which the vesicles are added is defined as the *cis* side, the other side is called th*e trans* side. The reference electrode is incorporated into the *cis* side and the command electrode into the *tran*s side. The *cis* side corresponds to the cytosolic side of the RyR and the *trans* side to its luminal side (Figure 24). Since the SR contains ion channels (such as chloride and K^+ channels) other than the RyR, it is necessary to block these channels in order to prevent interferences with RyR recordings. The Cesium methanesulphonate (CH_3CsO_3S) is commonly used as the principal salt in the bathing solutions. The RyR is quite permeable to Cesium (Cs^+), which increases its conductance, whereas other ion channels in the SR do not conduct Cs^+. In addition, Cs^+ blocks the K^+ channels whereas CH_3O_3S blocks the chloride ones. A [Cs^+] gradient across the bilayer (300 mM in the *cis* chamber and 50 mM in the *trans* one) and a rigorous stirring of both the *cis* and the *trans* side of the preparation are crucial for SR vesicle incorporation into the lipid bilayer. When a vesicle has fused with a bilayer, the ion channels, notably the RyR embedded in the vesicle incorporates into the bilayer. Once this happens, it is possible to determine the ionic conductance of a single channel and to

monitor its opening and closing state by measuring the current through the membrane in response to an applied electrochemical gradient. We observe a trace that reflects the alternance between the open and the closed state of the channel. Intermediate current levels correspond to a subconductance state of the channel. Thus we can determine the open probability of the channel by quantifying the time of each state (open, closed, subconductance) of the RyR.

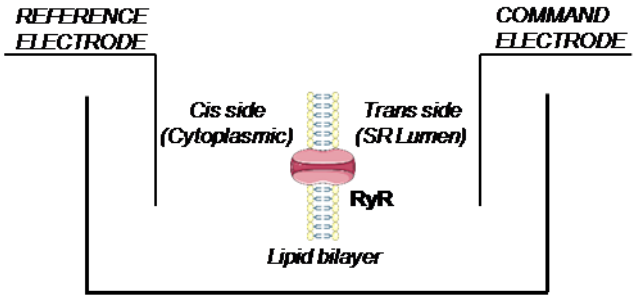

Figure 24: Single channel recording principle. The RyR contained in the SR vesicles incorporates into an artificial lipid bilayer. The side of the bilayer to which the vesicles are added is defined as the *cis* side, the other side is called the *trans* side. The reference electrode is incorporated into the *cis* side that corresponds to the RyR cytosolic side, and the command electrode into the *trans* side that corresponds to the RyR luminal side.

2) Protocol

Mice hearts were perfused with normal 100 mg/dl or high glucose 500 mg/dl Tyrode solution (Table 3). After 15 minutes of perfusion, the heart was removed and atriums discarded. Ventricles were directly frozen in nitrogen solution. A total of 5 mice hearts were pooled together for each condition and homogenized using a Teflon pestle in homogenization buffer (0.9% NaCl, Tris-HCl 10 mM pH = 6.8, plus protease inhibitors: 2 µM leupeptin, 100 µM phenylmethylsulphonyl fluoride, 500 µM benzamidine, 100 nM aprotinin, and phosphatase inhibitors: 50 mM NaF, 1 mM Na Orthovanadate, 5 mM Na pyrophosphate, 1 mM β-glycerolphosphate). Cardiac SR-enriched microsomes were prepared by differential centrifugation: Hearts homogenates were centrifuged at 1000 g for 3 minutes at 4°C, supernatants were centrifuged a second time at 8000 g for 20 minutes at 4°C. Supernatants were further centrifuged at 100 000 g for 35 minutes at 4°C. The pellets containing SR-

enriched microsomes were suspended in homogenization buffer supplemented with 0.3 M sucrose and stored at -80°C.

Planar lipid bilayers, composed of phospholipid mixture of phosphatidylethanolamine, phosphatidylserine and lecithin (1.0:0.9:0.1 ratio dissolved in n-decane to 50 mg/ml) (Matreya, LLC) were painted with a glass rod across an aperture of 150 μm diameter in a Delrin cup. The *cis* chamber represented the cytosolic side, which was held at virtual ground and contained the reference electrode. The *trans* chamber corresponded to the luminal side and contained the voltage command electrode. Electrodes were connected to the head stage of a 200B Axopatch amplifier. Both chambers contain 1000 μl of $CsCH_3SO_3$, 20 mM MOPS (3-(N-morpholino) propanesulfonic acid), pH = 7.2 with nominally free [Ca^{2+}] (~3-5 μM). Channel recordings were recorded at 0 mV holding potential, after filtration with a 8-pole low-pass Bessel filter set at 1 kHz and digitized at 4 kHz using a Digidata 1440A AD/DA interface. Data acquisition and analysis were performed with Axon Instruments (Burlingame, CA, USA) hardware and software (pClamp 10).

VI. Biochemical and biomolecular techniques

1) Western blot

We used this technique to assess the RyR phosphorylation level and Epac2 O-GlcNacylation under high glucose treatments.

a. Principle

The Western blot (WB) is a semi-quantitative technique used to assess protein expression level and/or protein post-translational modifications (phosphorylation, O-GlcNacylation) in a tissue or cells sample preparation. Proteins are separated based on their molecular weight by electrophoresis on an adequate gel. The proteins of the gel are transferred to a membrane by an application of a voltage difference, that is then blocked with a rich protein solution, and probed with a primary antibody specific to the protein of interest. The membrane should be well washed to avoid background noise signal and to remove unbound antibody. The protein-antibody complex is detected by asecondary antibody labeled with an enzyme such as horseradish peroxidase (HRP) (Figure 25).

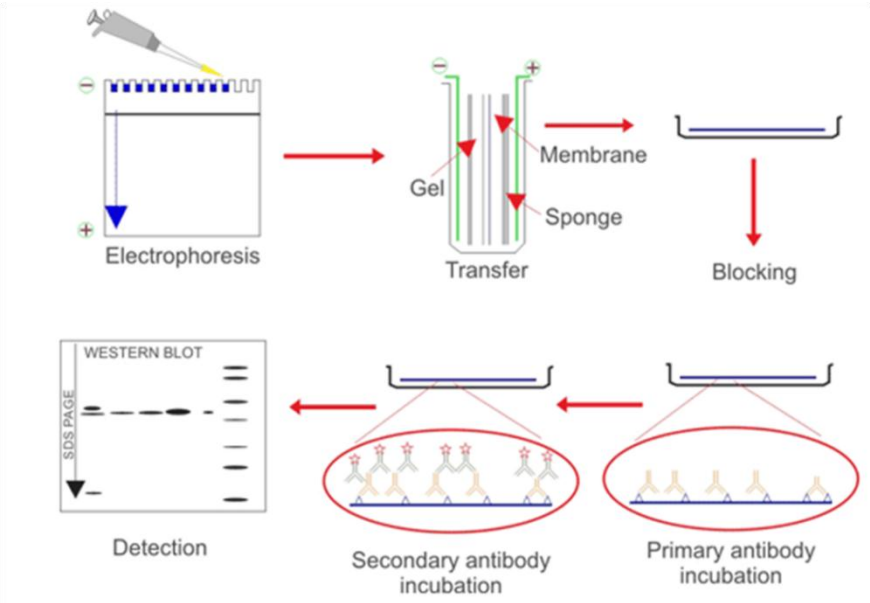

Figure 25: Western Blot principle, adapted from www.cusabio.com. The polyacrylamide gel is loaded with the same amount of denaturated proteins. The negatively charged proteins migrate, based on their molecular weight, toward the positive electrode upon current application. Once the migration is over, the proteins are then transferred to a membrane by an application of a voltage difference (negatively charged proteins migrate toward the positive electrode, thus from the gel to the membrane). The membrane is then blocked and incubated with the protein of interest specific primary antibody. After several washing, the membrane is incubated with a secondary labeled antibody that recognizes the primary antibody-protein complex. The protein of interest is then revealed by chemiluminescence.

b. Protocol

Protein extraction and dosage

Protein extraction

For the RyR phosphorylation state, proteins are extracted from mice adult hearts perfused 15 minutes with Tyrode solution (Table 3) containing different glucose concentration (100 mg/dl and 500 mg/dl) ± Epac2 inhibitor ESI-05 (Sigma Aldrich, SML 1907) at 10 µM. After heart perfusion, aorta and atriums are discarded and ventricles are frozen in liquid nitrogen.

For Epac2-O-GlcNacylation detection, ventricular cells are isolated from 3 mice and pooled together, then treated with different glucose concentrations and O-GlcNacase inhibitor as detailed in the Co-IP section below (VI.2) Co-Immunoprecipitation).

Hearts were then digested mechanically in 2 ml of RIPA-SDS (Radioimmunoprecipitation

assay sodium dodecyl sylfate) buffer (Table 4) using ultraturax on ice, followed by 15 pulses of sonication (375 watts) to destroy cell membrane. RIPA buffer is composed of several products to optimize protein extraction: detergents such as sodium deoxycolate acid (DOC), and sodium dodecyl sulfate (SDS) are used to induce the cell membrane rupture and to solubilize proteins and lipids. TrisHCl acts as a buffer providing an ionic environment similar to that of the cell *in vivo* and NaCl maintains the osmotic pressure. NP-40 is a non-ionic detergent used to prevent non-specific interaction between the proteins or the proteins with the tube. Proteases inhibitors are added to RIPA buffer to avoid protein degradation (Calbiochem, protease inhibitor cocktail set V, EDTA-free). Anti-phosphatases are also used to prevent dephosphorylation of the proteins: 1 mM sodium floride (NaF), a serine/threonine and acidic phosphatase irreversible inhibitor, 1 mM sodium orthovanadate (Na_3VO_4), a tyrosine and alkaline phosphatases irreversible inhibitor, 5 mM sodium pyrophosphate ($Na_4P_2O_7$) and 1 mM β-glycerolphosphate, both serine/threonine phosphatase irreversible inhibitors. The addition of anti-phosphatases is crucial for our experiments since we measured the phosphorylation state modification of the RyR under glucose treatment.

After the digestion, the homogenate is centrifuged at 4°C at 13200 RPM for 15 minutes to separate proteins from cells debris. The supernatant containing the proteins is aliquoted and stored at -80°C.

RIPA-SDS buffer composition

Product	**Concentration (mM)**
Tris HCl, pH = 8	50
NaCl	150
EDTA	2
DOC (sodium deoxycolateacid)	0.5%
SDS (sodium dodecyl sulfate)	0.5%
NP40	1%
H_2O	Completed to desired volume

Table 4: RIPA buffer composition, pH = 8

BCA Protein dosage test

The BCA (BiCinchoninic acid Assay) test was used to estimate protein concentration in the hearts homogenates (Thermo Scientific, Pierce BCA protein assay kit, 23225). This test is based on the reduction of Cu^{2+} to Cu^{+} by proteins in an alkaline medium at high temperature (37°C to 60°C), known as the Biuret reaction. The chelation of two BCA molecules with Cu^{+} gives a purple-coloured reaction product that exhibits a strong absorption at 562 nm that is nearly linear with increased protein concentrations. The protein concentration of our samples is then reported to a BSA, a common protein, standard absorbance curve. The following BSA standard range was used using a 1 µg/µl BSA stock solution for protein dosage: 30, 25, 20, 15, 10, 5, 2.5, 1.25 µg points with a blank point.

A 96-well flat transparent bottom plate was used to perform BCA dosage. Each 2 µl of sample were mixed with 98 µl of water and 100 µl of BCA reagent. Samples and BSA standard range were performed in triplicate. The plate was then heated 15 minutes at 60°C and absorbance measurements were done using Tecan or Victor Nivo Perkin instrument.

Western blot protocol

Samples preparation

A loading buffer containing an anionic detergent is used to charge proteins negatively allowing them to migrate toward the positive electrode after voltage application. 30 µg of proteins were loaded with a ThermoFisher LDS NuPAGE 4X (NP0008) loading buffer. This buffer contains lithium dodecyl sulfate at a pH of 8.4, which charges the protein negatively allowing their migration in the gel. The LDS NuPAGE 4X also contains the Coomassie G250 and Phenol Red, tracking dyes, to follow the protein migration. The coomassie also increases the density of the sample and thus keeps it in the bottom of the well. Additional strong reducing agents such as Beta-mercaptoethanol or Dithiothreitol (DTT) are added to break

disulfid bonds between cysteines residues. We used the ThermoFisher NuPAGE reducing agent 10X (NP0004) that contains DTT 10X. The samples are then heated 10 minutes at 70°C to break hydrogen bonds to unfold and linearize the protein.

Electrophoresis and migration

Electrophoresis is based on the molecule weight instead of the charge or the size of the proteins. That's why proteins must first get all charged in the same way and unfolded to their primary structure, to allow their migration based on their molecular weight only. Acrylamide gel is a three-dimensional mesh networks polymer which average pore sizes depends on the acrylamide percentage (the higher the percentage, the smaller the pores). Different acrylamide percentage migration gels are used depending on the size of the protein of interest. The biggest the protein size, the smaller the gel percentage allowing an easy migration of the protein through the pores of the gel.

For RyR (500 KDa) detection, we used a TGX Fast Cast Biorad (Tris-Glycine) 7.5% (1610181) gel that was prepared accordingly to the manufacturer instruction. For Epac2 (120 KDa) detection, we used a pre-cast Tris-Glycine 4-20% gel (Invitrogen, XP04200). Samples and protein ladder (Thermo Scientific, Page ruler prestained, 26620) were loaded in the wells of the gel and runned for 1 hour at 150 V in Tris-Glycine 1%.

Transfer

Once the migration is finished, the proteins of the gel are transferred (blotted) to a membrane (a nitrocellulose or PolyVinyliDene Fluoride (PVDF) membrane) using an electrical field. PVDF membrane has higher protein binding properties than nitrocellulose, but thereby a higher background noise signal. The proteins bind to nitrocellulose membrane through the non-specific hydrophobic interactions, and to the PVDF membrane through hydrophobic and dipole interaction. We transferred our gels to nitrocellulose membrane using an electrical

field as per the following protocol (1 min at 20 V, 4 minutes at 23 V, and 2 minutes at 25 V).

Blocking and probing

Since the protein of interest is later detected by its specific antibody, it is important to avoid the non-specific interactions of the antibody with the membrane. That's why non-specific binding sites of the membrane should be blocked with a high protein preparation (such as milk, BSA or gelatine) for 1 hour at room temperature. Membranes are then incubated overnight at 4°C on a tune roller with the primary antibody. Depending on the protein of interest, we used different blocking agent as reported in the summary table below.

Revelation

The next day, membranes were washed 3 times during 10 minutes with TBS-T 0.1% (Tris buffered saline with 0.1% tween 20), to avoid background noise signal and to remove unbound antibody. The protein-antibody complex is detected by the appropriate secondary antibody labeled with an enzyme such as horseradish peroxidase (HRP): Goat anti-mouse antibody for mice antibody (Invitrogen, 31430), and goat anti-rabbit antibody for rabbit antibodies (Invitrogen, 31460). The membrane is probed 1 hour at room temperature with secondary antibody coupled to HRP. The protein of interest is then revealed after incubation of the membrane with an HRP substrate (Supersignal West Dura Extended Duration substrate, ThermoFisher, 34076). The substrate is oxidized by peroxidase and emits a signal proportional to the amount of protein, as long as the detection is linear and the signal is not saturated, and is detected by chemiluminescence (iBright ™ FL1000 Imaging System, ThermoFisher Scientific).

Stripping

To detect other proteins, especially reference protein, membrane was stripped 10 minutes at

room temperature (Restore Plus Western Blot Stripping Buffer, ThermoFisher, 46428) to remove secondary antibody, and washed 5 minutes with water. Membrane was blocked again 1 hour at room temperature with appropriate blocking agent and incubated overnight at 4°C with protein of reference antibody to normalize our protein level expression. Washing and revelation were done as described above.

Summary antibody table

Antibody	Reference	Specie	Dilution	Gel	Transfert	Blocking
Epac2	Proteintech 19103-1-AP 40 µg / 150µl	Polyclonal rabbit	1/1000	PreCast Tris-Glycine 4-20%	Nitrocellulose	Gelatine
O-GlcNac	RL2 ThermoFisher MA1-072 2 mg / ml	Monoclonal mouse	1/1000	PreCast Tris-Glycine 4-20%	Nitrocellulose	Gelatine
Calsequestrine	ThermoScientific PA1-913	Polyclonal Rabbit	1/2500	PreCast Tris-Glycine 4-20%	Nitrocellulose	BSA 5% in TBS-T 0.1%
Total RyR	ThermoFisher C3-33 1 mg / ml	Monoclonal mouse	1/5000	Tris-Glycine 7%	Nitrocellulose	Gelatine
Phospho-RyR S2808	Badrilla A010-30AP	Monoclonal rabbit	1/2000	Tris-Glycine 7%	Nitrocellulose	BSA 5% in TBS-T 0.1%
Phospho-RyR S2814	Badrilla A010-31AP	Monoclonal rabbit	1/2000	Tris-Glycine 7%	Nitrocellulose	BSA 5% in TBS-T 0.1%

2) Co-Immunoprecipitation

We used this technique in order to assess direct Epac2-O-GlcNacylation under high glucose treatment in mice ventricular cardiomyocytes.

a. Principle

Co-immunoprecipitation (Co-IP) is a technique used to study the protein-protein interaction. Co-IP is developed from the immunoprecipitation (IP) technique based on the specific antigen-antibody reaction. For IP, the target protein is isolated out from a cell lysate by using a specific antibody. The entire protein complex is pulled out of solution and unknown members of the complex are then detected by WB analysis.

The first step is to immobilize the protein specific antibody (monoclonal or polyclonal) onto an insoluble support, such as agarose or magnetic beads. Magnetic beads covalently coupled to recombinant Protein G were used. Protein G are immunoglobulin (Ig)-binding proteins with a specificity for the heavy chains on the Fc region of antibodies. The small size of the magnetic beads (1 to 4 μm diameter) gives them sufficient surface area for high-capacity antibody binding. The antibody can covalently be attached to the Protein G-bound supports using bis(sulfosuccinimidyl)suberate (BS3), a cross-linker that links adjacent amines of the antibody and Protein G. The immobilized antibody on the chosen support is then incubated with the cell lysate containing the target protein. During the incubation period, gentle agitation of the lysate allows the target protein to bind to the immobilized antibody (non-covalent reversible bond between the Fab part of the antibody with its compatible epitope of the antigen). Irrelevant, non-binding proteins, antigens are then washed away. The targeted protein is eluted using an elution buffer with low pH (2.5 to 3) that dissociates antibody-antigen interaction (the Antibody-Protein G bond is not eluted since it is cross-linked). The

purified antigen is then analyzed by WB.

In our experiments we assessed a possible O-GlcNAcylation of Epac2. To do so, we immuo-precipitated Epac2 using Epac2 antibody immobilized on magnetic beads and then we revealed O-GlcNac residues by WB (Figure 26).

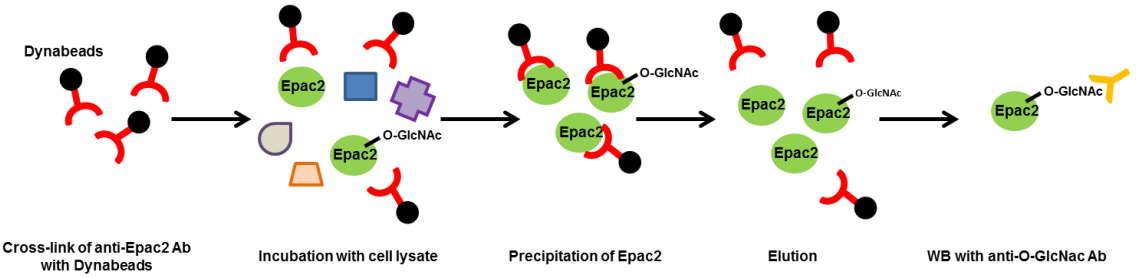

Figure 26: Co-IP principle. Epac2 antibody is immobilized on magnetic beads and incubated with cell lysate. Epac2 is precipitated and the antigene-antibody eluted. WB is performed to assess O-GlcNAcylation of Epac2.

b. Protocol

Left ventricular cardiomyocytes isolated from 3 mice were pooled together and treated with Tyrode solution at normal 100 mg/dl glucose + PUGNAC 50 µM (Sigma Aldrich, A7229) at 37°C for 45 minutes. Then, cells were separated into 3 groups as described below:

1. Control → cells are lysed directly as previously described with RIPA buffer
2. The supernatant is discarded and cells are treated with Tyrode solution at 500 mg/dl glucose + PUGNAC 50 µM for 30 minutes, then the cells are lysed
3. The supernatant is discarded and cells are treated with Tyrode solution at 500 mg/dl glucose + PUGNAC 50 µM + Uridine 5′-diphospho-N-acetylglucosamine sodium salt (UDP-GlcNac) 500 µM (Sigma Aldrich, U4375) for 30 minutes, then the cells are lysed. UDP-GlcNac is a direct substrate of O-GlcNAc transferase, and thus used as a positive control for the O-GlcNacylation reaction.

ThermoFisher magnetic DynabeadsProt G kit (10007D) was used in this experiment according to the manufacturer protocol. Dynabeads were firstly resuspended by gentle rotation on a roller (5 minutes) at room temperature, and 50 µl were used for each condition.

Each condition/tube was placed on magnet and supernatant was removed. Dynabeads were resuspended in 200 µl of Antibody Binding & Washing Buffer containing Epac2 antibody (Proteintech, 19103-1-AP) at a final concentration of 2 µg/µl. Rabbit IgG (sigma Aldrich, I5006) at 1 µg/µl was used as a negative control to ensure that the Epac2 antibody can only immuno-precipitate Epac2 and not unspecific proteins. The tubes were then incubated 15 minutes with agitation at 1000 RPM at room temperature. The tubes were placed on magnet and the supernatant discarded. The Dynabeads-Antibody complexes were washed with 200 µl of Antibody Binding & Washing Buffer (discard later the supernatant). We added 250 µl of BS3 (ThermoFisher, 21585) to allow cross-linking between the protein G of the Dynabeads and the antibody while shaking at room temperature for 30 minutes. We then added 12.5 µl of Tris-HCl pH = 7.4 to stop the cross-linking reaction and kept shaking 15 minutes at room temperature. We washed the Dynabeads twice with the Binding & Washing Buffer. We added 300 µg of our samples (completed the volume to 300 µl with lysis buffer) which corresponds to the Input, previously quantified by the BCA technique (VI.*1*)*Protein extraction and dosage*). The tubes were well sealed with parafilm and kept rotating on the roller at 4°C overnight. The next day the supernatant (lysate) were transferred to a clean tube (*i.e.* output control) and the Dynabeads washed 3 times with lysis buffer. Then, we resuspended the Dynabeads-Antibody-Antigene complex in 20 µl of the Elution Buffer to break the antibody-antigen bonds. We added 10 µl NuPAGE® LDS Sample Buffer and 3 µl NuPAGE® Reducing Agent and incubated 10 minutes at 70°C. We also prepared 20 µl of the output control (lysate) for the WB experiment.

We used precast Novex^{TM} Wedge Well^{TM} Tris-Glycine 4-20% gel (Invitrogen, XP04200). The migration was set at 220V for 45 minutes. The proteins were transferred into nitrocellulose membrane and blocked with gelatine. Membrane was then incubated overnight at 4°C with anti-O-GlcNAc monoclonal mouse antibody clone RL2 (Invitrogen, MA1-072) at

1/1000 dilution (0.002 mg/ml).The next day, membrane was washed 3 times 10 minutes with TBS-T 0.1 %, and incubated 1 hour at room temperature with anti-mouse secondary antibody coupled to HRP in order to reveal O-GlcNAc antibody. To make sure that Epac2 was immuno-precipitated, membrane was stripped 10 minutes at room temperature and washed 5 minutes with water. Membrane was blocked again 1 hour at room temperature with gelatine, and incubated overnight at 4°C with anti-Epac2 polyclonal rabbit antibody (Proteintech, 19103-1-AP) 1/1000. Washing and revelation were done as described above in the WB section.

3) PCR

This technique was used to genotype Epac2 mice line and to assess ECC components gene expression in h-iPSC-CM.

a. Principle

PCR for polymerase chain reaction technique is a technique that allows the generation of large amounts of a desoxyribonucleic acid (DNA) specific sequence (our gene of interest) from a small DNA amount.

First, the double DNA strand is disrupted by heating (destabilization of the hydrogen bounds between the adenine-guanine and cytosine-thymine at 95°C), it's the denaturation phase. Then, at lower temperature (55-65ºC) the specific primers that allow the synthesis of the target gene sequence hybridize with the single DNA strand, it's the annealing phase. At optimal temperature (70-75°C), DNA polymerase will synthesize the complementary DNA sequence, starting by the primer. It's the elongation phase. This cycle is repeated over several times allowing an exponential increase of the synthesized DNA sequences (Figure 27).

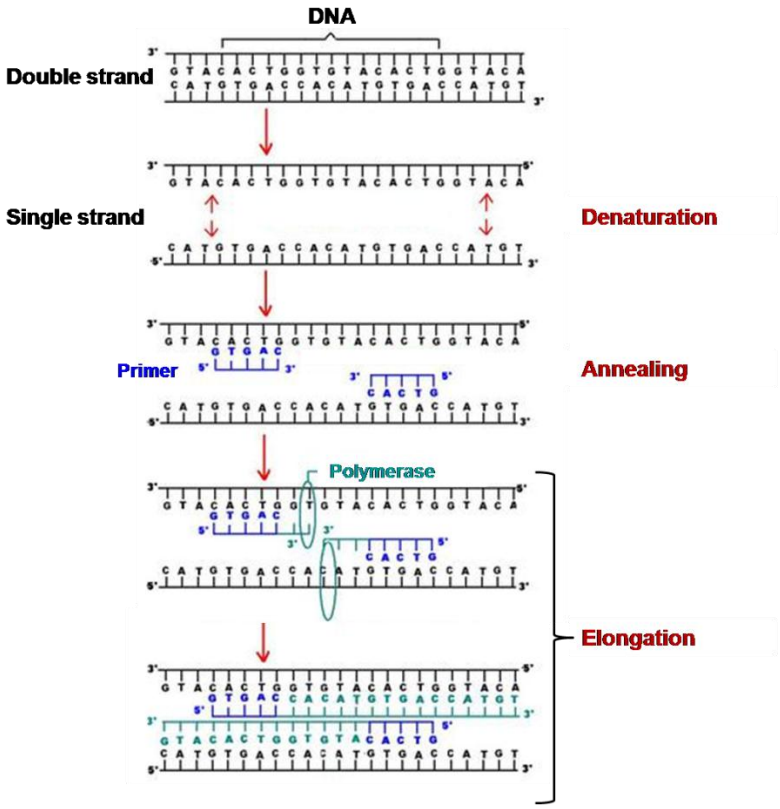

Figure 27: PCR principle, modified from www.technobio.fr. At the denaturation phase, the high temperature (95°C) disrupts the double DNA strand into single DNA strands. At the annealing phase, the lower temperature (55-65ºC) allows the hybridization of the specific primers with the single DNA strand for the synthesis of the target gene sequence. During the elongation phase (70-75°C), DNA polymerase synthesizes the complementary DNA sequence, starting by the primer. This cycle is repeated over several times allowing an exponential increase of the synthesized DNA sequences.

b. Protocols

Mice genotyping

DNA extraction

DNA was extracted from the end tail of the mice by NaOH 50 mM (1 hour at 95°C). Tris-HCl 1M (pH = 8) was added to stop the reaction. The solution is then centrifuged at 13000 RPM for 5 minutes and DNA was extracted from the supernatant. The DNA samples are used immediately for PCR or stored at -20°C for later measurements.

Epac2 genotyping PCR

Mix DreamTaq 2X (ThermoFisher, K1071) containing the polymerase enzyme and the

desoxyribonucleoside triphosphate (dNTP) was used for DNA replication along with 1 µl of DNA extract. EQP3 (5'-CCTCCCTTTTGCTCTCTCCT-3') and EQP4 (5'-CGCTCGCTGCATTTGTATTA-3') primers were used to amplify the Epac2 Wild Type (WT) band at 0.25 µM. Frtneo (5'- AATGGGCTGACCGCTTCCTCGT-3') and EQP4 for Epac2 KO band at 0.25 µM.

DNA replication was conducted with the following cycle repeated 38 times: 1 minute DNA denaturation at 95°C, followed by 1 minute annealing at 57.4°C, then 1 minute elongation at 72°C. Epac2 WT (300 bp) and KO (350 pb) bands are then separated over Tris acetate EDTA (TAE)-agarose 1.5 % gel at 150 V for 1 hour 30 minutes (Figure 28).

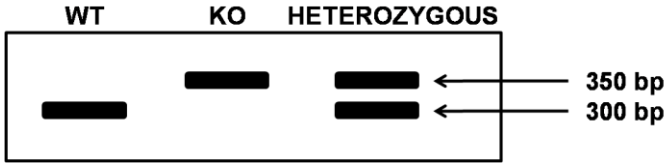

Figure 28: Epac2 genotyping. Upon separation on the gel, the Epac2 WT mice present a single band at 300 bp, the Epac2 KO mice present a single band at 350 bp, whereas the heterozygous Epac2 mice present the double bands.

RT-qPCR

Principle

RT-qPCR, for retrotranscription-quantitative polymerase chain reaction, is a technique used to assess the messenger ribose nucleic acid (mRNA) expression level of a gene. First the ribose nucleic acid (RNA) are extracted from the preparation, dosed and transcripted into cDNA (complementary DNA), then amplified with the specific primer of the gene of interest. The amplification of the cDNA is carried by a DNA polymerase with a denaturation, annealing and elongation phases. To quantify this amplification, a DNA intercalating agent, the SYBR Green, is used. SYBR Green emits fluorescence when it binds to double nucleic

acids strands. When the amount of DNA is sufficient so that the program can detect the SYBR Green fluorescence, we obtain the value of the cycle threshold called CT. This CT marks the beginning of the exponential amplification phase. The lower the CT value, the greater the number of initial copies of the gene of interest (Figure 29).

We used this technique to assess a possible modification of the gene expression of the ECC components in h-iPSC-CM after a chronic high glucose treatment.

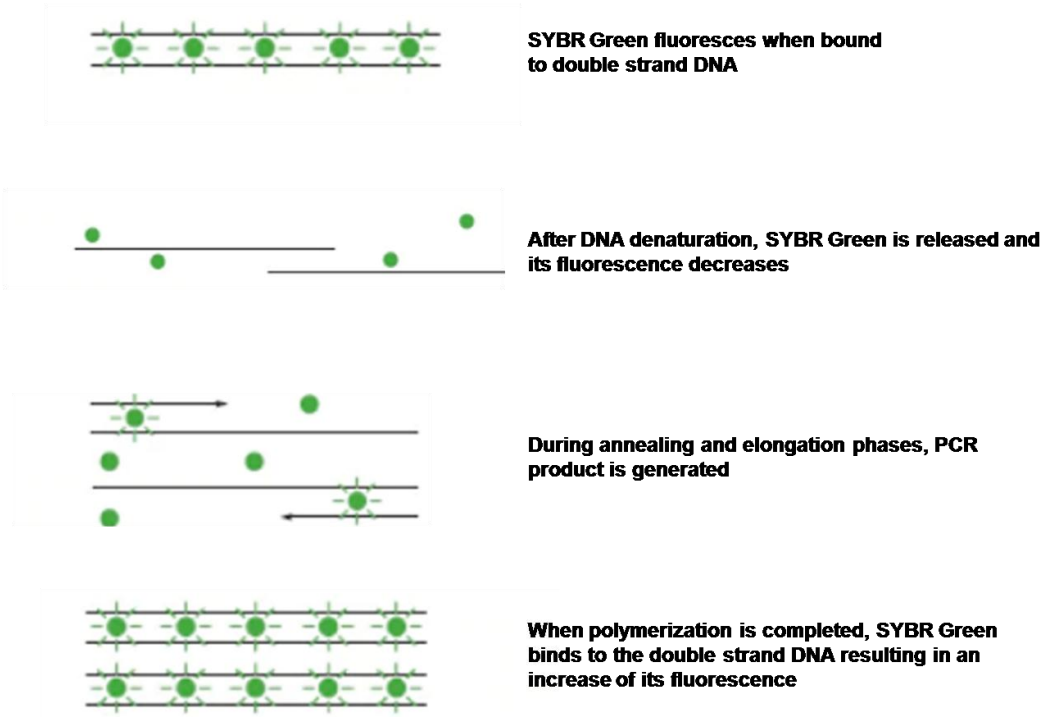

Figure 29: RT-qPCR principle with SYBR Green, adapted from www.thermofisher.com. SYBR Green fluorescences when bound to double DNA strand. During the denaturation phase, the double DNA strands disrupt in single strands, and SYBR Green fluorescence decreases. During the annealing and elongation phases, PCR products are generated until complete polymerization. SYBER Green then binds to double strands DNA resulting in an increase of its fluorescence.

RNA extraction

Total RNA was extracted from h-iPSC-CM treated chronically for 7 days with normal or high glucose concentration ± Epac2 inhibitor or mannitol. RNA was extracted by the common phenol-chloroform organic technique. The samples underwent mechanical lysis in the Bertin grinder-homogenizer in 1 ml of TRIzol (MRC, TR 118), which is a mix of phenol and guanidinium thiocyanate. Chloroform was added to the samples that were centrifuged at

12000 RPM for 15 minutes at 4°C. The mix phenol-chloroform-guanidinium thiocyanate possesses an acidic pH that allows, together with centrifugation, the separation of the DNA from RNA from proteins. Membrane debris and proteins stay in the lower organic chloroform-phenol phase, DNA at the interphase (the acid pH makes DNA less negatively charged and then less soluble in the upper aqueous phase), and total RNA in the upper aqueous phase. This upper phase was transferred to a new tube and total RNA was precipitated with isopropanol and centrifuged for 10 minutes at 12000 RPM at 4°C. The total RNA pellet was washed twice with ethanol before transfer in sterile RNAse-DNAse free water. The samples were heated 10 minutes at 60°C for better resuspension of RNA and stored at -80°C. The next day, RNAs were dosed with a spectrophotometer (NanoDrop ThermoFisher) at 260 nm. In addition to absorbance at 260 nm, the A260/280 and A260/230 ratios are also measured for purity control of the extraction. An A260/280 ratio < 1.5 indicates proteins contamination, while an A260/230 ratio < 2 indicates organic molecules contamination (such as EDTA, carbohydrates or phenols).

Reverse transcription

This step permits the synthesis of cDNA from the total RNAs previously extracted. Reverse transcription was performed using the iScript synthesis kit (Biorad). 1 µg of RNA is used for a reaction volume of 20 µl, along with 5X buffer (Biorad, 5X iScript^{TM} Reaction Mix, 64323295), RNAse and DNAse free water and the enzyme reverse transcriptase (Biorad, iScriptReverse Transcriptase, 64328365). Five minutes of initiation reaction at 25°C is followed by 30 minutes of annealing and elongation process at 42°C. Then the enzyme is inactivated 5 minutes with high temperature at 85°C. When the retro-transcription is over, cDNA are diluted to 1/10 (5 ng/µl as final concentration) and stored at -80°C.

qPCR protocol

A 96 well plates with a transparent bottom were used in this experiment. Each well was loaded with 10 µl of SuperMix and 5 µl of cDNA (5 ng/µl). The SuperMix consists of 7.5 µl of Sybr Green (Biorad, Sso Advanced Universal SYBER green supermix, 1725271) and 500 nM of forward and reverse primers. The double strand cDNA were separated 5 seconds at 95°C (denaturation phase), followed by the annealing and elongation phases at 60°C. This amplification cycle was repeated 40 times. The amplification and quantification were done with a CFX96 (Touch Real-Time PCR Detection System Biorad) device. Two different house-keeping genes were used for the analysis normalization, SLC4A1AP-R and NUBP1 (Table 5).

Analysis

We analyzed the results using the $2^{-\Delta\Delta CT}$ method as following:

ΔCT (gene of interest eg. Epac2 gene) = CT value of the sample X (eg. high glucose treatment) - CT value of the control sample (eg. normal glucose treatment).

ΔCT is calculated for the housekeeping genes in the same way as above for each sample. For the SLC4A1AP-R gene of the sample X for example:

ΔCT (SLC4A1AP-R gene) = CT value of the sample X (eg. high glucose treatment) - CT value of the control sample (eg. normal glucose treatment).

Then we normalized the ΔCT of each gene for each sample with its corresponding ΔCT value of the housekeeping gene as follows:

ΔΔCT= ΔCT of the gene of interest (eg Epac2 of sample X) - value of ΔCT of the house keeping gene (eg SLC4A1AP-R of sample X).

Then, the relative quantity of mRNA coding for the gene of interest of the sample X *vs*. the control sample (normalized with respect to a housekeeping gene), is expressed in "fold change" calculated by the formula $2^{-\Delta\Delta Ct}$.

qPCR primers tables

Gene	Forward	Reverse
Epac1	GCTCTTTGAACCACACAGCA	TGTCTTCTCGCAGGATGATG
Epac2	ATTAATGGACGCCTGTTTGC	CATGCACGCAGTTGAAGAGT
HCN4	ACTACATCATCCGGGAAGGC	TCAGCAGGCAGATCTCTCCA
NCX	ACCTGTTTGGCCAACCTGTCTTCA	TGCTGGTCAGTGGCTGCTTGT
SERCA2A	TCACCTGTGAGAATTGACTGG	AGAAAGAGTGTGCAGCGGAT
RyR2	TAGATTTATAAGGGGCCTTG	GATTCTTCAGGGCTCGTAGT
Cav1.2	CATCATCATCTTCTCCCTCCTG	CATCACCGAATTCCAGTCCT
House keeping genes		
SLC4A1AP-R human	CCTCTACGATCTGGGAAGCA	TCTGGTCCCTGCAGGATAAA
NUBP1 human	CAGAGGGGCTTCATGTCAGG	GATTTCCTCTATAGCCGTGTCC

Table 5: Primers of h-iPSC-CM genes

VII. Statistical Analysis

Data were expressed as mean ± SEM or median [5-95%] percentile. Significance was evaluated by a two way ANOVA or kruskal-Wallis test followed by a post-hoc test, as appropriate, using GraphPad.

Results

Results

The results of my thesis work are divided into 2 parts:

First the study of the implication of Epac2 in high glucose-mediated cardiac Ca^{2+} mishandling in mice ventricular cardiomyocytes and h-iPSC-CM is presented in the following manuscript. Second the characterization of the Ca^{2+} handling in cardio-specific Epac2-KO mice is reported in the second part.

I. Role of Epac2 in high glucose-mediated cardiac Ca^{2+} mishandling

Epac2 is a key player in cardiac Ca^{2+} homeostasis where it is implicated in SR Ca^{2+} leak and arrhythmias, also observed with high glucose concentration. In this manuscript, we studied the implication of Epac2 in high glucose-mediated Ca^{2+} mishandling in ventricular mice cardiomyocytes using control and constitutive Epac2-KO mice. Then we reported the mechanism of Epac2 activation under high glucose concentration pointing out the implication of the O-GlcNacylation pathway. Finally we studied the relevance of this mechanism in h-iPSC-CM which are emerging as an interesting model in studying cardiac pathologies.

Epac2 O-GlcNAcylation, a new mechanism of high glucose-mediated cardiac Ca^{2+} mishandling

Magali Samia El-Hayek[1], Pascal Gerbaud[1], Carmen R. Valdivia[2], Florence Lefebvre[1], Donald M. Bers[3], Ju CHEN[4], Jean-Pierre Bénitah[1], Ana-Maria Gomez[1], Laetitia Pereira[1]

[1]Université Paris-Saclay, Inserm, UMR-S 1180, 92296, Châtenay-Malabry, France.
[2] Division of Cardiovascular Medicine, Department of Medicine, University of Wisconsin School of Medicine and Public Health, Madison, Wisconsin.
[3]Dept. of Pharmacology, University of California Davis, Davis, CA95616.
[4]Department of Pharmacology, University of California Davis, Davis, CA, USA

Running title: Epac2 O-GlcNAcylation, a new mechanism of high glucose-mediated Ca^{2+} mishandling

Keywords: Calcium, Epac2, Hyperglycemia, Ryanodine Receptor

Corresponding author
Dr. Laetitia Pereira, Ph.D
Laboratory of signalling and cardiovascular pathophysiology
UMRS-1180, INSERM
5, Rue Jean-Baptiste Clément
92296 Châtenay-Malabry
FRANCE
Phone : +33 (0)1 46 83 58 07
Fax : (+33) (0)1 46 83 54 75
Email : laetitia.pereira@u-psud.fr

Abstract

Epac2 (Exchange Protein directly Activated by cAMP) has emerged as a critical player in cardiomyopathies, such as heart failure and arrhythmia, also seen in diabetes. Recently, we found that diabetic hyperglycemia leads to CaMKII-dependent SR Ca^{2+} leak, a downstream effector of Epac2. However, the role of Epac2 in hyperglycemia-mediated SR Ca^{2+} leak is still unknown. Here, we tested the significance of Epac2 in high glucose-mediated SR Ca^{2+} mishandling. We measured, using confocal microscopy, Ca^{2+} sparks frequency and Ca^{2+} waves to assess SR Ca^{2+} leak in isolated mice ventricular myocytes under acute hyperglycemic conditions (16.6 mM, 27.7mM *vs*. 5.5mM). High glucose enhanced SR Ca^{2+} leak, as observed by an increase in Ca^{2+} sparks frequency (1.07±0.39 at 27.7 mM *vs.* 0.158±0.06 at 5.5 mM, $p<0.01$) and Ca^{2+} waves, without alteration of SR Ca^{2+} load and Ca^{2+} transient. Both pharmacological (ESI-05) and genetic deletion of Epac2 (Epac2-KO) reduced high glucose-mediated SR Ca^{2+} leak. The Epac2-dependent alterations of Ca^{2+} signalling upon high glucose were associated with higher RyR open probability measured by single channel recording incorporated into lipid bilayers, which was prevented by Epac2 inhibition (median = 0.81 [0.50 (25%); 0.99 (75%)] at 27.7mM *vs.* 0.15 [0.02 ; 0.49], $p<0.001$). Interestingly, O-GlcNAcylation inhibition by diazo-5-oxonorleucine (DON) restored the open probability of the RyR under high glucose as well as high glucose-mediated activation of Epac-based FRET biosensor. In line with the murine model, we didn't find any alteration of the Ca^{2+} transient in acutely treated human induced pluripotent stem cells derived into cardiomyocytes (h-iPSC-CM). However a chronic treatment of high glucose reduces the Ca^{2+} transient amplitude in h-iPSC-CM in an Epac2-dependent manner. To conclude, our work suggest that hyperglycemia activates Epac2 by O-GlcNAcylation

to mediate SR Ca^{2+} leak and arrhythmia that leads to the reduction of the systolic Ca^{2+} release over long term exposure that may play a role in the cardiac alterations seen in diabetic-associated cardiomyopathy.

Introduction

Hyperglycemia represents an important factor in the development of diabetic cardiac complications. Indeed, several evidences have shown that hyperglycemic conditions trigger molecular and metabolic modifications such as oxidative stress, dysregulation of energetic metabolism and Ca^{2+} mishandling, all resulting in cardiomyocytes dysfunction[1]. Yet, the mechanisms underlying this glucose toxicity on Ca^{2+} signaling remain unclear. One of these mechanisms is the activation of the hexosamine biosynthesis pathway leading to post-translational modification of proteins induced by addition of an O-linked N-Acetyl Glucosamine group to serine or threonine residues[2]. This modification, referred as O-GlcNAcylation, increases in both human and animal model of diabetes and heart failure[3]. In cardiomyocytes, O-GlcNAcylation directly alters Ca^{2+} signaling during relaxation by reducing the re-uptake of Ca^{2+} by the SERCA pump into the sarcoplasmic reticulum (SR)[4, 5]. Indeed, high glucose or glucosamine treatment of neonatal cardiomyocytes prolonged the re-uptake of Ca^{2+} by down-regulation of the SERCA pump[4]. Moreover, *in vivo* overexpression of the O-GlcNAcase in streptozotocine-injected rats (type 1 diabetes), improves the decay of the SR Ca^{2+} release (Ca^{2+} transient) and the amount of Ca^{2+} stored into the SR (SR Ca^{2+} load) which is associated to an elevation of SERCA expression and the down-regulation of phospholamban[6]. CaMKII is also a target of O-GlcNAcylation under high glucose concentration leading to Ca^{2+} mishandling and

arrhythmias[7].

In the heart, Epac are **E**xchange **p**rotein directly **a**ctivated by **c**AMP that are emerging as critical players in heart failure and arrhythmias[8-12]. Epac2 activation mediates Ca^{2+}-dependent cardiac arrhythmias by increasing the diastolic SR Ca^{2+} leak from the ryanodine receptors (RyR) *via* CaMKII activation[8, 9, 13-16]. This enhanced SR Ca^{2+} leak depletes SR Ca^{2+} load and lowers systolic SR Ca^{2+} transient[8, 9, 13-15]. Recently, we found that, under hyperglycemic treatment and in type 2 diabetic rats, CaMKII, a downstream effector of Epac2, is activated enhancing SR Ca^{2+} leak and increasing the susceptibility to cardiac arrhythmias[7]. Since acute hyperglycemia increases SR Ca^{2+} leak, one can imagine that a chronic activation will dramatically lower SR Ca^{2+} transient and cardiac contraction. However, the role of Epac2 in high glucose-mediated Ca^{2+} signaling and its consequences on Ca^{2+} signaling after chronic activation are unknown.

In the present study, we propose Epac2 activation as a new mechanism involved in acute and chronic glucose-mediated alterations of cardiac Ca^{2+} signaling in rodent and human-induced pluripotent stem cell derived into cardiomyocytes (h-iPSC-CM). We found that acute high glucose treatment activates Epac2 to induce SR Ca^{2+} leak with small consequences on excitation-contraction coupling in adult mice cardiomyocytes and h-iPSC-CM. Interestingly, chronic Epac2 activation decreases global SR Ca^{2+} release. High glucose-mediated activation of Epac2 depends on O-GlcNAcylation pathway, leading, in chronic hyperglycemic conditions, to a reduced SR Ca^{2+} transient, which could underlie the impaired contraction seen in diabetic cardiomyopathy.

Methods

Cardiomyocytes Isolation

Experiments were carried out according to the ethical principles of the French Ministry of Agriculture, conformed to the guidelines from Directive 2010/63/EU of the European Parliament on the protection of animals, or approved by the University of California Davis Institutional Animal Care and Use Committee (IACUC) in accordance with the NIH Guide for the Care and Use of Laboratory Animals. Adult cardiomyocytes were isolated, as previously described[17], from 12 weeks old male C57Bl6 mice and 12 weeks old male Epac2-KO. Epac2-KO mouse line has been kindly provided by Dr. Ju Chen (UC San Diego)[15, 16, 18]. In summary, mice were euthanized by intraperitoneal injection of pentobarbital (100 mg/kg). Hearts were excised rapidly, cannulated above the aortic valve and placed in an ice-cold oxygenated solution containing (in mM): 113 NaCl, 0.6 NaH_2PO_4, 1.6 $NaHCO_3$, 4.7 KCl, 0.6 KH_2PO_4, 1.2 $MgSO_4$, 10 HEPES, 30 Taurine and 20 D-Glucose, pH 7.4 with NaOH. Cardiac myocytes were isolated, by retrograde Langendorff perfusion method, using 5 mg/ml Liberase (TM Research Grade). After isolation, cells were kept in Tyrode's solution (in mmol/litre): 140 NaCl, 4 KCl, 1.1 $MgCl_2$, 10 HEPES, 1.8 $CaCl_2$, and 5.5 D-Glucose, pH 7.4 with NaOH for 1 hour before experiments.

Confocal Microscopy

Freshly isolated adult cardiomyocytes were loaded for 30 min with 5 µM Fluo-4 acetoxymethyl ester (Fluo-4 AM, Invitrogen) diluted in a mixture of DMSO-pluronic acid 20%. Extracellular dye was washed out and myocytes were suspended in Tyrode's solution (in mmol/litre): 140 NaCl, 4 KCl, 1.1 $MgCl_2$, 10 HEPES, 1.8 $CaCl_2$, and 5.5 D-Glucose, pH 7.4 with NaOH. Ca^{2+} Transient, Ca^{2+} sparks and SR Ca^{2+}

load were recorded using confocal microscopy (Leica® TCS SP5X, Solms, Germany, x40 water immersion objective) in line scan mode while perfused for 2-5 mins with normal (5.5 mM), mild (16.6 mM) and high (27.7 mM) glucose concentrations. Fluo-4 AM was excited with a white light laser (λex=500 nm) and emission was collected at wavelengths > 510 nm. Ca^{2+} transients were evoked by field stimulation (1 Hz) and recorded in line scan at 400Hz. Spontaneous Ca^{2+} sparks were recorded in quiescent cells at 700 Hz after Ca^{2+} transient recording. SR Ca^{2+} load was estimated by a rapid application of caffeine (10 mM) after steady state pacing and recorded at 400 Hz.

The human-induced pluripotent stem cells (h-iPSC) were produced at Nantes iPSC core facility, France. h-iPSC were differentiated into cardiomyocytes using the matrix sandwich method. Experiments were conducted at 31±1 days after differentiation. h-iPSC derived cardiomyocytes (h-iPSC-CM) were loaded for 1h at 37°C, then 15 minutes at room temperature, with Calbryte™ 520 (BIOQUEST) diluted in 20% DMSO-Pluronic at a final concentration of 10 µM. The dye was washed out and cells were re-suspended in RPMI medium and B27 supplement (Fischer Scientist) at the desired glucose concentration (5.5 mM or 27.7 mM). h-iPSC-CM were incubated 2-5 mins (acute treatment) or 7 days (chronic treatment) with different glucose concentrations. Calbryte™ 520 was excited with a white light laser (λex=500 nm) and emission was collected at wavelengths >510 nm. Cells are kept in RPMI media at 37°C during the whole experiment. Spontaneous Ca^{2+} transients were recorded at 700 Hz. Image analysis was performed using ImageJ software and homemade routines in IDL (Interactive Data Language).

Fluorescence Resonance Energy Transfer

Adenovirus encoding for a full-length Epac-based FRET sensor (CFP-ICUE-YFP) or for a CFP-AKAR-YFP, provided by Dr. Y.K. Xiang (University of California, Davis), were transfected in cultured rabbit freshly isolated cardiomyocytes for 2-4 h (M.O.I. 10-100) (5% CO2, 37C) in PC-1 medium, as previously described[16]. Experiments were performed 24 h after transfection and FRET measured in frame scan mode using confocal microscopy (Zeiss LSM5 Pascal, ×40 water immersion objective). Donor (CFP) was excited with an Ar laser (λ_{ex} set at 458 nm). Images were analyzed using ImageJ software (NIH).

Single channel recordings

Cardiac SR-enriched microsomes for single channel recordings were prepared from frozen mouse hearts, perfused with normal 5.5 mM or high glucose 27.7 mM Tyrode solution. Hearts were homogenized by differential centrifugation. Briefly, 5 mouse hearts were pooled and homogenized using a Teflon pestle in homogenization buffer (0.9% NaCl, Tris-HCl 10 mM pH 6.8, plus protease inhibitors: 2 µM leupeptin, 100 µM phenylmethylsulphonyl fluoride, 500 µM benzamidine, 100 nM aprotinin, and phosphatase inhibitors: 50 mM NaF, 1 mM Na Orthovanadate, 5 mM Na pyrophosphate, 1 mM β-glycerolphosphate), and centrifuged at 1000 x g for 3 minutes at 4˚C, supernatants were centrifuged a second time at 8000 x g for 20 minutes at 4˚C. Supernatants were further centrifuged at 100,000 x g for 35 minutes at 4˚C. The pellets containing SR-enriched microsomes were suspended in homogenization buffer supplemented with 0.3 M sucrose.

Planar lipid bilayers, composed of phospholipid mixture of phosphatidylethanolamine, phosphatidylserine and lecithin (1.0:0.9:0.1 ratio dissolved in n-decane to 50 mg/ml)

(Matreya, LLC) were painted with a glass rod across an aperture of 150 µm diameter in a Delrin cup. The cis chamber represented the cytosolic side, which was held at virtual ground and contained the reference electrode. The trans chamber corresponded to the luminal side and contained the voltage command electrode. Electrodes were connected to the head stage of a 200B Axopatch amplifier. Both chambers contain 1000 µL of cesium methanesulphonate (CsCH3SO3), 20 mM MOPS (3-(N-morpholino) propanesulfonic acid), pH 7.2 with nominally free [Ca^{2+}] (~3-5 µM). Cs^{+} was selected as the charge carrier to increase the channel conductance, and to avoid any contribution from potassium channels present in the SR membrane. Chloride channels were inhibited by using the non-permeant anion methanesulfonate. A cesium gradient of cis (300 mM) and trans (50 mM) was used to favor channel incorporation, and SR-enriched microsomes were added to the cis chamber. Channel recordings were recorded at 0 mV holding potential, after filtration with a 8-pole low-pass Bessel filter set at 1 kHz and digitized at 4 kHz using a Digidata 1440A AD/DA interface. Data acquisition and analysis were performed with Axon Instruments (Burlingame, CA, USA) hardware and software (pClamp 10), and Origin.

Western Blotting

Mice hearts were perfused 15 mins with Tyrode solution containing normal (5.5 mM) or high glucose (27.7 mM) concentration ± ESI-05 10µM. Proteins were then extracted from the left ventricle with RIPA buffer. 30 µg of protein extracts were resolved on 7% SDS-PAGE gels and transferred to nitrocellulose membrane then incubated overnight with commercial p-$RyR2^{S2814}$ or p-$RyR2^{S2808}$ (Badrilla, 1/2000) and total RyR2 (ThermoFisher, 1/1000) primary antibody. Results were analysed

using Image J software.

Co-Immunoprecipitation

Ventricular cardiomyocytes were isolated from mice hearts and treated 30 mins with Tyrode solution containing PUGNAC 50 µM in normal (5.5 mM) or high glucose (27.7 mM) concentrations ± UDP-GlcNac 500 µM. Proteins were then extracted with RIPA buffer. For each condition, 50 µl of Dynabeads protein G (Invitrogen 10007) were suspended with Epac2 antibody rabbit antibody (Proteintech 1/1000) at a final concentration of 2 µg/µl. Rabbit IgG at 1 µg/µl was used as a negative control.
300 µg of our protein samples were pre-cleared with the Dynabeads-Epac2 Ab complex. WB experiments were then performed using 8-20% SDS-PAGE gels and transferred to nitrocellulose membrane then incubated with Epac2 (Proteintech 1/1000) and O-GlcNAc mouse antibody (ThermoFisher 1/1000).

Quantitative RT-qPCR

Total RNA was extracted by trizol. First cDNA strand was synthesized with a total of 1 µg mRNA in 20 µL using iScriptTM cDNA Synthesis Kit (Bio-Rad). Transcript levels of cDNA were analysed in triplicate by real-time polymerised chain reaction performed with CFX96 RT-PCR system (Bio-Rad) using SoAdvanced™ SYBER Green containing 0.5 µM of specific primers. SLC4A1AP-R human (Forward: 5'-CCTCTACGATCTGGGAAGCA-3', Reverse: 5'-TCTGGTCCCTGCAGGATAAA-3') and NUBP1 human (Forward: 5'-CAGAGGGGCTTCATGTCAGG-3', Reverse: 5'-GATTTCCTCTATAGCCGTGTCC-3') were used as housekeeping genes. Refer to the table below for primers sequences.

Gene	Forward	Reverse
Epac1	GCTCTTTGAACCACACAGCA	TGTCTTCTCGCAGGATGATG
Epac2	ATTAATGGACGCCTGTTTGC	CATGCACGCAGTTGAAGAGT
NCX	ACCTGTTTGGCCAACCTGTCTTCA	TGCTGGTCAGTGGCTGCTTGT
SERCA2A	TCACCTGTGAGAATTGACTGG	AGAAAGAGTGTGCAGCGGAT
RyR2	TAGATTTATAAGGGGCCTTG	GATTCTTCAGGGCTCGTAGT
Cav1.2	CATCATCATCTTCTCCCTCCTG	CATCACCGAATTCCAGTCCT

Statistical Analysis

Data were expressed as mean ± SEM or median [5-95%] percentile. Significance was evaluated by using two way ANOVA or kruskal-Wallis test followed by a post-hoc test, as appropriate.

Results

Epac2 mediates SR Ca^{2+} leak and pro-arrhythmic events during acute hyperglycemia

At 12 weeks old Epac2-KO do not present any cardiac hypertrophy or sign of heart failure (Suppl. Figure 1). The ESI-05, at the concentration used, prevents the 8-CPT-mediated SR Ca^{2+} transient decrease, transient decay lengthening and Ca^{2+} sparks release enhancement (Suppl. Figure 2) showing that ESI-05 effectively blocks 8-CPT-mediated Epac activation on Ca^{2+} transient and Ca^{2+} sparks frequency. Upon acute high glucose, SR Ca^{2+} leak increased, as shown by the significant raise of Ca^{2+} spark frequency (CaSpF) (Figure 1A-B) although SR Ca^{2+} load was similar in all groups (Figure 1C). This increase of CaSpF was associated with a raise in pro-arrhythmic events incidence with 25% increase in mild glucose and 36% increase in

high glucose (Figure 1D-E). Finally, Epac2 inhibition, by ESI-05, as well as genetic deletion prevented high glucose-mediated effects on CaSpF and pro-arrhythmic events (Figure 1B-E). The absence of effect upon 27.7 mM mannitol clearly rules out any osmotic-depend side effects. Those results clearly show that Epac2 does mediate acute high-glucose dependent SR Ca^{2+} leak and pro-arrhythmic events.

Acute hyperglycemia does not alter Ca^{2+} transient

The SR Ca^{2+} leak seen under high glucose concentrations does not affect neither SR Ca^{2+} load (Figure 1C) nor the Ca^{2+} transient amplitude upon the different glucose concentrations in both control and Epac2 KO cardiomyocytes (Figure 2A-B). Furthermore, the SERCA activity is not modified with hyperglycemia exposure since the Ca^{2+} transient decay time is not altered under any condition (Figure 2A-C).

Next, we verified whether the high glucose-mediated Epac2 regulation of Ca^{2+} signaling observed in rodent was transposable to human, we studied the impact of high glucose treatment and Epac2 inhibition in human pluripotent stem cells derived in cardiomyocytes (h-iPSC-CM) on Ca^{2+} handling. We found that acute treatment with high glucose concentration (27.7 mM) does not alter Ca^{2+} transient amplitude similarly to murine cardiomyocytes (Figure 3A-C). Besides, high glucose concentration did not alter h-iPSC-CM cycle length (Figure 3A-B). Even though Epac2 inhibition, under normal glucose concentration, increases the cell cycle length, this alteration had no impact on the amplitude of the Ca^{2+} transient amplitude (Figure 3C).

Chronic hyperglycemia alters Ca^{2+} transient in h-iPSC-CM

In diabetes, studies have shown that impaired contraction and relaxation is related to

a drop in SR Ca^{2+} release and SERCA pump dysfunction [19-21]. Here, we treated the h-iPSC-CM during 1 week with high glucose to mimic chronic hyperglycemia. Interestingly, contrarily to acute high glucose treatment, chronic high glucose exposure (27.7 mM) significantly decreased h-iPSC-CM Ca^{2+} transient amplitude ($p<0.05$) (Figure 4A-C). This effect on Ca^{2+} transient was prevented under Epac2 inhibition with ESI-05 suggesting that in human, Epac2 mediates high glucose-dependent Ca^{2+} signaling alterations (Figure 4A-C). Moreover, we observed a decrease of the cell cycle length with 27.7 mM glucose compared to 5.5 mM ($P<0.001$). A similar decrease was observed under 27.7 mM mannitol (Figure 4A-B) suggesting that osmolarity may affect the cell heart rate of spontaneously beating h-iPSC-CM without affecting the Ca^{2+} transient. The role of Epac2 in high glucose-mediated Ca^{2+} mishandling is more likely due to its activation rather than changes in expression level since the Epac1 mRNA (Supp. Figure 3A) or Epac2 mRNA (Suppl. Figure 3B) were not significantly altered by glucose concentrations variations. Those results clearly show that chronic high glucose conditions participate, *via* the activation of Epac2, in the drop of SR Ca^{2+} transient.

Epac2 increases ryanodine receptor activity during acute hyperglycemia

To test whether the SR Ca^{2+} leak is due to the modification of the RyR activity, we assessed the RyR2 channel current in lipid bilayers and microsome extracts containing RyR receptors. In microsomes obtained from *ex vivo*-perfused hearts with high glucose, RyR open probability is increased (Figure 5A-B). Those results are in line with the high-glucose-mediated increase of SR Ca^{2+} leak as shown in Figure 1. The higher RyR open probability in high glucose was prevented in presence of ESI-05, showing that RyR activation in high glucose depends on Epac2. Even though,

studies have shown that during β-adrenergic stimulation, Epac2 induces SR Ca^{2+} leak *via* CaMKII-dependent phosphorylation of RyR at serine 2814[9], we did not find any modifications of the RyR phosphorylation state neither at the CaMKII (S2814) (Figure 5C) nor at the PKA (S2808) site (Figure 5D) under high glucose concentration.

Epac2 undergoes O-GlcNAc-dependent activation during acute hyperglycemia

To decipher the mechanism of Epac2 activation in hyperglycemic condition, we used a full-length Epac-based FRET sensor activity (ICUE) in presence of normal (5.5 mM), high (16.6 mM) and very high (27.7 mM) glucose concentrations. First, Fig. 6A-B clearly shows that elevation of glucose concentration significantly increases ICUE activity in a concentration dependent-manner, as measured by the F_{CFP}/F_{YFP} ratio. This high-glucose mediated activation of the sensor is similar to the one obtained with Epac specific activator (8-CPT) or Epac physiological activation (ISO+H89). Interestingly, the level of the endogenous activator of Epac2, the cAMP, indirectly assessed by the activity of PKA-based FRET sensor [22], was unchanged (Suppl. Figure 4). However, inhibition of the hexosamine biosynthesis pathway with the 6-Diazo-5-oxo-L-norleucine (DON), a glutamine-fructose amidotransferase inhibitor, fully blocked the FRET signal induced by high glucose concentrations (Fig. 6B), showing that Epac2 activation by high glucose concentration is mediated by O-GlcNAcylation. Interestingly the increase of the RyR open probability was prevented by the inhibition of the O-GlcNAcylation pathway by the DON in a similar manner as seen with the inhibition of Epac2 (Figure 5A-B). This shows that RyR activation in high glucose is the result of Epac2 activation by O-GlcNAcylation. We then tested whether Epac2 undergoes O-GlcNAc modification using co-immunoprecipitation.

Interestingly, we could reveal for the first time a basal Epac2 co-immunoprecipitation with the O-GlcNAc moiety showing that Epac2 is O-GlcNAcylated at baseline (Figure 6C). Altogether, those results show that, under acute hyperglycemia, Epac2 is functionally activated by O-GlcNAcylation pathway.

Discussion

Epac2, a downstream effector of cAMP is a key regulator of Ca^{2+} handling in ventricular cardiomyocytes under pathological conditions[23, 24]. The activation of Epac2 induces abnormal pro-arrythmogenic diastolic Ca^{2+} leak[9, 15, 16, 18], a phenotype seen under high glucose concentration[7, 25]. Recently, it has been shown that hyperglycemic concentrations activate CaMKII, a downstream effector of Epac2, inducing Ca^{2+} mishandling[7] as seen under Epac2 activation[9, 15, 16, 18]. In cardiomyocytes, high glucose activates several deleterious pathways, including the alteration of the ECC [26, 27]. Yet, little is known about the underlying mechanisms [4, 7, 25, 28, 29]. Although high glucose-mediated CaMKII activation induces Ca^{2+} mishandling[7], the role of Epac2, in those alterations hasn't been elucidated yet. Here, we demonstrate for the first time that : 1) Epac2 mediates the high glucose-dependent Ca^{2+} signaling alteration and 2) this high-glucose activation of Epac2 is dependent of the O-GlcNAcylation pathway.

High glucose-induced SR Ca^{2+} leak is mediated by Epac2 and O-GlcNAcylation

Our work show for the first time that high glucose-mediated SR Ca^{2+} leak and subsequent arrhythmogenic events [7, 25] depends on Epac2 activation. Indeed, the increase of Ca^{2+} sparks frequency was reduced by the pharmacological inhibition of Epac2 by ESI-05. Although ESI-05 has off-target effects, including mitochondrial

stress-associated arrhythmogenic events at high concentrations (25 µM) [30], the absence of SR Ca^{2+} leak or arrhytmogenic events in Epac2-KO under high glucose, as seen under ESI-05, rule out any possible off-target effects. In our study, the increase of the SR Ca^{2+} leak under high glucose was associated with higher RyR open probability, rather than a modification of the SR Ca^{2+} load or change in phosphorylation state of RyR (CaMKII or PKA) as seen in HF [31-33] or under Epac2 activation [9]. In contrast, both Sommese *et al.* [34] and Federico *et al.*[28] have reported an increase of CaMKII-dependent RyR phosphorylation with an increase of the RyR activity, respectively, in cardiomyocytes of rat fed with high fructose diet and HEK293 cells treated with high glucose concentration (450mg/dl). Besides it is to note that Ser2814 is not the only CaMKII-dependent RyR phosphorylation site, and thus other potential phosphorylation sites, although not well described, should not be excluded[33]. Besides phosphorylation, RyR is also subject to oxidation [35, 36] which increases its activity and Ca^{2+} leak observed in HF [37-39]. One of the high glucose-mediated deleterious effects involves ROS production in the cell [40, 41] that has recently been reported to be CaMKII-dependent in mice cardiomyocytes [25]. Epac also activates CaMKII by a pathway involving a ROS related enzyme, the nitric oxide synthase 1 [42]. Altogether, these findings suggest a potential involvment of the oxidation pathway in the observed SR Ca^{2+} leak *via* a possible high glucose/Epac/CaMKII/ROS/RyR mechanism where oxidation can activate both RyR and CaMKII.

In high glucose Epac2 is activated by O-GlcNAcylation pathway

Our work reveals that Epac2 activation is mediated by the hexosamines biosynthesis pathway, a new mechanism of activation never described before. We found that the

inhibition of the O-GlcNAcylation pathway prevents the opening of the RyR under high glucose concentration as with Epac2 inhibition. This shows that both Epac2 and O-GlcNAcylation are required for the activation of RyR under high glucose concentrations. The O-GlcNAcylation dependent activation of Epac2 together with CaMKII direct O-GlycNAcylation [7] could synergize to potentiate SR Ca^{2+} leak under high glucose. The cardiomyocyte O-GlcNAcylation state also regulates phospholamban activity which compromises Ca^{2+} repumping by SERCA[43] participating in the generation of arrhythmogenic events seen under high glucose concentration by increasing diastolic Ca^{2+} levels [44]. Even though to date, cAMP is the only reported endogenous Epac activator [45, 46], we did not observe any increase of the cAMP levels in our study. Interestingly, we observed that activation of Epac under high glucose is prevented by the inhibition of the O-GlcNacyaltion pathway with DON, showing that Epac activation by glucose is mediated by O-GlcNAcylation. Since Epac possesses several serine and threonine residues[47, 48], Epac2 activation under high glucose could be the result of a direct O-GlcNAcylation of the protein. Indeed, our Co-IP experiments show for the first time that Epac2 is O-GlcNacylated and proteomic investigations, such as mass spectrometry[49], will be needed to determine the potential Epac O-GlcNAcylation sites.

Chronic high glucose reduces Ca^{2+} transient amplitude in h-iPSC-CM in an Epac2 dependent manner

We didn't observe any alteration of the Ca^{2+} transient in adult mice ventricular cells under high glucose, despite the observed SR Ca^{2+} leak which could be explained by an unchanged SR Ca^{2+} content[50] or absence of LTCC Ca^{2+} entry changes under acute Epac activation[9]. Those results are in line with Lu *et al.* study [25] that did not

observe any alteration of the Ca^{2+} transient in mice cardiomyocytes under high glucose. To test the relevance of this mechanism in human, we used h-iPSC-CM. Although this cellular model possesses spontaneous beating activity and lacks t-tubules organization, it expresses all the components of the ECC and is emerging as an interesting model in studying cardiac alterations despite its immature phenotype[51]. As observed in mice ventricular cells, there is no modification of the Ca^{2+} transient amplitude in the h-iPSC-CM under acute high glucose as seen by Lu *et al*.[25]. Interestingly, Lu et al. found an increase in the spontaneous Ca^{2+} release, as we described in mice cardiomyocytes, and that was associated with an increase of CaMKII-mediated ROS production[25]. However, a sustained SR Ca^{2+} leak under high glucose concentrations[25] is known to lower the SR Ca^{2+} load over time affecting the Ca^{2+} transient amplitude[50]. Thus, we studied the effect of longer high glucose exposure (7 days) on the Ca^{2+} transient in h-iPSC-CM. We observed a decrease in the Ca^{2+} transient amplitude, prevented by Epac2 that could affect cell shortening as described by Ng *et al*.[29] in h-iPSC-CM treated for 7 days with high glucose. Moreover, we didn't observe any alteration of the ECC components expressions such as the RyR, the LTCC, SERCA or NCX that might explain the Ca^{2+} transient amplitude reduction. This suggests that this same alteration of Ca^{2+} transient induced by Epac2 activation and subsequent cardiac contraction may also exist in adult human cardiomyocytes, a mechanism that could participate in the compromised systolic activity of diabetic patients leading to heart failure[52-54].

Epac2, a potential target of diabetic cardiomyopathy?

Diabetes mellitus is a metabolic disorder with a chronic hyperglycemic state, and constitutes a major risk factor of HF [55]. In diabetic patients, cardiovascular

complications represent the main cause of hospitalization and death. Growing evidences highlight the existence of a diabetic cardiomyopathy independent of vascular diseases, and defined by a reduction of cardiac contraction and relaxation [52, 53, 56].

In diabetes, Epac is up-regulated in diabetic kidney cells and mediates hypertrophy[57] and leptin resistance[58]. Furthermore, Epac2 is implicated in insulin secretion and pancreatic-specific Epac2-KO mice are prone to obesity and leptin resistance[58]. However, to date, no studies have investigated the role of Epac2 in diabetic cardiomyopathy. Ca^{2+} alterations have been described in diabetic animal models such as a decrease of the Ca^{2+} transient amplitude [19, 20, 59-61], as observed in our h-iPSC-CM model, which participates in the contractile diabetic dysfunction. Furthermore, O-GlcNAcylation levels are increased in diabetes participating in Ca^{2+} mishandling [6, 62, 63], where the inhibition of the O-GlcNAcylation pathway prevents cardiac fractional shortening reduction in diabetic type 2 mice [62] and improves diastolic function of perfused diabetic type 1 mice heart [6]. Since Epac2 is activated under high glucose by O-GlcNAcylation mediating Ca^{2+} mishandling as seen in diabetes, it would be interesting to investigate the possible role of Epac2 in ECC alteration seen in diabetes.

Conclusion

In this work, we deciphered a new mechanism of high glucose-mediated Ca^{2+} mishandling featuring Epac2. In mice ventricular cardiomyocytes, acute exposure of high glucose activated Epac2 by O-GlcNAcylation, inducing SR Ca^{2+} leak and arrhythmogenic events without affecting the Ca^{2+} transient. However, a longer exposure to high glucose, as observed in h-iPSC-CM decreases the Ca^{2+} transient

amplitude depending on Epac2 without modification of the ECC components expression. The decrease of the Ca^{2+} transient amplitude is known to participate in the reduction of the cardiac contractile activity as seen in diabetes. Thus, this described mechanism could be involved in the alteration of cardiac contraction observed in diabetes, placing Epac2 as a novel therapeutic target in the treatment of diabetic cardiomyopathy.

Acknowledgement

We thank Dr. Ju Chen from University of San Diego for providing the Epac2-KO and WT mice line. We also thank Saba Daneshpooy, Mikael Habtezion and Kayvon Jabbari for their technical assistance. This work funded by a MENSRI doctoral fellowship to M.SH and by a grant ANR-11-1DEX-0003-02 and Lefoulon Delalande post-doctoral fellowship to L.P. and as members of the Laboratory of Excellence LERMIT.

References

1. Joubert M, Manrique A, Cariou B and Prieur X. Diabetes-related cardiomyopathy: The sweet story of glucose overload from epidemiology to cellular pathways. *Diabetes Metab*. 2018.
2. Chatham JC and Marchase RB. The role of protein O-linked beta-N-acetylglucosamine in mediating cardiac stress responses. *Biochimica et biophysica acta*. 2010;1800:57-66.
3. Wright JN, Collins HE, Wende AR and Chatham JC. O-GlcNAcylation and cardiovascular disease. *Biochem Soc Trans*. 2017;45:545-553.
4. Clark RJ, McDonough PM, Swanson E, Trost SU, Suzuki M, Fukuda M and Dillmann WH. Diabetes and the accompanying hyperglycemia impairs cardiomyocyte calcium cycling through increased nuclear O-GlcNAcylation. *The Journal of biological chemistry*. 2003;278:44230-7.
5. Ren J, Gintant GA, Miller RE and Davidoff AJ. High extracellular glucose impairs cardiac E-C coupling in a glycosylation-dependent manner. *Am J Physiol*. 1997;273:H2876-83.
6. Hu Y, Belke D, Suarez J, Swanson E, Clark R, Hoshijima M and Dillmann WH.

Adenovirus-mediated overexpression of O-GlcNAcase improves contractile function in the diabetic heart. *Circulation research*. 2005;96:1006-13.
7. Erickson JR, Pereira L, Wang L, Han G, Ferguson A, Dao K, Copeland RJ, Despa F, Hart GW, Ripplinger CM and Bers DM. Diabetic hyperglycaemia activates CaMKII and arrhythmias by O-linked glycosylation. *Nature*. 2013;502:372-6.
8. Hothi SS, Gurung IS, Heathcote JC, Zhang Y, Booth SW, Skepper JN, Grace AA and Huang CL. Epac activation, altered calcium homeostasis and ventricular arrhythmogenesis in the murine heart. *Pflugers Arch*. 2008;457:253-70.
9. Pereira L, Metrich M, Fernandez-Velasco M, Lucas A, Leroy J, Perrier R, Morel E, Fischmeister R, Richard S, Benitah JP, Lezoualc'h F and Gomez AM. The cAMP binding protein Epac modulates Ca2+ sparks by a Ca2+/calmodulin kinase signalling pathway in rat cardiac myocytes. *The Journal of physiology*. 2007;583:685-94.
10. Pereira L, Ruiz-Hurtado G, Morel E, Laurent AC, Metrich M, Dominguez-Rodriguez A, Lauton-Santos S, Lucas A, Benitah JP, Bers DM, Lezoualc'h F and Gomez AM. Epac enhances excitation-transcription coupling in cardiac myocytes. *Journal of molecular and cellular cardiology*. 2012;52:283-91.
11. Ruiz-Hurtado G, Dominguez-Rodriguez A, Pereira L, Fernandez-Velasco M, Cassan C, Lezoualc'h F, Benitah JP and Gomez AM. Sustained Epac activation induces calmodulin dependent positive inotropic effect in adult cardiomyocytes. *Journal of molecular and cellular cardiology*. 2012;53:617-25.
12. Ruiz-Hurtado G, Morel E, Dominguez-Rodriguez A, Llach A, Lezoualc'h F, Benitah JP and Gomez AM. Epac in cardiac calcium signaling. *Journal of molecular and cellular cardiology*. 2013;58:162-71.
13. Oestreich EA, Malik S, Goonasekera SA, Blaxall BC, Kelley GG, Dirksen RT and Smrcka AV. Epac and phospholipase Cepsilon regulate Ca2+ release in the heart by activation of protein kinase Cepsilon and calcium-calmodulin kinase II. *The Journal of biological chemistry*. 2009;284:1514-22.
14. Oestreich EA, Wang H, Malik S, Kaproth-Joslin KA, Blaxall BC, Kelley GG, Dirksen RT and Smrcka AV. Epac-mediated activation of phospholipase C(epsilon) plays a critical role in beta-adrenergic receptor-dependent enhancement of Ca2+ mobilization in cardiac myocytes. *The Journal of biological chemistry*. 2007;282:5488-95.
15. Pereira L, Cheng H, Lao DH, Na L, van Oort RJ, Brown JH, Wehrens XH, Chen J and Bers DM. Epac2 mediates cardiac beta1-adrenergic-dependent sarcoplasmic reticulum Ca2+ leak and arrhythmia. *Circulation*. 2013;127:913-22.
16. Pereira L, Rehmann H, Lao DH, Erickson JR, Bossuyt J, Chen J and Bers DM. Novel Epac fluorescent ligand reveals distinct Epac1 vs. Epac2 distribution and function in cardiomyocytes. *Proceedings of the National Academy of Sciences of the United States of America*. 2015;112:3991-6.
17. Leroy J, Richter W, Mika D, Castro LR, Abi-Gerges A, Xie M, Scheitrum C, Lefebvre F, Schittl J, Mateo P, Westenbroek R, Catterall WA, Charpentier F, Conti M, Fischmeister R and Vandecasteele G. Phosphodiesterase 4B in the cardiac L-type Ca(2)(+) channel complex regulates Ca(2)(+) current and protects against ventricular arrhythmias in mice. *The Journal of clinical investigation*. 2011;121:2651-61.
18. Pereira L, Bare DJ, Galice S, Shannon TR and Bers DM. 0beta-Adrenergic induced SR Ca2+ leak is mediated by an Epac-NOS pathway. *Journal of molecular and cellular cardiology*. 2017.
19. Choi KM, Zhong Y, Hoit BD, Grupp IL, Hahn H, Dilly KW, Guatimosim S, Lederer WJ and Matlib MA. Defective intracellular Ca(2+) signaling contributes to cardiomyopathy in Type 1 diabetic rats. *American journal of physiology Heart and circulatory physiology*. 2002;283:H1398-408.

20. Pereira L, Matthes J, Schuster I, Valdivia HH, Herzig S, Richard S and Gomez AM. Mechanisms of [Ca2+]i transient decrease in cardiomyopathy of db/db type 2 diabetic mice. *Diabetes*. 2006;55:608-15.
21. Yaras N, Ugur M, Ozdemir S, Gurdal H, Purali N, Lacampagne A, Vassort G and Turan B. Effects of diabetes on ryanodine receptor Ca release channel (RyR2) and Ca2+ homeostasis in rat heart. *Diabetes*. 2005;54:3082-8.
22. Zhang H, Makarewich CA, Kubo H, Wang W, Duran JM, Li Y, Berretta RM, Koch WJ, Chen X, Gao E, Valdivia HH and Houser SR. Hyperphosphorylation of the cardiac ryanodine receptor at serine 2808 is not involved in cardiac dysfunction after myocardial infarction. *Circulation research*. 2012;110:831-40.
23. Gema Ruiz-Hurtado AD-R, Laetitia Pereira, María Fernández-Velasco, Cécile Cassan, Frank Lezoualc'h, Jean-Pierre Benitah, Ana M. Gómez. Sustained Epac activation induces calmodulin dependent positive inotropic effect in adult cardiomyocytes. *Journal of molecular and cellular cardiology*. 2012;53:617-625.
24. Lezoualc'h F, Fazal L, Laudette M and Conte C. Cyclic AMP Sensor EPAC Proteins and Their Role in Cardiovascular Function and Disease. *Circulation research*. 2016;118:881-97.
25. Lu S, Liao Z, Lu X, Katschinski DM, Mercola M, Chen J, Heller Brown J, Molkentin JD, Bossuyt J and Bers DM. Hyperglycemia Acutely Increases Cytosolic Reactive Oxygen Species via O-linked GlcNAcylation and CaMKII Activation in Mouse Ventricular Myocytes. *Circulation research*. 2020;126:e80-e96.
26. Bugger H and Abel ED. Molecular mechanisms of diabetic cardiomyopathy. *Diabetologia*. 2014;57:660-71.
27. Kolwicz SC, Jr. and Tian R. Glucose metabolism and cardiac hypertrophy. *Cardiovasc Res*. 2011;90:194-201.
28. Federico M, Portiansky EL, Sommese L, Alvarado FJ, Blanco PG, Zanuzzi CN, Dedman J, Kaetzel M, Wehrens XHT, Mattiazzi A and Palomeque J. Calcium-calmodulin-dependent protein kinase mediates the intracellular signalling pathways of cardiac apoptosis in mice with impaired glucose tolerance. *The Journal of physiology*. 2017;595:4089-4108.
29. Ng KM, Lau YM, Dhandhania V, Cai ZJ, Lee YK, Lai WH, Tse HF and Siu CW. Empagliflozin Ammeliorates High Glucose Induced-Cardiac Dysfuntion in Human iPSC-Derived Cardiomyocytes. *Sci Rep*. 2018;8:14872.
30. Yang Z, Kirton HM, Al-Owais M, Thireau J, Richard S, Peers C and Steele DS. Epac2-Rap1 Signaling Regulates Reactive Oxygen Species Production and Susceptibility to Cardiac Arrhythmias. *Antioxid Redox Signal*. 2016.
31. Huke S, Desantiago J, Kaetzel MA, Mishra S, Brown JH, Dedman JR and Bers DM. SR-targeted CaMKII inhibition improves SR Ca^{2+} handling, but accelerates cardiac remodeling in mice overexpressing CaMKII δ C. *Journal of molecular and cellular cardiology*. 2011;50:230-8.
32. van Oort RJ, McCauley MD, Dixit SS, Pereira L, Yang Y, Respress JL, Wang Q, De Almeida AC, Skapura DG, Anderson ME, Bers DM and Wehrens XH. Ryanodine receptor phosphorylation by calcium/calmodulin-dependent protein kinase II promotes life-threatening ventricular arrhythmias in mice with heart failure. *Circulation*. 2010;122:2669-79.
33. Wehrens XH, Lehnart SE, Reiken SR and Marks AR. Ca2+/calmodulin-dependent protein kinase II phosphorylation regulates the cardiac ryanodine receptor. *Circulation research*. 2004;94:e61-70.
34. Sommese L, Valverde CA, Blanco P, Castro MC, Rueda OV, Kaetzel M, Dedman J, Anderson ME, Mattiazzi A and Palomeque J. Ryanodine receptor phosphorylation by CaMKII promotes spontaneous Ca(2+) release events in a rodent model of early stage diabetes: The arrhythmogenic substrate. *Int J Cardiol*. 2016;202:394-406.

35. Boraso A and Williams AJ. Modification of the gating of the cardiac sarcoplasmic reticulum Ca(2+)-release channel by H2O2 and dithiothreitol. *Am J Physiol*. 1994;267:H1010-6.
36. Sun J, Yamaguchi N, Xu L, Eu JP, Stamler JS and Meissner G. Regulation of the cardiac muscle ryanodine receptor by O(2) tension and S-nitrosoglutathione. *Biochemistry*. 2008;47:13985-90.
37. Jung C, Martins AS, Niggli E and Shirokova N. Dystrophic cardiomyopathy: amplification of cellular damage by Ca2+ signalling and reactive oxygen species-generating pathways. *Cardiovasc Res*. 2008;77:766-73.
38. Lim G, Venetucci L, Eisner DA and Casadei B. Does nitric oxide modulate cardiac ryanodine receptor function? Implications for excitation-contraction coupling. *Cardiovasc Res*. 2008;77:256-64.
39. Terentyev D, Györke I, Belevych AE, Terentyeva R, Sridhar A, Nishijima Y, de Blanco EC, Khanna S, Sen CK, Cardounel AJ, Carnes CA and Györke S. Redox modification of ryanodine receptors contributes to sarcoplasmic reticulum Ca2+ leak in chronic heart failure. *Circulation research*. 2008;103:1466-72.
40. Brownlee M. The pathobiology of diabetic complications: a unifying mechanism. *Diabetes*. 2005;54:1615-25.
41. Giacco F and Brownlee M. Oxidative stress and diabetic complications. *Circulation research*. 2010;107:1058-70.
42. Pereira L, Bare DJ, Galice S, Shannon TR and Bers DM. beta-Adrenergic induced SR Ca2+ leak is mediated by an Epac-NOS pathway. *Journal of molecular and cellular cardiology*. 2017;108:8-16.
43. Yokoe S, Asahi M, Takeda T, Otsu K, Taniguchi N, Miyoshi E and Suzuki K. Inhibition of phospholamban phosphorylation by O-GlcNAcylation: implications for diabetic cardiomyopathy. *Glycobiology*. 2010;20:1217-26.
44. Bers DM. Calcium cycling and signaling in cardiac myocytes. *Annu Rev Physiol*. 2008;70:23-49.
45. de Rooij J, Zwartkruis FJ, Verheijen MH, Cool RH, Nijman SM, Wittinghofer A and Bos JL. Epac is a Rap1 guanine-nucleotide-exchange factor directly activated by cyclic AMP. *Nature*. 1998;396:474-7.
46. Kawasaki H, Springett GM, Mochizuki N, Toki S, Nakaya M, Matsuda M, Housman DE and Graybiel AM. A family of cAMP-binding proteins that directly activate Rap1. *Science (New York, NY)*. 1998;282:2275-9.
47. Rehmann H, Arias-Palomo E, Hadders MA, Schwede F, Llorca O and Bos JL. Structure of Epac2 in complex with a cyclic AMP analogue and RAP1B. *Nature*. 2008;455:124-7.
48. Rehmann H, Das J, Knipscheer P, Wittinghofer A and Bos JL. Structure of the cyclic-AMP-responsive exchange factor Epac2 in its auto-inhibited state. *Nature*. 2006;439:625-8.
49. Ma J and Hart GW. O-GlcNAc profiling: from proteins to proteomes. *Clinical proteomics*. 2014;11:8.
50. Eisner DA, Caldwell JL, Kistamás K and Trafford AW. Calcium and Excitation-Contraction Coupling in the Heart. *Circulation research*. 2017;121:181-195.
51. Karakikes I, Ameen M, Termglinchan V and Wu JC. Human induced pluripotent stem cell-derived cardiomyocytes: insights into molecular, cellular, and functional phenotypes. *Circulation research*. 2015;117:80-8.
52. de Simone G, Devereux RB, Chinali M, Lee ET, Galloway JM, Barac A, Panza JA and Howard BV. Diabetes and incident heart failure in hypertensive and normotensive participants of the Strong Heart Study. *J Hypertens*. 2010;28:353-60.
53. Devereux RB, Roman MJ, Paranicas M, O'Grady MJ, Lee ET, Welty TK, Fabsitz RR,

Robbins D, Rhoades ER and Howard BV. Impact of diabetes on cardiac structure and function: the strong heart study. *Circulation*. 2000;101:2271-6.
54. Rawshani A, Rawshani A, Franzen S, Sattar N, Eliasson B, Svensson AM, Zethelius B, Miftaraj M, McGuire DK, Rosengren A and Gudbjornsdottir S. Risk Factors, Mortality, and Cardiovascular Outcomes in Patients with Type 2 Diabetes. *N Engl J Med*. 2018;379:633-644.
55. Kannel WB and McGee DL. Diabetes and cardiovascular disease. The Framingham study. *Jama*. 1979;241:2035-8.
56. Rubler S, Dlugash J, Yuceoglu YZ, Kumral T, Branwood AW and Grishman A. New type of cardiomyopathy associated with diabetic glomerulosclerosis. *The American journal of cardiology*. 1972;30:595-602.
57. Sun L, Kondeti VK, Xie P, Raparia K and Kanwar YS. Epac1-mediated, high glucose-induced renal proximal tubular cells hypertrophy via the Akt/p21 pathway. *The American journal of pathology*. 2011;179:1706-18.
58. Hwang M, Go Y, Park JH, Shin SK, Song SE, Oh BC, Im SS, Hwang I, Jeon YH, Lee IK, Seino S and Song DK. Epac2a-null mice exhibit obesity-prone nature more susceptible to leptin resistance. *International journal of obesity (2005)*. 2017;41:279-288.
59. Belke DD, Swanson EA and Dillmann WH. Decreased sarcoplasmic reticulum activity and contractility in diabetic db/db mouse heart. *Diabetes*. 2004;53:3201-8.
60. Delucchi F, Berni R, Frati C, Cavalli S, Graiani G, Sala R, Chaponnier C, Gabbiani G, Calani L, Del Rio D, Bocchi L, Lagrasta C, Quaini F and Stilli D. Resveratrol treatment reduces cardiac progenitor cell dysfunction and prevents morpho-functional ventricular remodeling in type-1 diabetic rats. *PloS one*. 2012;7:e39836.
61. Depre C, Young ME, Ying J, Ahuja HS, Han Q, Garza N, Davies PJ and Taegtmeyer H. Streptozotocin-induced changes in cardiac gene expression in the absence of severe contractile dysfunction. *Journal of molecular and cellular cardiology*. 2000;32:985-96.
62. Fricovsky ES, Suarez J, Ihm SH, Scott BT, Suarez-Ramirez JA, Banerjee I, Torres-Gonzalez M, Wang H, Ellrott I, Maya-Ramos L, Villarreal F and Dillmann WH. Excess protein O-GlcNAcylation and the progression of diabetic cardiomyopathy. *Am J Physiol Regul Integr Comp Physiol*. 2012;303:R689-99.
63. Ramirez-Correa GA, Ma J, Slawson C, Zeidan Q, Lugo-Fagundo NS, Xu M, Shen X, Gao WD, Caceres V, Chakir K, DeVine L, Cole RN, Marchionni L, Paolocci N, Hart GW and Murphy AM. Removal of Abnormal Myofilament O-GlcNAcylation Restores Ca2+ Sensitivity in Diabetic Cardiac Muscle. *Diabetes*. 2015;64:3573-87.

Figures legends

<u>Fig1</u>: High glucose-mediated SR Ca^{2+} leak and pro-arrhythmogenic events is Epac2-dependent. (A) Representative examples of line-scan images recorded by confocal microscopy from control and Epac2-KO cardiomyocytes treated with different glucose concentration. **(B)** The corresponding mean of Ca^{2+} spark frequency (CaSpF) measured as number of sparks per 100 μm/s from control cardiomyocytes acutely treated (2-5 min) with normal (5.5 mM, n=28), high (16.6 mM, n=12), very high (27.7 mM, n=14) glucose concentrations ±ESI-05 10 μM (Epac2 specific inhibitor, n=12) and 27.7 mM mannitol (n=5), and from Epac2-KO myocytes under normal (5.5 mM; n=14) and high glucose (27.7 mM, n=15). **(C)** SR Ca^{2+} load in the same groups (for control cardiomyocytes treated with normal 5.5 mM (n=26), high 16.6mM (n=8), very high 27.7 mM glucose (n=14) with Epac2 specific inhibition (ESI-05, n=4), 27.7 mM mannitol (n=8) and from Epac2-KO cardiomyocytes under normal 5.5mM (n=14) and very high 27.7mM glucose concentration (n=9). **(D)** Representative examples of line-scan images recorded by confocal microscopy from control and Epac2-KO cardiomyocytes treated with different glucose concentrations. **(E)** Percentage of cardiomyocytes presenting waves and triggered activities in high *vs*. normal glucose concentration from control and Epac2-KO mice. *p<0.05.

<u>Fig2:</u> Acute high glucose does not alter Ca^{2+} transient in adult mice cardiomyocytes. (A) Representative examples of line-scan images recorded by confocal microscopy from adult mice cardiomyocytes paced at 1 Hz and treated acutely (2-5 mins) with different glucose concentrations and their respective Ca^{2+} transient profiles. **(B)** The corresponding Ca^{2+} transient amplitude and **(C)** Ca^{2+} decay time constants (τ) (ms) of control cardiomyocytes under normal 5.5 mM (n=38) and high 27.7 mM glucose concentration (n=26) ±ESI-05 10 μM (Epac-2 inhibitor, n=14), and 27.7 mM mannitol (n=8), and from Epac2-KO cardiomyocytes under normal 5.5 mM (n=10) and high 27.7 mM glucose concentration (n=9). P=N.S.

<u>Fig3:</u> h-iPSC-CM does not exhibit any alteration of Ca^{2+} homeostasis under acute high glucose. (A) Representative examples of line-scan images recorded by confocal microscopy from h-iPSC-CM treated acutely (2-5 mins) with different glucose concentration and their respective Ca^{2+} transient profile. **(B)** The corresponding cycle length average and **(C)** mean of Ca^{2+} transient amplitude without field-stimulation under normal 5.5 mM (n=39) ±ESI-05 10 μM (Epac-2 inhibitor, n=12) and high 27.7 mM glucose concentration (n=26) ±ESI-05 10 μM (n=12). *p<0.05.

<u>Fig4:</u> h-iPSC-CM exhibit an Epac2-dependant decrease of the Ca^{2+} transient amplitude under chronic high glucose. (A) Representative examples of line-scan images recorded by confocal microscopy from h-iPSC-CM chronically treated (7 days) with different glucose concentration and their respective Ca^{2+} transient profile. **(B)** The corresponding cycle length average and **(C)** mean of Ca^{2+} transient amplitude without field-stimulation under normal 5.5 mM (n=26) and high 27.7 mM glucose concentration (n=29) ±ESI-05 10 μM (Epac-2 inhibitor, n=14) and 27.7 mM mannitol (n=19). *p<0.05, ***p<0.001

Fig5: Epac2 and O-GlcNacylation increase RyR activity under high glucose condition. (A) Representative single cardiac RyR channel recording in lipid bilayers from microsomes extracted from mice hearts treated with different glucose concentrations. **(B)** The corresponding open probability (P_0) of RyR channels under normal 5.5 mM glucose concentration (n=9) *vs*. high glucose concentration 27.7 mM (n=7) glucose ± ESI-05 10μM (n=10), ±DON 50μM (n=7). **(C)** Representative immunoblot of RyR_2 phosphorylation on the CAMKII site (Ser 2814) compared to the total RyR_2 from perfused mice hearts. The corresponding mean of RyR_2 phosphorylation at S2814 normalized to the total RyR_2 in cardiomyocytes treated with normal 5.5 mM glucose concentration (n=6) *vs.* high 27.7mM glucose (n=6) ± Epac2 inhibitor ESI-05 10μM (n=6), and Isoproterenol 1μM (n=6). **(D)** Representative immunoblot of RyR_2 phosphorylation on the PKA site (Ser 2808) compared to the total RyR_2. The corresponding mean of RyR_2 phosphorylation at S2808 normalized to the total RyR_2 in cardiomyocytes treated with normal 5.5 mM glucose concentration (n=6) *vs*. high 27.7mM glucose (n=6) ± Epac2 inhibitor ESI-05 10 μM (n=6), and Isoproterenol 1μM (n=6). ******p<0.01.

Fig6: high glucose-mediated Epac2 activation is O-GlcNAcylation dependent. (A) Representative examples of FRET recording in isolated rabbit cardiomyocytes transfected with Epac-based FRET biosensor under different glucose concentration. **(B)** The corresponding T-Tubular Epac level activation under normal (5.5 mM, n=52), high glucose concentration (16.6 mM, n=36; 27.7 mM, n=22) ±O-GlcNAcylation inhibitor DON (n=13 and 5), 27.7 mM mannitol (n=13), *vs.* direct (8-pCPT, n=12) or β-AR–mediated activation (n=8 for ISO±H89) of Epac. **(C)** Representative example of Epac2 co-immunoprecipitation with O-GlcNAc-specific antibody in mice cardiomyocytes (n=3). *p<0.05, **p<0.01

Supplemental data

Suppl. Fig1: Normal cardiac phenotype in 12 weeks male Epac2-KO mice. (A) Heart weight/body weight ratio (HW/BW), **(B)** lung weight/body weight ratio (LW/BW), **(C)** heart weight/tibial length ratio (HW/TL), and **(D)** lung weight/tibial length ratio (LW/TL) in male Epac2-WT (n=8) and male Epac2-KO (n=5) mice. p=N.S.

Suppl. Fig2: Epac2 inhibitor (ESI-05) blocks Epac2 agonist (8-CPT) effects on Ca^{2+} transient. (A) The Ca^{2+} transient amplitude and the corresponding **(B)** Ca^{2+} decay time constants (τ) (ms) of control cardiomyocytes under normal 5.5 mM (n=9) ±8-CPT 10 μM (n=9), ±ESI-05 10 μM (n=6), and ±ESI-05 10 μM with 8-CPT 10 μM (n=6). **(C)** The mean of Ca^{2+} spark frequency (CaSpF) measured as number of sparks per 100 μm/s from control cardiomyocytes treated with normal normal 5.5 mM (n=6) ±8-CPT 10 μM (n=6), ±ESI-05 10 μM (n=3), and ±ESI-05 10 μM with 8-CPT 10 μM (n=3).

Suppl. Fig3: Chronic high glucose does not alter the ECC components mRNA expression. (A) Relative Epac1, **(B)** Epac2, **(C)** SERCA2a, **(D)** NCX, **(E)** RyR2, **(F)** Cav1.2 mRNA expression normalized to their respective control in h-iPSC-CM treated chronically (7 days) with normal (5.5 mM, n=7), high (16.6 mM, n=7) and very high (27.7 mM, n=7) glucose concentration and 27.7mM mannitol (n=7).

<u>Suppl. Fig4:</u> High glucose concentrations don't raise cAMP levels. (A) Examples of FRET recording in isolated rabbit cardiomyocytes transfected with PKA-based FRET biosensor under different glucose concentration. **(B)** The corresponding average PKA-based cAMP FRET biosensor activation under normal (5.5 mM, n=25), high (16.6 mM, n=10) and very high (27.7 mM, n=7) glucose concentration, 27.7 mM mannitol (n=3), and isoproterenol 100 nM (n=6). **p<0.01

<u>Suppl. Fig5</u>: O-GlcNacylation levels are enhanced in mice hearts following high glucose concentration perfusion. Representative immunoblot of O-GlcNAc levels in cardiomyocytes from hearts (used for Co-IP experiments) perfused 15 mins with normal 5.5 mM (n=3) and high 27.7 mM (n=3) glucose concentration ± UDP-GlcNAc 500 μM (substrate of the O-GlcNAcylation pathway), along with PUGNAC 50 μM (O-GlcNAcase inhibitor) (n=3).

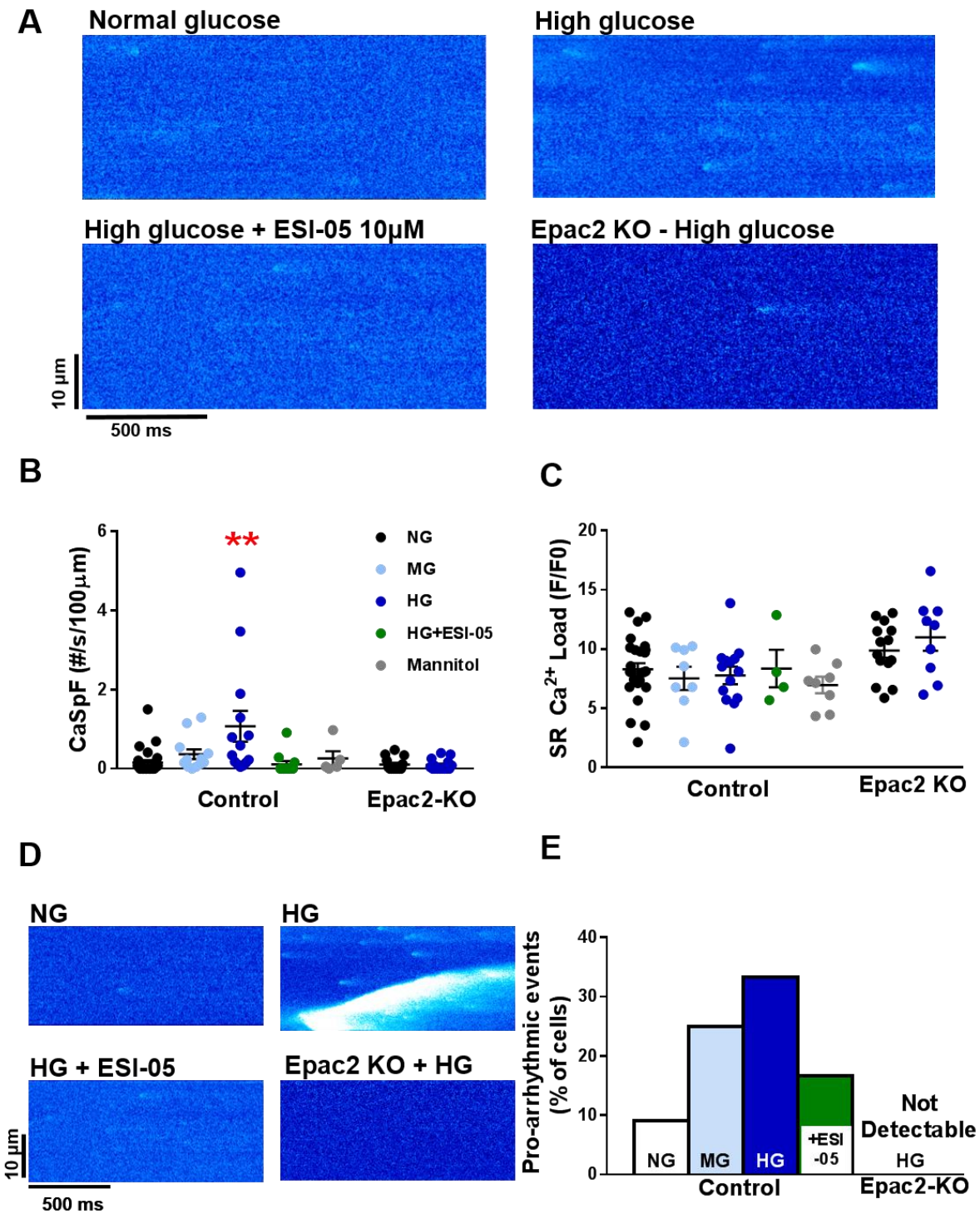
A
Normal glucose
High glucose
High glucose + ESI-05 10µM
Epac2 KO - High glucose
10 µm
500 ms
B
CaSpF (#/s/100µm)
**
NG
MG
HG
HG+ESI-05
Mannitol
Control
Epac2-KO
C
SR Ca2+ Load (F/F0)
Control
Epac2 KO
D
NG
HG
HG + ESI-05
Epac2 KO + HG
10 µm
500 ms
E
Pro-arrhythmic events (% of cells)
NG
MG
HG
+ESI -05
Not Detectable
HG
Control
Epac2-KO

Figure 1

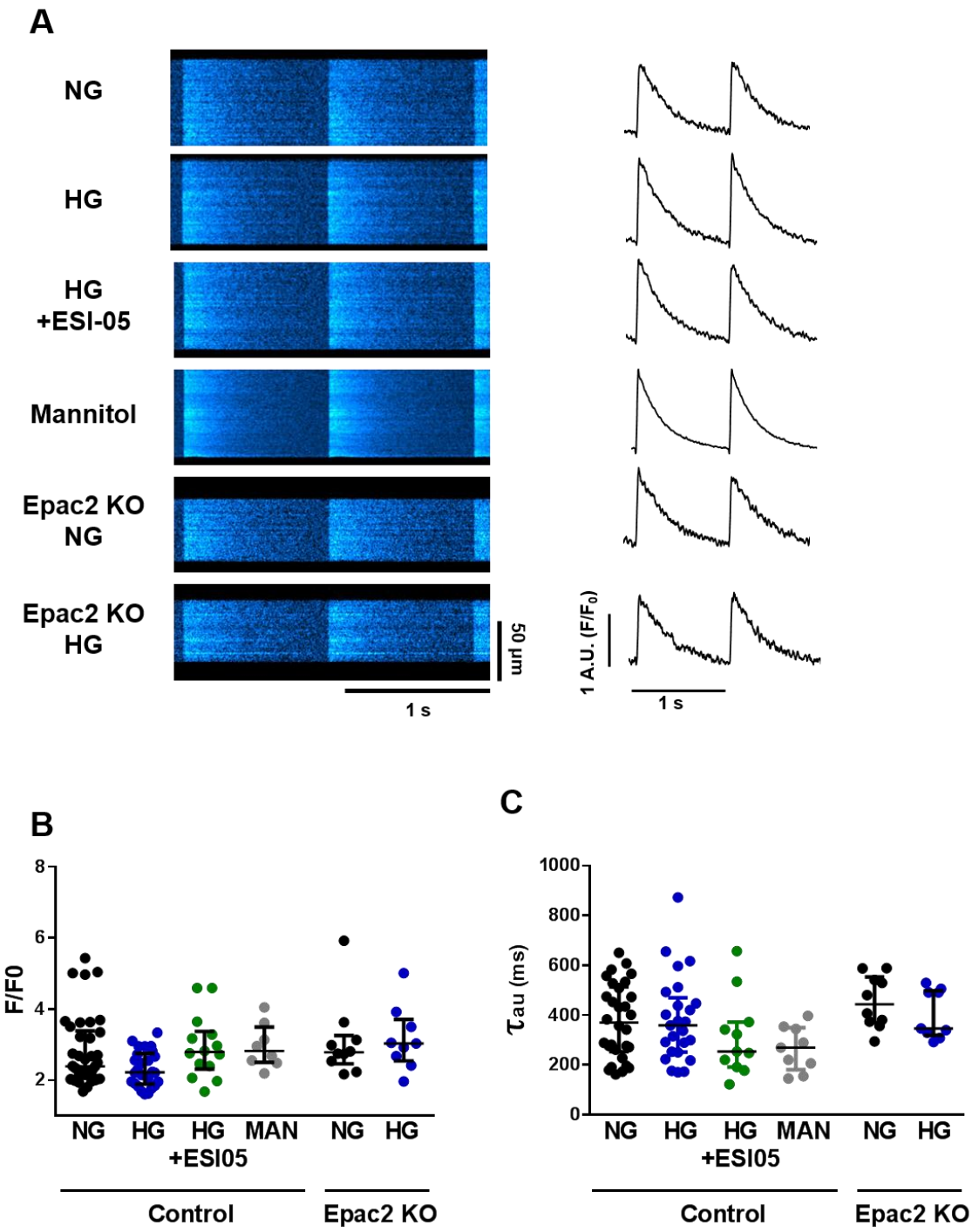
A
NG
HG
HG
+ESI-05
Mannitol
Epac2 KO
NG
Epac2 KO
HG
50 µm
1 s
1 A.U. (F/F0)
1 s
B
F/F0
8
6
4
2
NG
HG
HG
+ESI05
MAN
NG
HG
Control
Epac2 KO
C
τau (ms)
1000
800
600
400
200
0
NG
HG
HG
+ESI05
MAN
NG
HG
Control
Epac2 KO

Figure 2

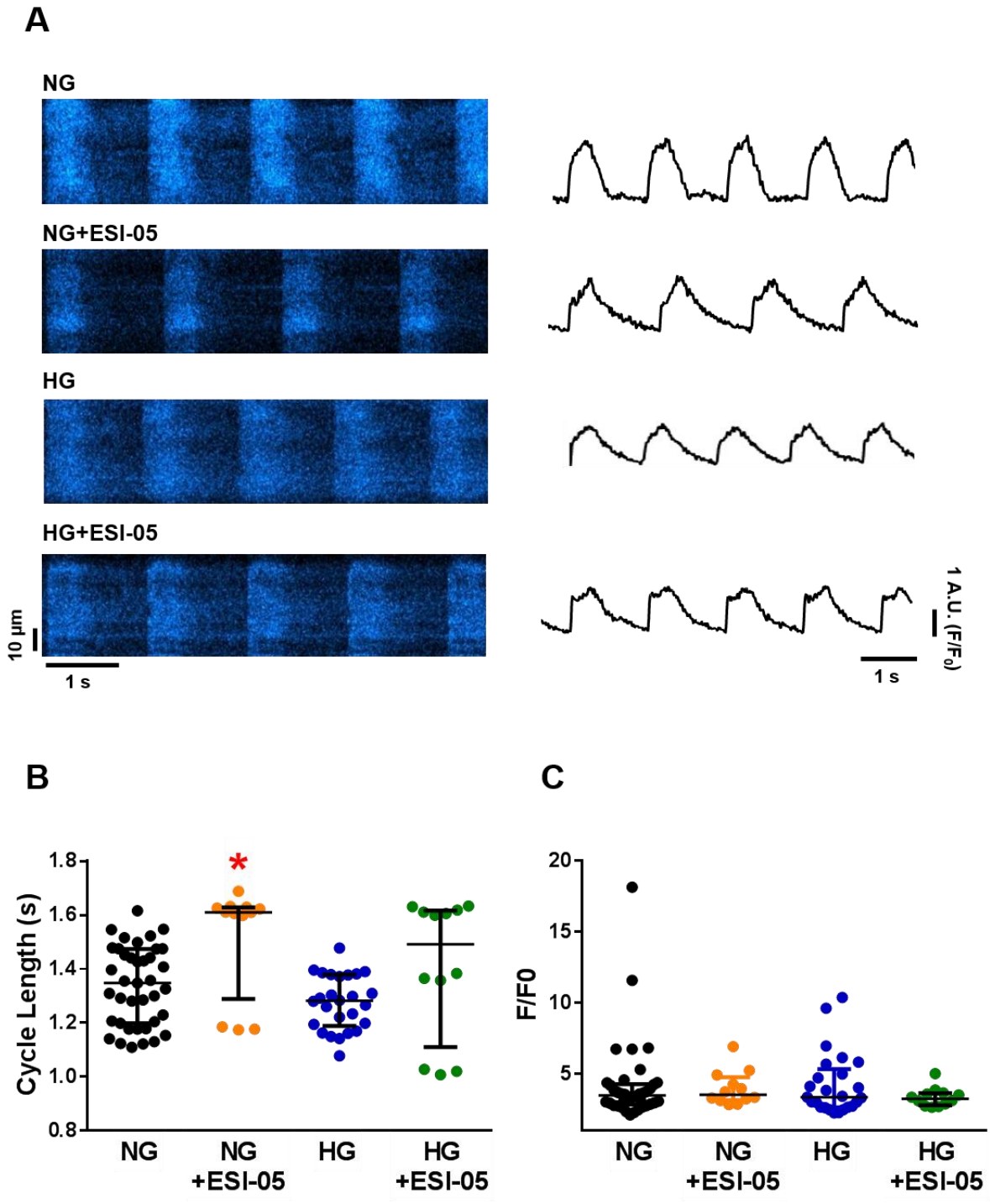
A
NG
NG+ESI-05
HG
HG+ESI-05
10 µm
1 s
1 A.U. (F/F0)
1 s
B
Cycle Length (s)
1.8
1.6
1.4
1.2
1.0
0.8
*
NG
NG +ESI-05
HG
HG +ESI-05
C
F/F0
20
15
10
5
NG
NG +ESI-05
HG
HG +ESI-05

Figure 3

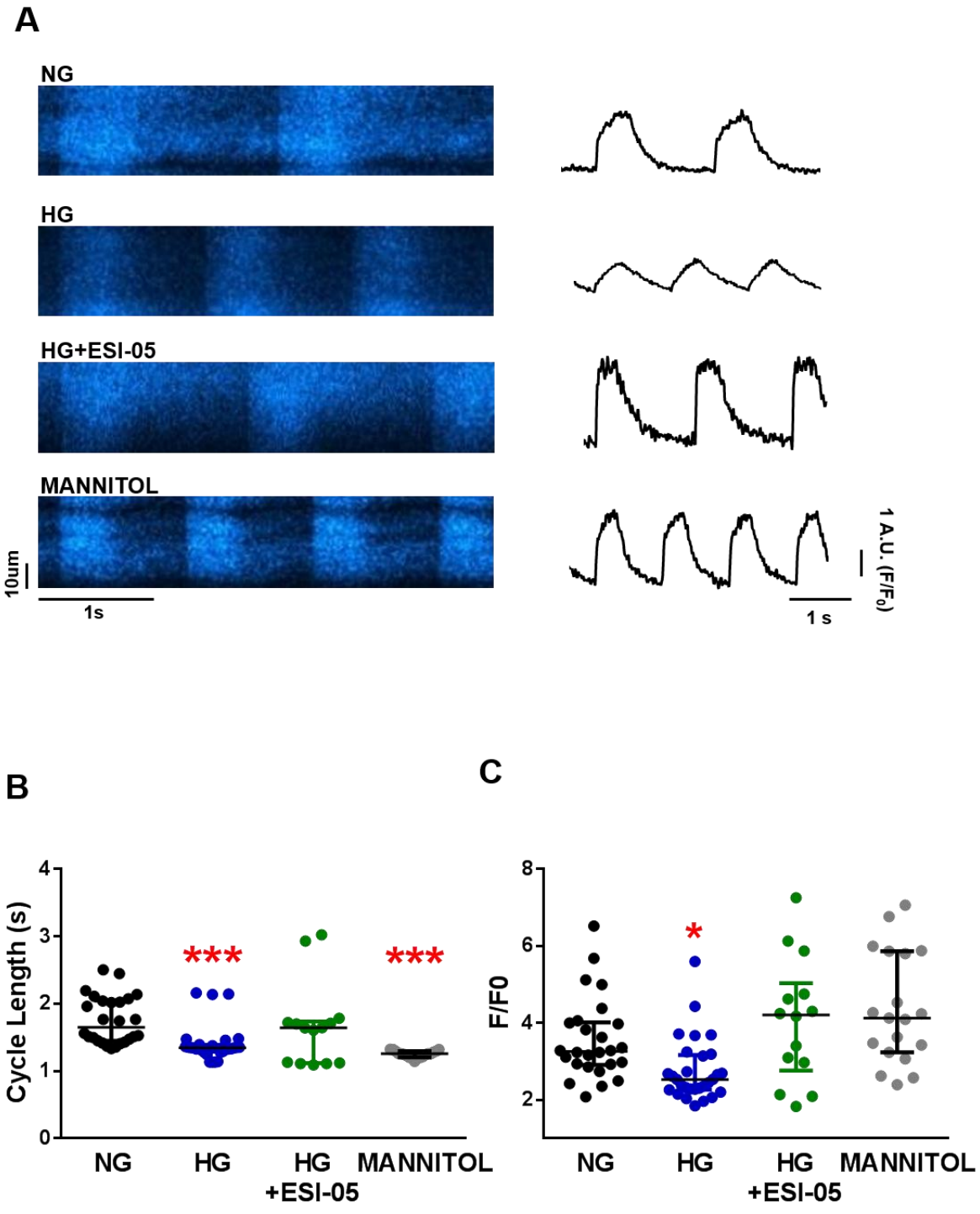
A
NG
HG
HG+ESI-05
MANNITOL
10um
1s
1 s
1 A.U. (F/F0)
B
Cycle Length (s)
***
***
NG
HG
HG +ESI-05
MANNITOL
C
F/F0
*
NG
HG
HG +ESI-05
MANNITOL

Figure 4

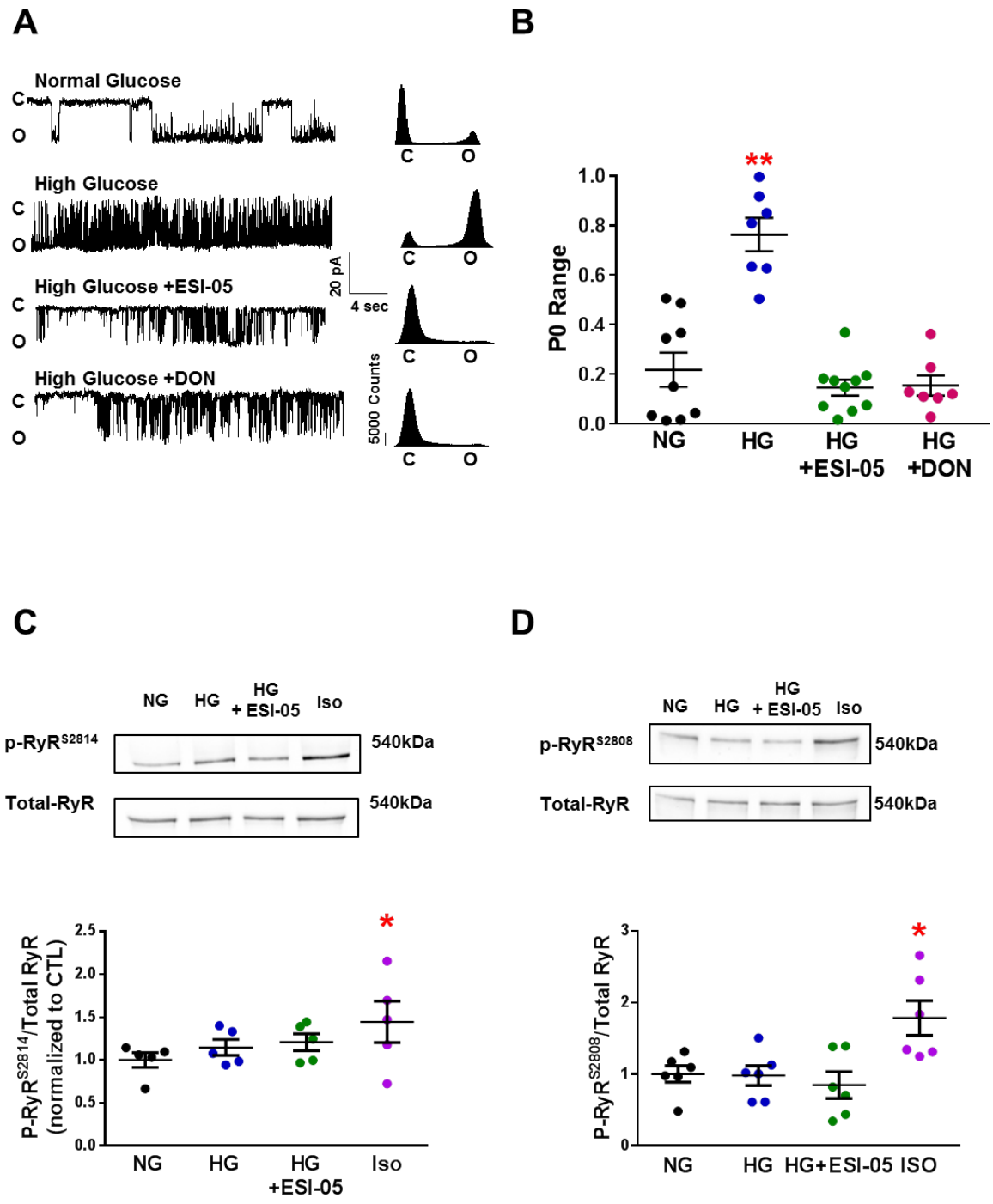
A
Normal Glucose
High Glucose
High Glucose +ESI-05
High Glucose +DON
C
O
20 pA
4 sec
5000 Counts
B
P0 Range
1.0
0.8
0.6
0.4
0.2
0.0
**
NG
HG
HG +ESI-05
HG +DON
C
NG
HG
HG + ESI-05
Iso
p-RyR S2814
Total-RyR
540kDa
P-RyR S2814/Total RyR (normalized to CTL)
2.5
2.0
1.5
1.0
0.5
0.0
*
NG
HG
HG +ESI-05
Iso
D
NG
HG
HG + ESI-05
Iso
p-RyR S2808
Total-RyR
540kDa
P-RyR S2808/Total RyR
3
2
1
0
*
NG
HG
HG+ESI-05
ISO

Figure 5

A

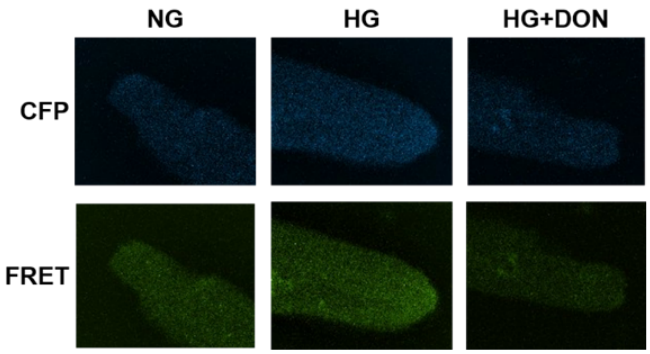
NG
HG
HG+DON
CFP
FRET

B

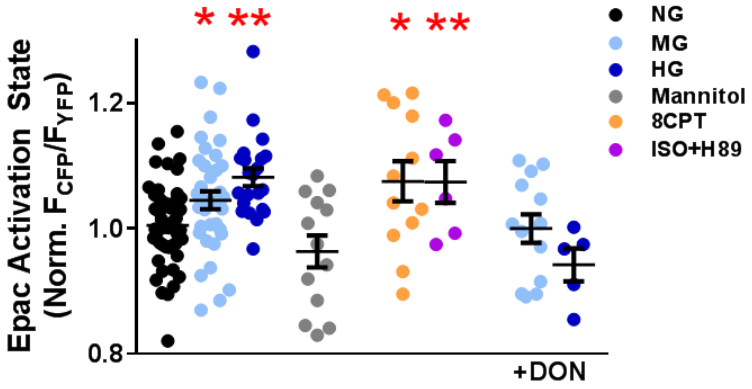
* **
* **
NG
MG
HG
Mannitol
8CPT
ISO+H89
Epac Activation State
(Norm. FCFP/FYFP)
1.2
1.0
0.8
+DON

C

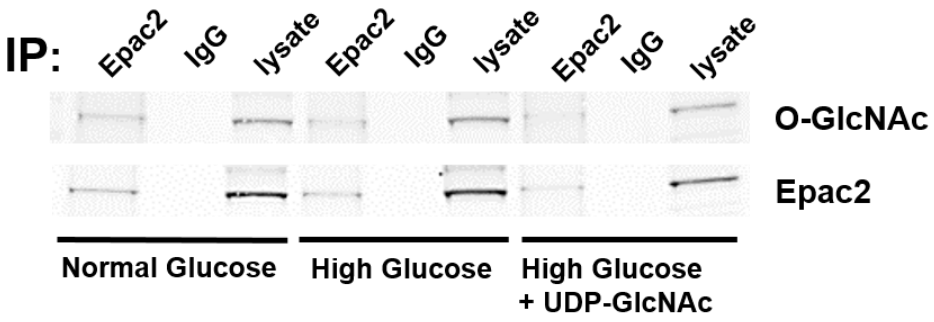
IP:
Epac2
IgG
lysate
Epac2
IgG
lysate
Epac2
IgG
lysate
O-GlcNAc
Epac2
Normal Glucose
High Glucose
High Glucose
+ UDP-GlcNAc

Figure 6

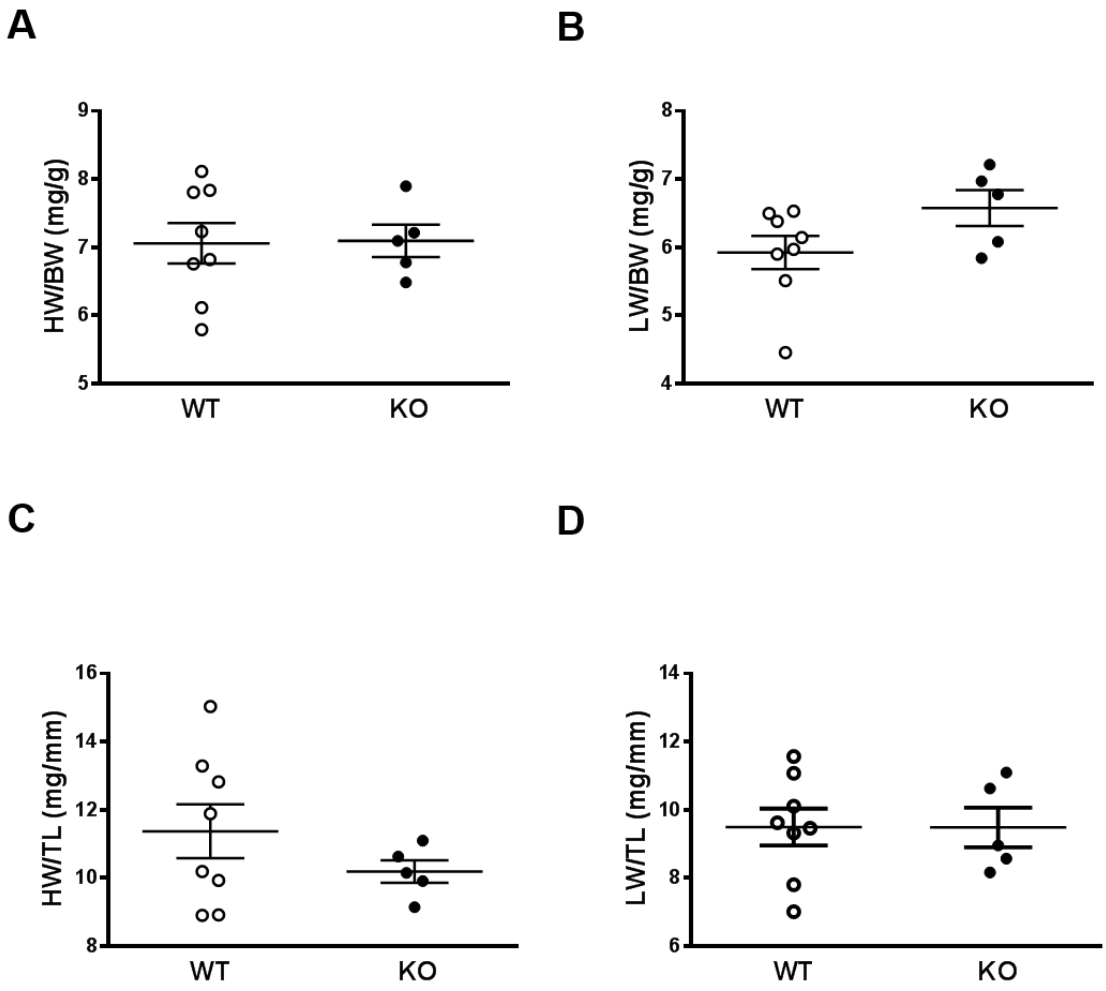

Supplemental Figure 1

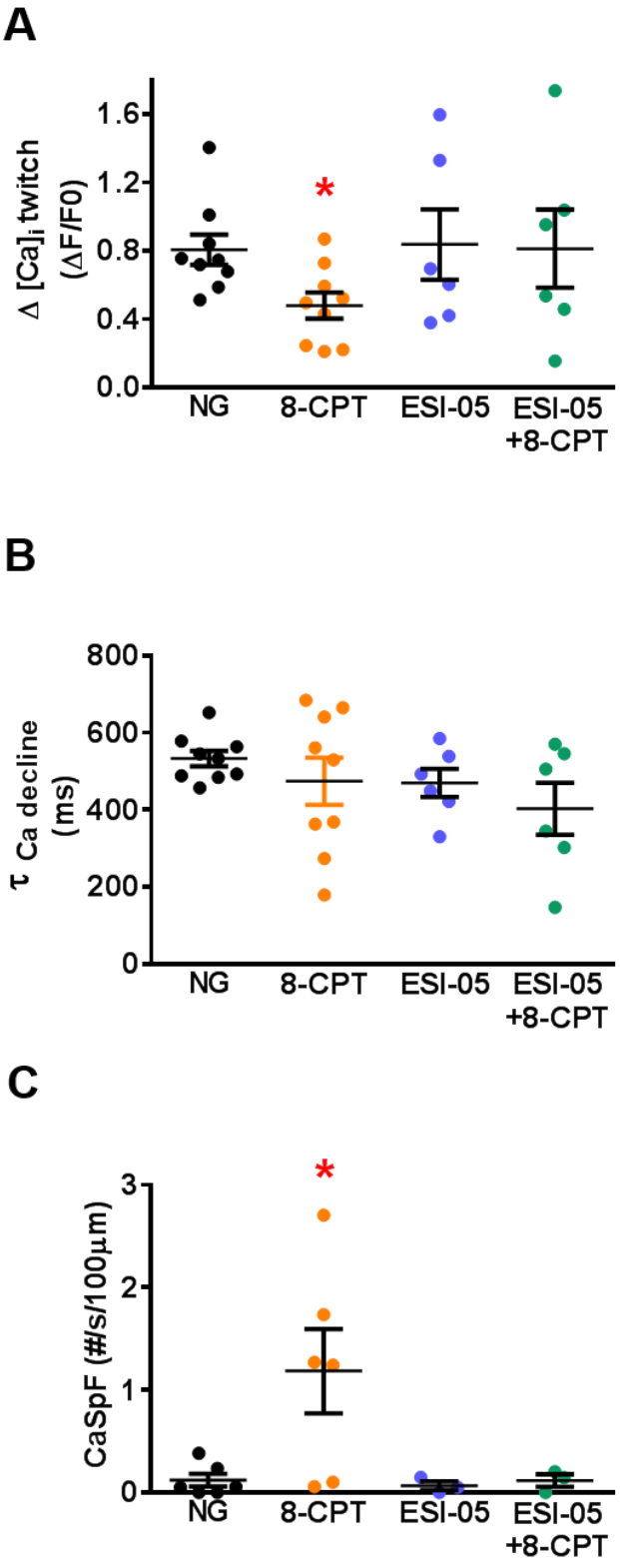

Supplemental Figure 2

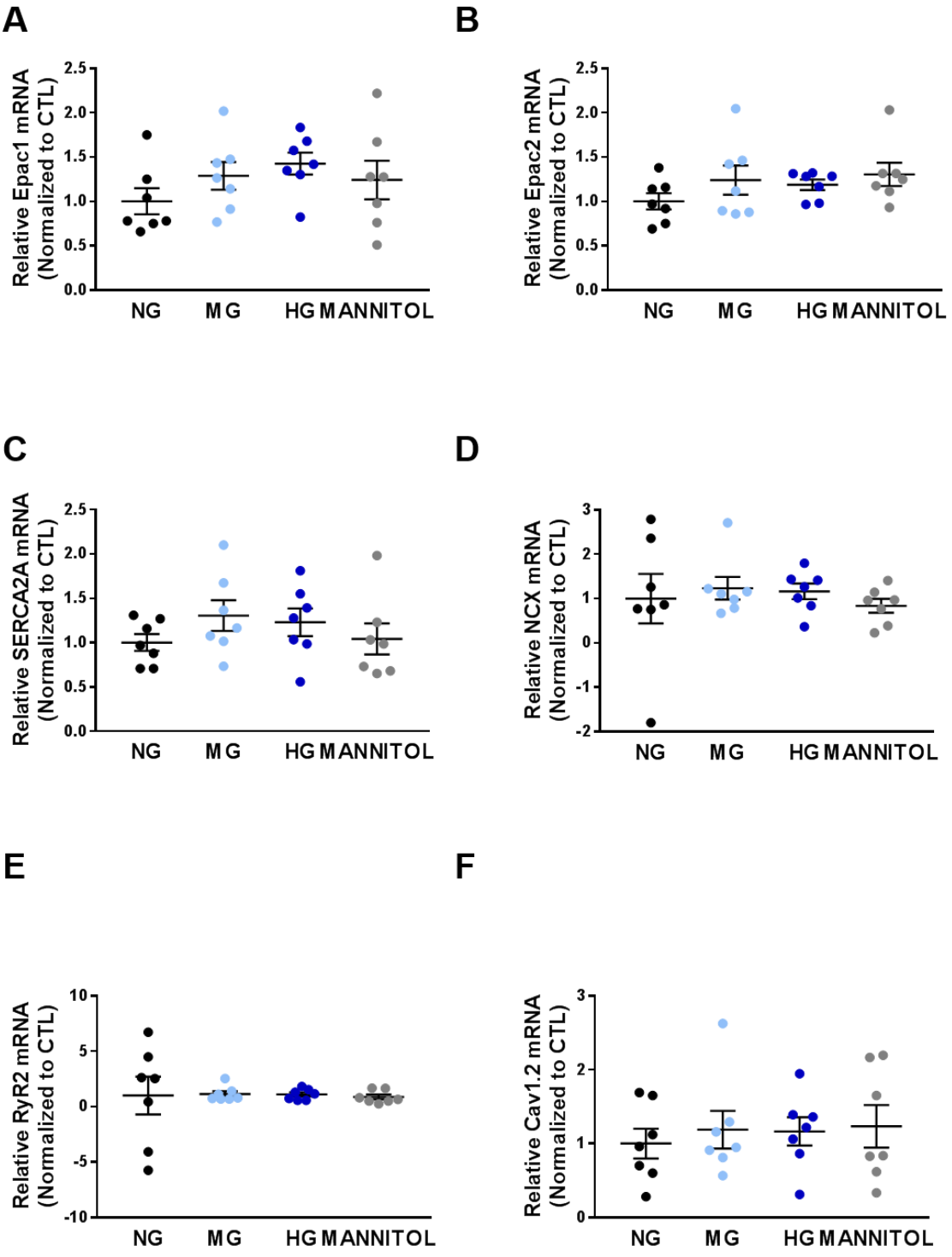

Supplemental Figure 3

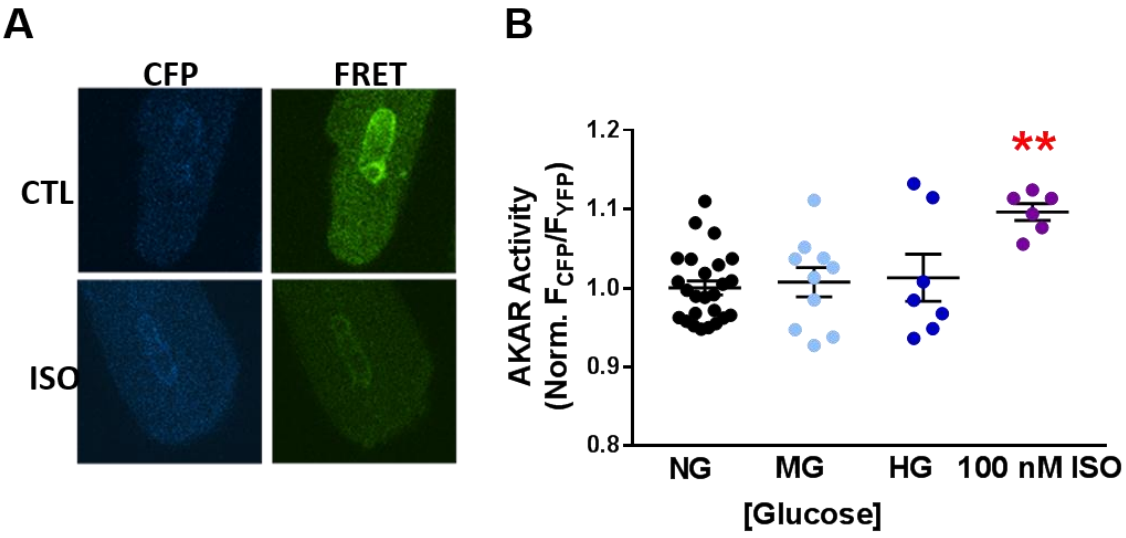

Supplemental Figure 4

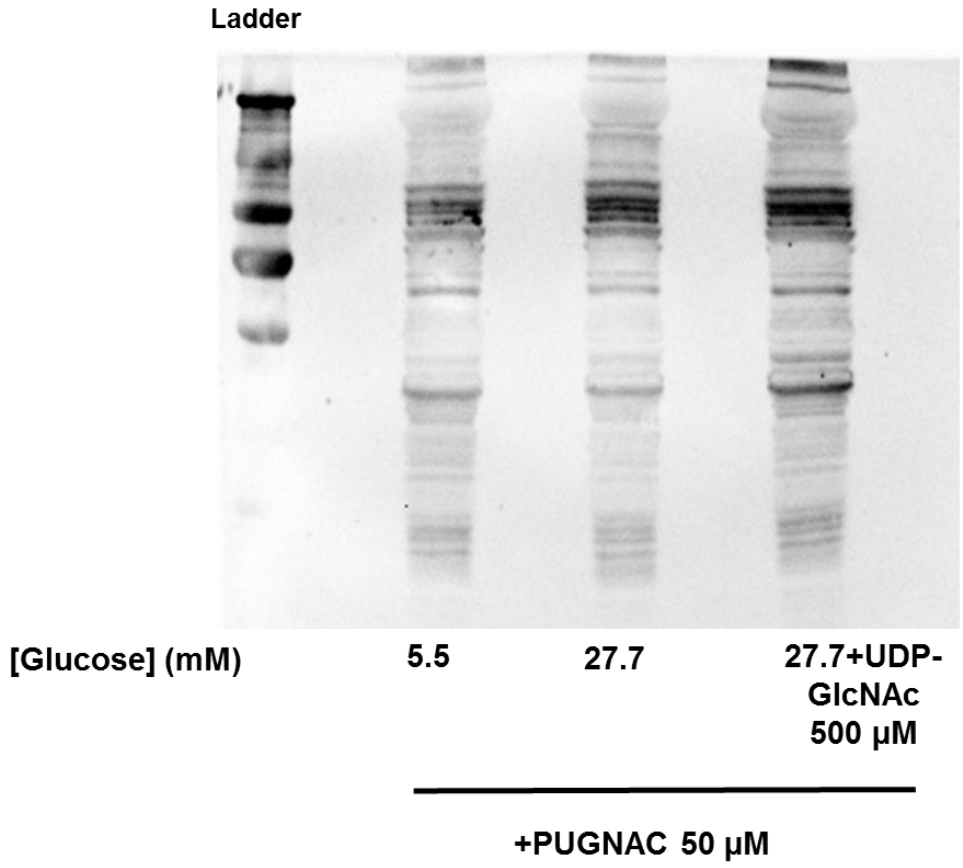

Supplemental Figure 5

II. Characterization of the ECC properties in Epac2 cardio-specific KO mice

Epac2 plays an important role in glucagon-like peptide (GLP-1)-mediated insulin secretion. Indeed, glucose induces the release of GLP-1 from the gastro-intestinal cells, which increases cAMP production in the β-pancreatic cells and subsequent Epac2-dependent insulin secretion (Fujimoto et al. 2002; Kang, Chepurny, and Holz 2001; Kang et al. 2006; Kang et al. 2003; Ozaki et al. 2000).The specific pancreatic β-cells Epac2-KO mice present a normal glucose and insulin sensitivity tolerance until 12 weeks of age (Hwang et al. 2017). However, they develop obesity under high-fat diet due to an impaired leptin signaling compared to their WT littermate (Hwang et al. 2017). Cardiac function was not assessed in these pancreatic β-cells KO mice to date.

Even though Pereira *et al.*(Pereira et al. 2013) didn't report any metabolic disturbances at 18 months in their constitutive Epac2-KO mice, an alteration of the insulin secretion can't be totally excluded. Therefore, it is interesting to generate cardio-specific Epac2-KO mice to avoid any possible metabolic alterations related to insulin secretion which can result from a constitutive KO. So in this study we studied the ECC in an Epac2 cardiac specific KO mice provided by Dr. Franck Lezoulc'h (Inserm UMR-1048, Institut des Maladies Métaboliques et Cardiovasculaires, Université Toulouse III). These mice have been generated by the excision of the exon 17 by the Cre-Lox technique under the control of cardiac specific promotor of the α-Myosin Heavy-Chain. We found that Epac2 deletion does not affect basal Ca^{2+} signaling, however it reduces β-adrenergic-induced pro-arrhythmic events.

1) Epac2 deletion does not affect mice morphometric parameters

First, we determine whether cardiac specific Epac2 deletion will alter cardiac morphometric parameters. The heart weight (HW) (Figure 30-A), heart weight/body weight (HW/BW) ratio (Figure 30-B), lung weight/body weight (LW/BW) ratio (Figure 30-C), and heart weight/tibial length (HW/TL) ratio (Figure 30-D), are similar between Epac2-KO and WT mice aged 9 to 23 weeks. The non-alteration of the morphometric characteristics reflects no evidence of obesity or cardiac hypertrophy in the mice with cardiac Epac2 deletion.

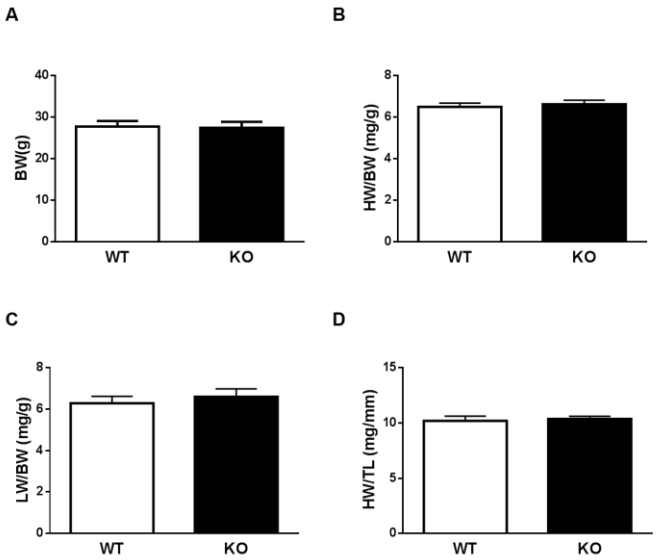

Figure 30: Cardiac Epac2-KO and WT present similar morphometric characteristics.(A) Body weight (BW) (B) Heart weight/body weight ratio (HW/BW), (C) lung weight/body weight ratio (LW/BW), (D) heart weight/tibial length ratio (HW/TL), in male Epac2-WT (n=7) and male Epac2-KO (n=9) mice. p=N.S.

2) Epac2 is not critical for basal ECC

Then we assessed whether Epac2 specific cardiac deletion will affect basal Ca^{2+} signaling using confocal microscopy. Basal Ca^{2+} transient amplitude (Figure 31-A) and decay time constant (Figure 31-B) (reflecting SERCA and NCX activity) are similar between Epac2-KO and WT mice. The SR Ca^{2+} content, estimated by rapid caffeine application (Figure 32-A)

and caffeine/evoked decay time were also similar between WT and KO cardiomyocytes (Figure 32-B). These results confirm that Epac2 in not required for the basal Ca^{2+} signaling which is in line with the Pereira *et al*. (Pereira et al. 2013) study performed in the constitutive Epac2-KO model.

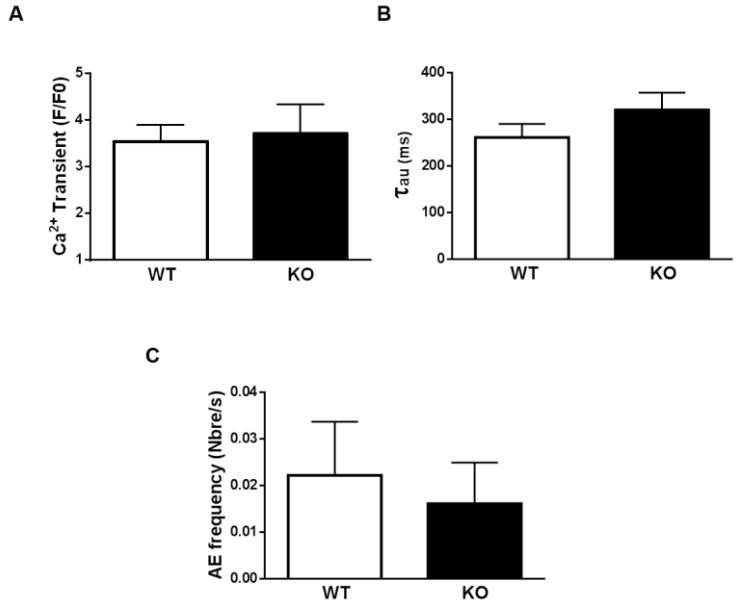

Figure 31: Epac2 deletion does not affect the basal Ca^{2+} signaling. (A) Ca^{2+} transient amplitude, (B) Ca^{2+} decay time constant (τ) (ms) and (C) Arrhythmogenic events frequency (number/s) in ventricular cardiomyocytes from Epac2 WT (N=4, n=8) and KO (N=8, n=11) mice. p=N.S.

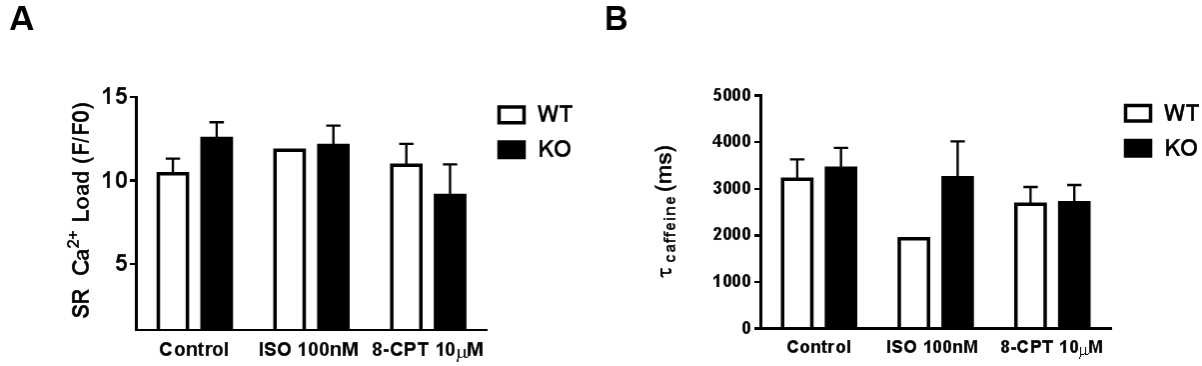

Figure 32: Epac2 deletion doesn't affect SR Ca^{2+} load nor NCX activity. (A) Ca^{2+} transient amplitude under caffeine application, and (B) Ca^{2+} decay time constant (τ) (ms) of cardiomyocytes in control tyrode solution (N=4, n=7), Isoproterenol 100 nM (N=1, n=1) and 8-CPT 10 µM (N=3, n=5) from Epac2-WT mice and, from Epac2-KO in control tyrode solution (N=4, n=9), Isoproterenol 100 nM (N=2, n=9) and 8-CPT 10 µM (N=4, n=4), p=N.S.

3) Epac2 deletion protects from β-adrenergic-mediated arrhythmogenic events

Since Epac2 is a downstream effector of cAMP, we studied the β-adrenergic response in these mice by 100 nM isoproterenol (β-adrenergic receptor agonist) application. Isoproterenol effect on the Ca^{2+} transient were similar between KO and WT mice, with an increase of the Ca^{2+} transient amplitude (Figure 33-A) and a decrease of the decay time constant (Figure 33-B). The SR Ca^{2+} load (Figure 32-A) and the NCX activity on the forward mode (Figure 32-B) were not affected by Epac2 deletion as well, consistent with Pereira *et al.* (Pereira et al. 2013) data. However, it has been reported that Epac2 is involved in the β-adrenergic-mediated SR Ca^{2+} leak and subsequent arrhythmogenic events (Pereira et al. 2013; Pereira et al. 2007). We found that Epac2 deletion drastically reduces the isoproterenol-induced arrhythmogenic events in KO mice compared to WT (Figure 33-C). This is in line with the Epac2 localization at the T-tubules (Pereira et al. 2015).

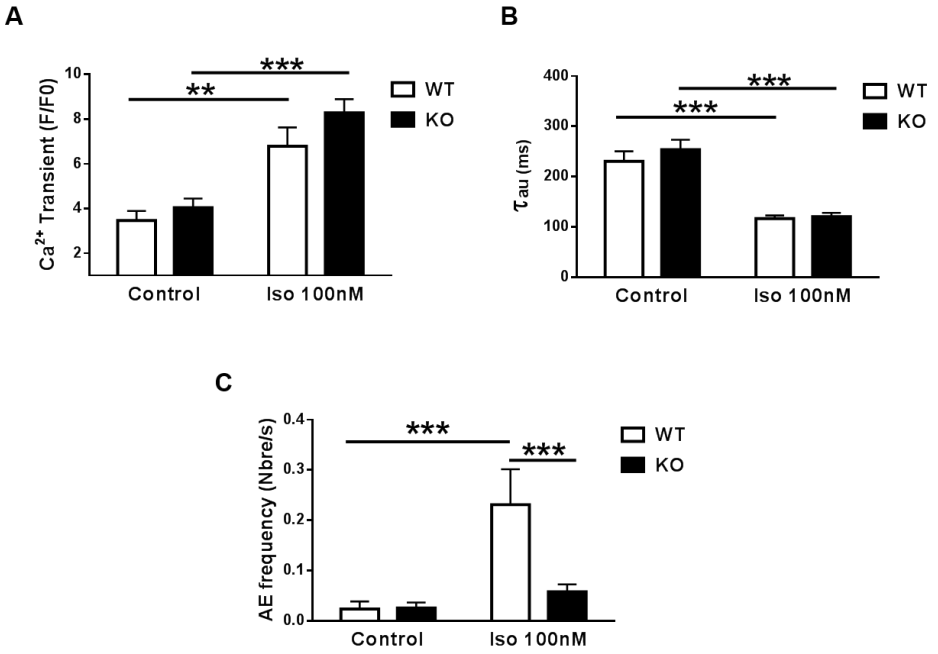

Figure 33: Epac2 deletion prevents Iso-mediated arrhythomgenic events. (A) Ca^{2+} transient amplitude, (B) Ca^{2+} decay time constant (τ) (ms) and (C) Arrhythmogenic events frequency (number/s) in ventricular cardiomyocytes from Epac2 WT (N=3, n=7) and KO (N=6, n=13) mice in control tyrode solution ± Isoproterenol 100 nM. **p<0.01, ***p<0.001.

4) Epac2 deletion doesn't prevent 8-CPT effects on Ca^{2+} signaling

It has been reported that Epac analog, 8-CPT induces SR Ca^{2+} leak and pro-arrhythmogenic events with a subsequent decrease of the SR Ca^{2+} load and the Ca^{2+} transient amplitude (Pereira et al. 2007). The 8-CPT effect on the Ca^{2+} leak was related to Epac2 and not Epac1 (Pereira et al. 2013). Even though we observed a decrease of the Ca^{2+} transient amplitude in WT and not Epac2-KO mice under 10µM 8-CPT (Figure 34-A), the SR Ca^{2+} load (Figure 32-A) and the arrhythmogenic events frequency (Figure 34-C) were similar in both cells groups. This could be explained by the potential off-target effects of 8-CPT notably on PDE's inhibition. Those off-target effects could increase cAMP level and a subsequent PKA activation that can affect SR Ca^{2+} leak (Poppe et al. 2008).

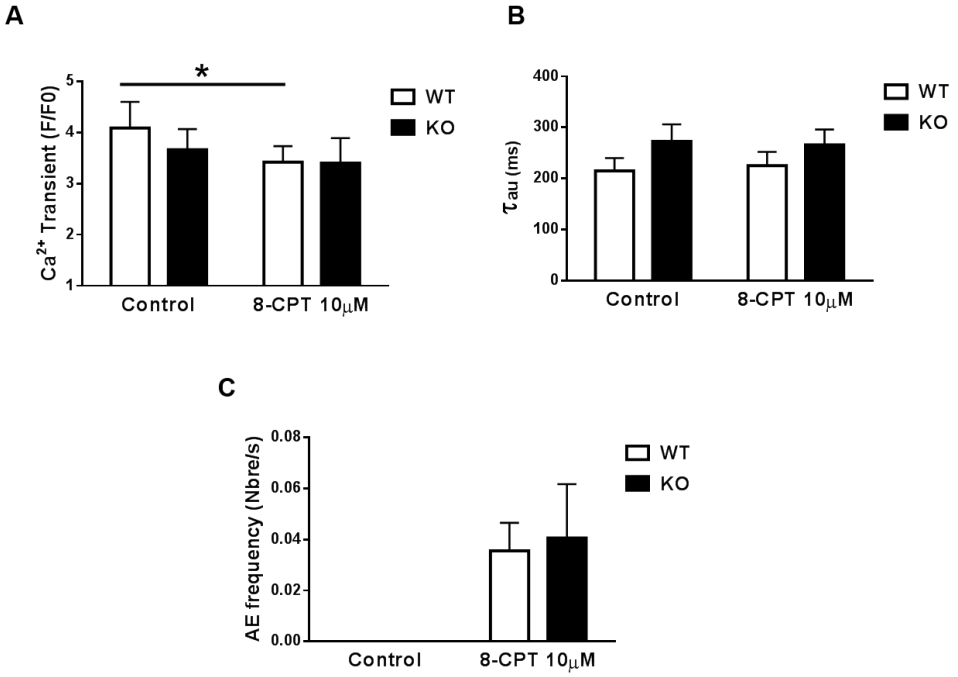

Figure 34: Epac2 deletion doesn't prevent 8-CPT effects of Ca^{2+} signaling. (A) Ca^{2+} transient amplitude, (B) Ca^{2+} decay time constant (τ) (ms) and (C) Arrhythmogenic events frequency (number/s) in ventricular cardiomyocytes from Epac2 WT (N=3, n=9) and KO (N=4, n=8) mice in control tyrode solution ± 8-CPT 10 µM. *p<0.05.

To conclude, our study shows that cardio-specific Epac2 deletion does not affect the basal cardiac ECC but reduces β-adrenergic-mediated arrhythmogenic events as already reported in the constitutive Epac2-KO model (Pereira et al. 2013; Pereira et al. 2015). Further investigation should be conducted to assess the basal cardiac function of these mice and the possible protecting role of cardiac Epac2 deletion in the development of MI, TAC or diabetes-mediated cardiac dysfunction.

Discussion and perspectives

Discussion and perspectives

The heart is a greedy organ with a nonstop activity that requires a constant energy supply derived from nutrient metabolism. Although fatty acids are the preferred energy source than glucose, the heart is able to utilize both of them to fulfill its needs (Pascual and Coleman 2016). Interestingly, studies have shown that excess glucose is harmful and activates several deleterious pathways that can disturb the cardiomyocytes activity such as the ECC (Bugger and Abel 2014; Kolwicz and Tian 2011). However, few studies (Clark et al. 2003; Erickson et al. 2013; Federico et al. 2017; Lu et al. 2020; Ng et al. 2018) have been conducted to decipher the molecular pathway underlying the high glucose-related ECC effects. In my thesis, I have described a new mechanism of high glucose-mediated Ca^{2+} mishandling, featuring Epac2 as a key player in glucose-mediated ECC regulation.

Epac2, a new player in high glucose-mediated cardiac Ca^{2+} leak

High glucose concentrations alter ECC by inducing in part SR Ca^{2+} leak and subsequent arrhythmogenic events (Erickson et al. 2013; Lu et al. 2020). Epac2 is a key player in ECC regulation, localized at the T-tubule region (Pereira et al. 2015) and participates in the SR Ca^{2+} leak (Pereira et al. 2017b; Pereira et al. 2013; Pereira et al. 2007; Pereira et al. 2015), as observed with high glucose concentrations (Erickson et al. 2013; Lu et al. 2020). However, the implication of Epac2 in high glucose-mediated Ca^{2+} mishandling was yet unknown. My thesis work has shown that Epac2 is involved in the previously described high-glucose-mediated Ca^{2+} alterations. Indeed, high glucose increases the Ca^{2+} sparks frequency without altering the SR Ca^{2+} load, which reflects an increase of the SR Ca^{2+} leak (Eisner et al. 2017), prevented by selective Epac2 inhibitor, the ESI-05. This high glucose-mediated SR Ca^{2+} leak

is associated with an increase of the Ca^{2+} waves and the arrhythmogenic events, similar to what it has been described in HF (Pogwizd and Bers 2004) and in catecholaminergic polymorphic ventricular tachycardia (Priori and Chen 2011), where this Ca^{2+} leak induces a NCX transient inward current that can result in an ectopic arrhythmogenic AP (Berlin, Cannell, and Lederer 1989; Ferrier, Saunders, and Mendez 1973; Kass et al. 1978; Lederer and Tsien 1976). The increase of the Ca^{2+} sparks frequency and subsequent arrhythmogenic events observed under high glucose was prevented by ESI-05. However, to overcome possible off-target effects of pharmacological tools, where it has been described that ESI-05 at high concentrations (25 µM) can induce arrhythmias associated with an increase of mitochondrial ROS production (Yang et al. 2016), we used freshly isolated cardiomyocytes from Epac2-KO mice. In line with our ESI-05 results, deletion of Epac2 protects ventricular cardiomyocytes from the high glucose-mediated SR Ca^{2+} leak and arrhythmogenic events.

The observed SR Ca^{2+} leak under high glucose concentrations was associated with an increase of RyR open probability prevented by Epac2 inhibition, confirming the role of Epac2 in the modulation of the RyR activity under high glucose concentration. The SR Ca^{2+} leak associated to an increase of the open probability of the RyR suggests the channel sensitization by its phosphorylation by CaMKII on its Ser2814 residue as described in HF models (Huke et al. 2011; Kohlhaas et al. 2006; van Oort et al. 2010; Wehrens et al. 2006). However, to our surprise, we didn't observe any increase of the RyR phosphorylation in our study at the Ser2814 in mice hearts perfused with high glucose. In contrast, Federico *et al*. (Federico et al. 2017) have demonstrated in another cell type, HEK cells, an increase of the RyR Ser2814 phosphorylation level under high glucose. Sommese *et al*. (Sommese et al. 2016) have also observed an increase of the RyR phosphorylation in cardiomyocytes of rat fed with high fructose diet. It is also worth to note, that Ser2814 is one of the CaMKII described RyR phosphorylation site, however RyR is a large macromolecule (Bers 2004) and

other CaMKII-related phosphorylation sites, although not yet well described, should not be excluded (Wehrens et al. 2004).

Besides phosphorylation, RyR is also subject to oxidation (Boraso and Williams 1994; Sun et al. 2008) which increases its activity and Ca^{2+} leak observed in HF (Jung et al. 2008; Lim et al. 2008; Terentyev et al. 2008). One of the high glucose-mediated deleterious effects involves ROS production in the cell (Brownlee 2005; Giacco and Brownlee 2010) that has recently been reported to be CaMKII-dependent in mice cardiomyocytes (Lu et al. 2020). Epac also activates CaMKII by a pathway involving a ROS related enzyme, the nitric oxide synthase 1 (Pereira et al. 2017b). Taking all these into consideration we can suggest a possible implication of the oxidation pathway in the observed Ca^{2+} leak *via* a possible high glucose/Epac/CaMKII/ROS/RyR mechanism where oxidation can activate both RyR and CaMKII.

O-GlcNacylation, a novel activation mechanism of Epac

Since Epac2 is involved in high glucose-mediated Ca^{2+} mishandling, we studied the underlying mechanism of Epac activation in these conditions. To date, cAMP is the only known activator of Epac (de Rooij et al. 1998; Kawasaki et al. 1998). Since O-GlcNacylation is a post-translationnal modification occurring on serine or threonine protein's residue upregulated under high glucose concentration (Hart, Housley, and Slawson 2007), and since Epac possess several serine and threonine residues (Rehmann et al. 2008; Rehmann et al. 2006) that could be potentially O-GlcNacylated, a possible direct interaction is thus possible. Indeed, we observed by Epac-based FRET biosensor an activation of Epac under high glucose prevented by the inhibition of the O-GlcNacylation pathway with DON, showing that Epac activation by glucose is mediated by the O-GlcNacylation pathway. These results were confirmed by Co-IP experiments that show for the first time a direct interaction between

Epac2 and O-GlcNacylation. Even though Co-IP are not quantifiable experiments, to our surprise we didn't find a detectable increase of the Epac O-GlcNacylation under high glucose or in positive control with O-GlcNacylation substrate (UDP-GlcNac) compared to normal glucose. Further proteomic investigations such as mass spectrometry (Ma and Hart 2014) are required to determine the potential Epac O-GlcNacylation sites. In parallel to our results, it has been recently reported that in retinal cells, angiotensin 1-7 increases cAMP production which inhibits OGT activity with a subsequent reduction of O-GlcNacylation levels in an Epac and not PKA-dependent manner (Dierschke et al. 2020). This paper (Dierschke et al. 2020) shows a possible interaction between Epac and O-GlcNac in retinal cells, as we describe for the first time in our work.

Epac2-O-GlcNacylation reduces Ca^{2+} transient amplitude under chronic high glucose

In mice cardiomyocytes, acute high glucose treatment didn't affect the Ca^{2+} transient amplitude in our study despite the observed SR Ca^{2+} leak, contrarily to what has been already described in some HF models where the SR Ca^{2+} leak decreases the Ca^{2+} transient amplitude and cell contraction (Belevych et al. 2007; Bers 2014; Eisner et al. 2017; Shannon, Pogwizd, and Bers 2003). The non-alteration of the Ca^{2+} transient in our study could be explained in part by the unmodified SR Ca^{2+} load since the leak has been assessed for a short time duration, probably not enough to induce detectable modifications of the SR Ca^{2+} load (Eisner et al. 2017). Besides, the Ca^{2+} transient amplitude depends also on the Ca^{2+} entry by the LTCC during the AP (Bers 2008; Eisner et al. 2017), which is reported to not be modified by acute Epac activation (Pereira et al. 2007). However, it has been described that acute high glucose increases Ca^{2+} entry by the LTCC in vascular arterial myocytes *via* PKA activation (Nystoriak et al. 2017). This same mechanism could also exist in ventricular cardiomoycytes,

also not reported to date, which could explain the non-alteration of the Ca^{2+} transient amplitude. Lu *et al*. (Lu et al. 2020) didn't observe any modification of the Ca^{2+} transient amplitude in mice cardiomyocytes treated with high glucose as well despite a slight decrease of the SR Ca^{2+} load, due to an increase of the fractional shortening, an intrinsic form of auto-regulation that stabilizes ECC (Trafford, Diaz, and Eisner 2001). In order to assess the relevance of the implication of Epac2 in high glucose-mediated Ca^{2+} mishandling in human, we used h-iPSC-CM that are gaining importance as a novel model in studying cardiac alterations (Yoshida and Yamanaka 2017). In our study we were the first to report the expression of both Epac isoforms in this cell line, which are not affected by glucose concentration. Acute treatment of h-iPSC-CM with high glucose concentration does not alter the Ca^{2+} transient amplitude, in line with what we observed in mice cardiomyocytes. Lu *et al*. (Lu et al. 2020) didn't neither observe an alteration of the Ca^{2+} transient amplitude in h-iPSC-CM treated with high glucose concentration, however they found an increase of the spontaneous Ca^{2+} release in line with the increase of the Ca^{2+} sparks frequency observed in our murine model, which was associated with an increase of CaMKII-mediated ROS production (Lu et al. 2020).

However, a sustained SR Ca^{2+} leak under high glucose concentrations (Lu et al. 2020) will lower the SR Ca^{2+} load over time affecting the Ca^{2+} transient amplitude (Bers 2004; Eisner et al. 2017). We thus studied the effect of longer high glucose exposure (7 days) on the Ca^{2+} transient in h-iPSC-CM, where we observed a decrease of the Ca^{2+} transient amplitude that is prevented by Epac2 inhibition. However, Ng *et al*. (Ng et al. 2018) have observed an increase of the Ca^{2+} transient amplitude in h-iPSC-CM treated 7 days with high glucose but a decrease of the cell shortening, suggesting that coupling of the Ca^{2+} transient and contraction is less effective under high glucose. The decrease of the Ca^{2+} transient amplitude is also observed in pathological models characterized by a chronic high glucose exposure such as diabetes

(Delucchi et al. 2012; Kranstuber et al. 2012; Pereira et al. 2006; Shao et al. 2007) and participate in the observed reduction of cardiac systolic function in some of these models (Kranstuber et al. 2012; Lu et al. 2007; Shao et al. 2007). The reduction of the observed Ca^{2+} transient amplitude can also be related to the decrease of the SR Ca^{2+} load (Lacombe et al. 2007; LaRocca et al. 2012; Pereira et al. 2006) or a decrease of the LTCC expression and or activity as observed in diabetic models (Bracken et al. 2004; Howarth et al. 2011; Lee et al. 1992; Lu et al. 2011; Lu et al. 2007; Pereira et al. 2006). O-GlcNacylation has also been described to be involved in high glucose-mediated Ca^{2+} mishandling, where it downregulates SERCA expression and activity resulting in Ca^{2+} transient prolongation (Clark et al. 2003) in neonatal rat cardiomyocytes under 48-72 hours of high glucose responsible, in part, of the diastolic dysfunction observed in type 2 diabetic mice (Fricovsky et al. 2012). We showed in our data that the increase of the RyR open probability is blunted by O-GlcNacylation inhibition as well as with Epac2 inhibition, confirming that both Epac and O-GlcNac are required for the modulation of the RyR activity under high glucose concentrations and subsequent SR Ca^{2+} leak.

Furthermore, it should be noted that although h-iPSC-CM express the key structural and functional cardiomyocyte genes (ECC components, myosin heavy and light chain, troponin), they present an immature development state (few or no T-tubules, spontaneous beating activity) contrarily to adult cardiomyocyte (Karakikes et al. 2015).

To conclude, our work on h-iPSC-CM has shown that chronic treatment with high glucose concentration reduces the systolic Ca^{2+} release in an Epac2-dependent manner which postulates the possible role of Epac2 in the alteration of the ECC in disease with a chronic high glucose exposure, such as diabetes.

Epac2, a potential target of diabetic cardiomyopathy?

Diabetes mellitus is a chronic metabolic pathology characterized by a hyperglycemic state, and constitutes a major risk factor of HF (Kannel and McGee 1979). Coronary artery diseases and hypertension were often considered as the underlying causes of HF in diabetic patients, until 1972, where Rubler *et al*. (Rubler et al. 1972) reported a HF associated with left ventricular hypertrophy in diabetic patients with no coronary artery disease or other etiological conditions explaining HF. Therefore, the concept of a specific myocardial dysfunction, called diabetic cardiomyopathy, was postulated and confirmed by several clinical studies (de Simone et al. 2010; Devereux et al. 2000), which is defined as "a cardiac dysfunction with impaired cardiac contraction and relaxation, leading to heart failure independently of coronary and/or valvular complications, hypertension, congenital cardiomyopathy or other HF known etiologies". However, the underlying molecular mechanisms of diabetic cardiomyopathy remain unclear (Bugger and Abel 2014). Several studies on animal diabetic models have reported an alteration of the ECC with a subsequent decrease of the Ca^{2+} transient amplitude (Belke, Swanson, and Dillmann 2004; Choi et al. 2002; Delucchi et al. 2012; Depre et al. 2000; Pereira et al. 2006), as observed in our h-iPSC-CM model, which participates in the systolic diabetic dysfunction. Furthermore, it is reported that O-GlcNacylation pathway is increased in diabetes and also participates in the alteration of the ECC (Fricovsky et al. 2012; Hu et al. 2005; Ramirez-Correa et al. 2015), where OGA overexpression prevents cardiac fractional shortening reduction in diabetic type 2 mice (Fricovsky et al. 2012) and improves diastolic function of perfused diabetic type 1 mice heart (Hu et al. 2005). All these data drive us to postulate a possible role of Epac2 in the cardiac alteration seen in diabetes, since we saw that it is activated under high glucose by O-GlcNacylation, 2 hallmarks of this metabolic disease, to induce alteration of the ECC as observed in diabetes. Few available studies have reported a role of Epac signaling during

diabetes. For instance, in diabetic kidney cells, Epac is up-regulated and mediates hypertrophy (Sun et al. 2011) and leptin resistance (Fukuda et al. 2011). However, no study has reported a role of Epac2 in diabetic cardiomyopathy that would be interesting to investigate, using Epac2 inhibition in diabetic animal models or by inducing diabetes in transgenic Epac2-KO mice. However, Epac2 is implicated in insulin secretion, thus a constitutive Epac2-KO model could induce metabolic alteration, although not reported to date (Pereira et al. 2013), as observed in pancreatic-specific Epac2-KO mice that are prone to obesity and leptin resistant (Hwang et al. 2017). Thus it is interesting to generate Epac2 cardio-specific KO mice to study the possible role of Epac2 in metabolic-related cardiac diseases such as diabetes which we tried to characterize in the second part of our work.

Specific cardiac Epac2 deletion does not affect basal ECC but protects from β-adrenergic-mediated arrhythmogenic events

Epac2 is a cAMP effector that plays a major role in ECC-cardiac Ca^{2+} handling even though the underlying mechanisms are not completely elucidated (Lezoualc'h et al. 2016). Thus, a generation of Epac2 cardio-specific KO mice seems interesting in order to further decipher the implication of Epac2 in cardiac diseases with associated etiology such as diabetes.

In our study, we observed that Epac2-KO and WT mice present similar morphometric features notably similar HW/TL and LW/BW, ruling out a possible cardiac hypertrophy or congestive HF, which should be however confirmed by echocardiography. We assessed the Ca^{2+} signaling in ventricular cardiomyocytes isolated from these mice. We observed that basal Ca^{2+} signaling is not altered by Epac2 deletion in line with what has already been reported in constitutive Epac2-KO mice (Pereira et al. 2013). Since Epac2 is not critical to basal ECC, it is also interesting to measure the cardiac function of these mice *in vivo* that we suppose won’t be affected, as observed in constitutive Epac2-KO model (Pereira et al. 2013).

Knowing that Epac1 and Epac2 are two isoforms with a lot of similarities, Epac1 expression should be assessed in Epac2-KO mice heart to verify a possible compensation mechanism by an increase of Epac1 expression.

In our study we confirmed that Epac2 is not required for the β-adrenergic-dependent modulation of the Ca^{2+} transient, where the amplitude increases and the decay time decreases in both mice cells under isoproterenol. This is in line with what have already been described by Pereira *et al.*(Pereira et al. 2013) in constitutive Epac2-KO mice and with that PKA is required for the β-adrenergic-mediated positive inotropic and lusitropic effects (Bers 2002), rather than Epac2. It would be interesting to assess the Ca^{2+} transient properties by inhibiting PKA (by H89 for example) under isoproterenol to validate the PKA-dependent inotropic and lusitropic effect in these Epac2-KO mice.

However, we confirmed that Epac2 is the cAMP effector responsible in part for the β-adrenergic-mediated arrhythmogenic events, where isoproterenol increases arrhythmogenic events frequencies in WT but not Epac2-KO mice, as in Epac2-KO constitutive deletion model (Pereira et al. 2013). It is reported that Epac2 activates CaMKII, its downstream effector, to mediate SR Ca^{2+} leak and subsequent phosphorylation of the RyR (Pereira et al. 2007) which are probably the underlying cause for the observed arrhythmogenic events. Besides, it is recognized that CaMKII–mediated RyR phosphorylation prevails over PKA-mediated RyR phosphorylation regarding SR Ca^{2+} leak and subsequent arrhythymias as observed in HF (Bers 2012). Thus, it would be interesting to assess the possible Epac2 deletion-mediated protection against β-adrenergic-induced ventricular-arrhythymia *in vivo* model. Furthermore, it is known that Epac2 expression is increased in isoproterenol-induced left ventricular hypertrophy in mice (Ulucan et al. 2007), it is judicious to test Epac2 deletion effect on the hypertrophy development in this HF model.

Conclusion

Conclusion

High glucose is an essential fuel for cardiac function. However, high glucose concentrations have been linked to cardiac alterations as seen in diabetes. Little is known about the underlying mechanisms of high glucose-mediated cardiac alteration, one is the Ca^{2+} mishandling. Besides, high glucose activates several deleterious mechanisms such as O-GlcNacylation altering protein activity, participating in cardiac function alteration.

Here, we deciphered a new mechanism of the high glucose-related Ca^{2+} mishandling featuring Epac2, a key regulator of Ca^{2+} homeostasis. In mice ventricular cardiomyocytes, high glucose activated Epac2 by O-GlcNcaylation pathway, to increase SR Ca^{2+} leak and arrhythmogenic events without affecting the Ca^{2+} transient. However, a longer exposure to high glucose, as observed in h-iPSC-CM decreases the Ca^{2+} transient amplitude depending on Epac2 without modification of the ECC components expression. However, the decrease of the Ca^{2+} transient amplitude participates in the reduction of the cardiac contractile activity as seen in diabetes, a metabolic disease characterized by a chronic state of glucose. Thus, this described mechanism can be involved in the alteration of cardiac contraction observed in diabetes, placing Epac2 as a novel therapeutic target in the treatment of diabetic cardiomyopathy. To further test this hypothesis, it would be interesting to study the cardiac function and the Ca^{2+} homeostasis in cardio-specific Epac2-KO diabetic mice, where the deletion of Epac2 could reduce the cardiac alteration in this disease, without altering insulin secretion.

References

References

'2. Classification and Diagnosis of Diabetes: Standards of Medical Care in Diabetes-2019'. 2019. *Diabetes Care*, 42: S13-s28.

Acsai, K., G. Antoons, L. Livshitz, Y. Rudy, and K. R. Sipido. 2011. 'Microdomain [Ca^{2+}] near ryanodine receptors as reported by L-type Ca^{2+} and Na+/Ca^{2+} exchange currents', *J Physiol*, 589: 2569-83.

Aflaki, M., X. Y. Qi, L. Xiao, B. Ordog, A. Tadevosyan, X. Luo, A. Maguy, Y. Shi, J. C. Tardif, and S. Nattel. 2014. 'Exchange protein directly activated by cAMP mediates slow delayed-rectifier current remodeling by sustained beta-adrenergic activation in guinea pig hearts', *Circ Res*, 114: 993-1003.

Ahles, A., and S. Engelhardt. 2014. 'Polymorphic variants of adrenoceptors: pharmacology, physiology, and role in disease', *Pharmacol Rev*, 66: 598-637.

Ahlquist, R. P. 1948. 'A study of the adrenotropic receptors', *Am J Physiol*, 153: 586-600.

Ai, X., J. W. Curran, T. R. Shannon, D. M. Bers, and S. M. Pogwizd. 2005. 'Ca2+/calmodulin-dependent protein kinase modulates cardiac ryanodine receptor phosphorylation and sarcoplasmic reticulum Ca2+ leak in heart failure', *Circ Res*, 97: 1314-22.

Akimoto, Y., L. K. Kreppel, H. Hirano, and G. W. Hart. 2000. 'Increased O-GlcNAc transferase in pancreas of rats with streptozotocin-induced diabetes', *Diabetologia*, 43: 1239-47.

Alderson, B. H., and J. J. Feher. 1987. 'The interaction of calcium and ryanodine with cardiac sarcoplasmic reticulum', *Biochim Biophys Acta*, 900: 221-9.

Amin, A. S., H. L. Tan, and A. A. Wilde. 2010. 'Cardiac ion channels in health and disease', *Heart Rhythm*, 7: 117-26.

Anderson, K., F. A. Lai, Q. Y. Liu, E. Rousseau, H. P. Erickson, and G. Meissner. 1989. 'Structural and functional characterization of the purified cardiac ryanodine receptor-Ca2+ release channel complex', *J Biol Chem*, 264: 1329-35.

Anderson, M. E. 2000. 'Connections count : excitation-contraction meets excitation-transcription coupling', *Circ Res*, 86: 717-9.

Anderson, M. E., A. P. Braun, H. Schulman, and B. A. Premack. 1994. 'Multifunctional Ca2+/calmodulin-dependent protein kinase mediates Ca(2+)-induced enhancement of the L-type Ca2+ current in rabbit ventricular myocytes', *Circ Res*, 75: 854-61.

Armoundas, A. A., I. A. Hobai, G. F. Tomaselli, R. L. Winslow, and B. O'Rourke. 2003. 'Role of sodium-calcium exchanger in modulating the action potential of ventricular myocytes from normal and failing hearts', *Circ Res*, 93: 46-53.

Asghari, P., M. Schulson, D. R. Scriven, G. Martens, and E. D. Moore. 2009. 'Axial tubules of rat ventricular myocytes form multiple junctions with the sarcoplasmic reticulum', *Biophys J*, 96: 4651-60.

Baddeley, D., I. D. Jayasinghe, L. Lam, S. Rossberger, M. B. Cannell, and C. Soeller. 2009. 'Optical single-channel resolution imaging of the ryanodine receptor distribution in rat cardiac myocytes', *Proc Natl Acad Sci U S A*, 106: 22275-80.

Bassani, J. W., R. A. Bassani, and D. M. Bers. 1994. 'Relaxation in rabbit and rat cardiac cells: species-dependent differences in cellular mechanisms', *J Physiol*, 476: 279-93.

Bassani, J. W., W. Yuan, and D. M. Bers. 1995. 'Fractional SR Ca release is regulated by trigger Ca and SR Ca content in cardiac myocytes', *Am J Physiol*, 268: C1313-9.

Beauchamp, P., T. Desplantez, M. L. McCain, W. Li, A. Asimaki, G. Rigoli, K. K. Parker, J. E. Saffitz, and A. G. Kleber. 2012. 'Electrical coupling and propagation in engineered

ventricular myocardium with heterogeneous expression of connexin43', *Circ Res*, 110: 1445-53.
Belevych, A., Z. Kubalova, D. Terentyev, R. L. Hamlin, C. A. Carnes, and S. Györke. 2007. 'Enhanced ryanodine receptor-mediated calcium leak determines reduced sarcoplasmic reticulum calcium content in chronic canine heart failure', *Biophys J*, 93: 4083-92.
Belke, D. D., E. A. Swanson, and W. H. Dillmann. 2004. 'Decreased sarcoplasmic reticulum activity and contractility in diabetic db/db mouse heart', *Diabetes*, 53: 3201-8.
Bell, R. M., M. M. Mocanu, and D. M. Yellon. 2011. 'Retrograde heart perfusion: the Langendorff technique of isolated heart perfusion', *J Mol Cell Cardiol*, 50: 940-50.
Benitah, J. P., J. L. Alvarez, and A. M. Gómez. 2010. 'L-type Ca(2+) current in ventricular cardiomyocytes', *J Mol Cell Cardiol*, 48: 26-36.
Benkusky, N. A., C. S. Weber, J. A. Scherman, E. F. Farrell, T. A. Hacker, M. C. John, P. A. Powers, and H. H. Valdivia. 2007. 'Intact beta-adrenergic response and unmodified progression toward heart failure in mice with genetic ablation of a major protein kinase A phosphorylation site in the cardiac ryanodine receptor', *Circ Res*, 101: 819-29.
Berisha, F., and V. O. Nikolaev. 2017. 'Cyclic nucleotide imaging and cardiovascular disease', *Pharmacol Ther*, 175: 107-15.
Berlin, J. R., M. B. Cannell, and W. J. Lederer. 1989. 'Cellular origins of the transient inward current in cardiac myocytes. Role of fluctuations and waves of elevated intracellular calcium', *Circ Res*, 65: 115-26.
Bers, D. M. 2002. 'Cardiac excitation-contraction coupling', *Nature*, 415: 198-205.
———. 2004. 'Macromolecular complexes regulating cardiac ryanodine receptor function', *J Mol Cell Cardiol*, 37: 417-29.
———. 2008. 'Calcium cycling and signaling in cardiac myocytes', *Annu Rev Physiol*, 70: 23-49.
———. 2012. 'Ryanodine receptor S2808 phosphorylation in heart failure: smoking gun or red herring', *Circ Res*, 110: 796-9.
———. 2014. 'Cardiac sarcoplasmic reticulum calcium leak: basis and roles in cardiac dysfunction', *Annu Rev Physiol*, 76: 107-27.
Bers, D. M., and T. R. Shannon. 2013. 'Calcium movements inside the sarcoplasmic reticulum of cardiac myocytes', *J Mol Cell Cardiol*, 58: 59-66.
Bertrand, L., S. Horman, C. Beauloye, and J. L. Vanoverschelde. 2008. 'Insulin signalling in the heart', *Cardiovasc Res*, 79: 238-48.
Blechschmidt, S., V. Haufe, K. Benndorf, and T. Zimmer. 2008. 'Voltage-gated Na+ channel transcript patterns in the mammalian heart are species-dependent', *Prog Biophys Mol Biol*, 98: 309-18.
Bodi, I., G. Mikala, S. E. Koch, S. A. Akhter, and A. Schwartz. 2005. 'The L-type calcium channel in the heart: the beat goes on', *J Clin Invest*, 115: 3306-17.
Bodiga, V. L., S. R. Eda, and S. Bodiga. 2014. 'Advanced glycation end products: role in pathology of diabetic cardiomyopathy', *Heart Fail Rev*, 19: 49-63.
Boraso, A., and A. J. Williams. 1994. 'Modification of the gating of the cardiac sarcoplasmic reticulum Ca(2+)-release channel by H2O2 and dithiothreitol', *Am J Physiol*, 267: H1010-6.
Bracken, N. K., A. J. Woodall, F. C. Howarth, and J. Singh. 2004. 'Voltage-dependence of contraction in streptozotocin-induced diabetic myocytes', *Mol Cell Biochem*, 261: 235-43.
Brahma, M. K., M. E. Pepin, and A. R. Wende. 2017. 'My Sweetheart Is Broken: Role of Glucose in Diabetic Cardiomyopathy', *Diabetes Metab J*, 41: 1-9.

Brette, F., E. Blandin, C. Simard, R. Guinamard, and L. Sallé. 2013. 'Epac activator critically regulates action potential duration by decreasing potassium current in rat adult ventricle', *J Mol Cell Cardiol*, 57: 96-105.

Brillantes, A. B., K. Ondrias, A. Scott, E. Kobrinsky, E. Ondriasová, M. C. Moschella, T. Jayaraman, M. Landers, B. E. Ehrlich, and A. R. Marks. 1994. 'Stabilization of calcium release channel (ryanodine receptor) function by FK506-binding protein', *Cell*, 77: 513-23.

Brodde, O. E., H. Bruck, K. Leineweber, and T. Seyfarth. 2001. 'Presence, distribution and physiological function of adrenergic and muscarinic receptor subtypes in the human heart', *Basic Res Cardiol*, 96: 528-38.

Brownlee, M. 2005. 'The pathobiology of diabetic complications: a unifying mechanism', *Diabetes*, 54: 1615-25.

Bugger, H., and E. D. Abel. 2014. 'Molecular mechanisms of diabetic cardiomyopathy', *Diabetologia*, 57: 660-71.

Bünemann, M., B. L. Gerhardstein, T. Gao, and M. M. Hosey. 1999. 'Functional regulation of L-type calcium channels via protein kinase A-mediated phosphorylation of the beta(2) subunit', *J Biol Chem*, 274: 33851-4.

Cannell, M. B., H. Cheng, and W. J. Lederer. 1995. 'The control of calcium release in heart muscle', *Science*, 268: 1045-9.

Cannell, M. B., C. H. Kong, M. S. Imtiaz, and D. R. Laver. 2013. 'Control of sarcoplasmic reticulum Ca2+ release by stochastic RyR gating within a 3D model of the cardiac dyad and importance of induction decay for CICR termination', *Biophys J*, 104: 2149-59.

Carnicer, R., A. B. Hale, S. Suffredini, X. Liu, S. Reilly, M. H. Zhang, N. C. Surdo, J. K. Bendall, M. J. Crabtree, G. B. Lim, N. J. Alp, K. M. Channon, and B. Casadei. 2012. 'Cardiomyocyte GTP cyclohydrolase 1 and tetrahydrobiopterin increase NOS1 activity and accelerate myocardial relaxation', *Circ Res*, 111: 718-27.

Catane, R., D. D. Von Hoff, D. L. Glaubiger, and F. M. Muggia. 1979. 'Azaserine, DON, and azotomycin: three diazo analogs of L-glutamine with clinical antitumor activity', *Cancer Treat Rep*, 63: 1033-8.

Catterall, W. A. 2011. 'Voltage-gated calcium channels', *Cold Spring Harb Perspect Biol*, 3: a003947.

Cazorla, O., A. Lucas, F. Poirier, A. Lacampagne, and F. Lezoualc'h. 2009. 'The cAMP binding protein Epac regulates cardiac myofilament function', *Proc Natl Acad Sci U S A*, 106: 14144-9.

Cens, T., M. Rousset, J. P. Leyris, P. Fesquet, and P. Charnet. 2006. 'Voltage- and calcium-dependent inactivation in high voltage-gated Ca(2+) channels', *Prog Biophys Mol Biol*, 90: 104-17.

Chatham, J. C., J. Zhang, and A. R. Wende. 2020. 'Role of O-Linked N-acetylglucosamine (O-GlcNAc) Protein Modification in Cellular (Patho)Physiology', *Physiol Rev*.

Chelu, M. G., C. I. Danila, C. P. Gilman, and S. L. Hamilton. 2004. 'Regulation of ryanodine receptors by FK506 binding proteins', *Trends Cardiovasc Med*, 14: 227-34.

Chen, G., D. R. Gulbranson, Z. Hou, J. M. Bolin, V. Ruotti, M. D. Probasco, K. Smuga-Otto, S. E. Howden, N. R. Diol, N. E. Propson, R. Wagner, G. O. Lee, J. Antosiewicz-Bourget, J. M. Teng, and J. A. Thomson. 2011. 'Chemically defined conditions for human iPSC derivation and culture', *Nat Methods*, 8: 424-9.

Chen, H., T. Tsalkova, O. G. Chepurny, F. C. Mei, G. G. Holz, X. Cheng, and J. Zhou. 2013. 'Identification and characterization of small molecules as potent and specific EPAC2 antagonists', *J Med Chem*, 56: 952-62.

Chen, X., C. Weber, E. T. Farrell, F. J. Alvarado, Y. T. Zhao, A. M. Gómez, and H. H.

Valdivia. 2018. 'Sorcin ablation plus β-adrenergic stimulation generate an arrhythmogenic substrate in mouse ventricular myocytes', *J Mol Cell Cardiol*, 114: 199-210.
Cheng, H., M. R. Lederer, W. J. Lederer, and M. B. Cannell. 1996. 'Calcium sparks and [Ca2+]i waves in cardiac myocytes', *Am J Physiol*, 270: C148-59.
Cheng, H., W. J. Lederer, and M. B. Cannell. 1993. 'Calcium sparks: elementary events underlying excitation-contraction coupling in heart muscle', *Science*, 262: 740-4.
Choi, K. M., Y. Zhong, B. D. Hoit, I. L. Grupp, H. Hahn, K. W. Dilly, S. Guatimosim, W. J. Lederer, and M. A. Matlib. 2002. 'Defective intracellular Ca(2+) signaling contributes to cardiomyopathy in Type 1 diabetic rats', *Am J Physiol Heart Circ Physiol*, 283: H1398-408.
Clark, R. J., P. M. McDonough, E. Swanson, S. U. Trost, M. Suzuki, M. Fukuda, and W. H. Dillmann. 2003. 'Diabetes and the accompanying hyperglycemia impairs cardiomyocyte calcium cycling through increased nuclear O-GlcNAcylation', *J Biol Chem*, 278: 44230-7.
Colatsky, T. J. 1980. 'Voltage clamp measurements of sodium channel properties in rabbit cardiac Purkinje fibres', *J Physiol*, 305: 215-34.
Consonni, S. V., M. Gloerich, E. Spanjaard, and J. L. Bos. 2012. 'cAMP regulates DEP domain-mediated binding of the guanine nucleotide exchange factor Epac1 to phosphatidic acid at the plasma membrane', *Proc Natl Acad Sci U S A*, 109: 3814-9.
Conti, M., and J. Beavo. 2007. 'Biochemistry and physiology of cyclic nucleotide phosphodiesterases: essential components in cyclic nucleotide signaling', *Annu Rev Biochem*, 76: 481-511.
Coraboeuf, E., and E. Carmeliet. 1982. 'Existence of two transient outward currents in sheep cardiac Purkinje fibers', *Pflugers Arch*, 392: 352-9.
Coraboeuf, E., and S. Weidmann. 1954. 'Temperature effects on the electrical activity of Purkinje fibres', *Helv Physiol Pharmacol Acta*, 12: 32-41.
Cotecchia, S., C. D. Del Vescovo, M. Colella, S. Caso, and D. Diviani. 2015. 'The alpha1-adrenergic receptors in cardiac hypertrophy: signaling mechanisms and functional implications', *Cell Signal*, 27: 1984-93.
Courilleau, D., P. Bouyssou, R. Fischmeister, F. Lezoualc'h, and J. P. Blondeau. 2013. 'The (R)-enantiomer of CE3F4 is a preferential inhibitor of human exchange protein directly activated by cyclic AMP isoform 1 (Epac1)', *Biochem Biophys Res Commun*, 440: 443-8.
Davis, R. L., H. Weintraub, and A. B. Lassar. 1987. 'Expression of a single transfected cDNA converts fibroblasts to myoblasts', *Cell*, 51: 987-1000.
De Blasio, M. J., N. Huynh, M. Deo, L. E. Dubrana, J. Walsh, A. Willis, D. Prakoso, H. Kiriazis, D. G. Donner, J. C. Chatham, and R. H. Ritchie. 2020. 'Defining the Progression of Diabetic Cardiomyopathy in a Mouse Model of Type 1 Diabetes', *Front Physiol*, 11: 124.
de Rooij, J., H. Rehmann, M. van Triest, R. H. Cool, A. Wittinghofer, and J. L. Bos. 2000. 'Mechanism of regulation of the Epac family of cAMP-dependent RapGEFs', *J Biol Chem*, 275: 20829-36.
de Rooij, J., F. J. Zwartkruis, M. H. Verheijen, R. H. Cool, S. M. Nijman, A. Wittinghofer, and J. L. Bos. 1998. 'Epac is a Rap1 guanine-nucleotide-exchange factor directly activated by cyclic AMP', *Nature*, 396: 474-7.
de Simone, G., R. B. Devereux, M. Chinali, E. T. Lee, J. M. Galloway, A. Barac, J. A. Panza, and B. V. Howard. 2010. 'Diabetes and incident heart failure in hypertensive and normotensive participants of the Strong Heart Study', *J Hypertens*, 28: 353-60.
Delgado, C., A. Artiles, A. M. Gómez, and G. Vassort. 1999. 'Frequency-dependent increase

in cardiac Ca2+ current is due to reduced Ca2+ release by the sarcoplasmic reticulum', *J Mol Cell Cardiol*, 31: 1783-93.

Delucchi, F., R. Berni, C. Frati, S. Cavalli, G. Graiani, R. Sala, C. Chaponnier, G. Gabbiani, L. Calani, D. Del Rio, L. Bocchi, C. Lagrasta, F. Quaini, and D. Stilli. 2012. 'Resveratrol treatment reduces cardiac progenitor cell dysfunction and prevents morpho-functional ventricular remodeling in type-1 diabetic rats', *PLoS One*, 7: e39836.

DeMarco, K. R., and C. E. Clancy. 2016. 'Cardiac Na Channels: Structure to Function', *Curr Top Membr*, 78: 287-311.

Depre, C., M. E. Young, J. Ying, H. S. Ahuja, Q. Han, N. Garza, P. J. Davies, and H. Taegtmeyer. 2000. 'Streptozotocin-induced changes in cardiac gene expression in the absence of severe contractile dysfunction', *J Mol Cell Cardiol*, 32: 985-96.

Despa, S., F. Brette, C. H. Orchard, and D. M. Bers. 2003. 'Na/Ca exchange and Na/K-ATPase function are equally concentrated in transverse tubules of rat ventricular myocytes', *Biophys J*, 85: 3388-96.

Devereux, R. B., M. J. Roman, M. Paranicas, M. J. O'Grady, E. T. Lee, T. K. Welty, R. R. Fabsitz, D. Robbins, E. R. Rhoades, and B. V. Howard. 2000. 'Impact of diabetes on cardiac structure and function: the strong heart study', *Circulation*, 101: 2271-6.

Dierschke, S. K., A. L. Toro, A. J. Barber, A. C. Arnold, and M. D. Dennis. 2020. 'Angiotensin-(1-7) Attenuates Protein O-GlcNAcylation in the Retina by EPAC/Rap1-Dependent Inhibition of O-GlcNAc Transferase', *Invest Ophthalmol Vis Sci*, 61: 24.

Diviani, D., K. L. Dodge-Kafka, J. Li, and M. S. Kapiloff. 2011. 'A-kinase anchoring proteins: scaffolding proteins in the heart', *Am J Physiol Heart Circ Physiol*, 301: H1742-53.

Diviani, D., E. Reggi, M. Arambasic, S. Caso, and D. Maric. 2016. 'Emerging roles of A-kinase anchoring proteins in cardiovascular pathophysiology', *Biochim Biophys Acta*, 1863: 1926-36.

Domingo, D., P. Neco, E. Fernández-Pons, S. Zissimopoulos, P. Molina, J. Olagüe, M. P. Suárez-Mier, F. A. Lai, A. M. Gómez, and E. Zorio. 2015. 'Non-ventricular, Clinical, and Functional Features of the RyR2(R420Q) Mutation Causing Catecholaminergic Polymorphic Ventricular Tachycardia', *Rev Esp Cardiol (Engl Ed)*, 68: 398-407.

Dominguez-Rodriguez, A., G. Ruiz-Hurtado, J. Sabourin, A. M. Gomez, J. L. Alvarez, and J. P. Benitah. 2015. 'Proarrhythmic effect of sustained EPAC activation on TRPC3/4 in rat ventricular cardiomyocytes', *J Mol Cell Cardiol*, 87: 74-8.

Drago, G. A., J. Colyer, and W. J. Lederer. 1998. 'Immunofluorescence localization of SERCA2a and the phosphorylated forms of phospholamban in intact rat cardiac ventricular myocytes', *Ann N Y Acad Sci*, 853: 273-9.

Du, X. L., D. Edelstein, L. Rossetti, I. G. Fantus, H. Goldberg, F. Ziyadeh, J. Wu, and M. Brownlee. 2000. 'Hyperglycemia-induced mitochondrial superoxide overproduction activates the hexosamine pathway and induces plasminogen activator inhibitor-1 expression by increasing Sp1 glycosylation', *Proc Natl Acad Sci U S A*, 97: 12222-6.

Duquesnes, N., M. Derangeon, M. Metrich, A. Lucas, P. Mateo, L. Li, E. Morel, F. Lezoualc'h, and B. Crozatier. 2010. 'Epac stimulation induces rapid increases in connexin43 phosphorylation and function without preconditioning effect', *Pflugers Arch*, 460: 731-41.

Eder, P. 2017. 'Cardiac Remodeling and Disease: SOCE and TRPC Signaling in Cardiac Pathology', *Adv Exp Med Biol*, 993: 505-21.

'Effect of intensive therapy on the microvascular complications of type 1 diabetes mellitus'. 2002. *JAMA*, 287: 2563-9.

Eisner, D. A., J. L. Caldwell, K. Kistamás, and A. W. Trafford. 2017. 'Calcium and

Excitation-Contraction Coupling in the Heart', *Circ Res*, 121: 181-95.
Elder, D. H., J. S. Singh, D. Levin, L. A. Donnelly, A. M. Choy, J. George, A. D. Struthers, A. S. Doney, and C. C. Lang. 2016. 'Mean HbA1c and mortality in diabetic individuals with heart failure: a population cohort study', *Eur J Heart Fail*, 18: 94-102.
Enserink, J. M., A. E. Christensen, J. de Rooij, M. van Triest, F. Schwede, H. G. Genieser, S. O. Døskeland, J. L. Blank, and J. L. Bos. 2002. 'A novel Epac-specific cAMP analogue demonstrates independent regulation of Rap1 and ERK', *Nat Cell Biol*, 4: 901-6.
Erickson, J. R., L. Pereira, L. Wang, G. Han, A. Ferguson, K. Dao, R. J. Copeland, F. Despa, G. W. Hart, C. M. Ripplinger, and D. M. Bers. 2013. 'Diabetic hyperglycaemia activates CaMKII and arrhythmias by O-linked glycosylation', *Nature*, 502: 372-6.
Erqou, S., C. T. Lee, M. Suffoletto, J. B. Echouffo-Tcheugui, R. A. de Boer, J. P. van Melle, and A. I. Adler. 2013. 'Association between glycated haemoglobin and the risk of congestive heart failure in diabetes mellitus: systematic review and meta-analysis', *Eur J Heart Fail*, 15: 185-93.
Fabiato, A., and F. Fabiato. 1979. 'Calcium and cardiac excitation-contraction coupling', *Annu Rev Physiol*, 41: 473-84.
Farrell, E. F., A. Antaramian, A. Rueda, A. M. Gómez, and H. H. Valdivia. 2003. 'Sorcin inhibits calcium release and modulates excitation-contraction coupling in the heart', *J Biol Chem*, 278: 34660-6.
Fawcett, D. W., and N. S. McNutt. 1969. 'The ultrastructure of the cat myocardium. I. Ventricular papillary muscle', *J Cell Biol*, 42: 1-45.
Federico, M., E. L. Portiansky, L. Sommese, F. J. Alvarado, P. G. Blanco, C. N. Zanuzzi, J. Dedman, M. Kaetzel, X. H. T. Wehrens, A. Mattiazzi, and J. Palomeque. 2017. 'Calcium-calmodulin-dependent protein kinase mediates the intracellular signalling pathways of cardiac apoptosis in mice with impaired glucose tolerance', *J Physiol*, 595: 4089-108.
Ferrier, G. R., J. H. Saunders, and C. Mendez. 1973. 'A cellular mechanism for the generation of ventricular arrhythmias by acetylstrophanthidin', *Circ Res*, 32: 600-9.
Frank, J. S., G. Mottino, D. Reid, R. S. Molday, and K. D. Philipson. 1992. 'Distribution of the Na(+)-Ca2+ exchange protein in mammalian cardiac myocytes: an immunofluorescence and immunocolloidal gold-labeling study', *J Cell Biol*, 117: 337-45.
Frank, K. F., B. Bölck, Z. Ding, D. Krause, N. Hattebuhr, A. Malik, K. Brixius, R. J. Hajjar, J. Schrader, and R. H. Schwinger. 2005. 'Overexpression of sorcin enhances cardiac contractility in vivo and in vitro', *J Mol Cell Cardiol*, 38: 607-15.
Fricovsky, E. S., J. Suarez, S. H. Ihm, B. T. Scott, J. A. Suarez-Ramirez, I. Banerjee, M. Torres-Gonzalez, H. Wang, I. Ellrott, L. Maya-Ramos, F. Villarreal, and W. H. Dillmann. 2012. 'Excess protein O-GlcNAcylation and the progression of diabetic cardiomyopathy', *Am J Physiol Regul Integr Comp Physiol*, 303: R689-99.
Fujimoto, K., T. Shibasaki, N. Yokoi, Y. Kashima, M. Matsumoto, T. Sasaki, N. Tajima, T. Iwanaga, and S. Seino. 2002. 'Piccolo, a Ca2+ sensor in pancreatic beta-cells. Involvement of cAMP-GEFII.Rim2. Piccolo complex in cAMP-dependent exocytosis', *J Biol Chem*, 277: 50497-502.
Fujioka, Y., M. Komeda, and S. Matsuoka. 2000. 'Stoichiometry of Na+-Ca2+ exchange in inside-out patches excised from guinea-pig ventricular myocytes', *J Physiol*, 523 Pt 2: 339-51.
Fukuda, M., K. W. Williams, L. Gautron, and J. K. Elmquist. 2011. 'Induction of leptin resistance by activation of cAMP-Epac signaling', *Cell Metab*, 13: 331-9.
Fülöp, N., M. M. Mason, K. Dutta, P. Wang, A. J. Davidoff, R. B. Marchase, and J. C.

Chatham. 2007. 'Impact of Type 2 diabetes and aging on cardiomyocyte function and O-linked N-acetylglucosamine levels in the heart', *Am J Physiol Cell Physiol*, 292: C1370-8.

Furuichi, T., D. Furutama, Y. Hakamata, J. Nakai, H. Takeshima, and K. Mikoshiba. 1994. 'Multiple types of ryanodine receptor/Ca2+ release channels are differentially expressed in rabbit brain', *J Neurosci*, 14: 4794-805.

Ganesan, A. N., C. Maack, D. C. Johns, A. Sidor, and B. O'Rourke. 2006. 'Beta-adrenergic stimulation of L-type Ca2+ channels in cardiac myocytes requires the distal carboxyl terminus of alpha1C but not serine 1928', *Circ Res*, 98: e11-8.

Gauthier, C., G. Tavernier, F. Charpentier, D. Langin, and H. Le Marec. 1996. 'Functional beta3-adrenoceptor in the human heart', *J Clin Invest*, 98: 556-62.

Gellen, B., M. Fernández-Velasco, F. Briec, L. Vinet, K. LeQuang, P. Rouet-Benzineb, J. P. Bénitah, M. Pezet, G. Palais, N. Pellegrin, A. Zhang, R. Perrier, B. Escoubet, X. Marniquet, S. Richard, F. Jaisser, A. M. Gómez, F. Charpentier, and J. J. Mercadier. 2008. 'Conditional FKBP12.6 overexpression in mouse cardiac myocytes prevents triggered ventricular tachycardia through specific alterations in excitation-contraction coupling', *Circulation*, 117: 1778-86.

Gema Ruiz-Hurtado, Alejandro Domínguez-Rodríguez , Laetitia Pereira, María Fernández-Velasco, Cécile Cassan, Frank Lezoualc'h, Jean-Pierre Benitah, Ana M. Gómez. 2012. 'Sustained Epac activation induces calmodulin dependent positive inotropic effect in adult cardiomyocytes', *J Mol Cell Cardiol*, 53: 617-25.

Geraldes, P., and G. L. King. 2010. 'Activation of protein kinase C isoforms and its impact on diabetic complications', *Circ Res*, 106: 1319-31.

Giacco, F., and M. Brownlee. 2010. 'Oxidative stress and diabetic complications', *Circ Res*, 107: 1058-70.

Gloerich, M., and J. L. Bos. 2010. 'Epac: defining a new mechanism for cAMP action', *Annu Rev Pharmacol Toxicol*, 50: 355-75.

Golob, M., R. L. Moss, and N. C. Chesler. 2014. 'Cardiac tissue structure, properties, and performance: a materials science perspective', *Ann Biomed Eng*, 42: 2003-13.

Gómez, A. M., I. Schuster, J. Fauconnier, J. Prestle, G. Hasenfuss, and S. Richard. 2004. 'FKBP12.6 overexpression decreases Ca2+ spark amplitude but enhances [Ca2+]i transient in rat cardiac myocytes', *Am J Physiol Heart Circ Physiol*, 287: H1987-93.

Gonano, L. A., and P. P. Jones. 2017. 'FK506-binding proteins 12 and 12.6 (FKBPs) as regulators of cardiac Ryanodine Receptors: Insights from new functional and structural knowledge', *Channels (Austin)*, 11: 415-25.

Gong, D., X. Chi, J. Wei, G. Zhou, G. Huang, L. Zhang, R. Wang, J. Lei, S. R. W. Chen, and N. Yan. 2019. 'Modulation of cardiac ryanodine receptor 2 by calmodulin', *Nature*, 572: 347-51.

Gopal, S., H. A. B. Multhaupt, and J. R. Couchman. 2020. 'Calcium in Cell-Extracellular Matrix Interactions', *Adv Exp Med Biol*, 1131: 1079-102.

Gordan, R., J. K. Gwathmey, and L. H. Xie. 2015. 'Autonomic and endocrine control of cardiovascular function', *World J Cardiol*, 7: 204-14.

Greene, A. L., M. J. Lalli, Y. Ji, G. J. Babu, I. Grupp, M. Sussman, and M. Periasamy. 2000. 'Overexpression of SERCA2b in the heart leads to an increase in sarcoplasmic reticulum calcium transport function and increased cardiac contractility', *J Biol Chem*, 275: 24722-7.

Guatimosim, S., K. Dilly, L. F. Santana, M. Saleet Jafri, E. A. Sobie, and W. J. Lederer. 2002. 'Local Ca(2+) signaling and EC coupling in heart: Ca(2+) sparks and the regulation of the [Ca(2+)](i) transient', *J Mol Cell Cardiol*, 34: 941-50.

Guo, T., R. L. Cornea, S. Huke, E. Camors, Y. Yang, E. Picht, B. R. Fruen, and D. M. Bers.

2010. 'Kinetics of FKBP12.6 binding to ryanodine receptors in permeabilized cardiac myocytes and effects on Ca sparks', *Circ Res*, 106: 1743-52.

Guo, T., T. Zhang, R. Mestril, and D. M. Bers. 2006. 'Ca2+/Calmodulin-dependent protein kinase II phosphorylation of ryanodine receptor does affect calcium sparks in mouse ventricular myocytes', *Circ Res*, 99: 398-406.

Gurdon, J. B., T. R. Elsdale, and M. Fischberg. 1958. 'Sexually mature individuals of Xenopus laevis from the transplantation of single somatic nuclei', *Nature*, 182: 64-5.

Györke, I., and S. Györke. 1998. 'Regulation of the cardiac ryanodine receptor channel by luminal Ca2+ involves luminal Ca2+ sensing sites', *Biophys J*, 75: 2801-10.

Györke, I., N. Hester, L. R. Jones, and S. Györke. 2004. 'The role of calsequestrin, triadin, and junctin in conferring cardiac ryanodine receptor responsiveness to luminal calcium', *Biophys J*, 86: 2121-8.

Györke, S., and M. Fill. 1993. 'Ryanodine receptor adaptation: control mechanism of Ca(2+)-induced Ca2+ release in heart', *Science*, 260: 807-9.

Györke, S., and D. Terentyev. 2008. 'Modulation of ryanodine receptor by luminal calcium and accessory proteins in health and cardiac disease', *Cardiovasc Res*, 77: 245-55.

Haltiwanger, R. S., K. Grove, and G. A. Philipsberg. 1998. 'Modulation of O-linked N-acetylglucosamine levels on nuclear and cytoplasmic proteins in vivo using the peptide O-GlcNAc-beta-N-acetylglucosaminidase inhibitor O-(2-acetamido-2-deoxy-D-glucopyranosylidene)amino-N-phenylcarbamate', *J Biol Chem*, 273: 3611-7.

Hart, G. W., M. P. Housley, and C. Slawson. 2007. 'Cycling of O-linked beta-N-acetylglucosamine on nucleocytoplasmic proteins', *Nature*, 446: 1017-22.

Hawkins, M., N. Barzilai, R. Liu, M. Hu, W. Chen, and L. Rossetti. 1997. 'Role of the glucosamine pathway in fat-induced insulin resistance', *J Clin Invest*, 99: 2173-82.

Hilgemann, D. W., A. Collins, and S. Matsuoka. 1992. 'Steady-state and dynamic properties of cardiac sodium-calcium exchange. Secondary modulation by cytoplasmic calcium and ATP', *J Gen Physiol*, 100: 933-61.

Hilgemann, D. W., S. Matsuoka, G. A. Nagel, and A. Collins. 1992. 'Steady-state and dynamic properties of cardiac sodium-calcium exchange. Sodium-dependent inactivation', *J Gen Physiol*, 100: 905-32.

Hoivik, E. A., S. L. Witsoe, I. R. Bergheim, Y. Xu, I. Jakobsson, A. Tengholm, S. O. Doskeland, and M. Bakke. 2013. 'DNA methylation of alternative promoters directs tissue specific expression of Epac2 isoforms', *PLoS One*, 8: e67925.

Hothi, S. S., I. S. Gurung, J. C. Heathcote, Y. Zhang, S. W. Booth, J. N. Skepper, A. A. Grace, and C. L. Huang. 2008. 'Epac activation, altered calcium homeostasis and ventricular arrhythmogenesis in the murine heart', *Pflugers Arch*, 457: 253-70.

Howarth, F. C., M. A. Qureshi, Z. Hassan, L. T. Al Kury, D. Isaev, K. Parekh, S. R. Yammahi, M. Oz, T. E. Adrian, and E. Adeghate. 2011. 'Changing pattern of gene expression is associated with ventricular myocyte dysfunction and altered mechanisms of Ca2+ signalling in young type 2 Zucker diabetic fatty rat heart', *Exp Physiol*, 96: 325-37.

Hu, Y., D. Belke, J. Suarez, E. Swanson, R. Clark, M. Hoshijima, and W. H. Dillmann. 2005. 'Adenovirus-mediated overexpression of O-GlcNAcase improves contractile function in the diabetic heart', *Circ Res*, 96: 1006-13.

Hudmon, A., H. Schulman, J. Kim, J. M. Maltez, R. W. Tsien, and G. S. Pitt. 2005. 'CaMKII tethers to L-type Ca2+ channels, establishing a local and dedicated integrator of Ca2+ signals for facilitation', *J Cell Biol*, 171: 537-47.

Huke, S., and D. M. Bers. 2008. 'Ryanodine receptor phosphorylation at Serine 2030, 2808 and 2814 in rat cardiomyocytes', *Biochem Biophys Res Commun*, 376: 80-5.

Huke, S., J. Desantiago, M. A. Kaetzel, S. Mishra, J. H. Brown, J. R. Dedman, and D. M.

Bers. 2011. 'SR-targeted CaMKII inhibition improves SR Ca^{2+} handling, but accelerates cardiac remodeling in mice overexpressing CaMKIIδC', *J Mol Cell Cardiol*, 50: 230-8.

Hulme, J. T., R. E. Westenbroek, T. Scheuer, and W. A. Catterall. 2006. 'Phosphorylation of serine 1928 in the distal C-terminal domain of cardiac CaV1.2 channels during beta1-adrenergic regulation', *Proc Natl Acad Sci U S A*, 103: 16574-9.

Hüser, J., D. M. Bers, and L. A. Blatter. 1998. 'Subcellular properties of [Ca2+]i transients in phospholamban-deficient mouse ventricular cells', *Am J Physiol*, 274: H1800-11.

Huxley, A. F. 1971. 'The activation of striated muscle and its mechanical response', *Proc R Soc Lond B Biol Sci*, 178: 1-27.

Huxley, H., and J. Hanson. 1954. 'Changes in the cross-striations of muscle during contraction and stretch and their structural interpretation', *Nature*, 173: 973-6.

Hwang, M., Y. Go, J. H. Park, S. K. Shin, S. E. Song, B. C. Oh, S. S. Im, I. Hwang, Y. H. Jeon, I. K. Lee, S. Seino, and D. K. Song. 2017. 'Epac2a-null mice exhibit obesity-prone nature more susceptible to leptin resistance', *Int J Obes (Lond)*, 41: 279-88.

Iribarren, C., A. J. Karter, A. S. Go, A. Ferrara, J. Y. Liu, S. Sidney, and J. V. Selby. 2001. 'Glycemic control and heart failure among adult patients with diabetes', *Circulation*, 103: 2668-73.

Isenberg, G., and U. Klöckner. 1982. 'Calcium currents of isolated bovine ventricular myocytes are fast and of large amplitude', *Pflugers Arch*, 395: 30-41.

Izu, L. T., W. G. Wier, and C. W. Balke. 2001. 'Evolution of cardiac calcium waves from stochastic calcium sparks', *Biophys J*, 80: 103-20.

Jan, L. Y., and Y. N. Jan. 1997. 'Voltage-gated and inwardly rectifying potassium channels', *J Physiol*, 505 (Pt 2): 267-82.

Jayasinghe, I. D., M. B. Cannell, and C. Soeller. 2009. 'Organization of ryanodine receptors, transverse tubules, and sodium-calcium exchanger in rat myocytes', *Biophys J*, 97: 2664-73.

Jeevaratnam, K., K. R. Chadda, C. L. Huang, and A. J. Camm. 2018. 'Cardiac Potassium Channels: Physiological Insights for Targeted Therapy', *J Cardiovasc Pharmacol Ther*, 23: 119-29.

Jensen, B. C., T. D. O'Connell, and P. C. Simpson. 2014. 'Alpha-1-adrenergic receptors in heart failure: the adaptive arm of the cardiac response to chronic catecholamine stimulation', *J Cardiovasc Pharmacol*, 63: 291-301.

Jensen, R. V., I. Andreadou, D. J. Hausenloy, and H. E. Bøtker. 2019. 'The Role of O-GlcNAcylation for Protection against Ischemia-Reperfusion Injury', *Int J Mol Sci*, 20.

Jeyakumar, L. H., L. Ballester, D. S. Cheng, J. O. McIntyre, P. Chang, H. E. Olivey, L. Rollins-Smith, J. V. Barnett, K. Murray, H. B. Xin, and S. Fleischer. 2001. 'FKBP binding characteristics of cardiac microsomes from diverse vertebrates', *Biochem Biophys Res Commun*, 281: 979-86.

Jia, G., M. A. Hill, and J. R. Sowers. 2018. 'Diabetic Cardiomyopathy: An Update of Mechanisms Contributing to This Clinical Entity', *Circ Res*, 122: 624-38.

Jiang, M. T., A. J. Lokuta, E. F. Farrell, M. R. Wolff, R. A. Haworth, and H. H. Valdivia. 2002. 'Abnormal Ca2+ release, but normal ryanodine receptors, in canine and human heart failure', *Circ Res*, 91: 1015-22.

Jones, E. M., E. C. Roti Roti, J. Wang, S. A. Delfosse, and G. A. Robertson. 2004. 'Cardiac IKr channels minimally comprise hERG 1a and 1b subunits', *J Biol Chem*, 279: 44690-4.

Jung, C., A. S. Martins, E. Niggli, and N. Shirokova. 2008. 'Dystrophic cardiomyopathy: amplification of cellular damage by Ca2+ signalling and reactive oxygen species-generating pathways', *Cardiovasc Res*, 77: 766-73.

Jurevicius, J., and R. Fischmeister. 1996. 'cAMP compartmentation is responsible for a local activation of cardiac Ca2+ channels by beta-adrenergic agonists', *Proc Natl Acad Sci U S A*, 93: 295-9.

Kang, G., O. G. Chepurny, and G. G. Holz. 2001. 'cAMP-regulated guanine nucleotide exchange factor II (Epac2) mediates Ca2+-induced Ca2+ release in INS-1 pancreatic beta-cells', *J Physiol*, 536: 375-85.

Kang, G., O. G. Chepurny, B. Malester, M. J. Rindler, H. Rehmann, J. L. Bos, F. Schwede, W. A. Coetzee, and G. G. Holz. 2006. 'cAMP sensor Epac as a determinant of ATP-sensitive potassium channel activity in human pancreatic beta cells and rat INS-1 cells', *J Physiol*, 573: 595-609.

Kang, G., J. W. Joseph, O. G. Chepurny, M. Monaco, M. B. Wheeler, J. L. Bos, F. Schwede, H. G. Genieser, and G. G. Holz. 2003. 'Epac-selective cAMP analog 8-pCPT-2'-O-Me-cAMP as a stimulus for Ca2+-induced Ca2+ release and exocytosis in pancreatic beta-cells', *J Biol Chem*, 278: 8279-85.

Kannel, W. B., and D. L. McGee. 1979. 'Diabetes and cardiovascular disease. The Framingham study', *JAMA*, 241: 2035-8.

Karakikes, I., M. Ameen, V. Termglinchan, and J. C. Wu. 2015. 'Human induced pluripotent stem cell-derived cardiomyocytes: insights into molecular, cellular, and functional phenotypes', *Circ Res*, 117: 80-8.

Kass, R. S., W. J. Lederer, R. W. Tsien, and R. Weingart. 1978. 'Role of calcium ions in transient inward currents and aftercontractions induced by strophanthidin in cardiac Purkinje fibres', *J Physiol*, 281: 187-208.

Katz, A. M., M. Tada, and M. A. Kirchberger. 1975. 'Control of calcium transport in the myocardium by the cyclic AMP-Protein kinase system', *Adv Cyclic Nucleotide Res*, 5: 453-72.

Kawasaki, H., G. M. Springett, N. Mochizuki, S. Toki, M. Nakaya, M. Matsuda, D. E. Housman, and A. M. Graybiel. 1998. 'A family of cAMP-binding proteins that directly activate Rap1', *Science*, 282: 2275-9.

Kehat, I., D. Kenyagin-Karsenti, M. Snir, H. Segev, M. Amit, A. Gepstein, E. Livne, O. Binah, J. Itskovitz-Eldor, and L. Gepstein. 2001. 'Human embryonic stem cells can differentiate into myocytes with structural and functional properties of cardiomyocytes', *J Clin Invest*, 108: 407-14.

Keizer, J., and G. D. Smith. 1998. 'Spark-to-wave transition: saltatory transmission of calcium waves in cardiac myocytes', *Biophys Chem*, 72: 87-100.

Kenyon, J. L., and W. R. Gibbons. 1979a. '4-Aminopyridine and the early outward current of sheep cardiac Purkinje fibers', *J Gen Physiol*, 73: 139-57.

———. 1979b. 'Influence of chloride, potassium, and tetraethylammonium on the early outward current of sheep cardiac Purkinje fibers', *J Gen Physiol*, 73: 117-38.

Kohlhaas, M., T. Zhang, T. Seidler, D. Zibrova, N. Dybkova, A. Steen, S. Wagner, L. Chen, J. H. Brown, D. M. Bers, and L. S. Maier. 2006. 'Increased sarcoplasmic reticulum calcium leak but unaltered contractility by acute CaMKII overexpression in isolated rabbit cardiac myocytes', *Circ Res*, 98: 235-44.

Kolwicz, S. C., Jr., and R. Tian. 2011. 'Glucose metabolism and cardiac hypertrophy', *Cardiovasc Res*, 90: 194-201.

Kranias, E. G., A. Schwartz, and R. A. Jungmann. 1982. 'Characterization of cyclic 3':5'-amp-dependent protein kinase in sarcoplasmic reticulum and cytosol of canine myocardium', *Biochim Biophys Acta*, 709: 28-37.

Kranstuber, A. L., C. Del Rio, B. J. Biesiadecki, R. L. Hamlin, J. Ottobre, S. Gyorke, and V. A. Lacombe. 2012. 'Advanced glycation end product cross-link breaker attenuates diabetes-induced cardiac dysfunction by improving sarcoplasmic reticulum calcium

handling', *Front Physiol*, 3: 292.
Kronlage, M., M. Dewenter, J. Grosso, T. Fleming, U. Oehl, L. H. Lehmann, I. Falcão-Pires, A. F. Leite-Moreira, N. Volk, H. J. Gröne, O. J. Müller, A. Sickmann, H. A. Katus, and J. Backs. 2019. 'O-GlcNAcylation of Histone Deacetylase 4 Protects the Diabetic Heart From Failure', *Circulation*, 140: 580-94.
Kuschel, M., P. Karczewski, P. Hempel, W. P. Schlegel, E. G. Krause, and S. Bartel. 1999. 'Ser16 prevails over Thr17 phospholamban phosphorylation in the beta-adrenergic regulation of cardiac relaxation', *Am J Physiol*, 276: H1625-33.
Kuschel, M., Y. Y. Zhou, H. Cheng, S. J. Zhang, Y. Chen, E. G. Lakatta, and R. P. Xiao. 1999. 'G(i) protein-mediated functional compartmentalization of cardiac beta(2)-adrenergic signaling', *J Biol Chem*, 274: 22048-52.
Lacombe, V. A., S. Viatchenko-Karpinski, D. Terentyev, A. Sridhar, S. Emani, J. D. Bonagura, D. S. Feldman, S. Györke, and C. A. Carnes. 2007. 'Mechanisms of impaired calcium handling underlying subclinical diastolic dysfunction in diabetes', *Am J Physiol Regul Integr Comp Physiol*, 293: R1787-97.
Lakatta, E. G., V. A. Maltsev, and T. M. Vinogradova. 2010. 'A coupled SYSTEM of intracellular Ca2+ clocks and surface membrane voltage clocks controls the timekeeping mechanism of the heart's pacemaker', *Circ Res*, 106: 659-73.
Larbig, R., N. Torres, J. H. Bridge, J. I. Goldhaber, and K. D. Philipson. 2010. 'Activation of reverse Na+-Ca2+ exchange by the Na+ current augments the cardiac Ca2+ transient: evidence from NCX knockout mice', *J Physiol*, 588: 3267-76.
LaRocca, T. J., F. Fabris, J. Chen, D. Benhayon, S. Zhang, L. McCollum, A. D. Schecter, J. Y. Cheung, E. A. Sobie, R. J. Hajjar, and D. Lebeche. 2012. 'Na+/Ca2+ exchanger-1 protects against systolic failure in the Akitains2 model of diabetic cardiomyopathy via a CXCR4/NF-κB pathway', *Am J Physiol Heart Circ Physiol*, 303: H353-67.
Laver, D. R., C. H. Kong, M. S. Imtiaz, and M. B. Cannell. 2013. 'Termination of calcium-induced calcium release by induction decay: an emergent property of stochastic channel gating and molecular scale architecture', *J Mol Cell Cardiol*, 54: 98-100.
Lederer, W. J., and R. W. Tsien. 1976. 'Transient inward current underlying arrhythmogenic effects of cardiotonic steroids in Purkinje fibres', *J Physiol*, 263: 73-100.
Lee, S. L., I. Ostadalova, F. Kolar, and N. S. Dhalla. 1992. 'Alterations in Ca(2+)-channels during the development of diabetic cardiomyopathy', *Mol Cell Biochem*, 109: 173-9.
Lehnart, S. E. 2007. 'Novel targets for treating heart and muscle disease: stabilizing ryanodine receptors and preventing intracellular calcium leak', *Curr Opin Pharmacol*, 7: 225-32.
Leney, A. C., D. El Atmioui, W. Wu, H. Ovaa, and A. J. R. Heck. 2017. 'Elucidating crosstalk mechanisms between phosphorylation and O-GlcNAcylation', *Proc Natl Acad Sci U S A*, 114: E7255-e61.
Lezcano, N., J. I. E. Mariángelo, L. Vittone, X. H. T. Wehrens, M. Said, and C. Mundiña-Weilenmann. 2018. 'Early effects of Epac depend on the fine-tuning of the sarcoplasmic reticulum Ca(2+) handling in cardiomyocytes', *J Mol Cell Cardiol*, 114: 1-9.
Lezoualc'h, F., L. Fazal, M. Laudette, and C. Conte. 2016. 'Cyclic AMP Sensor EPAC Proteins and Their Role in Cardiovascular Function and Disease', *Circ Res*, 118: 881-97.
Li, G. R., J. Feng, L. Yue, M. Carrier, and S. Nattel. 1996. 'Evidence for two components of delayed rectifier K+ current in human ventricular myocytes', *Circ Res*, 78: 689-96.
Li, L., J. Desantiago, G. Chu, E. G. Kranias, and D. M. Bers. 2000. 'Phosphorylation of phospholamban and troponin I in beta-adrenergic-induced acceleration of cardiac relaxation', *Am J Physiol Heart Circ Physiol*, 278: H769-79.

Li, Y., S. Asuri, J. F. Rebhun, A. F. Castro, N. C. Paranavitana, and L. A. Quilliam. 2006. 'The RAP1 guanine nucleotide exchange factor Epac2 couples cyclic AMP and Ras signals at the plasma membrane', *J Biol Chem*, 281: 2506-14.

Li, Y., E. G. Kranias, G. A. Mignery, and D. M. Bers. 2002. 'Protein kinase A phosphorylation of the ryanodine receptor does not affect calcium sparks in mouse ventricular myocytes', *Circ Res*, 90: 309-16.

Lim, G., L. Venetucci, D. A. Eisner, and B. Casadei. 2008. 'Does nitric oxide modulate cardiac ryanodine receptor function? Implications for excitation-contraction coupling', *Cardiovasc Res*, 77: 256-64.

Linz, K. W., and R. Meyer. 1998. 'Control of L-type calcium current during the action potential of guinea-pig ventricular myocytes', *J Physiol*, 513 (Pt 2): 425-42.

Liu, C., M. Takahashi, Y. Li, S. Song, T. J. Dillon, U. Shinde, and P. J. Stork. 2008. 'Ras is required for the cyclic AMP-dependent activation of Rap1 via Epac2', *Mol Cell Biol*, 28: 7109-25.

Liu, D. W., G. A. Gintant, and C. Antzelevitch. 1993. 'Ionic bases for electrophysiological distinctions among epicardial, midmyocardial, and endocardial myocytes from the free wall of the canine left ventricle', *Circ Res*, 72: 671-87.

Lohse, M. J., S. Engelhardt, and T. Eschenhagen. 2003. 'What is the role of beta-adrenergic signaling in heart failure?', *Circ Res*, 93: 896-906.

Lokuta, A. J., M. B. Meyers, P. R. Sander, G. I. Fishman, and H. H. Valdivia. 1997. 'Modulation of cardiac ryanodine receptors by sorcin', *J Biol Chem*, 272: 25333-8.

Lopatin, A. N., and C. G. Nichols. 2001. 'Inward rectifiers in the heart: an update on I(K1)', *J Mol Cell Cardiol*, 33: 625-38.

Louch, W. E., V. Bito, F. R. Heinzel, R. Macianskiene, J. Vanhaecke, W. Flameng, K. Mubagwa, and K. R. Sipido. 2004. 'Reduced synchrony of Ca2+ release with loss of T-tubules-a comparison to Ca2+ release in human failing cardiomyocytes', *Cardiovasc Res*, 62: 63-73.

Loughrey, C. M., T. Seidler, S. L. Miller, J. Prestle, K. E. MacEachern, D. F. Reynolds, G. Hasenfuss, and G. L. Smith. 2004. 'Over-expression of FK506-binding protein FKBP12.6 alters excitation-contraction coupling in adult rabbit cardiomyocytes', *J Physiol*, 556: 919-34.

Lu, S., Z. Liao, X. Lu, D. M. Katschinski, M. Mercola, J. Chen, J. Heller Brown, J. D. Molkentin, J. Bossuyt, and D. M. Bers. 2020. 'Hyperglycemia Acutely Increases Cytosolic Reactive Oxygen Species via O-linked GlcNAcylation and CaMKII Activation in Mouse Ventricular Myocytes', *Circ Res*, 126: e80-e96.

Lu, Z., L. M. Ballou, Y. P. Jiang, I. S. Cohen, and R. Z. Lin. 2011. 'Restoration of defective L-type Ca2+ current in cardiac myocytes of type 2 diabetic db/db mice by Akt and PKC-ι', *J Cardiovasc Pharmacol*, 58: 439-45.

Lu, Z., Y. P. Jiang, X. H. Xu, L. M. Ballou, I. S. Cohen, and R. Z. Lin. 2007. 'Decreased L-type Ca2+ current in cardiac myocytes of type 1 diabetic Akita mice due to reduced phosphatidylinositol 3-kinase signaling', *Diabetes*, 56: 2780-9.

Lundby, A., G. N. Tseng, and N. Schmitt. 2010. 'Structural basis for K(V)7.1-KCNE(x) interactions in the I(Ks) channel complex', *Heart Rhythm*, 7: 708-13.

Luo, W., I. L. Grupp, J. Harrer, S. Ponniah, G. Grupp, J. J. Duffy, T. Doetschman, and E. G. Kranias. 1994. 'Targeted ablation of the phospholamban gene is associated with markedly enhanced myocardial contractility and loss of beta-agonist stimulation', *Circ Res*, 75: 401-9.

Ma, J., and G. W. Hart. 2014. 'O-GlcNAc profiling: from proteins to proteomes', *Clin Proteomics*, 11: 8.

Maack, C., and M. Böhm. 2011. 'Targeting mitochondrial oxidative stress in heart failure

throttling the afterburner', *J Am Coll Cardiol*, 58: 83-6.
Macauley, M. S., and D. J. Vocadlo. 2010. 'Increasing O-GlcNAc levels: An overview of small-molecule inhibitors of O-GlcNAcase', *Biochim Biophys Acta*, 1800: 107-21.
MacDonnell, S. M., G. García-Rivas, J. A. Scherman, H. Kubo, X. Chen, H. Valdivia, and S. R. Houser. 2008. 'Adrenergic regulation of cardiac contractility does not involve phosphorylation of the cardiac ryanodine receptor at serine 2808', *Circ Res*, 102: e65-72.
MacLennan, D. H., and E. G. Kranias. 2003. 'Phospholamban: a crucial regulator of cardiac contractility', *Nat Rev Mol Cell Biol*, 4: 566-77.
Mailleux, F., R. Gelinas, C. Beauloye, S. Horman, and L. Bertrand. 2016. 'O-GlcNAcylation, enemy or ally during cardiac hypertrophy development?', *Biochim Biophys Acta*, 1862: 2232-43.
Marbán, E. 2002. 'Cardiac channelopathies', *Nature*, 415: 213-8.
Marban, E., T. Yamagishi, and G. F. Tomaselli. 1998. 'Structure and function of voltage-gated sodium channels', *J Physiol*, 508 (Pt 3): 647-57.
Marshall, S., V. Bacote, and R. R. Traxinger. 1991. 'Discovery of a metabolic pathway mediating glucose-induced desensitization of the glucose transport system. Role of hexosamine biosynthesis in the induction of insulin resistance', *J Biol Chem*, 266: 4706-12.
Marx, S. O., J. Gaburjakova, M. Gaburjakova, C. Henrikson, K. Ondrias, and A. R. Marks. 2001. 'Coupled gating between cardiac calcium release channels (ryanodine receptors)', *Circ Res*, 88: 1151-8.
Marx, S. O., S. Reiken, Y. Hisamatsu, T. Jayaraman, D. Burkhoff, N. Rosemblit, and A. R. Marks. 2000. 'PKA phosphorylation dissociates FKBP12.6 from the calcium release channel (ryanodine receptor): defective regulation in failing hearts', *Cell*, 101: 365-76.
Maurer, P., and E. Hohenester. 1997. 'Structural and functional aspects of calcium binding in extracellular matrix proteins', *Matrix Biol*, 15: 569-80; discussion 81.
McCall, E., L. Li, H. Satoh, T. R. Shannon, L. A. Blatter, and D. M. Bers. 1996. 'Effects of FK-506 on contraction and Ca2+ transients in rat cardiac myocytes', *Circ Res*, 79: 1110-21.
Meissner, G. 1994. 'Ryanodine receptor/Ca2+ release channels and their regulation by endogenous effectors', *Annu Rev Physiol*, 56: 485-508.
———. 2017. 'The structural basis of ryanodine receptor ion channel function', *J Gen Physiol*, 149: 1065-89.
Meissner, G., and J. S. Henderson. 1987. 'Rapid calcium release from cardiac sarcoplasmic reticulum vesicles is dependent on Ca2+ and is modulated by Mg2+, adenine nucleotide, and calmodulin', *J Biol Chem*, 262: 3065-73.
Metrich, M., A. C. Laurent, M. Breckler, N. Duquesnes, I. Hmitou, D. Courillau, J. P. Blondeau, B. Crozatier, F. Lezoualc'h, and E. Morel. 2010. 'Epac activation induces histone deacetylase nuclear export via a Ras-dependent signalling pathway', *Cell Signal*, 22: 1459-68.
Metrich, M., A. Lucas, M. Gastineau, J. L. Samuel, C. Heymes, E. Morel, and F. Lezoualc'h. 2008. 'Epac mediates beta-adrenergic receptor-induced cardiomyocyte hypertrophy', *Circ Res*, 102: 959-65.
Meyers, M. B., A. Fischer, Y. J. Sun, C. M. Lopes, T. Rohacs, T. Y. Nakamura, Y. Y. Zhou, P. C. Lee, R. A. Altschuld, S. A. McCune, W. A. Coetzee, and G. I. Fishman. 2003. 'Sorcin regulates excitation-contraction coupling in the heart', *J Biol Chem*, 278: 28865-71.
Meyers, M. B., V. M. Pickel, S. S. Sheu, V. K. Sharma, K. W. Scotto, and G. I. Fishman. 1995. 'Association of sorcin with the cardiac ryanodine receptor', *J Biol Chem*, 270:

26411-8.
Mika, D., J. Leroy, G. Vandecasteele, and R. Fischmeister. 2012. 'PDEs create local domains of cAMP signaling', *J Mol Cell Cardiol*, 52: 323-9.
Mitchell, R. D., H. K. Simmerman, and L. R. Jones. 1988. 'Ca2+ binding effects on protein conformation and protein interactions of canine cardiac calsequestrin', *J Biol Chem*, 263: 1376-81.
Montaigne, D., X. Marechal, A. Coisne, N. Debry, T. Modine, G. Fayad, C. Potelle, J. M. El Arid, S. Mouton, Y. Sebti, H. Duez, S. Preau, I. Remy-Jouet, F. Zerimech, M. Koussa, V. Richard, R. Neviere, J. L. Edme, P. Lefebvre, and B. Staels. 2014. 'Myocardial contractile dysfunction is associated with impaired mitochondrial function and dynamics in type 2 diabetic but not in obese patients', *Circulation*, 130: 554-64.
Morel, E., A. Marcantoni, M. Gastineau, R. Birkedal, F. Rochais, A. Garnier, A. M. Lompre, G. Vandecasteele, and F. Lezoualc'h. 2005. 'cAMP-binding protein Epac induces cardiomyocyte hypertrophy', *Circ Res*, 97: 1296-304.
Munshi, N. V. 2012. 'Gene regulatory networks in cardiac conduction system development', *Circ Res*, 110: 1525-37.
Münzel, T., G. G. Camici, C. Maack, N. R. Bonetti, V. Fuster, and J. C. Kovacic. 2017. 'Impact of Oxidative Stress on the Heart and Vasculature: Part 2 of a 3-Part Series', *J Am Coll Cardiol*, 70: 212-29.
Münzel, T., T. Gori, R. M. Bruno, and S. Taddei. 2010. 'Is oxidative stress a therapeutic target in cardiovascular disease?', *Eur Heart J*, 31: 2741-8.
Näbauer, M. 1998. 'Electrical heterogeneity in the ventricular wall--and the M cell', *Cardiovasc Res*, 40: 248-50.
Neco, P., B. Rose, N. Huynh, R. Zhang, J. H. Bridge, K. D. Philipson, and J. I. Goldhaber. 2010. 'Sodium-calcium exchange is essential for effective triggering of calcium release in mouse heart', *Biophys J*, 99: 755-64.
Negretti, N., S. C. O'Neill, and D. A. Eisner. 1993. 'The effects of inhibitors of sarcoplasmic reticulum function on the systolic Ca2+ transient in rat ventricular myocytes', *J Physiol*, 468: 35-52.
Nerbonne, J. M., and W. Guo. 2002. 'Heterogeneous expression of voltage-gated potassium channels in the heart: roles in normal excitation and arrhythmias', *J Cardiovasc Electrophysiol*, 13: 406-9.
Nerbonne, J. M., and R. S. Kass. 2005. 'Molecular physiology of cardiac repolarization', *Physiol Rev*, 85: 1205-53.
Neylon, C. B., S. M. Richards, M. A. Larsen, A. Agrotis, and A. Bobik. 1995. 'Multiple types of ryanodine receptor/Ca2+ release channels are expressed in vascular smooth muscle', *Biochem Biophys Res Commun*, 215: 814-21.
Ng, K. M., Y. M. Lau, V. Dhandhania, Z. J. Cai, Y. K. Lee, W. H. Lai, H. F. Tse, and C. W. Siu. 2018. 'Empagliflozin Ammeliorates High Glucose Induced-Cardiac Dysfuntion in Human iPSC-Derived Cardiomyocytes', *Sci Rep*, 8: 14872.
Niedergerke, R., and S. Page. 1977. 'Analysis of catecholamine effects in single atrial trabeculae of the frog heart', *Proc R Soc Lond B Biol Sci*, 197: 333-62.
Niggli, E., N. D. Ullrich, D. Gutierrez, S. Kyrychenko, E. Poláková, and N. Shirokova. 2013. 'Posttranslational modifications of cardiac ryanodine receptors: Ca(2+) signaling and EC-coupling', *Biochim Biophys Acta*, 1833: 866-75.
Niimura, M., T. Miki, T. Shibasaki, W. Fujimoto, T. Iwanaga, and S. Seino. 2009. 'Critical role of the N-terminal cyclic AMP-binding domain of Epac2 in its subcellular localization and function', *J Cell Physiol*, 219: 652-8.
Nikolaev, V. O., M. Bünemann, E. Schmitteckert, M. J. Lohse, and S. Engelhardt. 2006. 'Cyclic AMP imaging in adult cardiac myocytes reveals far-reaching beta1-adrenergic

but locally confined beta2-adrenergic receptor-mediated signaling', *Circ Res*, 99: 1084-91.

Nikolaev, V. O., A. Moshkov, A. R. Lyon, M. Miragoli, P. Novak, H. Paur, M. J. Lohse, Y. E. Korchev, S. E. Harding, and J. Gorelik. 2010. 'Beta2-adrenergic receptor redistribution in heart failure changes cAMP compartmentation', *Science*, 327: 1653-7.

Noble, D., and R. W. Tsien. 1969. 'Outward membrane currents activated in the plateau range of potentials in cardiac Purkinje fibres', *J Physiol*, 200: 205-31.

Nystoriak, M. A., M. Nieves-Cintrón, T. Patriarchi, O. R. Buonarati, M. P. Prada, S. Morotti, E. Grandi, J. D. Fernandes, K. Forbush, F. Hofmann, K. C. Sasse, J. D. Scott, S. M. Ward, J. W. Hell, and M. F. Navedo. 2017. 'Ser1928 phosphorylation by PKA stimulates the L-type Ca2+ channel CaV1.2 and vasoconstriction during acute hyperglycemia and diabetes', *Sci Signal*, 10.

Oestreich, E. A., S. Malik, S. A. Goonasekera, B. C. Blaxall, G. G. Kelley, R. T. Dirksen, and A. V. Smrcka. 2009. 'Epac and phospholipase Cepsilon regulate Ca2+ release in the heart by activation of protein kinase Cepsilon and calcium-calmodulin kinase II', *J Biol Chem*, 284: 1514-22.

Oestreich, E. A., H. Wang, S. Malik, K. A. Kaproth-Joslin, B. C. Blaxall, G. G. Kelley, R. T. Dirksen, and A. V. Smrcka. 2007. 'Epac-mediated activation of phospholipase C(epsilon) plays a critical role in beta-adrenergic receptor-dependent enhancement of Ca2+ mobilization in cardiac myocytes', *J Biol Chem*, 282: 5488-95.

Olson, A. K., B. Bouchard, W. Z. Zhu, J. C. Chatham, and C. Des Rosiers. 2020. 'First characterization of glucose flux through the hexosamine biosynthesis pathway (HBP) in ex vivo mouse heart', *J Biol Chem*, 295: 2018-33.

Opthof, T. 2000. 'The normal range and determinants of the intrinsic heart rate in man', *Cardiovasc Res*, 45: 173-6.

Orkand, R. K., and R. Niedergerke. 1964. 'HEART ACTION POTENTIAL: DEPENDENCE ON EXTERNAL CALCIUM AND SODIUM IONS', *Science*, 146: 1176-7.

Osterrieder, W., G. Brum, J. Hescheler, W. Trautwein, V. Flockerzi, and F. Hofmann. 1982. 'Injection of subunits of cyclic AMP-dependent protein kinase into cardiac myocytes modulates Ca2+ current', *Nature*, 298: 576-8.

Otsu, K., H. F. Willard, V. K. Khanna, F. Zorzato, N. M. Green, and D. H. MacLennan. 1990. 'Molecular cloning of cDNA encoding the Ca2+ release channel (ryanodine receptor) of rabbit cardiac muscle sarcoplasmic reticulum', *J Biol Chem*, 265: 13472-83.

Ozaki, N., T. Shibasaki, Y. Kashima, T. Miki, K. Takahashi, H. Ueno, Y. Sunaga, H. Yano, Y. Matsuura, T. Iwanaga, Y. Takai, and S. Seino. 2000. 'cAMP-GEFII is a direct target of cAMP in regulated exocytosis', *Nat Cell Biol*, 2: 805-11.

Page, E., and M. Surdyk-Droske. 1979. 'Distribution, surface density, and membrane area of diadic junctional contacts between plasma membrane and terminal cisterns in mammalian ventricle', *Circ Res*, 45: 260-7.

Pascual, F., and R. A. Coleman. 2016. 'Fuel availability and fate in cardiac metabolism: A tale of two substrates', *Biochim Biophys Acta*, 1861: 1425-33.

Pereira, L., D. J. Bare, S. Galice, T. R. Shannon, and D. M. Bers. 2017a. '0beta-Adrenergic induced SR Ca2+ leak is mediated by an Epac-NOS pathway', *J Mol Cell Cardiol*.

———. 2017b. 'beta-Adrenergic induced SR Ca2+ leak is mediated by an Epac-NOS pathway', *J Mol Cell Cardiol*, 108: 8-16.

Pereira, L., H. Cheng, D. H. Lao, L. Na, R. J. van Oort, J. H. Brown, X. H. Wehrens, J. Chen, and D. M. Bers. 2013. 'Epac2 mediates cardiac beta1-adrenergic-dependent sarcoplasmic reticulum Ca2+ leak and arrhythmia', *Circulation*, 127: 913-22.

Pereira, L., J. Matthes, I. Schuster, H. H. Valdivia, S. Herzig, S. Richard, and A. M. Gomez. 2006. 'Mechanisms of [Ca2+]i transient decrease in cardiomyopathy of db/db type 2

diabetic mice', *Diabetes*, 55: 608-15.
Pereira, L., M. Metrich, M. Fernandez-Velasco, A. Lucas, J. Leroy, R. Perrier, E. Morel, R. Fischmeister, S. Richard, J. P. Benitah, F. Lezoualc'h, and A. M. Gomez. 2007. 'The cAMP binding protein Epac modulates Ca2+ sparks by a Ca2+/calmodulin kinase signalling pathway in rat cardiac myocytes', *J Physiol*, 583: 685-94.
Pereira, L., H. Rehmann, D. H. Lao, J. R. Erickson, J. Bossuyt, J. Chen, and D. M. Bers. 2015. 'Novel Epac fluorescent ligand reveals distinct Epac1 vs. Epac2 distribution and function in cardiomyocytes', *Proc Natl Acad Sci U S A*, 112: 3991-6.
Pereira, L., G. Ruiz-Hurtado, E. Morel, A. C. Laurent, M. Metrich, A. Dominguez-Rodriguez, S. Lauton-Santos, A. Lucas, J. P. Benitah, D. M. Bers, F. Lezoualc'h, and A. M. Gomez. 2012. 'Epac enhances excitation-transcription coupling in cardiac myocytes', *J Mol Cell Cardiol*, 52: 283-91.
Pidoux, G., and K. Taskén. 2010. 'Specificity and spatial dynamics of protein kinase A signaling organized by A-kinase-anchoring proteins', *J Mol Endocrinol*, 44: 271-84.
Pitt, G. S. 2007. 'Calmodulin and CaMKII as molecular switches for cardiac ion channels', *Cardiovasc Res*, 73: 641-7.
Pitt, G. S., R. D. Zühlke, A. Hudmon, H. Schulman, H. Reuter, and R. W. Tsien. 2001. 'Molecular basis of calmodulin tethering and Ca2+-dependent inactivation of L-type Ca2+ channels', *J Biol Chem*, 276: 30794-802.
Pogwizd, S. M., and D. M. Bers. 2004. 'Cellular basis of triggered arrhythmias in heart failure', *Trends Cardiovasc Med*, 14: 61-6.
Ponsioen, B., M. Gloerich, L. Ritsma, H. Rehmann, J. L. Bos, and K. Jalink. 2009. 'Direct spatial control of Epac1 by cyclic AMP', *Mol Cell Biol*, 29: 2521-31.
Poppe, H., S. D. Rybalkin, H. Rehmann, T. R. Hinds, X. B. Tang, A. E. Christensen, F. Schwede, H. G. Genieser, J. L. Bos, S. O. Doskeland, J. A. Beavo, and E. Butt. 2008. 'Cyclic nucleotide analogs as probes of signaling pathways', *Nat Methods*, 5: 277-8.
Potenza, D. M., R. Janicek, M. Fernandez-Tenorio, E. Camors, R. Ramos-Mondragón, H. H. Valdivia, and E. Niggli. 2019. 'Phosphorylation of the ryanodine receptor 2 at serine 2030 is required for a complete β-adrenergic response', *J Gen Physiol*, 151: 131-45.
Powell, T., D. A. Terrar, and V. W. Twist. 1980. 'Electrical properties of individual cells isolated from adult rat ventricular myocardium', *J Physiol*, 302: 131-53.
Prestle, J., P. M. Janssen, A. P. Janssen, O. Zeitz, S. E. Lehnart, L. Bruce, G. L. Smith, and G. Hasenfuss. 2001. 'Overexpression of FK506-binding protein FKBP12.6 in cardiomyocytes reduces ryanodine receptor-mediated Ca(2+) leak from the sarcoplasmic reticulum and increases contractility', *Circ Res*, 88: 188-94.
Priori, S. G., and S. R. Chen. 2011. 'Inherited dysfunction of sarcoplasmic reticulum Ca2+ handling and arrhythmogenesis', *Circ Res*, 108: 871-83.
Qin, C. X., R. Sleaby, A. J. Davidoff, J. R. Bell, M. J. De Blasio, L. M. Delbridge, J. C. Chatham, and R. H. Ritchie. 2017. 'Insights into the role of maladaptive hexosamine biosynthesis and O-GlcNAcylation in development of diabetic cardiac complications', *Pharmacol Res*, 116: 45-56.
Ramirez-Correa, G. A., J. Ma, C. Slawson, Q. Zeidan, N. S. Lugo-Fagundo, M. Xu, X. Shen, W. D. Gao, V. Caceres, K. Chakir, L. DeVine, R. N. Cole, L. Marchionni, N. Paolocci, G. W. Hart, and A. M. Murphy. 2015. 'Removal of Abnormal Myofilament O-GlcNAcylation Restores Ca2+ Sensitivity in Diabetic Cardiac Muscle', *Diabetes*, 64: 3573-87.
Reeves, J. P., and C. C. Hale. 1984. 'The stoichiometry of the cardiac sodium-calcium exchange system', *J Biol Chem*, 259: 7733-9.
Rehmann, H., E. Arias-Palomo, M. A. Hadders, F. Schwede, O. Llorca, and J. L. Bos. 2008. 'Structure of Epac2 in complex with a cyclic AMP analogue and RAP1B', *Nature*, 455:

124-7.
Rehmann, H., J. Das, P. Knipscheer, A. Wittinghofer, and J. L. Bos. 2006. 'Structure of the cyclic-AMP-responsive exchange factor Epac2 in its auto-inhibited state', *Nature*, 439: 625-8.
Rehmann, H., B. Prakash, E. Wolf, A. Rueppel, J. de Rooij, J. L. Bos, and A. Wittinghofer. 2003. 'Structure and regulation of the cAMP-binding domains of Epac2', *Nat Struct Biol*, 10: 26-32.
Rehmann, H., A. Rueppel, J. L. Bos, and A. Wittinghofer. 2003. 'Communication between the regulatory and the catalytic region of the cAMP-responsive guanine nucleotide exchange factor Epac', *J Biol Chem*, 278: 23508-14.
Rehmann, H., F. Schwede, S. O. Doskeland, A. Wittinghofer, and J. L. Bos. 2003. 'Ligand-mediated activation of the cAMP-responsive guanine nucleotide exchange factor Epac', *J Biol Chem*, 278: 38548-56.
Rehmann, H., A. Wittinghofer, and J. L. Bos. 2007. 'Capturing cyclic nucleotides in action: snapshots from crystallographic studies', *Nat Rev Mol Cell Biol*, 8: 63-73.
Ren, J., G. A. Gintant, R. E. Miller, and A. J. Davidoff. 1997. 'High extracellular glucose impairs cardiac E-C coupling in a glycosylation-dependent manner', *Am J Physiol*, 273: H2876-83.
Richard, S., E. Perrier, J. Fauconnier, R. Perrier, L. Pereira, A. M. Gõmez, and J. P. Bénitah. 2006. "Ca(2+)-induced Ca(2+) entry' or how the L-type Ca(2+) channel remodels its own signalling pathway in cardiac cells', *Prog Biophys Mol Biol*, 90: 118-35.
Rousseau, E., J. S. Smith, J. S. Henderson, and G. Meissner. 1986. 'Single channel and 45Ca2+ flux measurements of the cardiac sarcoplasmic reticulum calcium channel', *Biophys J*, 50: 1009-14.
Rubler, S., J. Dlugash, Y. Z. Yuceoglu, T. Kumral, A. W. Branwood, and A. Grishman. 1972. 'New type of cardiomyopathy associated with diabetic glomerulosclerosis', *Am J Cardiol*, 30: 595-602.
Ruiz-Hurtado, G., A. Dominguez-Rodriguez, L. Pereira, M. Fernandez-Velasco, C. Cassan, F. Lezoualc'h, J. P. Benitah, and A. M. Gomez. 2012. 'Sustained Epac activation induces calmodulin dependent positive inotropic effect in adult cardiomyocytes', *J Mol Cell Cardiol*, 53: 617-25.
Salata, J. J., N. K. Jurkiewicz, B. Jow, K. Folander, P. J. Guinosso, Jr., B. Raynor, R. Swanson, and B. Fermini. 1996. 'IK of rabbit ventricle is composed of two currents: evidence for IKs', *Am J Physiol*, 271: H2477-89.
Sanguinetti, M. C., M. E. Curran, A. Zou, J. Shen, P. S. Spector, D. L. Atkinson, and M. T. Keating. 1996. 'Coassembly of K(V)LQT1 and minK (IsK) proteins to form cardiac I(Ks) potassium channel', *Nature*, 384: 80-3.
Sanguinetti, M. C., C. Jiang, M. E. Curran, and M. T. Keating. 1995. 'A mechanistic link between an inherited and an acquired cardiac arrhythmia: HERG encodes the IKr potassium channel', *Cell*, 81: 299-307.
Santana, L. F., A. M. Gómez, E. G. Kranias, and W. J. Lederer. 1997. 'Amount of calcium in the sarcoplasmic reticulum: influence on excitation-contraction coupling in heart muscle', *Heart Vessels*, Suppl 12: 44-9.
Santana, L. F., E. G. Kranias, and W. J. Lederer. 1997. 'Calcium sparks and excitation-contraction coupling in phospholamban-deficient mouse ventricular myocytes', *J Physiol*, 503 (Pt 1): 21-9.
Satoh, H., L. A. Blatter, and D. M. Bers. 1997. 'Effects of [Ca2+]i, SR Ca2+ load, and rest on Ca2+ spark frequency in ventricular myocytes', *Am J Physiol*, 272: H657-68.
Schmitt, N., M. Grunnet, and S. P. Olesen. 2014. 'Cardiac potassium channel subtypes: new roles in repolarization and arrhythmia', *Physiol Rev*, 94: 609-53.

Schwede, F., D. Bertinetti, C. N. Langerijs, M. A. Hadders, H. Wienk, J. H. Ellenbroek, E. J. de Koning, J. L. Bos, F. W. Herberg, H. G. Genieser, R. A. Janssen, and H. Rehmann. 2015. 'Structure-guided design of selective Epac1 and Epac2 agonists', *PLoS Biol*, 13: e1002038.

Scriven, D. R., P. Asghari, and E. D. Moore. 2013. 'Microarchitecture of the dyad', *Cardiovasc Res*, 98: 169-76.

Seidler, T., S. L. Miller, C. M. Loughrey, A. Kania, A. Burow, S. Kettlewell, N. Teucher, S. Wagner, H. Kögler, M. B. Meyers, G. Hasenfuss, and G. L. Smith. 2003. 'Effects of adenovirus-mediated sorcin overexpression on excitation-contraction coupling in isolated rabbit cardiomyocytes', *Circ Res*, 93: 132-9.

Sham, J. S., L. S. Song, Y. Chen, L. H. Deng, M. D. Stern, E. G. Lakatta, and H. Cheng. 1998. 'Termination of Ca2+ release by a local inactivation of ryanodine receptors in cardiac myocytes', *Proc Natl Acad Sci U S A*, 95: 15096-101.

Shannon, T. R., K. S. Ginsburg, and D. M. Bers. 2000. 'Potentiation of fractional sarcoplasmic reticulum calcium release by total and free intra-sarcoplasmic reticulum calcium concentration', *Biophys J*, 78: 334-43.

———. 2002. 'Quantitative assessment of the SR Ca2+ leak-load relationship', *Circ Res*, 91: 594-600.

Shannon, T. R., T. Guo, and D. M. Bers. 2003. 'Ca2+ scraps: local depletions of free [Ca2+] in cardiac sarcoplasmic reticulum during contractions leave substantial Ca2+ reserve', *Circ Res*, 93: 40-5.

Shannon, T. R., S. M. Pogwizd, and D. M. Bers. 2003. 'Elevated sarcoplasmic reticulum Ca2+ leak in intact ventricular myocytes from rabbits in heart failure', *Circ Res*, 93: 592-4.

Shannon TR1, Pogwizd SM, Bers DM. 2003. 'Elevated sarcoplasmic reticulum Ca2+ leak in intact ventricular myocytes from rabbits in heart failure.', *Circ Res.*, 93: 592-94.

Shao, C. H., G. J. Rozanski, K. P. Patel, and K. R. Bidasee. 2007. 'Dyssynchronous (non-uniform) Ca2+ release in myocytes from streptozotocin-induced diabetic rats', *J Mol Cell Cardiol*, 42: 234-46.

Shattock, M. J., M. Ottolia, D. M. Bers, M. P. Blaustein, A. Boguslavskyi, J. Bossuyt, J. H. Bridge, Y. Chen-Izu, C. E. Clancy, A. Edwards, J. Goldhaber, J. Kaplan, J. B. Lingrel, D. Pavlovic, K. Philipson, K. R. Sipido, and Z. J. Xie. 2015. 'Na+/Ca2+ exchange and Na+/K+-ATPase in the heart', *J Physiol*, 593: 1361-82.

Shibasaki, T., H. Takahashi, T. Miki, Y. Sunaga, K. Matsumura, M. Yamanaka, C. Zhang, A. Tamamoto, T. Satoh, J. Miyazaki, and S. Seino. 2007. 'Essential role of Epac2/Rap1 signaling in regulation of insulin granule dynamics by cAMP', *Proc Natl Acad Sci U S A*, 104: 19333-8.

Simmerman, H. K., J. H. Collins, J. L. Theibert, A. D. Wegener, and L. R. Jones. 1986. 'Sequence analysis of phospholamban. Identification of phosphorylation sites and two major structural domains', *J Biol Chem*, 261: 13333-41.

Simmerman, H. K., and L. R. Jones. 1998. 'Phospholamban: protein structure, mechanism of action, and role in cardiac function', *Physiol Rev*, 78: 921-47.

Singh, R. M., T. Waqar, F. C. Howarth, E. Adeghate, K. Bidasee, and J. Singh. 2018. 'Hyperglycemia-induced cardiac contractile dysfunction in the diabetic heart', *Heart Fail Rev*, 23: 37-54.

Sitsapesan, R., and A. J. Williams. 1994. 'Regulation of the gating of the sheep cardiac sarcoplasmic reticulum Ca(2+)-release channel by luminal Ca2+', *J Membr Biol*, 137: 215-26.

Slawson, C., M. P. Housley, and G. W. Hart. 2006. 'O-GlcNAc cycling: how a single sugar post-translational modification is changing the way we think about signaling

networks', *J Cell Biochem*, 97: 71-83.
Smith, J. S., E. Rousseau, and G. Meissner. 1989. 'Calmodulin modulation of single sarcoplasmic reticulum Ca2+-release channels from cardiac and skeletal muscle', *Circ Res*, 64: 352-9.
Snyders, D. J. 1999. 'Structure and function of cardiac potassium channels', *Cardiovasc Res*, 42: 377-90.
Soeller, C., and M. B. Cannell. 1999. 'Examination of the transverse tubular system in living cardiac rat myocytes by 2-photon microscopy and digital image-processing techniques', *Circ Res*, 84: 266-75.
Soltysinska, E., S. P. Olesen, T. Christ, E. Wettwer, A. Varró, M. Grunnet, and T. Jespersen. 2009. 'Transmural expression of ion channels and transporters in human nondiseased and end-stage failing hearts', *Pflugers Arch*, 459: 11-23.
Somekawa, S., S. Fukuhara, Y. Nakaoka, H. Fujita, Y. Saito, and N. Mochizuki. 2005. 'Enhanced functional gap junction neoformation by protein kinase A-dependent and Epac-dependent signals downstream of cAMP in cardiac myocytes', *Circ Res*, 97: 655-62.
Sommese, L., C. A. Valverde, P. Blanco, M. C. Castro, O. V. Rueda, M. Kaetzel, J. Dedman, M. E. Anderson, A. Mattiazzi, and J. Palomeque. 2016. 'Ryanodine receptor phosphorylation by CaMKII promotes spontaneous Ca(2+) release events in a rodent model of early stage diabetes: The arrhythmogenic substrate', *Int J Cardiol*, 202: 394-406.
Spencer, C. I., and J. R. Berlin. 1995. 'Control of sarcoplasmic reticulum calcium release during calcium loading in isolated rat ventricular myocytes', *J Physiol*, 488 (Pt 2): 267-79.
Stehle, R., and B. Iorga. 2010. 'Kinetics of cardiac sarcomeric processes and rate-limiting steps in contraction and relaxation', *J Mol Cell Cardiol*, 48: 843-50.
Stern, M. D. 1992. 'Theory of excitation-contraction coupling in cardiac muscle', *Biophys J*, 63: 497-517.
Stoyanovsky, D., T. Murphy, P. R. Anno, Y. M. Kim, and G. Salama. 1997. 'Nitric oxide activates skeletal and cardiac ryanodine receptors', *Cell Calcium*, 21: 19-29.
Sun, J., N. Yamaguchi, L. Xu, J. P. Eu, J. S. Stamler, and G. Meissner. 2008. 'Regulation of the cardiac muscle ryanodine receptor by O(2) tension and S-nitrosoglutathione', *Biochemistry*, 47: 13985-90.
Sun, L., V. K. Kondeti, P. Xie, K. Raparia, and Y. S. Kanwar. 2011. 'Epac1-mediated, high glucose-induced renal proximal tubular cells hypertrophy via the Akt/p21 pathway', *Am J Pathol*, 179: 1706-18.
Tada, M., M. A. Kirchberger, and A. M. Katz. 1975. 'Phosphorylation of a 22,000-dalton component of the cardiac sarcoplasmic reticulum by adenosine 3':5'-monophosphate-dependent protein kinase', *J Biol Chem*, 250: 2640-7.
Tada, M., T. Yamamoto, and Y. Tonomura. 1978. 'Molecular mechanism of active calcium transport by sarcoplasmic reticulum', *Physiol Rev*, 58: 1-79.
Takahashi, K., and S. Yamanaka. 2006. 'Induction of pluripotent stem cells from mouse embryonic and adult fibroblast cultures by defined factors', *Cell*, 126: 663-76.
Terentyev, D., I. Györke, A. E. Belevych, R. Terentyeva, A. Sridhar, Y. Nishijima, E. C. de Blanco, S. Khanna, C. K. Sen, A. J. Cardounel, C. A. Carnes, and S. Györke. 2008. 'Redox modification of ryanodine receptors contributes to sarcoplasmic reticulum Ca2+ leak in chronic heart failure', *Circ Res*, 103: 1466-72.
Thomas, M. J., I. Sjaastad, K. Andersen, P. J. Helm, J. A. Wasserstrom, O. M. Sejersted, and O. P. Ottersen. 2003. 'Localization and function of the Na+/Ca2+-exchanger in normal and detubulated rat cardiomyocytes', *J Mol Cell Cardiol*, 35: 1325-37.

Thrainsdottir, I. S., T. Aspelund, G. Thorgeirsson, V. Gudnason, T. Hardarson, K. Malmberg, G. Sigurdsson, and L. Ryden. 2005. 'The association between glucose abnormalities and heart failure in the population-based Reykjavik study', *Diabetes Care*, 28: 612-6.

Timerman, A. P., H. Onoue, H. B. Xin, S. Barg, J. Copello, G. Wiederrecht, and S. Fleischer. 1996. 'Selective binding of FKBP12.6 by the cardiac ryanodine receptor', *J Biol Chem*, 271: 20385-91.

Tourneur, Y., R. Mitra, M. Morad, and O. Rougier. 1987. 'Activation properties of the inward-rectifying potassium channel on mammalian heart cells', *J Membr Biol*, 97: 127-35.

Trafford, A. W., M. E. Diaz, and D. A. Eisner. 2001. 'Coordinated control of cell Ca(2+) loading and triggered release from the sarcoplasmic reticulum underlies the rapid inotropic response to increased L-type Ca(2+) current', *Circ Res*, 88: 195-201.

Tsalkova, T., F. C. Mei, S. Li, O. G. Chepurny, C. A. Leech, T. Liu, G. G. Holz, V. L. Woods, Jr., and X. Cheng. 2012. 'Isoform-specific antagonists of exchange proteins directly activated by cAMP', *Proc Natl Acad Sci U S A*, 109: 18613-8.

Tseng, G. N., and B. F. Hoffman. 1989. 'Two components of transient outward current in canine ventricular myocytes', *Circ Res*, 64: 633-47.

Tsien, R. W., B. P. Bean, P. Hess, J. B. Lansman, B. Nilius, and M. C. Nowycky. 1986. 'Mechanisms of calcium channel modulation by beta-adrenergic agents and dihydropyridine calcium agonists', *J Mol Cell Cardiol*, 18: 691-710.

Ulucan, C., X. Wang, E. Baljinnyam, Y. Bai, S. Okumura, M. Sato, S. Minamisawa, S. Hirotani, and Y. Ishikawa. 2007. 'Developmental changes in gene expression of Epac and its upregulation in myocardial hypertrophy', *Am J Physiol Heart Circ Physiol*, 293: H1662-72.

Valdivia, H. H., J. H. Kaplan, G. C. Ellis-Davies, and W. J. Lederer. 1995. 'Rapid adaptation of cardiac ryanodine receptors: modulation by Mg2+ and phosphorylation', *Science*, 267: 1997-2000.

van Oort, R. J., M. D. McCauley, S. S. Dixit, L. Pereira, Y. Yang, J. L. Respress, Q. Wang, A. C. De Almeida, D. G. Skapura, M. E. Anderson, D. M. Bers, and X. H. Wehrens. 2010. 'Ryanodine receptor phosphorylation by calcium/calmodulin-dependent protein kinase II promotes life-threatening ventricular arrhythmias in mice with heart failure', *Circulation*, 122: 2669-79.

Vangheluwe, P., W. E. Louch, M. Ver Heyen, K. Sipido, L. Raeymaekers, and F. Wuytack. 2003. 'Ca2+ transport ATPase isoforms SERCA2a and SERCA2b are targeted to the same sites in the murine heart', *Cell Calcium*, 34: 457-64.

Vogel, S. S., C. Thaler, and S. V. Koushik. 2006. 'Fanciful FRET', *Sci STKE*, 2006: re2.

Vozzi, C., E. Dupont, S. R. Coppen, H. I. Yeh, and N. J. Severs. 1999. 'Chamber-related differences in connexin expression in the human heart', *J Mol Cell Cardiol*, 31: 991-1003.

Wang, H., S. Viatchenko-Karpinski, J. Sun, I. Györke, N. A. Benkusky, M. J. Kohr, H. H. Valdivia, E. Murphy, S. Györke, and M. T. Ziolo. 2010. 'Regulation of myocyte contraction via neuronal nitric oxide synthase: role of ryanodine receptor S-nitrosylation', *J Physiol*, 588: 2905-17.

Weber, C. R., K. S. Ginsburg, K. D. Philipson, T. R. Shannon, and D. M. Bers. 2001. 'Allosteric regulation of Na/Ca exchange current by cytosolic Ca in intact cardiac myocytes', *J Gen Physiol*, 117: 119-31.

Weber, C. R., V. Piacentino, 3rd, K. S. Ginsburg, S. R. Houser, and D. M. Bers. 2002. 'Na(+)-Ca(2+) exchange current and submembrane [Ca(2+)] during the cardiac action potential', *Circ Res*, 90: 182-9.

Wehrens, X. H., S. E. Lehnart, F. Huang, J. A. Vest, S. R. Reiken, P. J. Mohler, J. Sun, S.

Guatimosim, L. S. Song, N. Rosemblit, J. M. D'Armiento, C. Napolitano, M. Memmi, S. G. Priori, W. J. Lederer, and A. R. Marks. 2003. 'FKBP12.6 deficiency and defective calcium release channel (ryanodine receptor) function linked to exercise-induced sudden cardiac death', *Cell*, 113: 829-40.

Wehrens, X. H., S. E. Lehnart, S. R. Reiken, and A. R. Marks. 2004. 'Ca2+/calmodulin-dependent protein kinase II phosphorylation regulates the cardiac ryanodine receptor', *Circ Res*, 94: e61-70.

Wehrens, X. H., S. E. Lehnart, S. Reiken, J. A. Vest, A. Wronska, and A. R. Marks. 2006. 'Ryanodine receptor/calcium release channel PKA phosphorylation: a critical mediator of heart failure progression', *Proc Natl Acad Sci U S A*, 103: 511-8.

Weishaar, R. E., D. C. Kobylarz-Singer, R. P. Steffen, and H. R. Kaplan. 1987. 'Subclasses of cyclic AMP-specific phosphodiesterase in left ventricular muscle and their involvement in regulating myocardial contractility', *Circ Res*, 61: 539-47.

Wettwer, E., G. J. Amos, H. Posival, and U. Ravens. 1994. 'Transient outward current in human ventricular myocytes of subepicardial and subendocardial origin', *Circ Res*, 75: 473-82.

Whitworth, G. E., M. S. Macauley, K. A. Stubbs, R. J. Dennis, E. J. Taylor, G. J. Davies, I. R. Greig, and D. J. Vocadlo. 2007. 'Analysis of PUGNAc and NAG-thiazoline as transition state analogues for human O-GlcNAcase: mechanistic and structural insights into inhibitor selectivity and transition state poise', *J Am Chem Soc*, 129: 635-44.

Wu, P., G. Deng, X. Sai, H. Guo, H. Huang, and P. Zhu. 2020. 'Maturation strategies and limitations of induced pluripotent stem cell-derived cardiomyocytes', *Biosci Rep*.

Wu, X., P. Eder, B. Chang, and J. D. Molkentin. 2010. 'TRPC channels are necessary mediators of pathologic cardiac hypertrophy', *Proc Natl Acad Sci U S A*, 107: 7000-5.

Wu, X., T. Zhang, J. Bossuyt, X. Li, T. A. McKinsey, J. R. Dedman, E. N. Olson, J. Chen, J. H. Brown, and D. M. Bers. 2006. 'Local InsP3-dependent perinuclear Ca2+ signaling in cardiac myocyte excitation-transcription coupling', *J Clin Invest*, 116: 675-82.

Wuytack, F., L. van den Bosch, M. Ver Heyen, F. Baba-Aïssa, L. Raeymaekers, and R. Casteels. 1998. 'Regulation of alternative splicing of the SERCA2 pre-mRNA in muscle', *Ann N Y Acad Sci*, 853: 372-5.

Xiao, B., M. T. Jiang, M. Zhao, D. Yang, C. Sutherland, F. A. Lai, M. P. Walsh, D. C. Warltier, H. Cheng, and S. R. Chen. 2005. 'Characterization of a novel PKA phosphorylation site, serine-2030, reveals no PKA hyperphosphorylation of the cardiac ryanodine receptor in canine heart failure', *Circ Res*, 96: 847-55.

Xiao, B., C. Sutherland, M. P. Walsh, and S. R. Chen. 2004. 'Protein kinase A phosphorylation at serine-2808 of the cardiac Ca2+-release channel (ryanodine receptor) does not dissociate 12.6-kDa FK506-binding protein (FKBP12.6)', *Circ Res*, 94: 487-95.

Xiao, R. P., H. Cheng, W. J. Lederer, T. Suzuki, and E. G. Lakatta. 1994. 'Dual regulation of Ca2+/calmodulin-dependent kinase II activity by membrane voltage and by calcium influx', *Proc Natl Acad Sci U S A*, 91: 9659-63.

Xu, L., J. P. Eu, G. Meissner, and J. S. Stamler. 1998. 'Activation of the cardiac calcium release channel (ryanodine receptor) by poly-S-nitrosylation', *Science*, 279: 234-7.

Xu, L., G. Mann, and G. Meissner. 1996. 'Regulation of cardiac Ca2+ release channel (ryanodine receptor) by Ca2+, H+, Mg2+, and adenine nucleotides under normal and simulated ischemic conditions', *Circ Res*, 79: 1100-9.

Xu, L., and G. Meissner. 1998. 'Regulation of cardiac muscle Ca2+ release channel by sarcoplasmic reticulum lumenal Ca2+', *Biophys J*, 75: 2302-12.

———. 2004. 'Mechanism of calmodulin inhibition of cardiac sarcoplasmic reticulum Ca2+

release channel (ryanodine receptor)', *Biophys J*, 86: 797-804.
Yamaguchi, N., L. Xu, D. A. Pasek, K. E. Evans, and G. Meissner. 2003. 'Molecular basis of calmodulin binding to cardiac muscle Ca(2+) release channel (ryanodine receptor)', *J Biol Chem*, 278: 23480-6.
Yang, Z., H. M. Kirton, M. Al-Owais, J. Thireau, S. Richard, C. Peers, and D. S. Steele. 2016. 'Epac2-Rap1 Signaling Regulates Reactive Oxygen Species Production and Susceptibility to Cardiac Arrhythmias', *Antioxid Redox Signal*.
Yaras, N., E. Tuncay, N. Purali, B. Sahinoglu, G. Vassort, and B. Turan. 2007. 'Sex-related effects on diabetes-induced alterations in calcium release in the rat heart', *Am J Physiol Heart Circ Physiol*, 293: H3584-92.
Yaras, N., M. Ugur, S. Ozdemir, H. Gurdal, N. Purali, A. Lacampagne, G. Vassort, and B. Turan. 2005. 'Effects of diabetes on ryanodine receptor Ca release channel (RyR2) and Ca2+ homeostasis in rat heart', *Diabetes*, 54: 3082-8.
Yatani, A., and A. M. Brown. 1989. 'Rapid beta-adrenergic modulation of cardiac calcium channel currents by a fast G protein pathway', *Science*, 245: 71-4.
Yokoe, S., M. Asahi, T. Takeda, K. Otsu, N. Taniguchi, E. Miyoshi, and K. Suzuki. 2010. 'Inhibition of phospholamban phosphorylation by O-GlcNAcylation: implications for diabetic cardiomyopathy', *Glycobiology*, 20: 1217-26.
Yokoyama, U., H. H. Patel, N. C. Lai, N. Aroonsakool, D. M. Roth, and P. A. Insel. 2008. 'The cyclic AMP effector Epac integrates pro- and anti-fibrotic signals', *Proc Natl Acad Sci U S A*, 105: 6386-91.
Yoshida, Y., and S. Yamanaka. 2017. 'Induced Pluripotent Stem Cells 10 Years Later: For Cardiac Applications', *Circ Res*, 120: 1958-68.
Yu, P., L. Hu, J. Xie, S. Chen, L. Huang, Z. Xu, X. Liu, Q. Zhou, P. Yuan, X. Yan, J. Jin, Y. Shen, W. Zhu, L. Fu, Q. Chen, J. Yu, J. Hu, Q. Cao, R. Wan, and K. Hong. 2018. 'O-GlcNAcylation of cardiac Nav1.5 contributes to the development of arrhythmias in diabetic hearts', *Int J Cardiol*, 260: 74-81.
Yue, D. T., S. Herzig, and E. Marban. 1990. 'Beta-adrenergic stimulation of calcium channels occurs by potentiation of high-activity gating modes', *Proc Natl Acad Sci U S A*, 87: 753-7.
Zachara, N. E., N. O'Donnell, W. D. Cheung, J. J. Mercer, J. D. Marth, and G. W. Hart. 2004. 'Dynamic O-GlcNAc modification of nucleocytoplasmic proteins in response to stress. A survival response of mammalian cells', *J Biol Chem*, 279: 30133-42.
Zahradníková, A., I. Minarovic, R. C. Venema, and L. G. Mészáros. 1997. 'Inactivation of the cardiac ryanodine receptor calcium release channel by nitric oxide', *Cell Calcium*, 22: 447-54.
Zeidan, Q., and G. W. Hart. 2010. 'The intersections between O-GlcNAcylation and phosphorylation: implications for multiple signaling pathways', *J Cell Sci*, 123: 13-22.
Zhang, H., C. A. Makarewich, H. Kubo, W. Wang, J. M. Duran, Y. Li, R. M. Berretta, W. J. Koch, X. Chen, E. Gao, H. H. Valdivia, and S. R. Houser. 2012. 'Hyperphosphorylation of the cardiac ryanodine receptor at serine 2808 is not involved in cardiac dysfunction after myocardial infarction', *Circ Res*, 110: 831-40.
Zhang, L., J. Kelley, G. Schmeisser, Y. M. Kobayashi, and L. R. Jones. 1997. 'Complex formation between junctin, triadin, calsequestrin, and the ryanodine receptor. Proteins of the cardiac junctional sarcoplasmic reticulum membrane', *J Biol Chem*, 272: 23389-97.
Zühlke, R. D., G. S. Pitt, K. Deisseroth, R. W. Tsien, and H. Reuter. 1999. 'Calmodulin supports both inactivation and facilitation of L-type calcium channels', *Nature*, 399: 159-62.

Annexes

Annexes

Annex 1:

This paper is published in *Frontiers physiology*, 2019

Gender-Dependent Alteration of Ca^{2+} and TNFα Signaling in *db*/ *db* Mice, an Obesity-Linked Type 2 Diabetic Model

Carmen DELGADO, Ana-Maria GOMEZ, **Magali SAMIA EL HAYEK**, Gema RUIZ-HURTADO, Laetitia PEREIRA.

Annex 2:

This paper is under revision in *Journal of cardiac failure*

Cardiac phosphodiesterases are differentially increased in diabetic cardiomyopathy

Rita HANNA, Wared NOUR-ELDINE, Youakim SALIBA, Carole DAGHER-HAMALIAN, Pia HACHEM, Pamela ABOU-KHALIL, **Magali SAMIA EL HAYEK**, Laëtitia PEREIRA, Nassim FARÈS, Grégoire VANDECASTEELE, Aniella ABI-GERGES

Annex 3:

This review is under revision in *Archives of cardiovascular diseases*

The role of hyperglycemia in the development of diabetic cardiomyopathy

Magali SAMIA EL HAYEK, Laura ERNANDE, Jean-Pierre Bénitah, Ana-Maria GOMEZ, Laetitia PEREIRA.

Annex 1

frontiers in Physiology

ORIGINAL RESEARCH
published: 07 February 2019
doi: 10.3389/fphys.2019.00040

Gender-Dependent Alteration of Ca^{2+} and TNFα Signaling in *db/db* Mice, an Obesity-Linked Type 2 Diabetic Model

Carmen Delgado[1], Ana-Maria Gomez[2]*, Magali Samia El Hayek[2], Gema Ruiz-Hurtado[3†] and Laetitia Pereira[2†]*

[1]Instituto de Investigaciones Biomédicas "Alberto Sols" (CSIC-UAM)/CIBER-CV, Madrid, Spain, [2]INSERM UMR-S 1180, University of Paris-Sud, University of Paris-Saclay, Châtenay-Malabry, France, [3]Cardiorenal Translational Laboratory, Institute of Research i+12, Hospital Universitario 12 de Octubre/CIBER-CV, Madrid, Spain

OPEN ACCESS

Edited by:
José Antonio Pariente, Universidad de Extremadura, Spain

Reviewed by:
Juan Martinez-Pinna, University of Alicante, Spain
Gines M. Salido, Universidad de Extremadura, Spain
Belma Turan, Ankara University, Turkey

***Correspondence:**
Carmen Delgado
cdelgado@iib.uam.es
Ana-Maria Gomez
ana-maria.gomez@inserm.fr

†These authors have contributed equally to this work

Specialty section:
This article was submitted to Membrane Physiology and Membrane Biophysics, a section of the journal Frontiers in Physiology

Received: *04 November 2018*
Accepted: *14 January 2019*
Published: *07 February 2019*

Citation:
Delgado C, Gomez A-M, Samia El Hayek M, Ruiz-Hurtado G and Pereira L (2019) Gender-Dependent Alteration of Ca^{2+} and TNFα Signaling in db/db Mice, an Obesity-Linked Type 2 Diabetic Model. Front. Physiol. 10:40. doi: 10.3389/fphys.2019.00040

Cardiovascular complications are the primary death cause in type 2 diabetes, where inflammation can play a role. We, and others, have previously shown that, in diabetic cardiomyopathy, cardiac dysfunction is associated with Ca^{2+} mishandling. It is possible that diabetic cardiomyopathy differently affects men and women, as the latter present higher risk to develop heart failure and a higher plasmatic level of the pro-inflammatory cytokine, tumor necrosis factor alpha (TNFα), than men. However, the gender-dependent regulation of Ca^{2+} signaling in diabetes and its relationship with TNFα signaling are still unclear. Here, we analyzed TNFα signaling pathway and its role in Ca^{2+} signaling dysfunction in male and female rodent models of type 2 diabetes linked to obesity (*db/db* mice) using confocal microscopy in freshly isolated cardiomyocytes. TNFα increased $[Ca^{2+}]_i$ transient amplitude and accelerated its decay without affecting SR Ca^{2+} load or Ca^{2+} spark frequency in cells from control mice. All TNFα effects on Ca^{2+} handling were prevented by the inhibition of the ceramidase and the phospholipase A2 (PLA2). While the plasmatic level of TNFα was similar in male and female *db/db* mice, only male *db/db* hearts over-expressed both TNFα converting enzyme (TACE) and the protective TNFα receptors 2 (TNF-R2). TNFα receptor 1 (TNF-R1) expression, involved in negative inotropic response of TNFα, was unchanged in both male and female *db/db* mice compared to controls. We found that male *db/db* mice cardiomyocytes presented a decrease in $[Ca^{2+}]_i$ transient amplitude associated to a drop of sarcoplasmic reticulum Ca^{2+} load, not seen in female *db/db* mice. Interestingly, sustained incubation with TNFα did not restored Ca^{2+} signaling alteration observed in male *db/db* mice but still induces an increase in Ca^{2+} spark frequency as seen in control littermates. In cardiomyocytes from female *db/db* mice, TNFα had no visible effects on Ca^{2+} handling. In conclusion, our study shows that the alteration of Ca^{2+} signaling and TNFα, seen in *db/db* mice, is gender specific presenting an increase in TNFα cardio-protective pathway in male mice.

Keywords: diabetic cardiomyopathy, TNFα, calcium, gender difference, *db/db* mice

INTRODUCTION

Cardiovascular complications, such as coronary artery diseases, hypertension, and heart failure, are a leading cause of death in type 2 diabetes (Laakso, 1999; Bauters et al., 2003; Bell, 2007). Preclinical studies have shown that diabetic cardiac dysfunction, with depressed contraction and relaxation, results from dysregulation of metabolism, mitochondrial function, oxidative stress, and Ca^{2+} handling (Bugger and Abel, 2014). These knowledge result almost exclusively from male animal studies. However, in the clinical setting, the risk for developing cardiac diseases in diabetes is known to be gender specific (Galderisi et al., 1991; Rutter et al., 2003; Toedebusch et al., 2018). Indeed, the Framingham Heart Study showed that diabetic women present a 5.1-fold increased risk to develop heart failure than non-diabetic patients, whereas in diabetic men, this risk is only multiplied by 2.4 (Galderisi et al., 1991; Rutter et al., 2003). In addition, the hospital admission rate for cardiovascular diseases is higher in diabetic women compared to diabetic men. Yet, the gender differences in the alterations of cardiac cellular function in diabetes are unclear, notably regarding Ca^{2+} mishandling.

Ca^{2+} regulates contraction through the excitation-contraction coupling in cardiomyocytes. For each heartbeat, sarcolemmal L type Ca^{2+} channels open during the action potential, leading to Ca^{2+} influx that activates Ca^{2+} release from the ryanodine receptors (RyR) located at the sarcoplasmic reticulum (SR). This release of Ca^{2+} by the RyR (visualized as a $[Ca^{2+}]_i$ transient) activates contractile myofibrils to generate cardiomyocyte contraction. After the contraction, the Ca^{2+} is re-uptaken into the SR by the SERCA pump and extruded outside the cardiomyocytes mainly by the Na^+/Ca^{2+} exchanger, resulting in cardiomyocyte relaxation. We and others have shown that, in animal models of type 2 diabetes linked to obesity, contractile dysfunction is associated with a decrease in the Ca^{2+} transient amplitude. This lower Ca^{2+} transient amplitude is associated to reduced L-type Ca^{2+} current density combined with downregulation of RyR expression (Belke et al., 2004; Pereira et al., 2006b, 2014). We found that these alterations may be different in male and female *db*/*db* mice (Pereira et al., 2014); however, the mechanisms remain unclear.

Clinical and preclinical studies pointed out an increase in plasmatic level of TNFα, in type 2 diabetes, notably in women (Yamakawa et al., 1995; Pereira et al., 2006a; Preciado-Puga et al., 2014). TNFα is an inflammatory cytokine commonly associated to infectious and non-infectious cardiomyopathy, such as viral myocarditis, congestive heart failure, and myocardial infarction. The level of TNFα seems correlated to the development of cardiac dysfunction (Feldman et al., 2000; Blum and Miller, 2001), and its over-expression leads to cardiac hypertrophy, fibrosis, arrhythmia, and dysfunction (Kubota et al., 1997; Kadokami et al., 2000; London et al., 2003). Yet, whether TNFα is a cause or a consequence of cardiac dysfunction is still under debate. The biological response of TNFα is mediated through two receptors, the TNFα receptor 1 (TNF-R1) and TNFα receptor 2 (TNF-R2). TNF-R1 activation is responsible for a cardiac negative inotropic response, whereas TNF-R2 mediates cardiac positive inotropic response (Meldrum, 1998). At the cellular level, TNFα regulates contraction either by direct regulation of Ca^{2+} signaling in acute condition or *via* iNOS activation in sustained conditions (Fernandez-Velasco et al., 2007). Still, whether TNFα activation positively or negatively alters the Ca^{2+} transient is quite controversial, and studies found either a decrease, an increase, or no effect on Ca^{2+} transient. Those discrepancies seem to depend on the animal model, the concentration of TNFα used, and the incubation time (Yokoyama et al., 1993; Goldhaber et al., 1996; Bick et al., 1997; Sugishita et al., 1999; Li et al., 2003; Zhang et al., 2005; Duncan et al., 2010; Greensmith and Nirmalan, 2013). In addition, whether the regulation of TNFα signaling in type 2 diabetic cardiomyopathy linked to obesity is gender specific remains unknown.

Considering all these controversial findings surrounding TNFα regulation of Ca^{2+} handling, we first studied the effect of TNFα on Ca^{2+} signaling in WT mice. Then, using the *db*/*db* mice, an animal model of type 2 diabetes with insulin resistance linked to obesity, we found that both Ca^{2+} and TNFα signaling underwent distinct alterations in male compared to female. Here, we found that male *db*/*db* mice presented a depressed Ca^{2+} transient associated with a lower SR Ca^{2+} load, not seen in female *db*/*db* mice. More interestingly, in male *db*/*db*, cardiomyocytes seem to put in place a protective mechanism to counteract those alterations by increasing the expression of cardio-protective TNF-R2 signaling pathway.

MATERIALS AND METHODS

Cell Isolation

Experiments were carried out according to the ethical principles of the French Ministry of Agriculture and the European Parliament on the protection of animals. Ventricular adult cardiomyocytes were isolated from 8 weeks old male C56Bl6 mice, male and female 15 weeks old *db*/*db* (Janvier), and their control littermates (*db*/+). Mice were euthanized by intraperitoneal injection of sodium pentobarbital (100 mg/kg). Cardiac ventricular myocyte isolation was performed by standard enzymatic methods (collagenase type II, Worthington) using the Langendorff perfusion as previously described (Pereira et al., 2006b, 2007, 2012; Leroy et al., 2011; Ruiz-Hurtado et al., 2015). After isolation, cells were kept in 1 mM $[Ca^{2+}]$ for an hour prior experiments. Only rod-shaped cells and quiescent cells when unstimulated and excitable were used for the Ca^{2+} experiments.

Abbreviations: ATK, arachidonyl trifluoromethyl ketone; TNFα, tumor necrosis factor alpha; TNF-R1, TNFα receptor 1; TNF-R2, TNFα receptor 2; KO, knock-out; NO, nitric oxide; NOE, n-oleoylethanolamine; o.i., oil immersion; PKA, protein kinase A; PLA2, phospholipase A2; RyR, cardiac ryanodine receptor; SR, sarcoplasmic reticulum; SERCA, sarco/endoplasmic reticulum Ca^{2+}-ATPase; TACE, TNFα converting enzyme.

Measurements of Plasmatic TNFα

TNFα determination by ELISA Soluble TNFα concentration was determined in plasma samples from mice using commercial ELISA test (BIOTRAK, Amersham Life Science, Sweden).

Confocal Microscopy

Ca^{2+} handling was recorded in freshly isolated ventricular adult cardiomyocytes loaded with the fluorescent Ca^{2+} dye, the Fluo-3 acetoxymethyl ester (Fluo-3 AM, Molecular Probes) at 5 μM diluted in a mixture of DMSO-pluronic acid 20%. A line scan across the longitudinal axis of the myocyte was performed to measure cardiomyocyte shortening. Cardiomyocyte shortening corresponds to the difference between cardiomyocyte length at rest and cardiomyocyte length during contraction (during electrical stimulation), as previously described (Fernandez-Velasco et al., 2009). Ca^{2+} transient, Ca^{2+} sparks, and SR Ca^{2+} load were recorded using confocal microscopy (Meta Zeiss LSM 510, objective w.i. 63×, n.a. 1.2) in line scan mode (1.54 ms) along the longitudinal axis of the cell. Ca^{2+} transients were evoked by field stimulation (1 Hz) applied through two parallel platinum electrodes. Spontaneous Ca^{2+} sparks were recorded in quiescent cells after Ca^{2+} transient recording. Ca^{2+} transient decay time corresponds to the kinetic of the relaxation phase due to the re-uptake of Ca^{2+} into the SR by the SERCA pump as well as the extrusion of Ca^{2+} by the Na^{2+}/Ca^{2+} exchanger. Ca^{2+} transient decay time is calculated using a mono-exponential function to fit the Ca^{2+} transient decline phase. SR Ca^{2+} load was assessed by rapid caffeine application (10 mM) after 1 min pacing to reach the steady state. Parameters were studied with or without TNFα (1 h to 1 h 30 min) supplemented or not with a ceramidase inhibitor n-oleoylethanolamine (NOE, 5 μM) and a phospholipase A2 (PLA2) inhibitor (ATK, 10 μM) (Sigma-Aldrich). Fluo-3 AM was excited with an Argon laser (λ_{ex} = 488 nm), and emission was collected at wavelengths >505 nm. Image analysis was performed using homemade routines in interactive data language (IDL).

Western-Blot Analysis

Adult ventricular homogenates were quickly frozen in liquid nitrogen and then placed in Tris solution (50 mmol/L, pH = 7.4) containing proteases and phosphatase inhibitors (10 μg/ml leupeptin, 10 μg/ml trypsin inhibitor, 2 μg/ml aprotinin, and 5 μM okadaic acid). Homogenization was performed on ice using a Politron. Homogenate was centrifuged at 18,925 g for 10 min at 4°C. Proteins were resuspended in Laemmli (5%) sample buffer, boiled (90°C for 5–10 min), and separated by sodium dodecyl sulfate polyacrylamide gel electrophoresis (SDS-PAGE) using 10% polyacrylamide gels. After separation, proteins were transferred to polyvinylidene fluoride membranes (Amersham Biosciences), and non-specific binding sites were blocked overnight at 4°C in 5% dried milk and Tris-buffer saline (TBS, pH = 7.4) and 0.01% Tween 20. Membranes were incubated overnight (at 4°C) for the rabbit polyclonal anti-TACE (1:300; Proscience) and the rabbit polyclonal anti-TNFR2 (H-202) (1:250; Santa Cruz), at room temperature for 1 h 30 min for the rabbit polyclonal anti-TNFR1 (H-271) (1:500; Santa Cruz). A secondary horseradish peroxidase-conjugated goat anti-rabbit IgG (Amersham Biosciences) was used in combination with an enhanced chemiluminescence detection system (SuperSignal West Pico Chemiluminescent Substrate, Pierce) to visualize the primary antibodies. Band densities were determined with a laser-scanning densitometer (HP-3970) and Quantity One software (BioRad SA). Protein loading was controlled by probing all Western blots with anti-GADPH antibody (1:4,000) (Ambion).

Statistical Analysis

Results were expressed as mean ± SEM. Significance between two groups was determined using unpaired Student's *t* test or non-parametric Mann-Whitney test. Data involving more than two groups were analyzed using either one-way ANOVA or two-way ANOVA as appropriate. We used GraphPad Prism 7 (GraphPad) for statistical comparison. Differences with values of $p < 0.05$ were considered significant.

RESULTS

Sustained TNFα Exposure Increases Ca^{2+}-Induced Ca^{2+} Release

TNFα-mediated Ca^{2+} signaling regulation is quite controversial, which is probably due to protocol differences. Therefore, we first studied, in our experimental settings, the effect of sustained activation (1–1 h 30 min) of TNFα on Ca^{2+} handling parameters such as Ca^{2+} transient, Ca^{2+} spark frequency, and SR Ca^{2+} load (**Figure 1**). In our hands, 10 and 50 ng/ml TNFα treatment significantly increased Ca^{2+} transient amplitude (F/F_0 of 3.1 ± 0.3 for 10 ng/ml, 3.5 ± 0.3 for 50 ng/ml vs. 2.5 ± 0.14 for baseline, $p < 0.05$). Moreover, TNFα significantly accelerated the Ca^{2+} re-uptake into the SR as shown by the faster SR Ca^{2+} transient decay time (**Figures 1A,B**) (~29% faster for 10 ng/ml and ~25% for 50 ng/ml, $p < 0.01$). This acceleration of Ca^{2+} re-uptake did not modified SR Ca^{2+} load (**Figure 1D**) and did not affect Ca^{2+} spark frequency (**Figures 1E,F**) at any concentration studied. However, 100 ng/ml of TNFα had no effects on either Ca^{2+} transient amplitude, Ca^{2+} spark frequency, or SR Ca^{2+} load. However, 100 ng/ml of TNFα still accelerated the Ca^{2+} transient decay (**Figure 1C**). These results clearly show that sustained TNFα activation mediates an increase in systolic Ca^{2+} release. Altogether, our results lean toward the idea of a positive inotropic effect.

PLA2 and Ceramidase Mediate TNFα Regulation of Ca^{2+} Signaling

Previous work has suggested that TNFα response is mediated by the sphingosine signaling pathway (Hofmann et al., 2003). To investigate the signaling pathway involved in TNFα regulation of Ca^{2+} signaling, we used a ceramidase inhibitor

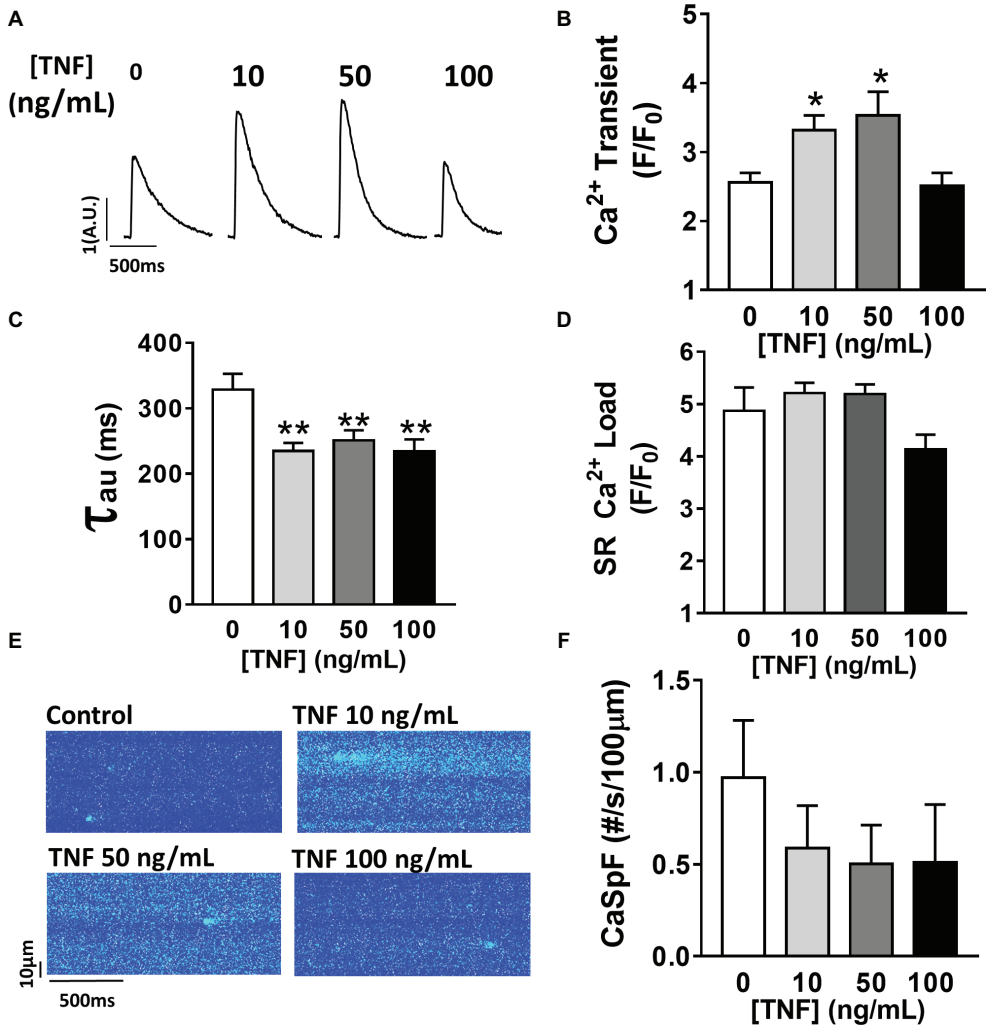

FIGURE 1 | Positive inotropic effect of TNFα incubation. **(A)** Examples of Ca^{2+} transient recordings in freshly isolated cardiomyocytes (5 µM Fluo-3 AM) at baseline, at 10 ng/ml TNFα and 100 ng/ml TNFα. **(B)** Mean Ca^{2+} transient amplitude from cardiomyocytes at baseline (n = 22) and with incremental TNFα treatment (n = 21 for 10 ng/ml, n = 15 for 50 ng/ml, n = 10 for 100 ng/ml). **(C)** Ca^{2+} transient decay time (in ms) at baseline (n = 20) and with incremental TNFα treatments (n = 20 for 10 ng/ml, n = 15 for 50 ng/ml, n = 9 for 100 ng/ml). **(D)** Mean of sarcoplasmic reticulum (SR) Ca^{2+} load obtained by caffeine application after 1 min field stimulation in same conditions (respectively, n = 10, n = 11, n = 11, and n = 7). **(E)** Examples Ca^{2+} spark frequency (CaSpF) recording in freshly isolated cardiomyocytes at baseline, at 10 ng/ml TNFα and 100 ng/ml TNFα. **(F)** Mean of CaSpF (number of sparks (#) per second per 100 µm) obtained in same groups as in **(A)** (respectively, n = 19, n = 20, n = 15, and n = 7). *$p < 0.05$, **$p < 0.01$.

(5 µM NOE) and a PLA2 inhibitor (10 µM ATK). NOE fully prevented the increase of Ca^{2+} transient amplitude (**Figures 2A,B**) and the faster Ca^{2+} transient decay time induced by 10 ng/ml of TNFα (**Figure 2C**). NOE had no significant effects on neither the Ca^{2+} spark frequency nor the SR Ca^{2+} load (**Figures 2D–F**). Similarly, the phospholipase A2 inhibitor blunted all TNFα-mediated effects on the Ca^{2+} transient and the Ca^{2+} transient decay time (**Figures 2B,C**). As for NOE, ATK had no effect on SR Ca^{2+} load (**Figure 2D**). However, ATK, contrarily to NOE, did significantly reduce basal Ca^{2+} spark frequency. Altogether, those results suggest that TNFα alters Ca^{2+} signaling *via* the activation of the ceramidase and phospholipase A2 signaling pathway.

Gender Differences in Upstream TNFα Signaling Pathway in Obesity-Linked Type 2 Diabetic Mice (*db/db*)

Since plasmatic TNFα level is significantly elevated in type 2 diabetic patients, we first measured the plasmatic level of TNFα in male and female *db*/*db* mice. At 15 weeks old, *db*/*db* mice develop a type 2 diabetes linked to obesity with associated cardiomyopathy (Pereira et al., 2006b). Surprisingly, neither male nor female *db*/*db* mice presented an increase in their plasmatic level of TNFα compared to control (**Figure 3A**). Then, we measured the expression of key proteins involved in the TNFα signaling pathway, such as type 1 and type 2 TNFα receptors and the TNFα conversion enzyme TACE in both male and female *db*/*db*

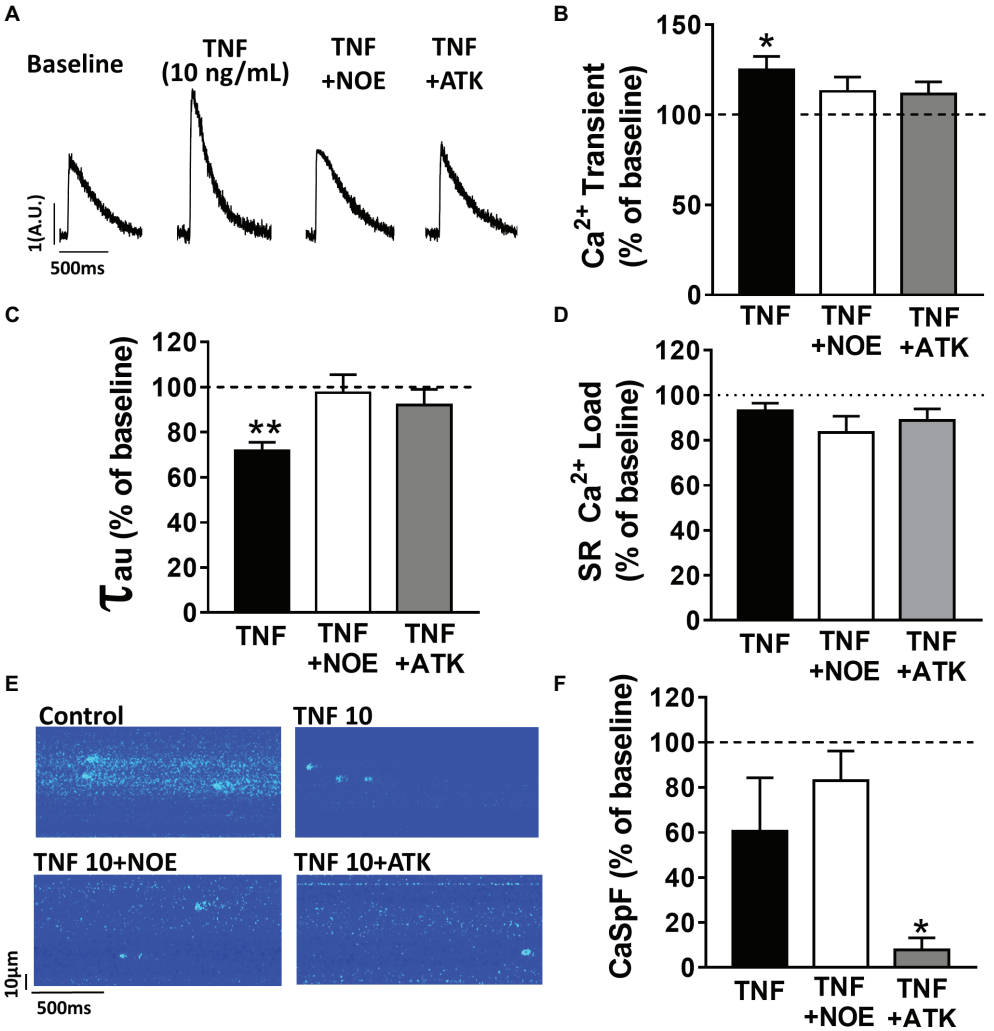

FIGURE 2 | TNFα regulates Ca^{2+} signaling *via* the sphingosine pathway. **(A)** Representative Ca^{2+} transient examples obtained at baseline, at 10 ng/ml TNFα ± ceramide inhibitor (NOE) or phospholipase A2 inhibitor (ATK). **(B)** Percentage of effect on Ca^{2+} transient amplitude of TNFα treatment ±NOE or ATK (n = 20 for 10 ng/ml TNFα, n = 10 for TNFα+NOE, and n = 10 for TNFα+ATK). **(C)** Ca^{2+} transient decay time (in ms) in same groups (respectively, n = 19, n = 10, and n = 10). **(D)** Mean of SR Ca^{2+} load in the same groups (respectively, n = 11, n = 10, and n = 9). **(E)** Examples Ca^{2+} spark frequency recording in freshly isolated cardiomyocytes at baseline, at TNFα ± NOE or ATK. **(F)** Mean of CaSpF obtained in conditions (respectively, n = 20, n = 10, and n = 10). $^{*}p < 0.05$, $^{**}p < 0.01$.

mice. Interestingly, TACE expression was significantly higher in male *db*/*db* mice compared to controls, whereas no change was detectable in the female group (**Figure 3B**). Moreover, while TNF-R1 receptor expression was unchanged in both *db*/*db* groups (**Figure 3C**), TNF-R2 in the *db*/*db* male group was significantly increased (**Figure 3D**). These results clearly suggest that in male *db*/*db* mice hearts, the TNF-R2, known to mediate a cardio-protective pathway, is over-expressed, probably to protect the heart from diabetic-induced stress.

Gender Differences in Obesity-Linked Type 2 Diabetic (*db*/*db*) Ca^{2+} Mishandling

In *db*/*db* mice, cardiac dysfunction has been associated with a decrease in SR Ca^{2+} transient amplitude and SR Ca^{2+} load (Belke et al., 2004; Pereira et al., 2006b, 2014). Here, we confirmed, in isolated cardiac myocytes from male *db*/*db* mice, that Ca^{2+} transient amplitude is significantly decreased (**Figures 4A,B**). This drop in Ca^{2+} transient amplitude (~51% lower than control, $p < 0.01$) is correlated with a drop in SR Ca^{2+} load (**Figure 4D**) (~51% lower than control, $p < 0.01$), which could explain the smaller (although not significant) cardiac cell shortening (**Figure 4C**). In our experimental conditions, Ca^{2+} spark frequency does not seem to be altered in *db*/*db* compared to control (*db*/+) (p = N.S.) (**Figures 4E,F**). In female *db*/*db* mice, the Ca^{2+} handling was similar in *db*/*db* compared to their control littermates (**Figure 5**). Indeed, all parameters such as Ca^{2+} transient amplitude (**Figure 5A**), Ca^{2+} spark frequency (**Figure 5C**), SR Ca^{2+} load (**Figure 5D**), and cell shortening (**Figure 5B**) were not significantly modified in freshly isolated cardiomyocytes in female *db*/*db* compared to control. In

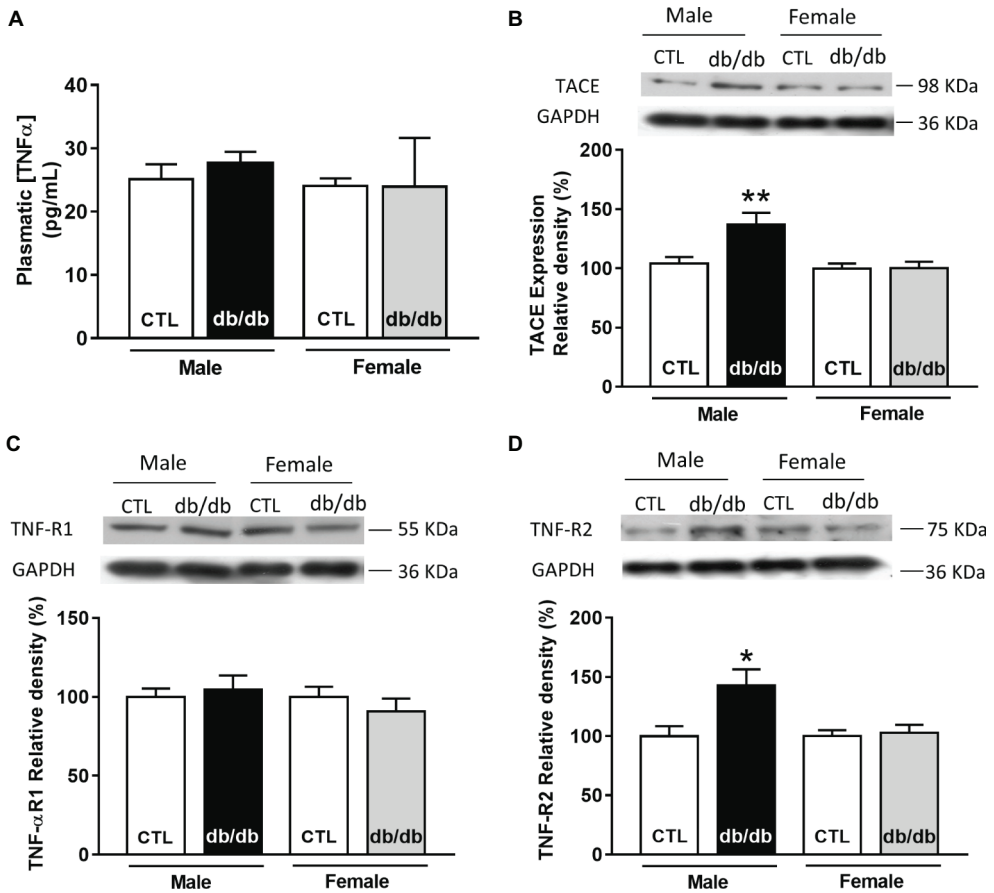

FIGURE 3 | Gender-dependent alteration of the TNFα signaling pathway in type 2 diabetic mice (*db/db*). **(A)** Plasmatic level of TNFα obtained in male and female control and *db/db* heart tissue homogenates (male control: $n = 5$, male *db/db*: $n = 7$; female control and *db/db*: $n = 8$). **(B)** Representative Western-blot example of TACE (98 kDa) and the percent of relative density normalized by GAPDH signal from male and female control ($n = 15$, $n = 17$) and *db/db* ($n = 14$, $n = 17$) heart tissue homogenates. **(C)** Representative Western-blot example of TNF-R1 (55 kDa) expression and percentage of relative density normalized by GAPDH signal in male and female control ($n = 16$, $n = 18$) and *db/db* ($n = 16$, $n = 18$) heart tissue homogenates. **(D)** Representative Western-blot example of TNF-R2 (75 kDa) expression and percentage of relative density normalized by GAPDH signal in male and female control ($n = 13$, $n = 13$) and *db/db* ($n = 13$, $n = 15$) heart tissue homogenates. *$p < 0.05$.

conclusion, we found a gender-specific alteration of Ca^{2+} handling in *db*/*db* mice, with lower SR Ca^{2+} release associated to a drop in SR Ca^{2+} load in male, not seen in female.

Gender Differences of TNFα-Mediated Effect in Type 2 Diabetic (*db/db*)

Next, we compared TNFα regulation of Ca^{2+} signaling between male and female *db*/*db* mice. In male *db*/*db* mice, 10 ng/ml TNFα did not alter Ca^{2+} transient amplitude, cell shortening, nor SR Ca^{2+} load (**Figures 4A–C,F**). However, 10 ng/ml of TNFα similarly increased Ca^{2+} spark frequency in both control (~3.29 fold, $p < 0.05$) and *db*/*db* (1.5 fold, $p = 0.06$) (**Figure 4D**). In female control, the higher Ca^{2+} transient amplitude and cell shortening did not reach significance. Both female *db*/*db* and control had unchanged Ca^{2+} spark frequency. Those results suggest that, in 15 weeks old female *db*/*db*, the excitation-contraction coupling is unchanged compared to female control. Moreover, TNFα fails to show the effects found in male *db*/*db* (**Figure 4D**). Therefore, there are gender differences in Ca^{2+} mishandling and the underlying mechanisms in type 2 diabetes.

DISCUSSION

We have previously shown that cardiac dysfunction in type 2 diabetes is associated with cardiomyocyte Ca^{2+} mishandling, resulting from a decrease in the Ca^{2+} channels involved in the Ca^{2+}-induced Ca^{2+} release process (RyR and L-Type Ca^{2+} channels) (Belke et al., 2004; Pereira et al., 2006b). Although TNFα is elevated in diabetic patient and animal model of diabetes (Yamakawa et al., 1995; Pereira et al., 2006a; Preciado-Puga et al., 2014), little was known about its role in cellular alteration, notably regarding the Ca^{2+} signaling pathway and gender specificity in animal model of diabetes linked to obesity. Here, we found a gender-specific alteration of Ca^{2+} and TNFα signaling in *db*/*db* mice, a common model of type 2 diabetes linked to obesity. Indeed, we found that male *db*/*db* mice, not

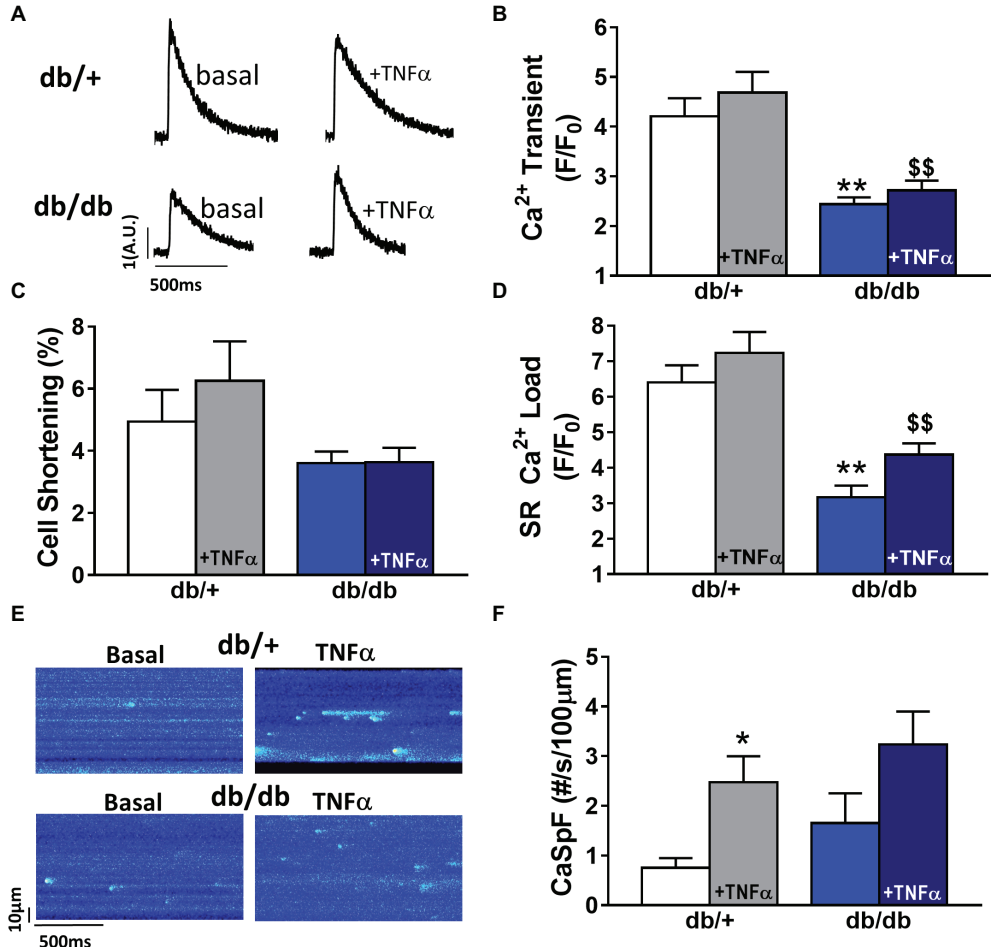

FIGURE 4 | Ca^{2+} signaling is impaired in male type 2 diabetic mice. **(A)** Line scan images of Ca^{2+} transient recorded in male cardiomyocytes from *db*/+, *db*/*db* ± TNFα (10 ng/ml). **(B)** Mean of Ca^{2+} transient amplitude from *db*/*db* ± TNFα (n = 21 and n = 19) cardiomyocytes and their control littermates (*db*/+, n = 14 and n = 20). **(C)** Cell shortening measured in intact *db*/*db* ± TNFα (n = 13 and n = 15) and *db*/+ cardiomyocytes (n = 10 and n = 13) stimulated at 1 Hz. **(D)** Mean of SR Ca^{2+} load in intact *db*/*db* ± TNFα (n = 6 and n = 11) and *db*/+ cardiomyocytes (n = 10 and 11). **(E)** Examples Ca^{2+} spark frequency recording in freshly isolated cardiomyocytes at in *db*/+ and *db*/*db* with or without TNFα **(F)** Ca^{2+} spark frequency in the same groups (for *db*/*db*: n = 12 and 17, for *db*/+: n = 12 and n = 18) $^{**}p < 0.01$ compared to *db*/+ and $^{\$\$}p < 0.05$ compared to *db*/*db* without TNFα treatment.

female, presented the previously described Ca^{2+} mishandling with lower systolic Ca^{2+} release and SR Ca^{2+} load. More interestingly, we found that male and female *db*/*db* mice expressed differently TNF-R2, with an increased expression in male *db*/*db* mice that might reflect the activation of the TNFα cardio-protective TNF-R2-dependent pathway, not seen in female *db*/*db*.

Cardiac Positive Inotropic Effect of TNFα

Discrepancies regarding the TNFα regulation of Ca^{2+} signaling are quite important in the literature with reported positive or negative ionotropic effect. For instance, in cat cardiomyocytes, short time exposure of TNFα reduced Ca^{2+} transient amplitude in response to a disruption of Ca^{2+} influx *via* L type Ca^{2+} channels leading to cellular shortening, supporting, then, a negative ionotropic effect of TNFα (Yokoyama et al., 1993). This negative inotropic effect of TNFα has been also described, in rabbit and guinea pigs, with TNFα-induced impaired cellular shortening cardiomyocytes mediated by NO dependent but Ca^{2+} independent (Goldhaber et al., 1996; Sugishita et al., 1999). However, various studies performed in rodents have shown that TNFα can lead to inotropic positive effects (Bick et al., 1997; Greensmith and Nirmalan, 2013). Here, we found that TNFα treatments (10 and 50 ng/ml) induced a time and concentration-dependent effect leading to a significant increase in Ca^{2+} transient amplitude between 1 h and 1 h 30 min suggesting a positive inotropic effect. Our results are in concordance with Bick et al. study (Bick et al., 1997), who have found that TNFα incubation increases Ca^{2+} transient and cellular contraction in neo-natal cardiomyocytes. In adult rat cardiomyocytes treated with 50 ng/ml of TNFα (Greensmith and Nirmalan, 2013), Ca^{2+} transient amplitude and cellular shortening were also increased (Greensmith and Nirmalan, 2013). The absence of effect observed under 100 ng/ml of TNFα might be explained by its bimodal effect, as previously described in cardiomyocytes, depending on exposure time or dose (Amadou et al., 2002; Shanmugam et al., 2016). Then, 100 ng/ml TNFα

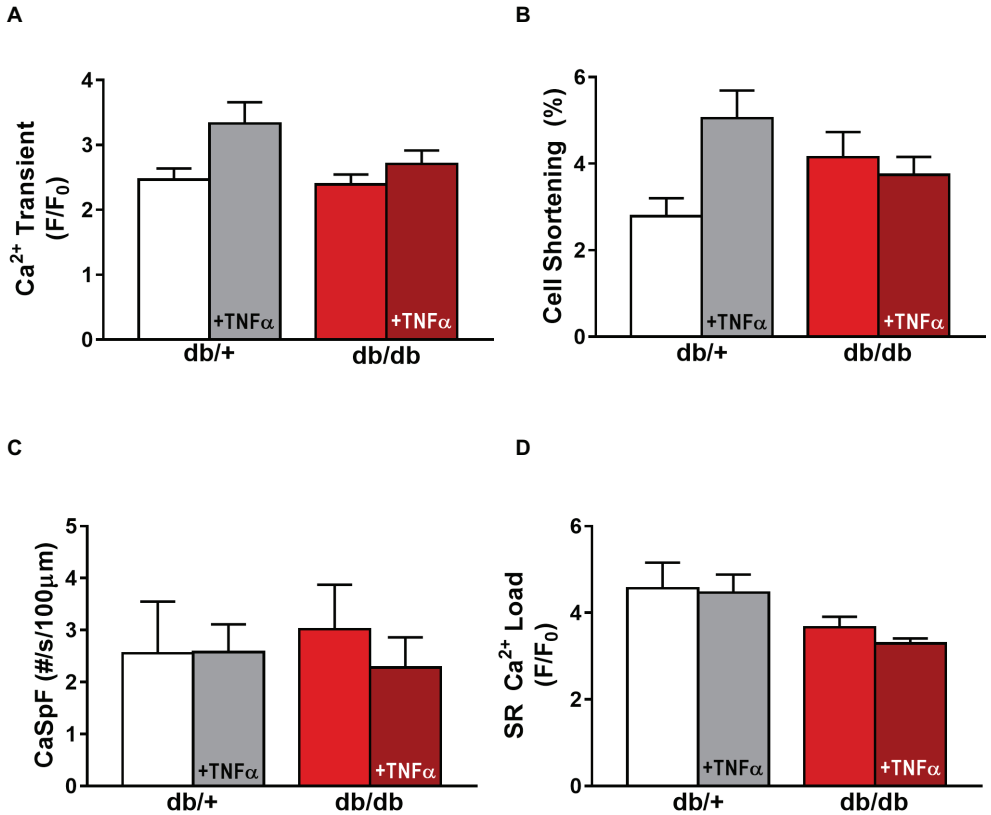

FIGURE 5 | EC coupling is unchanged in type 2 diabetic female mice. **(A)** Mean Ca^{2+} transient amplitude from *db/db* ± TNFα (n = 27 and n = 23) cardiomyocytes and their control littermates (*db/+*, n = 11 and n = 18). **(B)** Cell shortening measured in intact *db/db* ± TNFα (n = 12 and n = 9) and *db/+* cardiomyocytes (n = 8 and n = 14). **(C)** Ca^{2+} spark frequency in the same groups (for *db/db*: n = 9 and n = 12, for *db/+*: n = 10 and n = 17). **(D)** Mean of SR Ca^{2+} load in intact *db/db* ± TNFα (n = 17 and n = 18) and *db/+* cardiomyocytes (n = 9 and n = 14). p = N.S.

or higher doses, and with prolonged exposure, is expected to induce negative inotropic effects on Ca^{2+} handling.

In Mice Cardiomyocytes, TNFα Regulates Ca^{2+} Signaling *via* the Sphingosine and PLA2 Pathways

Previous studies have shown that TNFα produces myocardial effects (negative or positive inotropic effect) through different mechanisms such as PLA2 or sphingosine signaling pathway (Murray and Freeman, 1996; Oral et al., 1997; Liu and McHowat, 1998). Here, we found that exposure of TNFα (1 h to 1 h 30 min) mediates Ca^{2+} transient increase *via* the activation of both ceramidase (sphingosine precursor) and PLA2 (for arachidonic acid production). Sphingosine is commonly associated to short-term (within minutes) negative inotropic effect of TNFα (Oral et al., 1997). However, other studies have shown that ceramide enhanced SR Ca^{2+} release and SR Ca^{2+} re-uptake in adult ventricular myocytes (Liu and Kennedy, 2003). Those results are in line with our prevention of TNFα-mediated elevation of systolic Ca^{2+} release and Ca^{2+} transient decay time in cardiomyocytes treated with the ceramidase inhibitor NOE (**Figures 2B,C**). Moreover, inhibition of the PLA2 prevented TNFα-mediated increase in Ca^{2+} transient amplitude and SR Ca^{2+} transient decay time, suggesting that TNFα induces Ca^{2+} mishandling *via* PLA2-mediated phosphorylation of RyR. Indeed, 10 ng/ml of TNFα has been shown to increase Ca^{2+} transient amplitude as a result of PLA-2 mediated RyR PKA phosphorylation at serine 2,808 in wild-type mice of RASSF1A knock out (Mohamed et al., 2014). This PKA-dependent mediated effect of PLA-2/arachidonic acid on the RyR phosphorylation state perfectly explains why we observed a dramatic drop of Ca^{2+} spark frequency under the inhibition of the PLA-2 (**Figure 2F**). In addition, TNFα also accelerates SR Ca^{2+} re-uptake reflecting an increase in SERCA pump activity as seen under PKA phosphorylation of phospholamban supporting the TNFα/PLA-2/PKA pathway. This mechanism is confirmed by the restoration of the TNFα-mediated acceleration Ca^{2+} transient decay time under ATK, the PLA-2 inhibitor (**Figures 2B,C**).

Gender-Dependent Ca^{2+} Mishandling in *db/db* Mice, an Obesity-Linked Type 2 Diabetic Model

Type 2 diabetes is the most common form of diabetes. In western countries, 80% of type 2 diabetic patients have developed a diabetes linked to obesity resulting in severe glucose intolerance

compared to lean type 2 diabetic patients (Schaffer and Mozaffari, 1996). Our study was performed in *db*/*db* mice, a model that recapitulates, in that sense, the human pathology. Indeed, the leptin receptor mutation of *db*/*db* mice impairs the satiety feeling and leads to obesity around 4–5 weeks of age, which is followed by diabetic state with hyperglycemia and insulin resistance (Coleman, 1978). In type 2 diabetes linked to obesity, cardiac dysfunction has been associated to Ca^{2+} mishandling and structural remodeling (Belke et al., 2004; Pereira et al., 2006b; Falcao-Pires and Leite-Moreira, 2012). Indeed, overall, animal models of type 2 diabetes present a reduced Na^+/Ca^{2+} exchanger activity, and depressed Ca^{2+} transient linked to downregulation of Ca^{2+} channels, RyRs, and reduced SERCA activity (Netticadan et al., 2001; Zhong et al., 2001; Abe et al., 2002; Belke et al., 2004; Pereira et al., 2006b; Boudina and Abel, 2010). Here, our results show that those effects are recapitulated in male *db*/*db* mice (**Figure 4**), but not in female *db*/*db* mice. However, the gender-specific regulation in Ca^{2+} handling and/or β-adrenergic response has been previously described (Parks et al., 2014). Supporting this idea, we found that basal Ca^{2+} transient amplitude is lower in female control compared to male control cardiomyocytes. Although Parks et al. (2014) have shown that Ca^{2+} current, diastolic Ca^{2+}, and SR Ca^{2+} load were similar between control male and female, basal cAMP level was lower in control female compared to control male due to higher PDE4B expression in female. These results are in line with our previous work showing that *db*/*db* female mice have reduced phosphorylation of the RyR, which reduce Ca^{2+} spark frequency and could explain the preserve SR Ca^{2+} load and Ca^{2+} transient seen in female *db*/*db* compared to *db*/*db* male. Our results are paradoxical compared to the higher risk to develop heart failure for type 2 diabetic women compared to diabetic men. This discrepancy could be explain as follow: the decrease in $[Ca^{2+}]_i$ transient in male *db*/*db* mice could be protective at long term, maybe by preventing Ca^{2+} toxic effects such as apoptosis or preserve ATP content by limiting the ATP expense in pumping Ca^{2+} (Javorkova et al., 2010; Parks et al., 2014). Future studies will be needed to confirm this hypothesis.

Gender Dependent Alteration of Molecular TNFα Signaling Pathway in *db/db*

To our knowledge, plasmatic TNFα level parallels the degree of cardiac dysfunction in diabetic patients. In the *db*/*db* mice, we did not observe any changes in the plasmatic level of TNFα compared to control. Even though circulating TNFα is unchanged, male *db*/*db* mice present an increase in TACE expression suggesting a paracrine elevation of TNFα in the heart. Surprisingly, despite cardiomyocyte treatment with 10 ng/ml of TNFα, a concentration within the *in vivo* range measured under stress and injury (Bitterman et al., 1991), TNFα did not induce an increase in Ca^{2+} transient amplitude or decay time in *db*/*db*, as seen in C57Bl6 mice (**Figures 4B,C**). One explanation could be that in *db*/*db* control littermate strain background (C57BKS/J strain), TNFα is not as effective as in C57Bl6 strain. Indeed, genetic background, such as between C57BL6/J and C57BL6/N, has been shown to influence cardiac phenotype and propensity to develop cardiomyopathies (Tian et al., 2011; Simon et al., 2013). This could also explain the ineffective response of TNFα in female control and *db*/*db* mice (**Figure 5**). Although TNFα activation has been linked with oxidative stress, no gender-specific difference in cardiomyocytes redox state at baseline or during pathology has been observed (Ren, 2007; Bell et al., 2015). Another possibility could be that in male *db*/*db*, the dramatically reduced SR Ca^{2+} load would prevent the high Ca^{2+} systolic release induced by TNFα probably due to the phosphorylation of the RyR *via* the activation of PLA2. Indeed, we found in the presence of TNFα an increase in Ca^{2+} spark frequency in both *db*/+ and *db*/*db* mice reflecting an elevated diastolic RyR opening resulting from RyR phosphorylation by PKA previously described in male *db*/*db* (Pereira et al., 2014). Interestingly, in male *db*/*db* mice, the TNF-R2 was overexpressed, which is known to exert cardio-protective effects *via* the activation of NF-κB (Burchfield et al., 2010). Indeed, in liver, TNFα inhibits PDE3 expression elevating cAMP level and PKA activation (Ke et al., 2015). This activation of PKA could explain, in cardiomyocytes, the elevation of Ca^{2+} spark frequency in male *db*/+ cardiomyocytes treated with TNFα (**Figure 4F**). Moreover, TNF-R2 is known to be involved in positive cardiac inotropic effect (Defer et al., 2007). As a result, $[Ca^{2+}]$ overload was prevented and Ca^{2+} transient increased leading to an increase in inotropic response. The over-expressed TNF-R2 in a male *db*/*db* appears as an attempt to counteract the already present Ca^{2+} mishandling to protect from cardiac dysfunction. Indeed, prolonged activation of the TNF-R2 pathway in the *db*/*db* male cardiomyocytes could then activate phosphorylation of excitation-contraction coupling key proteins, such as phospholamban, to restore Ca^{2+} transient and cardiomyocytes contraction.

In conclusion, we found for the first time that both Ca^{2+} and TNFα signaling are altered only in male type 2 diabetic mice, whereas female does not seem to be affected. Although this study has several limitations in the interpretation such as non-comparable hormonal state between female *db*/*db* mice and diabetic women, lower effect of TNFα in *db*/+ than C57BL6 control, we still clearly show that male *db*/*db* mice develop Ca^{2+} mishandling leading to impaired contraction already at a young age, while woman seemed to be protected. Moreover, we found that male *db*/*db* mice put into place a protective mechanism to counteract those negative effects by over-expressing TNF-R2 cardio-protective signaling pathway.

DATA AVAILABILITY

The datasets generated for this study are available on request to the corresponding author.

ETHICS STATEMENT

The study was carried out in accordance to the ethical principles of the French Ministry of Agriculture and the European Parliament on the protection of animals. The protocol was

approved by the French Ministry of Agriculture and Bioethical Committee of the CSIC following recommendation of the Spanish Animal Care and the European Parliament on the protection of animals.

AUTHOR CONTRIBUTIONS

CD and AG conceived and designed the project, supervised the data acquisition and participated in analysis. LP and GR performed most of the experiments and analyses. LP interpreted the data and wrote the first draft of the manuscript. MS participated in the figure preparation. All authors have edited the manuscript.

FUNDING

This work has been funded by Acuerdos Bilaterales España-Francia (CSIC-INSERM) grant no. 2005FR0020 and partially by SAF2017-84777R from the Spanish Ministerio de Industria, Economia y Competitividad (to CD) and partially by CP15/00129 and PI17/01093 (to GR), and the ANR-11-1DEX-0003-02 to LP as members of the Laboratory of Excellence LERMIT.

REFERENCES

Abe, T., Ohga, Y., Tabayashi, N., Kobayashi, S., Sakata, S., Misawa, H., et al. (2002). Left ventricular diastolic dysfunction in type 2 diabetes mellitus model rats. *Am. J. Physiol. Heart Circ. Physiol.* 282, H138–H148. doi: 10.1152/ajpheart.2002.282.1.H138

Amadou, A., Nawrocki, A., Best-Belpomme, M., Pavoine, C., and Pecker, F. (2002). Arachidonic acid mediates dual effect of TNF-alpha on Ca^{2+} transients and contraction of adult rat cardiomyocytes. *Am. J. Phys. Cell Physiol.* 282, C1339–C1347. doi: 10.1152/ajpcell.00471.2001

Bauters, C., Lamblin, N., Mc Fadden, E. P., Van Belle, E., Millaire, A., and de Groote, P. (2003). Influence of diabetes mellitus on heart failure risk and outcome. *Cardiovasc. Diabetol.* 2:1. doi: 10.1186/1475-2840-2-1

Belke, D. D., Swanson, E. A., and Dillmann, W. H. (2004). Decreased sarcoplasmic reticulum activity and contractility in diabetic db/db mouse heart. *Diabetes* 53, 3201–3208. doi: 10.2337/diabetes.53.12.3201

Bell, D. S. (2007). Heart failure in the diabetic patient. *Cardiol. Clin.* 25, 523–538; vi. doi: 10.1016/j.ccl.2007.08.003

Bell, J. R., Raaijmakers, A. J., Curl, C. L., Reichelt, M. E., Harding, T. W., Bei, A., et al. (2015). Cardiac CaMKIIdelta splice variants exhibit target signaling specificity and confer sex-selective arrhythmogenic actions in the ischemic-reperfused heart. *Int. J. Cardiol.* 181, 288–296. doi: 10.1016/j.ijcard.2014.11.159

Bick, R. J., Liao, J. P., King, T. W., LeMaistre, A., McMillin, J. B., and Buja, L. M. (1997). Temporal effects of cytokines on neonatal cardiac myocyte Ca^{2+} transients and adenylate cyclase activity. *Am. J. Phys.* 272, H1937–H1944. doi: 10.1152/ajpheart.1997.272.4.H1937

Bitterman, H., Kinarty, A., Lazarovich, H., and Lahat, N. (1991). Acute release of cytokines is proportional to tissue injury induced by surgical trauma and shock in rats. *J. Clin. Immunol.* 11, 184–192. doi: 10.1007/BF00917424

Blum, A., and Miller, H. (2001). Pathophysiological role of cytokines in congestive heart failure. *Annu. Rev. Med.* 52, 15–27. doi: 10.1146/annurev.med.52.1.15

Boudina, S., and Abel, E. D. (2010). Diabetic cardiomyopathy, causes and effects. *Rev. Endocr. Metab. Disord.* 11, 31–39. doi: 10.1007/s11154-010-9131-7

Bugger, H., and Abel, E. D. (2014). Molecular mechanisms of diabetic cardiomyopathy. *Diabetologia* 57, 660–671. doi: 10.1007/s00125-014-3171-6

Burchfield, J. S., Dong, J. W., Sakata, Y., Gao, F., Tzeng, H. P., Topkara, V. K., et al. (2010). The cytoprotective effects of tumor necrosis factor are conveyed through tumor necrosis factor receptor-associated factor 2 in the heart. *Circ. Heart Fail.* 3, 157–164. doi: 10.1161/CIRCHEARTFAILURE.109.899732

Coleman, D. L. (1978). Obese and diabetes: two mutant genes causing diabetes-obesity syndromes in mice. *Diabetologia* 14, 141–148. doi: 10.1007/BF00429772

Defer, N., Azroyan, A., Pecker, F., and Pavoine, C. (2007). TNFR1 and TNFR2 signaling interplay in cardiac myocytes. *J. Biol. Chem.* 282, 35564–35573. doi: 10.1074/jbc.M704003200

Duncan, D. J., Yang, Z., Hopkins, P. M., Steele, D. S., and Harrison, S. M. (2010). TNF-alpha and IL-1beta increase Ca^{2+} leak from the sarcoplasmic reticulum and susceptibility to arrhythmia in rat ventricular myocytes. *Cell Calcium* 47, 378–386. doi: 10.1016/j.ceca.2010.02.002

Falcao-Pires, I., and Leite-Moreira, A. F. (2012). Diabetic cardiomyopathy: understanding the molecular and cellular basis to progress in diagnosis and treatment. *Heart Fail. Rev.* 17, 325–344. doi: 10.1007/s10741-011-9257-z

Feldman, A. M., Combes, A., Wagner, D., Kadakomi, T., Kubota, T., Li, Y. Y., et al. (2000). The role of tumor necrosis factor in the pathophysiology of heart failure. *J. Am. Coll. Cardiol.* 35, 537–544.

Fernandez-Velasco, M., Rueda, A., Rizzi, N., Benitah, J. P., Colombi, B., Napolitano, C., et al. (2009). Increased Ca^{2+} sensitivity of the ryanodine receptor mutant RyR2R4496C underlies catecholaminergic polymorphic ventricular tachycardia. *Circ. Res.* 104, 201–209, 212p following 209. doi: 10.1161/CIRCRESAHA.108.177493

Fernandez-Velasco, M., Ruiz-Hurtado, G., Hurtado, O., Moro, M. A., and Delgado, C. (2007). TNF-alpha downregulates transient outward potassium current in rat ventricular myocytes through iNOS overexpression and oxidant species generation. *Am. J. Physiol. Heart Circ. Physiol.* 293, H238–H245. doi: 10.1152/ajpheart.01122.2006

Galderisi, M., Anderson, K. M., Wilson, P. W., and Levy, D. (1991). Echocardiographic evidence for the existence of a distinct diabetic cardiomyopathy (the Framingham Heart Study). *Am. J. Cardiol.* 68, 85–89. doi: 10.1016/0002-9149(91)90716-X

Goldhaber, J. I., Kim, K. H., Natterson, P. D., Lawrence, T., Yang, P., and Weiss, J. N. (1996). Effects of TNF-alpha on $[Ca^{2+}]i$ and contractility in isolated adult rabbit ventricular myocytes. *Am. J. Phys.* 271, H1449–H1455. doi: 10.1152/ajpheart.1996.271.4.H1449

Greensmith, D. J., and Nirmalan, M. (2013). The effects of tumor necrosis factor-alpha on systolic and diastolic function in rat ventricular myocytes. *Phys. Rep.* 1:e00093. doi: 10.1002/phy2.93

Hofmann, U., Domeier, E., Frantz, S., Laser, M., Weckler, B., Kuhlencordt, P., et al. (2003). Increased myocardial oxygen consumption by TNF-alpha is mediated by a sphingosine signaling pathway. *Am. J. Physiol. Heart Circ. Physiol.* 284, H2100–H2105. doi: 10.1152/ajpheart.00888.2002

Javorkova, V., Mezesova, L., Vlkovicova, J., and Vrbjar, N. (2010). Influence of sub-chronic diabetes mellitus on functional properties of renal Na(+),K(+)-ATPase in both genders of rats. *Gen. Physiol. Biophys.* 29, 266–274. doi: 10.4149/gpb_2010_03_266

Kadokami, T., McTiernan, C. F., Kubota, T., Frye, C. S., and Feldman, A. M. (2000). Sex-related survival differences in murine cardiomyopathy are associated with differences in TNF-receptor expression. *J. Clin. Invest.* 106, 589–597. doi: 10.1172/JCI9307

Ke, B., Zhao, Z., Ye, X., Gao, Z., Manganiello, V., Wu, B., et al. (2015). Inactivation of NF-kappaB p65 (RelA) in liver improves insulin sensitivity and inhibits cAMP/PKA pathway. *Diabetes* 64, 3355–3362. doi: 10.2337/db15-0242

Kubota, T., McTiernan, C. F., Frye, C. S., Slawson, S. E., Lemster, B. H., Koretsky, A. P., et al. (1997). Dilated cardiomyopathy in transgenic mice with cardiac-specific overexpression of tumor necrosis factor-alpha. *Circ. Res.* 81, 627–635. doi: 10.1161/01.RES.81.4.627

Laakso, M. (1999). Hyperglycemia and cardiovascular disease in type 2 diabetes. *Diabetes* 48, 937–942. doi: 10.2337/diabetes.48.5.937

Leroy, J., Richter, W., Mika, D., Castro, L. R., Abi-Gerges, A., Xie, M., et al. (2011). Phosphodiesterase 4B in the cardiac L-type Ca(2)(+) channel complex regulates Ca(2)(+) current and protects against ventricular arrhythmias in mice. *J. Clin. Invest.* 121, 2651–2661. doi: 10.1172/JCI44747

Li, X. Q., Zhao, M. G., Mei, Q. B., Zhang, Y. F., Guo, W., Wang, H. F., et al. (2003). Effects of tumor necrosis factor-alpha on calcium movement in rat ventricular myocytes. *Acta Pharmacol. Sin.* 24, 1224–1230.

Liu, S. J., and Kennedy, R. H. (2003). Positive inotropic effect of ceramide in adult ventricular myocytes: mechanisms dissociated from its reduction in Ca^{2+} influx. *Am. J. Physiol. Heart Circ. Physiol.* 285, H735–H744. doi: 10.1152/ajpheart.01098.2002

Liu, S. J., and McHowat, J. (1998). Stimulation of different phospholipase A2 isoforms by TNF-alpha and IL-1beta in adult rat ventricular myocytes. *Am. J. Phys.* 275, H1462–H1472.

London, B., Baker, L. C., Lee, J. S., Shusterman, V., Choi, B. R., Kubota, T., et al. (2003). Calcium-dependent arrhythmias in transgenic mice with heart failure. *Am. J. Physiol. Heart Circ. Physiol.* 284, H431–H441. doi: 10.1152/ajpheart.00431.2002

Meldrum, D. R. (1998). Tumor necrosis factor in the heart. *Am. J. Phys.* 274, R577–R595.

Mohamed, T. M., Zi, M., Prehar, S., Maqsood, A., Abou-Leisa, R., Nguyen, L., et al. (2014). The tumour suppressor Ras-association domain family protein 1A (RASSF1A) regulates TNF-alpha signalling in cardiomyocytes. *Cardiovasc. Res.* 103, 47–59. doi: 10.1093/cvr/cvu111

Murray, D. R., and Freeman, G. L. (1996). Tumor necrosis factor-alpha induces a biphasic effect on myocardial contractility in conscious dogs. *Circ. Res.* 78, 154–160. doi: 10.1161/01.RES.78.1.154

Netticadan, T., Temsah, R. M., Kent, A., Elimban, V., and Dhalla, N. S. (2001). Depressed levels of Ca^{2+}-cycling proteins may underlie sarcoplasmic reticulum dysfunction in the diabetic heart. *Diabetes* 50, 2133–2138. doi: 10.2337/diabetes.50.9.2133

Oral, H., Dorn, G. W., 2nd, and Mann, D. L. (1997). Sphingosine mediates the immediate negative inotropic effects of tumor necrosis factor-alpha in the adult mammalian cardiac myocyte. *J. Biol. Chem.* 272, 4836–4842. doi: 10.1074/jbc.272.8.4836

Parks, R. J., Ray, G., Bienvenu, L. A., Rose, R. A., and Howlett, S. E. (2014). Sex differences in SR Ca(2+) release in murine ventricular myocytes are regulated by the cAMP/PKA pathway. *J. Mol. Cell. Cardiol.* 75, 162–173. doi: 10.1016/j.yjmcc.2014.07.006

Pereira, F. O., Frode, T. S., and Medeiros, Y. S. (2006a). Evaluation of tumour necrosis factor alpha, interleukin-2 soluble receptor, nitric oxide metabolites, and lipids as inflammatory markers in type 2 diabetes mellitus. *Mediat. Inflamm.* 2006:39062. doi: 10.1155/MI/2006/39062

Pereira, L., Matthes, J., Schuster, I., Valdivia, H. H., Herzig, S., Richard, S., et al. (2006b). Mechanisms of [Ca2+]i transient decrease in cardiomyopathy of db/db type 2 diabetic mice. *Diabetes* 55, 608–615. doi: 10.2337/diabetes.55.03.06.db05-1284

Pereira, L., Metrich, M., Fernandez-Velasco, M., Lucas, A., Leroy, J., Perrier, R., et al. (2007). The cAMP binding protein Epac modulates Ca^{2+} sparks by a Ca^{2+}/calmodulin kinase signalling pathway in rat cardiac myocytes. *J. Physiol.* 583, 685–694. doi: 10.1113/jphysiol.2007.133066

Pereira, L., Ruiz-Hurtado, G., Morel, E., Laurent, A. C., Metrich, M., Dominguez-Rodriguez, A., et al. (2012). Epac enhances excitation-transcription coupling in cardiac myocytes. *J. Mol. Cell. Cardiol.* 52, 283–291. doi: 10.1016/j.yjmcc.2011.10.016

Pereira, L., Ruiz-Hurtado, G., Rueda, A., Mercadier, J. J., Benitah, J. P., and Gomez, A. M. (2014). Calcium signaling in diabetic cardiomyocytes. *Cell Calcium* 56, 372–380. doi: 10.1016/j.ceca.2014.08.004

Preciado-Puga, M. C., Malacara, J. M., Fajardo-Araujo, M. E., Wrobel, K., Wrobel, K., Kornhauser-Araujo, C., et al. (2014). Markers of the progression of complications in patients with type 2 diabetes: a one-year longitudinal study. *Exp. Clin. Endocrinol. Diabetes* 122, 484–490. doi: 10.1055/s-0034-1372594

Ren, J. (2007). Influence of gender on oxidative stress, lipid peroxidation, protein damage and apoptosis in hearts and brains from spontaneously hypertensive rats. *Clin. Exp. Pharmacol. Physiol.* 34, 432–438. doi: 10.1111/j.1440-1681.2007.04591.x

Ruiz-Hurtado, G., Li, L., Fernandez-Velasco, M., Rueda, A., Lefebvre, F., Wang, Y., et al. (2015). Reconciling depressed Ca^{2+} sparks occurrence with enhanced RyR2 activity in failing mice cardiomyocytes. *J. Gen. Physiol.* 146, 295–306. doi: 10.1085/jgp.201511366

Rutter, M. K., Parise, H., Benjamin, E. J., Levy, D., Larson, M. G., Meigs, J. B., et al. (2003). Impact of glucose intolerance and insulin resistance on cardiac structure and function: sex-related differences in the Framingham Heart Study. *Circulation* 107, 448–454. doi: 10.1161/01.CIR.0000045671.62860.98

Schaffer, S. W., and Mozaffari, M. (1996). Abnormal mechanical function in diabetes: relation to myocardial calcium handling. *Coron. Artery Dis.* 7, 109–115. doi: 10.1097/00019501-199602000-00003

Shanmugam, G., Narasimhan, M., Sakthivel, R., Kumar, R. R., Davidson, C., Palaniappan, S., et al. (2016). A biphasic effect of TNF-alpha in regulation of the Keap1/Nrf2 pathway in cardiomyocytes. *Redox Biol.* 9, 77–89. doi: 10.1016/j.redox.2016.06.004

Simon, M. M., Greenaway, S., White, J. K., Fuchs, H., Gailus-Durner, V., Wells, S., et al. (2013). A comparative phenotypic and genomic analysis of C57BL/6J and C57BL/6N mouse strains. *Genome Biol.* 14:R82. doi: 10.1186/gb-2013-14-7-r82

Sugishita, K., Kinugawa, K., Shimizu, T., Harada, K., Matsui, H., Takahashi, T., et al. (1999). Cellular basis for the acute inhibitory effects of IL-6 and TNF- alpha on excitation-contraction coupling. *J. Mol. Cell. Cardiol.* 31, 1457–1467. doi: 10.1006/jmcc.1999.0989

Tian, C., Shao, C. H., Moore, C. J., Kutty, S., Walseth, T., DeSouza, C., et al. (2011). Gain of function of cardiac ryanodine receptor in a rat model of type 1 diabetes. *Cardiovasc. Res.* 91, 300–309. doi: 10.1093/cvr/cvr076

Toedebusch, R., Belenchia, A., and Pulakat, L. (2018). Diabetic cardiomyopathy: impact of biological sex on disease development and molecular signatures. *Front. Physiol.* 9:453. doi: 10.3389/fphys.2018.00453

Yamakawa, T., Tanaka, S., Yamakawa, Y., Kiuchi, Y., Isoda, F., Kawamoto, S., et al. (1995). Augmented production of tumor necrosis factor-alpha in obese mice. *Clin. Immunol. Immunopathol.* 75, 51–56. doi: 10.1006/clin.1995.1052

Yokoyama, T., Vaca, L., Rossen, R. D., Durante, W., Hazarika, P., and Mann, D. L. (1993). Cellular basis for the negative inotropic effects of tumor necrosis factor-alpha in the adult mammalian heart. *J. Clin. Invest.* 92, 2303–2312. doi: 10.1172/JCI116834

Zhang, M., Xu, Y. J., Saini, H. K., Turan, B., Liu, P. P., and Dhalla, N. S. (2005). TNF-alpha as a potential mediator of cardiac dysfunction due to intracellular Ca^{2+}-overload. *Biochem. Biophys. Res. Commun.* 327, 57–63. doi: 10.1016/j.bbrc.2004.11.131

Zhong, Y., Ahmed, S., Grupp, I. L., and Matlib, M. A. (2001). Altered SR protein expression associated with contractile dysfunction in diabetic rat hearts. *Am. J. Physiol. Heart Circ. Physiol.* 281, H1137–H1147. doi: 10.1152/ajpheart.2001.281.3.H1137

Conflict of Interest Statement: The authors declare that the research was conducted in the absence of any commercial or financial relationships that could be construed as a potential conflict of interest.

Annex 2

Cardiac phosphodiesterases are differentially increased in diabetic cardiomyopathy.

Rita Hanna[1]*, Wared Nour-Eldine[1]*, Youakim Saliba[2], Carole Dagher-Hamalian[1], Pia Hachem[1], Pamela Abou-Khalil[1], Magali Samia El Hayek[3], Laëtitia Pereira[3], Nassim Farès[2], Grégoire Vandecasteele[3], Aniella Abi-Gerges[1].

[1]Gilbert and Rose-Marie Chagoury School of Medicine, Lebanese American University, P.O. Box 36, Byblos, Lebanon.

[2] Faculté de Médecine, Laboratoire de Recherche en Physiologie et Physiopathologie, LRPP, Pôle Technologie Santé, Université Saint Joseph, Beirut, Lebanon.

[3]Signaling and Cardiovascular Pathophysiology, UMR-S1180, Université Paris-Saclay, 92296 Châtenay-Malabry, France.

*These authors contributed equally to the work and are listed by alphabetical order.

Running title: Cardiac PDEs, MRP4 and Epac in diabetic cardiomyopathy.

Correspondence to:

Dr. Aniella Abi-Gerges
Gilbert and Rose-Marie Chagoury School of Medicine
Lebanese American University
P.O. Box 36, Byblos
Lebanon.
Tel
Fax
Email: aniella.abigerges@lau.edu.lb

Abstract

Background: Diabetic cardiomyopathy (DCM) is a diabetes-induced pathophysiological condition associated with cardiac hypertrophy, fibrosis and contractile dysfunction. Adrenergic impairment in the diabetic hearts has been attributed to β_1-AR dysfunction as well as defects involving post-receptor proteins however, much remains to be understood as to whether the expression of cardiac cyclic nucleotide phosphodiesterases (PDEs) is affected in DCM. Besides, as some PDE isoforms have been proposed as potential therapeutic targets in DCM, understanding their alterations could be a promising therapeutic approach for a better management of diabetic patients.

Objective: Characterize the expression pattern of cardiac PDE isoforms (PDE 1-5) in a streptozotocin (STZ)–induced type 1 diabetes adult rat model at 4, 8 and 12 weeks following either vehicle or STZ injection.

Results: Diabetic rats exhibited cardiomyopathy at week 4, attested by an early onset of cardiac hypertrophy along with steatosis and diastolic dysfunction with preserved ejection fraction, and which were followed by myocardial fibrosis at week 12. We show that DCM is associated with an early and exclusive increase in PDE4B and PDE4D mRNA expression at week 4. This was followed by a transient up-regulation in the mRNA expression of PDE1A, PDE2A, PDE3A and PDE5A in diabetic rats at week 8, compared to their age-matched controls while no change was noted in the gene expression of PDE4A regardless of the disease stage. These changes were reflected in transient increases in protein expression of both PDE3A and PDE4B in diabetic rats at week 8. Moreover, we assessed the expression of other proteins involved in cyclic adenosine

3’-5’ monophosphate (cAMP) signaling pathway, such as the multidrug-resistance protein 4 (MRP4) and the exchange protein Epac 1-2. Up-regulation in Epac1 mRNA expression occurred at week 8 in diabetic rats and was maintained until week 12 when an increase in Epac2 and MRP4 mRNA expression emerged. Interestingly, alterations in Epac2 mRNA were not reflected in similar changes of the protein expression.

Conclusion: We show herein for the first time that the gene and protein expression of cardiac PDE2A, PDE3A, PDE4B, PDE4D, PDE5A are subjected to a differential and time-specific regulation in DCM.

Keywords: 3′-5′ cyclic nucleotide phosphodiesterase, diabetes type 1, diabetic cardiomyopathy, multidrug-resistance protein 4, exchange protein directly activated by cAMP.

Introduction

Diabetes mellitus (DM) represents a major global health problem with an estimation of 285 million people affected in 2010, which is expected to grow to almost 700 million by 2040 (1). In 1974, Framingham study showed that diabetic patients, suffering neither from coronary artery disease (CAD) nor hypertension, have 2 to 5 times higher risk of developing heart failure (HF) than age-matched, non-diabetic patients (2). These findings suggest that in addition to the well-known pathological triggers, DM contributes to the development of HF through a more disease-specific variety of mechanisms, which seem to be mostly driven by hyperglycemia, hyperinsulinemia, metabolic changes, and oxidative stress (3). Diabetic cardiomyopathy (DCM) is DM-induced pathophysiological condition in which HF occurs in the absence of CAD, hypertension, and valvular heart disease and comprises a spectrum of cardiac abnormalities (4). These include cardiac hypertrophy (CH), myocardial fibrosis, diabetic microangiopathy, diastolic and systolic dysfunction. Diabetes-ensued non-ischemic HF has received much less attention than coronary and cerebral vascular events (5); hence, the pathophysiology of DCM is still not fully understood.

Impairment of cyclic adenosine 3'-5' monophosphate (cAMP) signaling pathway, which is attributed to the chronic activation of the sympathetic nervous system (6), is a hallmark of the hypertrophied and failing heart. However, data on actual changes affecting this pathway in DCM are still missing. In the normal myocardium and upon β-adrenergic receptors (β-ARs) stimulation, cAMP exerts its effects mainly through cAMP-dependent protein kinase A (PKA) activation, hence regulating the key components of the cardiac excitation-contraction coupling (ECC). Moreover, cAMP also directly activates the exchange proteins Epac1 and Epac2, which are

associated with pro-hypertrophic effects of β-AR stimulation, promotion of sarcoplasmic reticulum (SR) Ca^{2+} leak, and cardiomyocyte apoptosis (7).

In normal cardiac myocytes, intracellular cAMP content is finely tuned by its rate of synthesis by adenylyl cyclases (AC5/6) (8), its rate of degradation by cyclic nucleotide phosphodiesterases (PDEs) (8) and to some extent by its extrusion by an ATP-dependent transport mechanism involving multidrug-resistance protein 4 (MRP4) (9).

PDEs fall into 11 families (PDE 1-11) and 21 genes encoding nearly 100 isoforms arising from multiple transcription start sites as well as alternative splicing (10). Of these, PDE 1–5, PDE8, PDE9 and PDE10 (11) are expressed and display different functional roles in the normal and pathological heart. In the normal myocardium, PDE3 and PDE4 are the predominating families (12). PDE3 is encoded by two genes (PDE3A and PDE3B), with PDE3A being the predominant form expressed in cardiac myocytes (13). PDE4 family consists of four genes (PDE4A to D), but only PDE4A, PDE4B, and PDE4D appear to be expressed in the rat heart (14). These multiple PDEs terminate hormonal signals and prevent global rises in cAMP, known to be deleterious (15). They display distinct intracellular localization (16-18), thereby shaping intracellular-signaling microdomains that maintain the specificity of cellular responses (19, 20).

Changes affecting cAMP pathway in hypertrophied and failing myocardium classically include decreased β_1-AR density (6) and AC activity (21, 22), uncoupling of β_2-AR from Gs and increased Gi expression (6). Downstream of cAMP, changes in PDE expression (23-28), increased expression levels of Epac1 and to a lesser extent Epac2 in experimental models of CH (29) as well as in left ventricular samples from human patients with HF were reported (30).

DM causes cardiac dysfunction and HF that are associated with metabolic abnormalities and autonomic impairment. Adrenergic impairment in the diabetic hearts may not be only due to a reduction in β_1-AR function but seems to be also involving post-receptor defects. While some studies reported decreased β_1-AR content in rat heart (31), others showed a similar β-AR density in normal and diabetic LV in mini-pigs despite a reduction in cAMP production (32). β-AR desensitization was mainly attributed to an increased Gi expression. Additionally, this impaired signaling has been shown to be mediated by a reduction in PKA activity and its catalytic subunit content in the hearts (33) and mesenteric artery (34) isolated from diabetic animals. Furthermore, abnormal vascular relaxation responsiveness, seen in superior mesenteric artery rings isolated from diabetic rats, was attributed to an increase in PDE activity (34), which was mainly associated with an up-regulation in PDE3A and PDE3B mRNA levels (35) and a reduction in AC5/6 expression (36). However, Abboud et al., reported a decrease in total cAMP and cGMP-PDE activity in aortic rings isolated from diabetic rats that was mainly due to a reduction in the activity of PDE1, PDE3 and PDE5 with no changes reported in PDE4 activity (37). Therefore, most of the defects affecting the expression and activity of PDEs have been well documented in diabetic animal models using aortic (37, 38) and mesenteric arteries (34), however these impairments, especially with respect to the different isoforms of cardiac PDEs, remain incompletely explored in the diabetic myocardium. A study performed on mice fed on high-fat diet and subjects developing diabetes type 2, showed an increase in cardiac PDE4D expression (39). This up-regulation was attributed to a reduced PKA phosphorylation of phospholamban thus leading to systolic and diastolic dysfunction. In particular, little is known about molecular changes affecting cAMP signaling pathway in diabetes type 1.

Taken together, the abovementioned studies suggest a potential role of the main actors of cAMP pathway in cardiac remodeling associated with diabetes. In the present study, we have

characterized the expression pattern of PDE isoforms (PDE 1-5), MRP4 and Epac 1-2 in a streptozotocin (STZ)–induced type 1 diabetes adult rat model 4, 8 and 12 weeks after diabetes induction. We show a differential and time-specific up-regulation in the expression of various cardiac PDE isoforms, mainly PDE3A and PDE4B in DCM. Besides, we also reveal an up-regulation in MRP4 and Epac 1-2 mRNA expression in diabetic hearts. To our knowledge, this is the first report that delineates differential changes in the expression of various PDE isoforms, MRP4 and Epac 1-2 with respect to the evolution of DCM at three different stages of the disease progression. Understanding their alterations is important as this knowledge may help to propose new therapeutic approaches for better management of diabetic patients and prevent the progression of DCM to HF.

Methods

Animal model

Animal care and investigations adhered to the Guide for the Care and Use of Laboratory Animals published by the US National Research Council committee. All protocols were approved by the Animal Care and Use Committee (LAU.ACUC.SOM.AA1.16/April/2018) at the Lebanese American University (LAU) (40). Sixty-nine adult male Wistar rats (LAU animal breeding program) were included in this study. Animals were placed under 12h light/12h dark cycle conditions at a constant temperature (22 ± 2 °C) and were fed with standard chow and tap water *ad libitum*. Five week-old male Wistar rats (80-130g) were randomized into two groups. After 12 hours fasting, one group received one intraperitoneal injection of streptozotocin (STZ, Sigma-Aldrich: 65 mg/kg in 0.1 M citrate buffer, pH=4.5) to induce diabetes mellitus type 1 while the

second age-matched control (CON) group was injected with vehicle (0.1 M citrate buffer, pH=4.5) (41). After 72 hours, fasting blood glucose levels were measured using Accu-Check® Performa glucometer (Roche, USA) and rats exhibiting blood glucose levels > 200mg/dl following STZ injection were considered diabetic and were included in the study. All experiments were performed at 4, 8 and 12 weeks after STZ or vehicle injection. Fasting blood glucose and body weight were monitored on a weekly basis for all control and diabetic rats.

Echocardiography

Cardiac function of all rats was monitored under anesthesia (4-5% of Sevoflurane). Transthoracic two-dimensional guided M-mode echocardiography was performed via the long axis of the left ventricle at the level of the papillary muscles using the SonoScape S2V high- resolution color Doppler ultrasound system equipped with a 4-8 MHz micro-convex C611 probe (SonoScape Co., Shenzhen, China) (42). Echocardiography provided the following measurements: end-systolic and end-diastolic interventricular septum thickness, left ventricle posterior wall thickness, internal end-diastolic and end-systolic diameters of the left ventricle, heart rate (HR), end diastolic volume (EDV), end systolic volume (ESV), stroke volume (SV), ejection fraction (EF) and fractional shortening (FS) of the left ventricular diameter (23). All measurements were performed in triplicate and after stabilization of the HR.

Anatomical study and blood extraction

At the end of the echocardiography measurements and while CON and STZ-treated rats were still under anesthesia (4-5% of sevoflurane), body weight (BW) was measured and the heart was rapidly excised, rinsed with fresh cold physiological saline solution and weighted. Heart was cut; the upper 2/3 part was fixed in a 10% neutral buffered formalin for histopathological evaluation of morphological changes while the remaining 1/3 part was stored in liquid nitrogen for real-time PCR and western blot analysis. Lungs, liver and kidneys were removed and weighted. Signs of congestive heart failure (ascites, serous cavity effusion, etc) were reported, if present.

Blood was collected from thoracic chamber after excision of the heart and left at room temperature for 30 min. Blood samples from all rats were subsequently centrifuged at 4500 rpm for 10 min, and the serum was preserved at −80°C for lipid profile, hepatic enzymes, CO_2, creatinine and urea measurements using a Cobas C311 analyzer.

Histopathology

Cardiac specimens were fixed in 10% neutral buffered formalin at 25°C, dehydrated in 95 % ethanol and then embedded in paraffin (43). Briefly, sections were stained with hematoxylin & eosin and Masson's Trichrome. The latter stain was used to assess cardiac fibrosis. Slides from control and diabetic rats at 4, 8 and 12 weeks following either vehicle or STZ injection were evaluated for pathological lesions and cardiac remodeling by an experienced board-certified pathologist using a light microscope (Zeiss). Two different sections were obtained from each heart and analyzed for inflammation (presence or absence of lymphocyte aggregates within the interstitial space), steatosis (presence or absence of intracellular clear vacuoles of lipids) and

interstitial fibrosis (present or not of collagen fibers highlighted by trichrome stain between cardiac myocytes). Quantitative analysis of fibrotic areas in both control and diabetic at 4, 8 and 12 weeks was performed using ImageJ software. Morphometric pixel analysis was conducted on 4 non-overlapping randomly chosen fields (40 X magnification) per section per rat. The total fibrotic stained area was corrected to the total stained area section of the heart tissue.

Real-time quantitative PCR (RT-qPCR)

Total RNA was extracted from frozen cardiac tissue isolated from control and diabetic rats at 4, 8 and 12 weeks using Trizol reagent (Ambion, life technologies, USA). The purity and integrity of RNA was detected by NanoDrop 2000 and 1 μg was reverse-transcribed using iscript cDNA synthesis kit (Bio-Rad) as per the manufacturer's instructions. Real-time PCR reactions were prepared using SsoAdvanced™ Universal SYBR® Green Supermix (Bio-Rad) and performed in a CFX96 Real-Time PCR Detection System (Bio-Rad). The specificity of each primer set was monitored by analyzing the dissociation curve. GAPDH was used as a housekeeping gene. Genes of interest included ANF, PDE1A, PDE2A, PDE3A, PDE4A, PDE4B, PDE4D, PDE5A, MRP4, Epac1 and Epac2. Forward and reverse primers used in this study are listed in **Table S1**. Cq values were obtained and the relative expression values of the target genes were calculated using the $2^{-\Delta\Delta Ct}$ method.

Western Blot

Frozen hearts from control and diabetic rats at 4, 8 and 12 weeks were homogenized in an ice-cold buffer containing 150 mM NaCl, 20 mM Hepes (pH 7.4), 2 mM EDTA, 1 mM

Phenylmethylsulfonyl fluoride (Sigma Aldrich) and supplemented with 10% Glycerol, 0,2% Triton, and Complete Protease Inhibitor Tablets from Roche Diagnostics (Basel, Switzerland). Protein lysates were kept on ice for 30 min then centrifuged at 13200 rpm for 15 min at 4°C. Supernatants were subjected to protein quantification and 50 µg of protein extracts were loaded on SDS-PAGE gels. PDE3A was detected with a rabbit anti-PDE3A antibody (1:1000). PDE4B was detected using a rabbit anti-PDE4B antibody (1:1000). Epac2 was detected using a rabbit polyclonal anti-Epac2 antibody (1:1000). Calsequestrin was detected using a rabbit anti-calsequestrin (1:2000). Immunoreactive bands were revealed in ChemiDoc Imaging Systems (Bio-Rad) or Thermofischer iBright Imaging system and analyzed using Image J. PDE3A antibody was a generous gift from Dr. Chen Yan (Rochester University, NY, USA). PDE4B antibody was kindly provided by Pr. Marco Conti (University of California San Francisco, CA, USA). Epac2 and Calsequestrin antibodies were purchased from Thermo Scientific PA1-913 and Proteintech 19103-1-AP, respectively.

Statistical analysis

Survival curves of CON and STZ-treated rats were compared using Log-rank test (Mantel-Cox test); and a difference was considered statistically significant when $P<0.05$. All quantitative data are reported as means ± SEM and analyzed by Prism (Version 7.0a). When only one variable (i.e STZ treatment) was present, t-test was used to compare between CON and STZ-treated groups at one-time point because the data followed a normal distribution that was verified with the Shapiro-Wilk test. When normality did not follow a normal distribution, the non-parametric Mann-Whitney test was used to compare between CON and STZ-treated groups at one-time point. When the effect of two independent variables (i.e. both the effect of STZ treatment and time) was studied,

two-way ANOVA test was performed followed by post hoc Sidak's multiple comparison test. $P<0.05$ was considered to indicate a statistically significant difference.

Results

Induction and characterization of diabetes type I model in adult rats.

To assess the consequences of a sustained hyperglycemia on cardiac function and DCM development, we generated a STZ–induced type 1 diabetes in adult rat. The survival rate and fasting blood glucose were assessed in both CON and STZ-treated rats over 4, 8 and 12 weeks following either vehicle or STZ injection. No death was reported in the CON group while the mortality rate was estimated to be 8%, 26% and 43% in STZ-treated rats, 4, 8 and 12 weeks respectively, following diabetes induction (**Figure 1A**). Fasting blood glucose levels were increased at least by 4-fold in all STZ-treated rats compared to their age-matched CON (**Figure 1B**).

Blood was collected from all rat groups included in this study and analyzed for lipid profile, liver and kidney function. As shown in **Table 1**, cholesterol and triglycerides levels were increased in STZ-treated rats at 8 (Cholesterol: +41%, $p<0.05$; Triglycerides: +174%, $p<0.01$) and 12 weeks (Cholesterol: +42%, $p=0.08$; Triglycerides: +188%, $p<0.05$) compared to their age-matched CON, while there was no change between both groups at 4 weeks. Furthermore, regardless of the disease stage, STZ-treated rats showed impaired liver and kidney functions attested by a significant increase in the level of alanine aminotransferase (ALT) and creatinine/body weight ratio (Cr/BW), respectively. However, CO_2 levels were similar between STZ-treated and CON rats at 4, 8 and 12 weeks attesting the absence of acidosis.

Effect of diabetes type I on the development of diabetic cardiomyopathy (DCM) in adult rats.

To assess the influence of diabetes type 1 on the heart, the development of the DCM was assessed by anatomic, echocardiographic and histopathological data at 4, 8 and 12 weeks following either vehicle or STZ injection. All diabetic rats had a significantly lower BW and heart weight (HW) compared to their age-matched control (**Table 2**). However, HW/BW ratio was significantly increased by ~ 34% in STZ-treated rats compared to the age-matched CON, attesting CH in diabetic rats (**Table 2; Figure 1C**). The weights of lungs, liver and kidneys normalized to BW were also significantly higher in 4, 8 and 12 week-STZ-treated rats compared to their age-matched CON (**Table 2**). No sign of ascites nor serous cavity effusion was observed.

CH detected by anatomic data in diabetic rats (**Figure 1C**) was confirmed by examining both the expression of atrial natriuretic factor (ANF), a CH marker, by real time qPCR (**Figure 1D)** as well as structural and functional changes by echocardiography **(Figure 2)** in the hearts of 4, 8 and 12 week-CON and STZ-treated rats. As shown in **Figure 1D**, ANF expression was strongly increased in STZ-treated rats compared to their age-matched CON, regardless of the disease stage.

Echocardiography revealed both structural and functional changes in the hearts of STZ-treated rats compared to controls (**Figure 2; Table 3**). Telediastolic and telesystolic interventricular septum, diastolic and systolic left ventricular posterior wall thickness, as well as left ventricular end diastolic and systolic diameters were decreased in STZ-treated rats compared to CON rats. However, given that the BW was lower in diabetic rats compared to controls, we normalized the abovementioned parameters to BW **(Table 3).** When normalized to BW, telediastolic and telesystolic interventricular septum, diastolic and systolic left ventricular posterior wall thickness as well as the left ventricular end diastolic and systolic diameters showed a significant increase in

STZ-treated rats at 4, 8 and 12 weeks compared to their age-matched CON **(Table 3)**. In contrast, EF (**Figure 2A**) and FS (**Figure 2B**) were quite similar in all groups of rats except for a slight increase in STZ-treated rats, 4 weeks following injection (FS was 41 ± 2% in 6 CON *versus* 51 ± 3% in 7 STZ).

To further characterize the progression of DCM in our model, cardiac function was evaluated by assessing the HR and changes in blood volumes during the cardiac cycle in 4, 8 and 12 week- STZ-treated rats as well as their age-matched CON. As shown in **Figure 2C**, all diabetic rats exhibited an approximate 28% decrease in HR compared to CON, regardless of the disease stage. Additionally, 4, 8 and 12 week-STZ-treated rats presented a decrease in the SV, ESV and EDV compared to their age-matched CON rats (**Figure 2D**).

Histological sections were obtained from the hearts of all CON and STZ-treated rats and analyzed for cardiac steatosis, inflammation and fibrosis (**Table S2** and **Figures 3** & **4**). Cardiac steatosis appeared exclusively and early on, starting 4 weeks after STZ injection, in 86% of diabetic rats **(Figures 3D and 4D)** and was maintained until 12 weeks in all STZ-treated rats (**Table S2; Figures 3F, 4F and 4H**). However, cardiac inflammation was apparent in 38% of diabetic rats (**Table S2 and Figure 3E**) and 17% of controls (**Table S2** and **Figure 3B)**) starting 8 weeks following either STZ or vehicle injection and was maintained until 12 weeks in 50% of both CON (**Table S2; Figure 3C**) and diabetic rats (**Table S2; Figure 3G**) with no significant difference between the 2 groups. Cardiac fibrosis was clearly apparent in all diabetic rats (n=10) at 12 weeks (**Table S2; Figure 4G**) compared to controls (1 case reported; **Table S2**). Quantitative analysis of fibrotic areas in both control and diabetic rats showed a strong increase in diabetic rats at 12 weeks compared to their age-matched controls, while no significant difference was reported between both groups at 4 and 8 weeks **(Figure 4I)**.

Our results also showed an accumulation of foamy macrophages in the alveoli of diabetic rats at 4, 8 and 12 weeks after STZ injection (**Table S2; Figure S1**). However, diabetes didn't seem to have a major effect on the liver as compared to controls with respect to liver portal inflammation, hepatic necro-inflammation, steatosis and perisinusoidal fibrosis. Besides, only 30% of STZ-treated rats developed liver portal fibrosis at 12 weeks while no cases were reported in controls (**Table S2; Figure S2)**.

Expression of PDEs transcripts in control and diabetic hearts.

Most of the defects affecting the expression and activity of PDEs have been well documented in diabetic animal models using aortic (37, 38) and mesenteric arteries (34, 35), however data on actual changes in cardiac PDE isoforms are still missing in the diabetic heart. Hence, we examined the variations in the expression of the major PDE isoforms (PDE1-5) with respect to DCM evolution at three different stages of the disease progression.

To start with, mRNA expression of different PDE isoforms was evaluated in the hearts of both CON and STZ-treated rats at 4, 8 and 12 weeks following either vehicle or STZ injection. As shown in **Figure 5**, there were no significant changes in PDE1A, PDE2A, PDE3A and PDE5A mRNA expression between both groups of rats at 4 weeks. The expression of all the latter was significantly and transiently increased in 8 week-STZ-treated rats compared to their age-matched CON. The expression of PDE4A mRNA did not change in diabetic rats compared to controls regardless of the disease stage (**Figure 5D**). In contrast, a significant increase in PDE4B and PDE4D mRNA expression was observed in STZ-treated rats compared to CON at 4 weeks

following injection. This increase was further maintained for both isoforms at 8 (**Figures 5E and 5F**) and eventually at 12 weeks for PDE4D only (**Figure 5F**).

Expression of PDE3A and PDE4B in control and diabetic hearts.

To further characterize the modifications in PDE isoforms expression in DCM, we assessed whether alterations in mRNA were reflected in similar changes of PDE protein expression. We focused on PDE3 and PDE4 families because they are the predominant forms expressed in the normal myocardium (44). Hence, their protein expression was measured in normal and diabetic hearts 4, 8 and 12 weeks following vehicle or STZ injection.

Equal amounts of proteins prepared from heart extracts from all CON or STZ-treated animals were separated on SDS/PAGE and PDE3A as well as PDE4B proteins were subsequently detected by Western blotting using PDE subtype-selective antibodies. Two bands migrating at approximately 125 kDa and 85 kDa were detected for PDE3A in both control and diabetic rat hearts (**Figure 6A**). PDE3A-125 kDa band appeared to be significantly increased in 8 week-diabetic hearts (n=3) compared to their age-matched control (n=4) (**Figure 6B; left panel**) with no change between both groups at 4 and 12 weeks. Expression of PDE3A-85 kDa did not change in diabetic rats compared to controls regardless of the disease stage (**Figure 6B; right panel**). A single band migrating at approximately 78 kDa was detected for PDE4B in rat hearts (**Figure 6C**). Its expression was only increased in 8 week-diabetic hearts (n=4) compared to their age-matched control (n=5) (**Figure 6D**).

Expression of MRP4 and Epac in control and diabetic hearts.

To further characterize the changes affecting the expression of key proteins involved in cAMP homeostasis in DCM, we assessed the mRNA expression of Epac 1-2 isoforms and MRP4. As shown in **Figure S3**, MRP4 mRNA increased in the 12 week-STZ-treated rats compared to their age-matched CON. Epac1 mRNA expression increased in the diabetic rats 8 and 12 weeks following STZ injection compared to their age matched CON (**Figure S4, Panel A**) while the up-regulation in Epac2 wasn't apparent in STZ-treated rats until week 12 (**Figure S4, Panel B)**. We then assessed whether alterations in Epac2 mRNA were reflected in similar changes of the protein expression. Equal amounts of proteins prepared from heart extracts from all CON or STZ-treated animals were separated on SDS/PAGE and Epac2 protein was detected by Western blotting using Epac2 selective antibody. A single band migrating at approximately 110 kDa was detected in rat hearts for Epac2 (**Figure S3; Panel C**). Its expression did not change in diabetic rats compared to controls regardless of the disease stage (**Figure S3; Panel D**).

Discussion

The main goal of the present study was to delineate the sequential changes in the expression of the following key cAMP signaling proteins: PDE isoforms (PDE 1-5), MRP4 and Epac 1-2 during the evolution of DCM. We provide herein the first evidence of a differential and time-specific up-regulation in the expression of various cardiac PDE isoforms, mainly PDE3A and PDE4B, MRP4 and Epac1-2 in a STZ–induced type 1 diabetes adult rat model. Actually, while increases in PDE4B and PDE4D mRNA expression occurred at week 4, a transient up-regulation was noted in the mRNA expression of PDE1A, PDE2A, PDE3A and PDE5A at week 8 in diabetic rats compared

to their age-matched controls. These changes were reflected in increases in protein expression of both PDE3A and PDE4B in diabetic rats at week 8. However, DCM was not associated with changes in the gene expression of PDE4A regardless of the disease stage. Moreover, Epac1 mRNA expression increased at week 8 in diabetic rats whereas the mRNA expression of Epac 2 and MRP4 was up-regulated at week 12.

We first assessed the influence of diabetes type 1 on the development and progression of the cardiomyopathy, 4, 8 and 12 weeks after diabetes induction in adult rats. Our results showed that sustained hyperglycemia in STZ-injected rats (**Figure 1B**) led to the development and progression of DCM characterized by an increase in the mortality rate (**Figure 1A**) as well as by structural and functional abnormalities. Cardiac steatosis, interstitial fibrosis, myocardial inflammation (**Table S2**), as well as left ventricular hypertrophy, attested by an increase in HW/BW (**Figure 1C)** and ANF expression (**Figure 1D**) are structural hallmarks associated with the diabetic heart. Echocardiographic measurements of diabetic rats showed a significant increase in LV posterior and septal wall thickness as well as LV end systolic and diastolic diameters, when normalized to BW, (**Table 3**), along with a preserved ejection fraction (**Figure 2**), pointing at the development of a concentric CH. The latter has been described as the early clinical manifestation of DCM-associated dysfunctional cardiac remodeling, usually followed by the development of interstitial fibrosis which was identified as a more advanced stage in the disease progression (1). These pathological changes of cardiac fibrosis and hypertrophy have been previously reported to cause LV diastolic stiffness and hence an early emergence of diastolic dysfunction which often evolves to asymptomatic HF with normal EF (45). Therefore, the timeline followed in this study (4, 8 and 12 weeks following diabetes type 1 onset) to assess the progression of DCM lies in the pathophysiological window that precedes the dilation of the left ventricle and the development of

systolic dysfunction accompanied by HF with reduced EF (45, 46). Except for the relative late onset of cardiac fibrosis on the 12th week after STZ injection, cardiac remodeling appeared early on the 4th week and were maintained until week 12. Besides, diabetic rats exhibited a reduced basal HR compared to their age-matched control at all studied time points as already described (47, 48). The decrease in the SV, ESV and EDV were most probably due to the decrease in the HW of diabetic rats (**Table 2**). In addition to cardiac remodeling, STZ-treated rats showed accumulation of foamy macrophages in the alveoli, structural and functional hepatic alterations starting week 4 [increase in ALT level (**Table 1**) and emergence of liver inflammation; (**Table S2** & **Figure S2**)] as well as renal dysfunction attested by an increase in the Cr/BW and urea levels (**Table 1**). Moreover, diabetic rats exhibited dyslipidemia (**Table 1**) with no symptoms of acidosis.

Molecular mechanisms linked to the underlying pathophysiological changes in DCM are still not fully understood. Studies showed a reduction in β_1-AR receptor function as well as defects involving post-receptor proteins (33, 34); however, much remains to be understood as to whether cardiac PDEs expression is affected in DCM. Hence, a molecular characterization of PDE 1-5 isoforms expressed in the heart was undertaken in both CON and STZ-treated rats at 4, 8 and 12 weeks. Consistent with other studies, transcripts of PDE1A, PDE2A, PDE3A, PDE4A, PDE4B, PDE4D and PDE5A were found in adult rat cardiac extracts (49). When compared to their age-matched controls, diabetic rats exhibited a differential and time-specific up-regulation of most PDE isoforms. Interestingly, DCM was associated with an early and exclusive increase in PDE4B and PDE4D mRNA expression at week 4, which was further maintained with the progression of DCM, mainly for PDE4D. Importantly, a transient up-regulation in PDE3A mRNA expression occurred at week 8 in diabetic rats compared to their age-matched controls, knowing that a strong increase, although not significant (p=0.053), was noted in PDE3A mRNA expression at week 4.

However, all other isoforms including PDE1A, PDE2A and PDE5A exhibited a transient increase in their mRNA expression at a later stage and at the same time point, in 8-week diabetic rats. Moreover, there were no apparent changes in the gene expression of PDE4A in diabetic rats compared to controls regardless of the disease stage. Taken together, these findings show a clear independent effect of STZ treatment on the expression of some PDE isoforms when comparing CON and diabetic rats at a specific time point of the disease. However, time did not exhibit any significant, independent change on PDE mRNA expression in the diabetic groups with respect to the progression of DCM. PDE3 and PDE4 are known to be one of the major cAMP-PDE isoforms in the heart (23, 50). Therefore, the next question was to examine whether these alterations were reflected in similar changes in PDE3A and PDE4B protein expression. The two immunoreactive bands detected in rat cardiac extracts most likely represent PDE3A1 (125 kDa) and PDE3A3 isoform (~85kDa) as previously reported (23). A single band migrating at approximately 78 kDa was detected in rat hearts for PDE4B. This isoform was previously detected in neonatal cardiac myocytes (50) and likely represents PDE4B2 short form. In contrast to earlier studies, we could not detect the expression of PDE4B long forms, such as PDE4B1 and PDEB3, which are expected to migrate at approximately 92 kDa (23). Expression of PDE3A-85 kDa protein was similar in both controls and diabetic rats regardless of the disease stage. However, a transient increase in PDE3A-125 kDa protein content appeared in STZ-treated rats at week 8 and could be explained by the upregulation of PDE3A gene expression that was noted at the same time point. Surprisingly, PDE4B protein expression exhibited a significant increase in 8-week-diabetic rats and hence, 4 weeks after the upregulation of its gene expression. Measurement of PDE4D protein expression was targeted in both controls and diabetic rats, however no specific band for PDE4D was detected with the tested antibody. Although the mechanisms were not explored, our results suggest that the

genes encoding for PDE3A and PDE4B are subjected to time-specific and differential regulation of their transcription and translation without excluding the possibility of changes in other PDE families, including PDE 8, 9 and 10 (11) in diabetic rats. Actually, the up-regulation that we report herein with respect to the various cardiac PDE isoforms in general and PDE3A and PDE4B specifically is consistent with an increased PDE3A gene expression resulting in significantly higher PDE3 activity in aortic smooth muscle cell isolated from diabetic rats (38). Some studies showed up-regulation in both PDE3A mRNA and protein levels with no changes in PDE4D in superior mesenteric artery rings isolated from diabetic rats, 12 weeks following STZ injection (35). However, the hydrolytic activities of PDE1, PDE3 and PDE5 were decreased in aortic rings from female diabetic rats, 4 weeks after STZ injection with no changes reported at 2 weeks. Concerning PDE4, a constant activity was reported at 2 and 4 weeks in the same model (37). Moreover, micro-array analysis showed no change in the gene expression of PDE2 in the left ventricle of diabetic rats 6 weeks following STZ injection (31). These different results might be attributed to the fact that PDE genes are expressed in a time and tissue-specific manner. Moreover, these multiple PDEs have been shown to be localized in specific compartments (16-18) so as to exert a local control of intracellular cAMP-signaling microdomains. Therefore, PDE4B was identified in the $Ca_{V1.2}$ complex (51), PDE4D3 with the ryanodine receptors (15) and with IKs potassium channel (52) and PDE4D5 with β-arrestin near the β_2-AR (53) while PDE4D8 has been shown to bind to the β_1-AR (54). In addition, PDE4D was shown to be associated with SERCA2a (55). Besides, some PDE isoforms have been proposed as potential therapeutic targets in DCM. A recent study has demonstrated that inhibition of PDE5A improves cardiac outcomes by enhancing β_2-AR stimulation in a mouse model of DCM (56). Therefore, understanding the exact behavior and regulation of PDE isoforms at the early asymptomatic stages of DCM could be a promising

therapeutic approach for a better management of diabetic patients and eventually for preventing the progression of DCM to HF. Importantly, increases in PDE4D mRNA and protein content have been reported in DCM-associated type 2 diabetes in both humans and mice while no change was noted in the mRNA expression of PDE2A, PDE3A, PDE4A, PDE4B and PDE5A (39). These findings are not in agreement with the increases we report in PDE2A, PDE3A, PDE4A and PDE5A and suggest different mechanisms underlying DCM induced by type 1 and type 2 diabetes.

MRP4, involved in cAMP extrusion, regulates the intracellular levels of this second messenger along with PDEs, although these latter are considered to be the major proteins involved in cAMP hydrolysis and hence homeostasis. Our results showed that DCM was associated with an increase in MRP4 mRNA expression 12 weeks following STZ injection. This upregulation in MRP4 levels occurred somehow at a later stage with respect to the onset of impairments in PDE gene and protein expression during the progression of DCM. This was not in accordance with an earlier increase in MRP4 levels, that was previously reported in diabetic left ventricular extracts from rats 6 weeks following STZ injection (31). Our results have been completed with data on Epac showing an increase in Epac1 mRNA expression in diabetic rats at week 8, and which coincided with the time point at which most of PDE isoforms levels increased. Epac1 upregulation was maintained until week 12 when an increase in Epac2 mRNA expression emerged. Interestingly, alterations in Epac2 mRNA were not reflected in similar changes of the protein expression within the pathophysiological window that was targeted in this study. A single band migrating at approximately 110 kDa was detected in rat hearts for Epac2 and its expression did not change in diabetic rats compared to controls regardless of the disease stage. Measurement of Epac1 protein expression was targeted in both controls and diabetic adult rats, however no specific band for Epac1 has been detected. This could be explained by developmental changes in gene expression

of Epac as some studies reported that Epac2, relative to Epac1, becomes dominant in the adult heart compared with fetal organs (29).

In light of the reported data, we cannot conclude whether abnormalities affecting PDEs, MRP4 and Epac1/2 in diabetes would participate to the well documented β-AR dysfunction (31) or simply represent a consequence. However, we believe that our results bridge a gap in the knowledge with respect to the alterations affecting cardiac PDEs, MRP4 and Epac in a same rat diabetic model. The early transient upregulation of all PDEs, mainly of PDE3A and PDE4B at week 8, might be regarded as a maladaptive process as it would exacerbate the effects of a reduction in cAMP production attributed to a decrease in β_1-AR (31) and AC5/6 (36) content and function. Moreover, the increase in Epac1 mRNA at the same time point might be even more deleterious to the heart since Epac1 has been previously shown to mediate pro-hypertrophic effects of β-AR stimulation (7) through its recruitment to β_1-ARs via β-arrestin2 (57). At week 12, while most PDEs returned to their normal levels, PDE4D and Epac1 remained upregulated and the onset of new increases in Epac2 and MRP4 mRNA levels appeared. Interestingly, Epac2 has been suggested to induce SR Ca^{2+} leak and arrhythmia, an effect that seems to be mediated by β_1-AR pathway (58) while MRP4 was reported to contribute to the pathogenesis of DCM since it decreases the positive inotropic effect upon β_1-AR stimulation (31). These late onset-alterations might participate in the progression of the disease. Concerning PDE4D, up-regulation of its expression was suggested to be a central mechanism contributing to cardiac dysfunction and HF and was mainly attributed to hyperinsulinemia, G-protein receptor kinase 2 (GRK2) and β-arrestin2-dependent transactivation of a β_2-AR-ERK signaling cascade (39). Interestingly, PDE4D5 isoform has been also reported to compete with Epac1 to interact with β-arrestin2 upon β_2-AR activation (57). Hence, the dissociation of PDE4D5 from β-arrestin2 allowed the recruitment of Epac1 to β_2-AR thus inducing

a switch from β_2-AR non-hypertrophic signaling to a β_1-AR-like pro-hypertrophic signaling cascade. These findings suggest the existence of different signaling cascade underlying β_1 and β_2 response.

In light of the novel provided evidence, we conclude that defects affecting the gene and protein expression of various cardiac PDEs, MRP4 and Epac1/2 in diabetes type 1 are subjected to a differential and time-specific regulation. It is more likely that the upregulation of all these proteins as per the progression of DCM is regarded as a maladaptive process that would participate in the loss of local control of intracellular cAMP-signaling microdomains (12) which in turn may lead to more severe pathophysiological impairments and hence progression to heart failure. Hence, a fine characterization of these specific defects becomes crucial for a better understanding of the pathophysiology of DCM, its progression and therefore its treatment through the identification of new therapeutic targets.

Acknowledgments

We thank Mr. Jean Karam and Mr. Elias Abi Ramia for their skillful technical assistance; Drs. Mary Deeb and Elma Nassar for their input to the statistical analysis and Dr. Jihane Soueid for the scientific discussions. We are also grateful to Dr. Chen Yan (Rochester University, NY, USA) and Pr. Marco Conti (University of California San Francisco, CA, USA) for providing us with the antibodies for PDE3A and PDE4B, respectively.

Funding

This study was jointly funded with the support of the National Council for Scientific Research (CNRS-L) in Lebanon and the Lebanese American University, CNRS-L/LAU **N° 858** to AAG. This work was also supported by a joint fellowship from the French and Lebanese governments, PHC CEDRE **N° 42338SA** to A.A.G and G.V.

References

1. Borghetti G, von Lewinski D, Eaton DM, Sourij H, Houser SR, Wallner M. Diabetic Cardiomyopathy: Current and Future Therapies. Beyond Glycemic Control. Frontiers in physiology. 2018;9:1514. PubMed PMID: 30425649. Pubmed Central PMCID: 6218509.
2. Kannel WB, Hjortland M, Castelli WP. Role of diabetes in congestive heart failure: the Framingham study. The American journal of cardiology. 1974 Jul;34(1):29-34. PubMed PMID: 4835750.
3. Davidoff AJ, Davidson MB, Carmody MW, Davis ME, Ren J. Diabetic cardiomyocyte dysfunction and myocyte insulin resistance: role of glucose-induced PKC activity. Molecular and cellular biochemistry. 2004 Jul;262(1-2):155-63. PubMed PMID: 15532720.
4. Dillmann WH. Diabetic Cardiomyopathy. Circulation research. 2019 Apr 12;124(8):1160-2. PubMed PMID: 30973809. Pubmed Central PMCID: 6578576.
5. Miki T, Yuda S, Kouzu H, Miura T. Diabetic cardiomyopathy: pathophysiology and clinical features. Heart Fail Rev. 2013 Mar;18(2):149-66. PubMed PMID: 22453289. Pubmed Central PMCID: PMC3593009. Epub 2012/03/29. eng.
6. Lohse MJ, Engelhardt S, Eschenhagen T. What is the role of beta-adrenergic signaling in heart failure? Circulation research. 2003 Nov 14;93(10):896-906. PubMed PMID: 14615493. Epub 2003/11/15. eng.
7. Lezoualc'h F, Fazal L, Laudette M, Conte C. Cyclic AMP Sensor EPAC Proteins and Their Role in Cardiovascular Function and Disease. Circulation research. 2016 Mar 4;118(5):881-97. PubMed PMID: 26941424.
8. Guellich A, Mehel H, Fischmeister R. Cyclic AMP synthesis and hydrolysis in the normal and failing heart. Pflugers Arch. 2014 Jun;466(6):1163-75. PubMed PMID: 24756197. Epub 2014/04/24. eng.
9. Sassi Y, Abi-Gerges A, Fauconnier J, Mougenot N, Reiken S, Haghighi K, et al. Regulation of cAMP homeostasis by the efflux protein MRP4 in cardiac myocytes. Faseb j. 2012 Mar;26(3):1009-17. PubMed PMID: 22090316. Pubmed Central PMCID: PMC3289499. Epub 2011/11/18. eng.

10. Bobin P, Belacel-Ouari M, Bedioune I, Zhang L, Leroy J, Leblais V, et al. Cyclic nucleotide phosphodiesterases in heart and vessels: A therapeutic perspective. Arch Cardiovasc Dis. 2016 Jun-Jul;109(6-7):431-43. PubMed PMID: 27184830. Epub 2016/05/18. eng.

11. Chen S, Zhang Y, Lighthouse JK, Mickelsen DM, Wu J, Yao P, et al. A Novel Role of Cyclic Nucleotide Phosphodiesterase 10A in Pathological Cardiac Remodeling and Dysfunction. Circulation. 2020 Jan 21;141(3):217-33. PubMed PMID: 31801360.

12. Fischmeister R, Castro LR, Abi-Gerges A, Rochais F, Jurevicius J, Leroy J, et al. Compartmentation of cyclic nucleotide signaling in the heart: the role of cyclic nucleotide phosphodiesterases. Circulation research. 2006 Oct 13;99(8):816-28. PubMed PMID: 17038651. Epub 2006/10/14. eng.

13. Shakur Y, Holst LS, Landstrom TR, Movsesian M, Degerman E, Manganiello V. Regulation and function of the cyclic nucleotide phosphodiesterase (PDE3) gene family. Prog Nucleic Acid Res Mol Biol. 2001;66:241-77. PubMed PMID: 11051766. Epub 2000/10/29. eng.

14. Kostic MM, Erdogan S, Rena G, Borchert G, Hoch B, Bartel S, et al. Altered Expression of PDE1 and PDE4 Cyclic Nucleotide Phosphodiesterase Isoforms in 7-oxo-prostacyclin-preconditioned Rat Heart. Journal of molecular and cellular cardiology. 1997 1997/11/01/;29(11):3135-46.

15. Lehnart SE, Wehrens XH, Reiken S, Warrier S, Belevych AE, Harvey RD, et al. Phosphodiesterase 4D deficiency in the ryanodine-receptor complex promotes heart failure and arrhythmias. Cell. 2005 Oct 7;123(1):25-35. PubMed PMID: 16213210. Pubmed Central PMCID: PMC2901878. Epub 2005/10/11. eng.

16. Kim GE, Kass DA. Cardiac Phosphodiesterases and Their Modulation for Treating Heart Disease. Handb Exp Pharmacol. 2017;243:249-69. PubMed PMID: 27787716. Pubmed Central PMCID: PMC5665023. Epub 2016/10/28. eng.

17. Lugnier C. Cyclic nucleotide phosphodiesterase (PDE) superfamily: a new target for the development of specific therapeutic agents. Pharmacol Ther. 2006 Mar;109(3):366-98. PubMed PMID: 16102838. Epub 2005/08/17. eng.

18. Patrucco E, Albergine MS, Santana LF, Beavo JA. Phosphodiesterase 8A (PDE8A) regulates excitation-contraction coupling in ventricular myocytes. Journal of molecular and cellular cardiology. 2010 Aug;49(2):330-3. PubMed PMID: 20353794. Pubmed Central PMCID: PMC2885478. Epub 2010/04/01. eng.

19. Jurevicius J, Fischmeister R. cAMP compartmentation is responsible for a local activation of cardiac Ca2+ channels by beta-adrenergic agonists. Proc Natl Acad Sci U S A. 1996 Jan 9;93(1):295-9. PubMed PMID: 8552625. Pubmed Central PMCID: PMC40225. Epub 1996/01/09. eng.

20. Rochais F, Abi-Gerges A, Horner K, Lefebvre F, Cooper DM, Conti M, et al. A specific pattern of phosphodiesterases controls the cAMP signals generated by different Gs-coupled receptors in adult rat ventricular myocytes. Circulation research. 2006 Apr 28;98(8):1081-8. PubMed PMID: 16556871. Pubmed Central PMCID: PMC2099453. Epub 2006/03/25. eng.

21. Chevalier B, Mansier P, Amrani FC-E, Swynghedauw B. β-Adrenergic System Is Modified in Compensatory Pressure Cardiac Overload in Rats: Physiological and Biochemical Evidence. Journal of Cardiovascular Pharmacology. 1989;13(3):412-20. PubMed PMID: 00005344-198903000-00009.

22. Holmer SR, Bruckschlegel G, Schunkert H, Rataj DB, Kromer EP, Riegger GA. Functional activity and expression of the myocardial postreceptor adenylyl cyclase system in pressure overload hypertrophy in rat. Cardiovasc Res. 1996 May;31(5):719-28. PubMed PMID: 8763401. Epub 1996/05/01. eng.

23. Abi-Gerges A, Richter W, Lefebvre F, Mateo P, Varin A, Heymes C, et al. Decreased expression and activity of cAMP phosphodiesterases in cardiac hypertrophy and its impact on beta-adrenergic cAMP signals. Circulation research. 2009 Oct 9;105(8):784-92. PubMed PMID: 19745166. Pubmed Central PMCID: PMC2792993. Epub 2009/09/12. eng.

24. Ding B, Abe JI, Wei H, Huang Q, Walsh RA, Molina CA, et al. Functional role of phosphodiesterase 3 in cardiomyocyte apoptosis: implication in heart failure. Circulation. 2005 May 17;111(19):2469-76. PubMed PMID: 15867171. Pubmed Central PMCID: PMC4108189. Epub 2005/05/04. eng.

25. Movsesian MA, Smith CJ, Krall J, Bristow MR, Manganiello VC. Sarcoplasmic reticulum-associated cyclic adenosine 5'-monophosphate phosphodiesterase activity in normal and failing human hearts. J Clin Invest. 1991 Jul;88(1):15-9. PubMed PMID: 1647414. Pubmed Central PMCID: PMC295996. Epub 1991/07/01. eng.

26. Senzaki H, Smith CJ, Juang GJ, Isoda T, Mayer SP, Ohler A, et al. Cardiac phosphodiesterase 5 (cGMP-specific) modulates beta-adrenergic signaling in vivo and is down-

regulated in heart failure. Faseb j. 2001 Aug;15(10):1718-26. PubMed PMID: 11481219. Epub 2001/08/02. eng.

27. Smith CJ, Huang R, Sun D, Ricketts S, Hoegler C, Ding JZ, et al. Development of decompensated dilated cardiomyopathy is associated with decreased gene expression and activity of the milrinone-sensitive cAMP phosphodiesterase PDE3A. Circulation. 1997 Nov 4;96(9):3116-23. PubMed PMID: 9386183. Epub 1997/12/31. eng.

28. Yanaka N, Kurosawa Y, Minami K, Kawai E, Omori K. cGMP-phosphodiesterase activity is up-regulated in response to pressure overload of rat ventricles. Biosci Biotechnol Biochem. 2003 May;67(5):973-9. PubMed PMID: 12834273. Epub 2003/07/02. eng.

29. Ulucan C, Wang X, Baljinnyam E, Bai Y, Okumura S, Sato M, et al. Developmental changes in gene expression of Epac and its upregulation in myocardial hypertrophy. American journal of physiology Heart and circulatory physiology. 2007 Sep;293(3):H1662-72. PubMed PMID: 17557924. Epub 2007/06/15. eng.

30. Métrich M, Lucas A, Gastineau M, Samuel JL, Heymes C, Morel E, et al. Epac mediates beta-adrenergic receptor-induced cardiomyocyte hypertrophy. Circulation research. 2008 Apr 25;102(8):959-65. PubMed PMID: 18323524. Epub 2008/03/08. eng.

31. Carillion A, Feldman S, Na N, Biais M, Carpentier W, Birenbaum A, et al. Atorvastatin reduces β-Adrenergic dysfunction in rats with diabetic cardiomyopathy. PLOS ONE. 2017;12(7):e0180103.

32. Roth DA, White CD, Hamilton CD, Hall JL, Stanley WC. Adrenergic desensitization in left ventricle from streptozotocin diabetic swine. Journal of molecular and cellular cardiology. 1995 Oct;27(10):2315-25. PubMed PMID: 8576946.

33. Bockus LB, Humphries KM. cAMP-dependent Protein Kinase (PKA) Signaling Is Impaired in the Diabetic Heart. J Biol Chem. 2015 Dec 4;290(49):29250-8. PubMed PMID: 26468277. Pubmed Central PMCID: PMC4705931. Epub 2015/10/16. eng.

34. Matsumoto T, Wakabayashi K, Kobayashi T, Kamata K. Diabetes-related changes in cAMP-dependent protein kinase activity and decrease in relaxation response in rat mesenteric artery. American journal of physiology Heart and circulatory physiology. 2004 Sep;287(3):H1064-71. PubMed PMID: 15130892. Epub 2004/05/08. eng.

35. Matsumoto T, Kobayashi T, Kamata K. Alterations in EDHF-type relaxation and phosphodiesterase activity in mesenteric arteries from diabetic rats. American journal of

physiology Heart and circulatory physiology. 2003 Jul;285(1):H283-91. PubMed PMID: 12793980.

36. Matsumoto T, Wakabayashi K, Kobayashi T, Kamata K. Functional changes in adenylyl cyclases and associated decreases in relaxation responses in mesenteric arteries from diabetic rats. American journal of physiology Heart and circulatory physiology. 2005 Nov;289(5):H2234-43. PubMed PMID: 15894571. Epub 2005/05/17. eng.

37. Abboud K, Bassila JC, Ghali-Ghoul R, Sabra R. Temporal changes in vascular reactivity in early diabetes mellitus in rats: role of changes in endothelial factors and in phosphodiesterase activity. American journal of physiology Heart and circulatory physiology. 2009 Aug;297(2):H836-45. PubMed PMID: 19542492. Epub 2009/06/23. eng.

38. Nagaoka T, Shirakawa T, Balon TW, Russell JC, Fujita-Yamaguchi Y. Cyclic nucleotide phosphodiesterase 3 expression in vivo: evidence for tissue-specific expression of phosphodiesterase 3A or 3B mRNA and activity in the aorta and adipose tissue of atherosclerosis-prone insulin-resistant rats. Diabetes. 1998;47(7):1135-44.

39. Wang Q, Liu Y, Fu Q, Xu B, Zhang Y, Kim S, et al. Inhibiting Insulin-Mediated beta2-Adrenergic Receptor Activation Prevents Diabetes-Associated Cardiac Dysfunction. Circulation. 2017 Jan 3;135(1):73-88. PubMed PMID: 27815373. Pubmed Central PMCID: 5302024.

40. Nasrallah P, Haidar EA, Stephan JS, El Hayek L, Karnib N, Khalifeh M, et al. Branched-chain amino acids mediate resilience to chronic social defeat stress by activating BDNF/TRKB signaling. Neurobiol Stress. 2019 Nov;11:100170. PubMed PMID: 31193350. Pubmed Central PMCID: PMC6526306. Epub 2019/06/14. eng.

41. Mahfoz AM, El-Latif HA, Ahmed LA, Hassanein NM, Shoka AA. Anti-diabetic and renoprotective effects of aliskiren in streptozotocin-induced diabetic nephropathy in female rats. Naunyn Schmiedebergs Arch Pharmacol. 2016 Dec;389(12):1315-24. PubMed PMID: 27612855. Epub 2016/09/11. eng.

42. Hajje G, Saliba Y, Itani T, Moubarak M, Aftimos G, Farès N. Hypothyroidism and its rapid correction alter cardiac remodeling. PLoS One. 2014;9(10):e109753. PubMed PMID: 25333636. Pubmed Central PMCID: PMC4198123. Epub 2014/10/22. eng.

43. Zeeni N, Dagher-Hamalian C, Dimassi H, Faour WH. Cafeteria diet-fed mice is a pertinent model of obesity-induced organ damage: a potential role of inflammation. Inflamm Res. 2015 Jul;64(7):501-12. PubMed PMID: 25966976. Epub 2015/05/15. eng.

44. Leroy J, Abi-Gerges A, Nikolaev VO, Richter W, Lechêne P, Mazet J-L, et al. Spatiotemporal Dynamics of β-Adrenergic cAMP Signals and L-Type Ca²⁺ Channel Regulation in Adult Rat Ventricular Myocytes. Circulation research. 2008;102(9):1091-100.

45. Jia G, Hill MA, Sowers JR. Diabetic Cardiomyopathy: An Update of Mechanisms Contributing to This Clinical Entity. Circulation research. 2018 Feb 16;122(4):624-38. PubMed PMID: 29449364. Pubmed Central PMCID: PMC5819359. Epub 2018/02/17. eng.

46. Maffei A, Cifelli G, Carnevale R, Iacobucci R, Pallante F, Fardella V, et al. PI3Kγ Inhibition Protects Against Diabetic Cardiomyopathy in Mice. Rev Esp Cardiol (Engl Ed). 2017 Jan;70(1):16-24. PubMed PMID: 27422446. Epub 2016/07/17. eng

spa.

47. Borges GR, de Oliveira M, Salgado HC, Fazan R, Jr. Myocardial performance in conscious streptozotocin diabetic rats. Cardiovasc Diabetol. 2006 Dec 4;5:26. PubMed PMID: 17144912. Pubmed Central PMCID: PMC1698470. Epub 2006/12/06. eng.

48. Hoit BD, Castro C, Bultron G, Knight S, Matlib MA. Noninvasive evaluation of cardiac dysfunction by echocardiography in streptozotocin-induced diabetic rats. J Card Fail. 1999 Dec;5(4):324-33. PubMed PMID: 10634674. Epub 2000/01/14. eng.

49. Mokni W, Keravis T, Etienne-Selloum N, Walter A, Kane MO, Schini-Kerth VB, et al. Concerted regulation of cGMP and cAMP phosphodiesterases in early cardiac hypertrophy induced by angiotensin II. PLoS One. 2010 Dec 3;5(12):e14227. PubMed PMID: 21151982. Pubmed Central PMCID: PMC2997062. Epub 2010/12/15. eng.

50. Mongillo M, McSorley T, Evellin S, Sood A, Lissandron V, Terrin A, et al. Fluorescence resonance energy transfer-based analysis of cAMP dynamics in live neonatal rat cardiac myocytes reveals distinct functions of compartmentalized phosphodiesterases. Circulation research. 2004 Jul 9;95(1):67-75. PubMed PMID: 15178638. Epub 2004/06/05. eng.

51. Leroy J, Richter W, Mika D, Castro LRV, Abi-Gerges A, Xie M, et al. Phosphodiesterase 4B in the cardiac L-type Ca2+ channel complex regulates Ca2+ current and protects against ventricular arrhythmias in mice. The Journal of Clinical Investigation. 2011 07/01/;121(7):2651-61.

52. Terrenoire C, Houslay MD, Baillie GS, Kass RS. The Cardiac IKs Potassium Channel Macromolecular Complex Includes the Phosphodiesterase PDE4D3. Journal of Biological Chemistry. 2009 April 3, 2009;284(14):9140-6.

53. Perry SJ, Baillie GS, Kohout TA, McPhee I, Magiera MM, Ang KL, et al. Targeting of cyclic AMP degradation to beta 2-adrenergic receptors by beta-arrestins. Science. 2002 Oct 25;298(5594):834-6. PubMed PMID: 12399592. Epub 2002/10/26. eng.

54. Richter W, Day P, Agrawal R, Bruss MD, Granier S, Wang YL, et al. Signaling from beta1- and beta2-adrenergic receptors is defined by differential interactions with PDE4. Embo j. 2008 Jan 23;27(2):384-93. PubMed PMID: 18188154. Pubmed Central PMCID: PMC2196435. Epub 2008/01/12. eng.

55. Kerfant BG, Zhao D, Lorenzen-Schmidt I, Wilson LS, Cai S, Chen SR, et al. PI3Kgamma is required for PDE4, not PDE3, activity in subcellular microdomains containing the sarcoplasmic reticular calcium ATPase in cardiomyocytes. Circulation research. 2007 Aug 17;101(4):400-8. PubMed PMID: 17615371. Epub 2007/07/07. eng.

56. West TM, Wang Q, Deng B, Zhang Y, Barbagallo F, Reddy GR, et al. Phosphodiesterase 5 Associates With β2 Adrenergic Receptor to Modulate Cardiac Function in Type 2 Diabetic Hearts. J Am Heart Assoc. 2019 Aug 6;8(15):e012273. PubMed PMID: 31311394. Pubmed Central PMCID: PMC6761630. Epub 2019/07/18. eng.

57. Berthouze-Duquesnes M, Lucas A, Sauliere A, Sin YY, Laurent AC, Gales C, et al. Specific interactions between Epac1, beta-arrestin2 and PDE4D5 regulate beta-adrenergic receptor subtype differential effects on cardiac hypertrophic signaling. Cellular signalling. 2013 Apr;25(4):970-80. PubMed PMID: 23266473.

58. Pereira L, Cheng H, Lao DH, Na L, van Oort RJ, Brown JH, et al. Epac2 mediates cardiac β1-adrenergic-dependent sarcoplasmic reticulum Ca2+ leak and arrhythmia. Circulation. 2013 Feb 26;127(8):913-22. PubMed PMID: 23363625. Pubmed Central PMCID: PMC3690126. Epub 2013/02/01. eng.

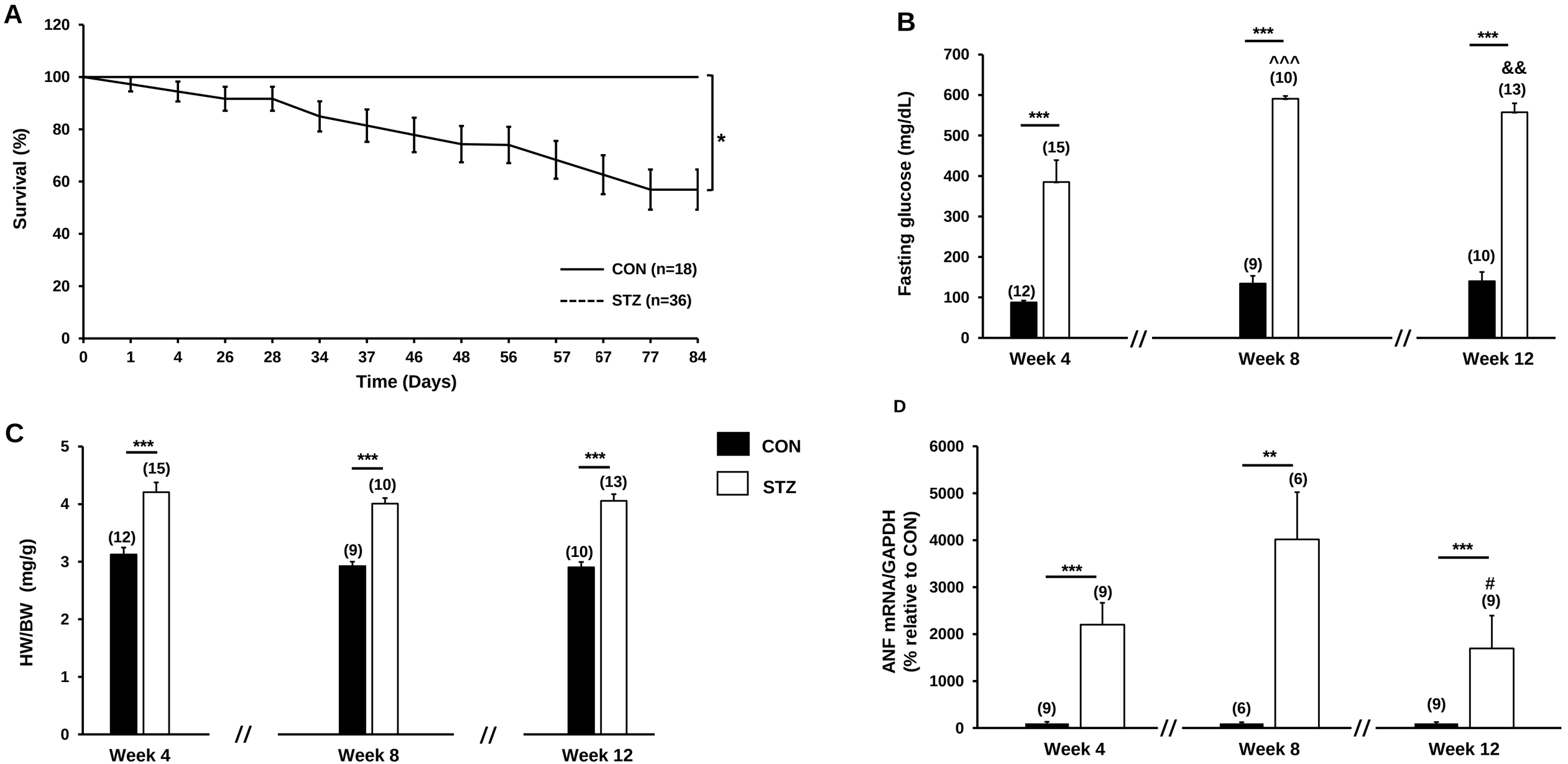
A
Survival (%)
120
100
80
60
40
20
0
0 1 4 26 28 34 37 46 48 56 57 67 77 84
Time (Days)
*
CON (n=18)
STZ (n=36)
B
Fasting glucose (mg/dL)
700
600
500
400
300
200
100
0
***
(15)
(12)
***
^^^
(10)
(9)
***
&&
(13)
(10)
Week 4
Week 8
Week 12
C
HW/BW (mg/g)
5
4
3
2
1
0
***
(15)
(12)
***
(10)
(9)
***
(13)
(10)
CON
STZ
Week 4
Week 8
Week 12
D
ANF mRNA/GAPDH
(% relative to CON)
6000
5000
4000
3000
2000
1000
0
***
(9)
(9)
**
(6)
(6)
***
#
(9)
(9)
Week 4
Week 8
Week 12

Figure 1

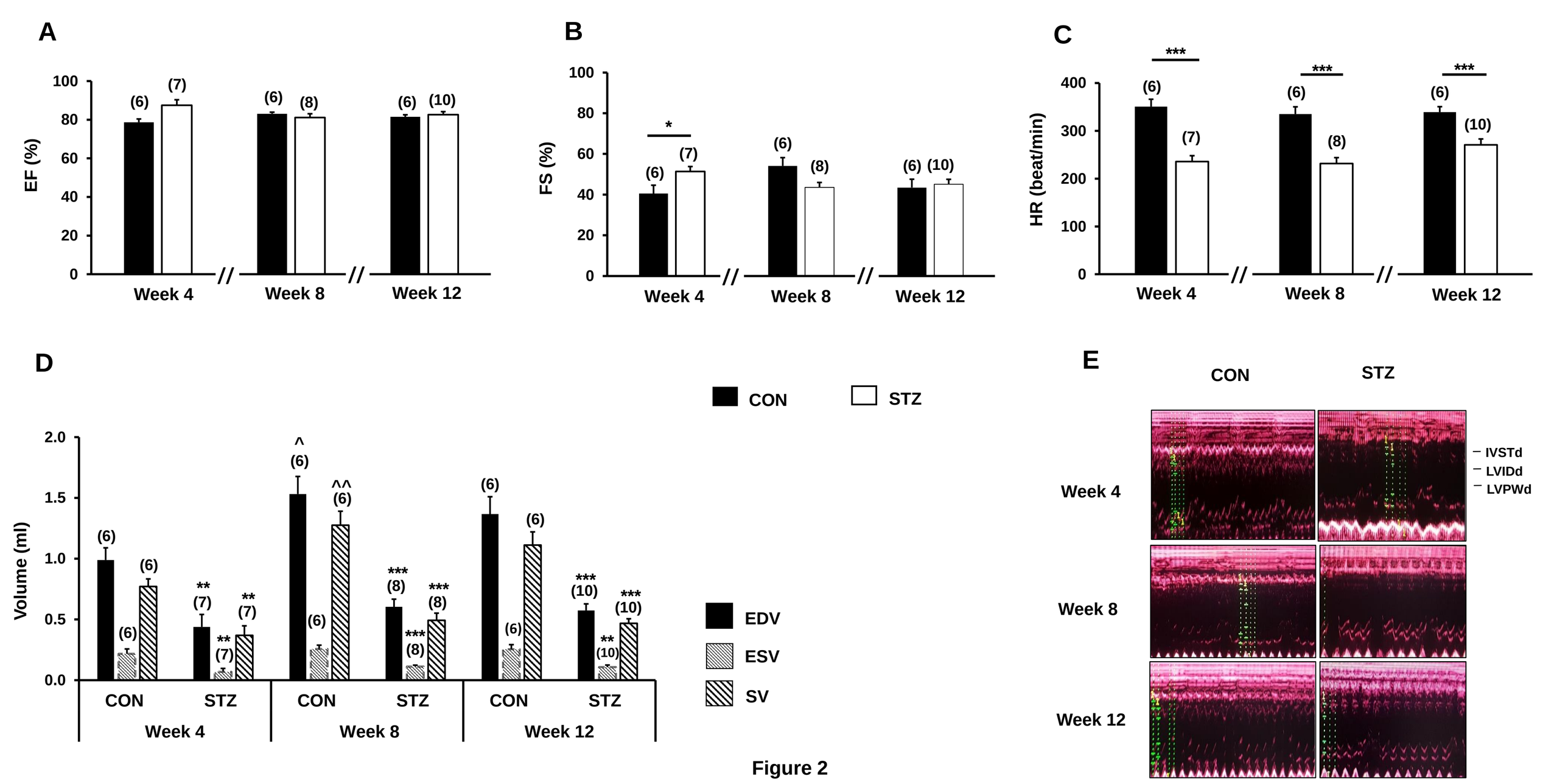
A
EF (%)
100
80
60
40
20
0
(6)
(7)
(6)
(8)
(6)
(10)
Week 4
Week 8
Week 12
B
FS (%)
100
80
60
40
20
0
*
(6)
(7)
(6)
(8)
(6)
(10)
Week 4
Week 8
Week 12
C
HR (beat/min)
400
300
200
100
0
***
***
***
(6)
(7)
(6)
(8)
(6)
(10)
Week 4
Week 8
Week 12
D
Volume (ml)
2.0
1.5
1.0
0.5
0.0
CON
STZ
EDV
ESV
SV
(6)
(6)
(6)
**
(7)
**
(7)
**
(7)
^
(6)
(6)
^^
(6)
***
(8)
***
(8)
***
(8)
(6)
(6)
(6)
***
(10)
**
(10)
***
(10)
CON
STZ
CON
STZ
CON
STZ
Week 4
Week 8
Week 12
E
CON
STZ
IVSTd
LVIDd
LVPWd
Week 4
Week 8
Week 12

Figure 2

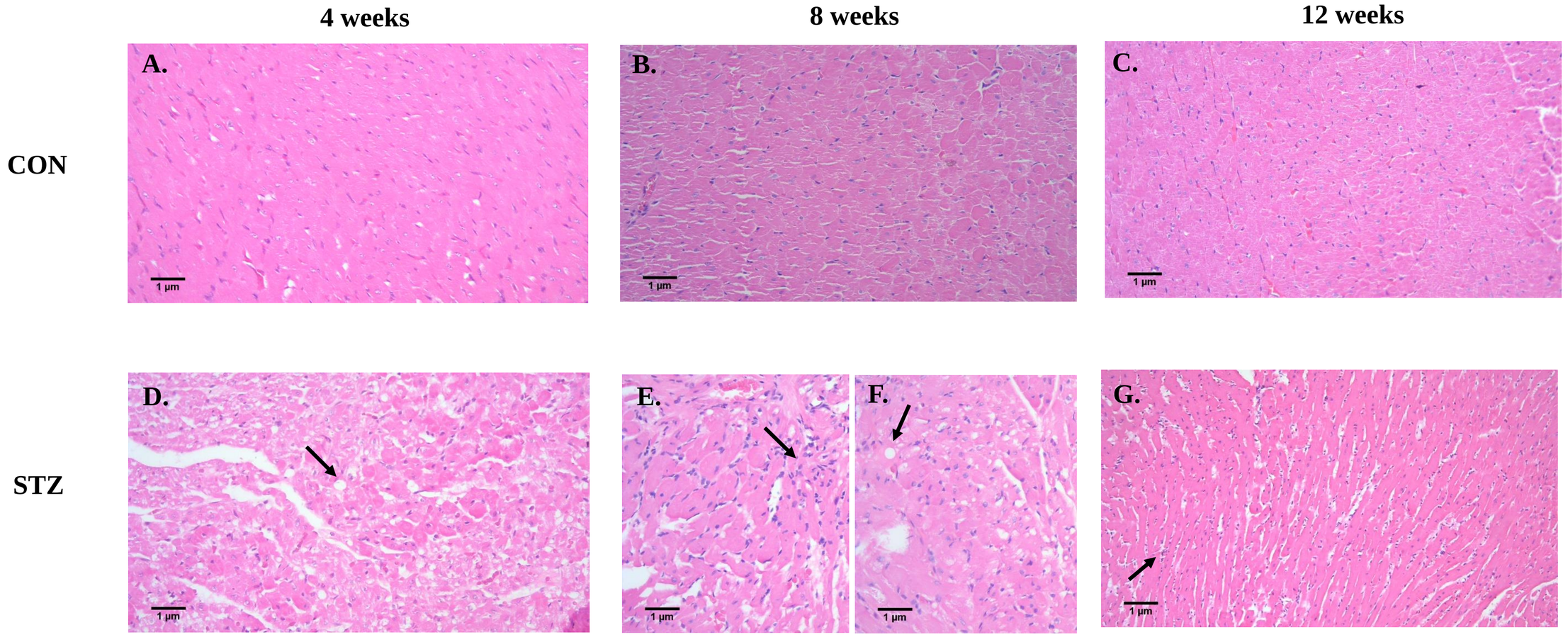

Figure 3

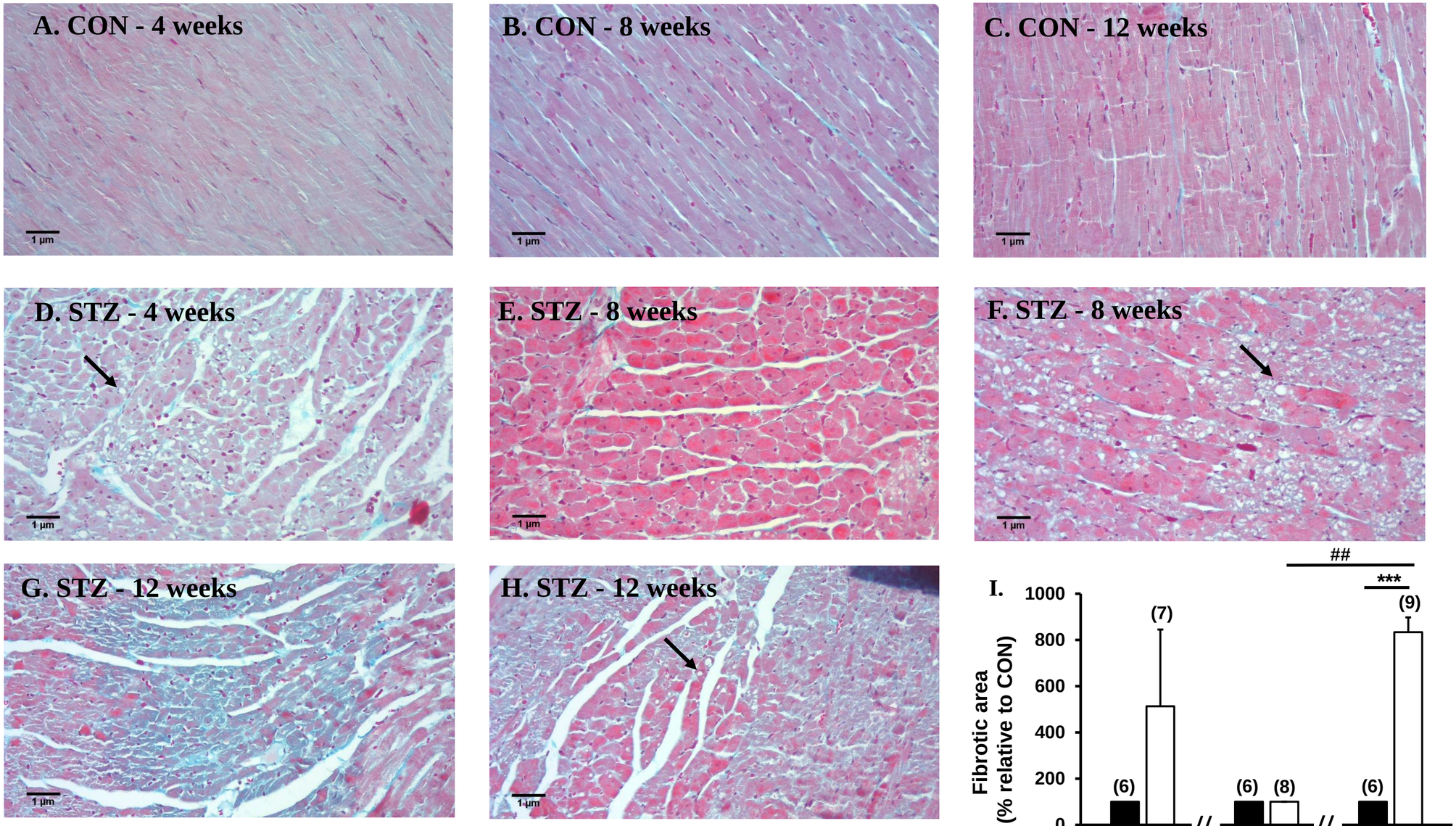
A. CON - 4 weeks
B. CON - 8 weeks
C. CON - 12 weeks
D. STZ - 4 weeks
E. STZ - 8 weeks
F. STZ - 8 weeks
G. STZ - 12 weeks
H. STZ - 12 weeks
1 µm
I.
Fibrotic area (% relative to CON)
1000
800
600
400
200
0
(6)
(7)
(6)
(8)
(6)
(9)
##
***
Week 4
Week 8
Week 12
CON
STZ

Figure 4

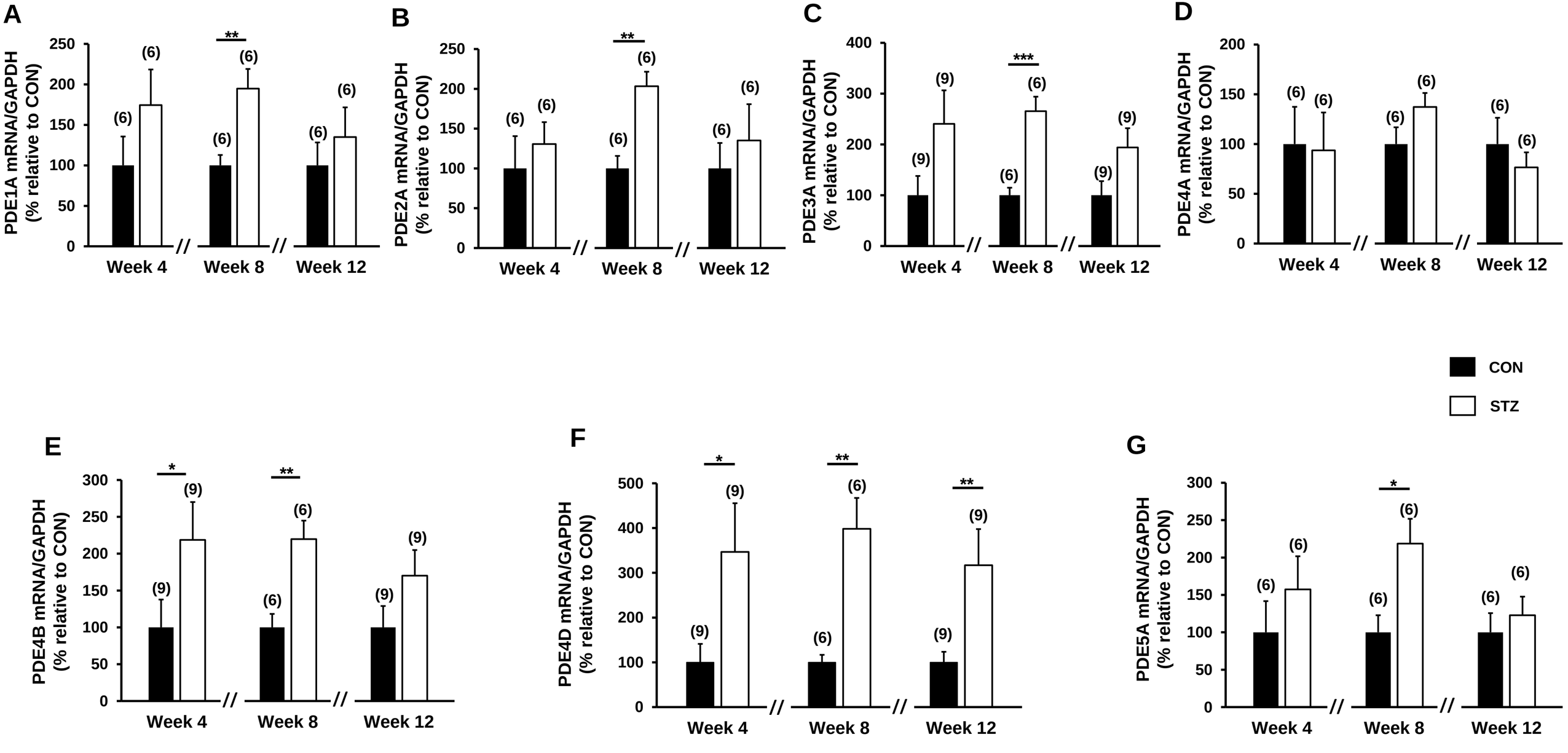
A
PDE1A mRNA/GAPDH
(% relative to CON)
B
PDE2A mRNA/GAPDH
(% relative to CON)
C
PDE3A mRNA/GAPDH
(% relative to CON)
D
PDE4A mRNA/GAPDH
(% relative to CON)
E
PDE4B mRNA/GAPDH
(% relative to CON)
F
PDE4D mRNA/GAPDH
(% relative to CON)
G
PDE5A mRNA/GAPDH
(% relative to CON)
Week 4
Week 8
Week 12
CON
STZ

Figure 5

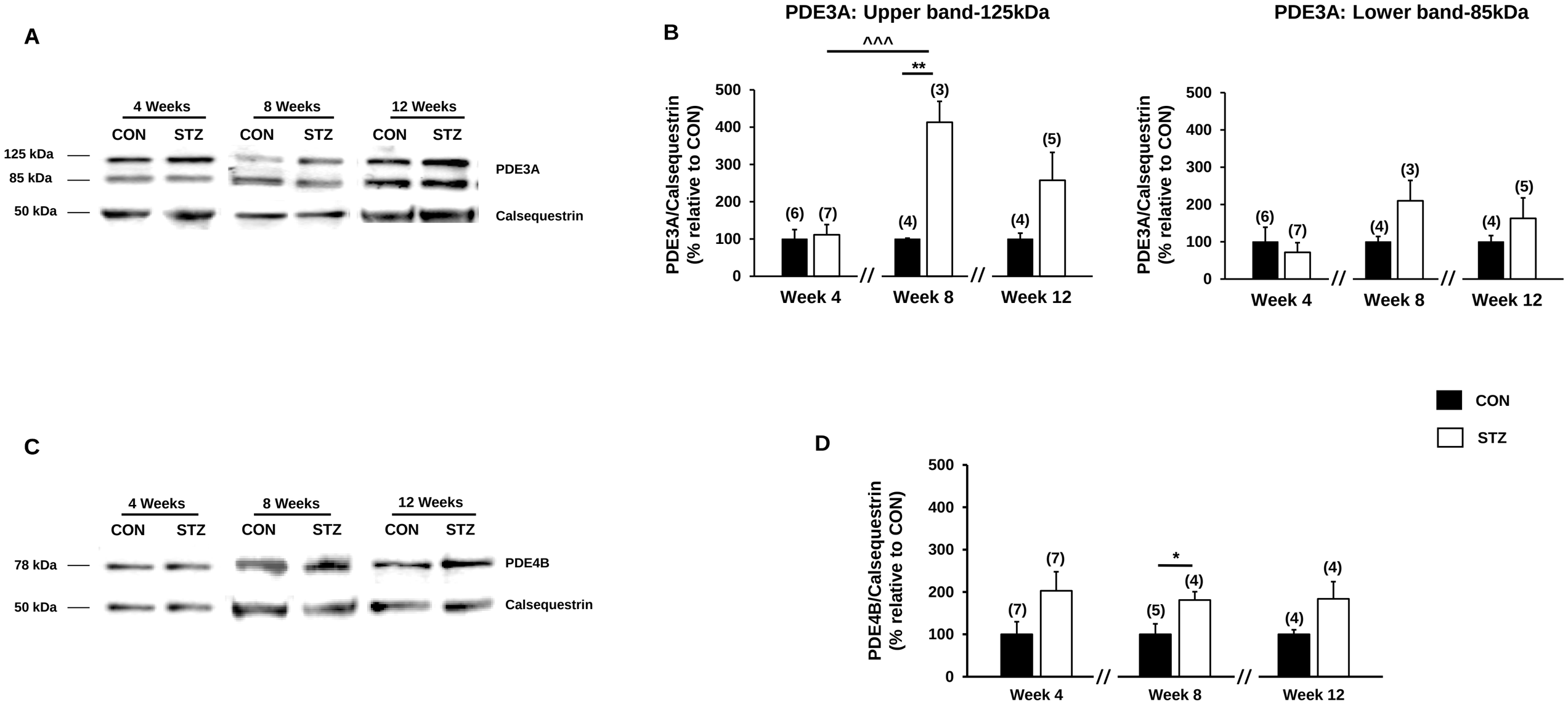
A
4 Weeks
8 Weeks
12 Weeks
CON
STZ
CON
STZ
CON
STZ
125 kDa
85 kDa
50 kDa
PDE3A
Calsequestrin
B
PDE3A: Upper band-125kDa
PDE3A: Lower band-85kDa
^^^
**
PDE3A/Calsequestrin
(% relative to CON)
500
400
300
200
100
0
(6)
(7)
(4)
(3)
(4)
(5)
Week 4
Week 8
Week 12
C
4 Weeks
8 Weeks
12 Weeks
CON
STZ
CON
STZ
CON
STZ
78 kDa
50 kDa
PDE4B
Calsequestrin
D
CON
STZ
PDE4B/Calsequestrin
(% relative to CON)
*
(7)
(7)
(5)
(4)
(4)
(4)
Week 4
Week 8
Week 12

Figure 6

	Week 4				Week 8				Week 12			
	CON	**n**	**STZ**	**n**	**CON**	**n**	**STZ**	**n**	**CON**	**n**	**STZ**	**n**
ALT (U/L)	49 ± 5	4	315 ± 99*	4	44 ± 4	4	146 ± 27*	4	42 ± 1	4	94 ± 14$^{*;\ \&}$	4
Cholesterol (mg/dl)	74 ± 7	4	70 ± 2	4	69 ± 5	4	97 ± 7*	4	67 ± 2	4	95 ± 13	4
HDL (mg/dl)	57 ± 4	6	49 ± 3	6	51 ± 3	6	67 ± 4**	6	55 ± 3	6	65 ± 9	6
Triglyceride (mg/dl)	149 ± 19	6	216 ± 37	6	121± 21	6	331 ± 52**	6	78 ± 17	6	225 ± 45*	6
CO_2 (mmol/L)	30.4 ± 0.4	4	27.8 ± 1.7	4	31.9 ± 0.7	4	27.9 ± 2.7	4	29 ± 1	4	29.4 ± 0.6	4
Cr (mg/dl)	0.190 ± 0.003	4	0.13 ± 0.01*	4	0.26 ± 0.02$^{\wedge}$	4	0.17 ± 0.01**	4	0.22 ± 0.01	4	0.15 ± 0.01**	4
Cr/BW ($\mu g.dl^{-1}.gr^{-1}$)	0.67 ± 0.03	4	1.3 ± 0.2*	4	0.7 ± 0.1	4	1.2 ± 0.1**	4	0.6 ± 0.1	4	1.05 ± 0.08*	4
Urea (mg/dl)	32 ± 3	4	53 ± 10	4	36 ± 3	4	57 ± 6*	4	32 ± 1	4	62 ± 4*	4

Table 1. Blood tests of control (CON) and diabetic (STZ) rats at 4, 8 and 12 weeks after injection of either streptozotocin or vehicle. All data are expressed as mean ± S.E.M. Abbreviations: ALT**,** alanine aminotransferase; HDL, high density lipoproteins; Cr, creatinine; BW, body weight. Statistically significant differences between CON and STZ rats of the same age are indicated as *, $p<0.05$; **, $p<0.01$. Statistically significant differences between CON-4 weeks and CON-8 weeks are indicated as $^{\wedge}$, $p<0.05$. Statistically significant differences between STZ-4 weeks and STZ-12 weeks are indicated as $^{\&}$, $p<0.05$

	Week 4		Week 8		Week 12	
	CON (n=12)	**STZ (n=15)**	**CON (n=9)**	**STZ (n=10)**	**CON (n=10)**	**STZ (n=13)**
BW (g)	281 ± 6	98 ± 8***	363 ± 12$^{\wedge\wedge\wedge}$	130 ± 7***	359 ± 17$^{\&\&\&}$	144 ± 9$^{***;\ \&\&}$
HW (g)	0.88 ± 0.04	0.41 ± 0.03***	1.06 ± 0.05$^{\wedge}$	0.52 ± 0.03***	1.04 ± 0.05$^{\&}$	0.58 ± 0.03$^{***;\ \&\&}$
HW/BW (mg/g)	3.1 ± 0.1	4.2 ± 0.2***	2.9 ± 0.1	4.0 ± 0.1***	2.9 ± 0.1	4.1 ± 0.1***
Lungs (g)	1.5 ± 0.1	0.73 ± 0.04***	1.6 ± 0.1	0.94 ± 0.05***	1.7 ± 0.1	1.01 ± 0.06$^{***;\ \&}$
Lungs/BW (mg/g)	5.3 ± 0.2	7.8 ± 0.4***	4.3 ± 0.2	7.4 ± 0.5***	4.9 ± 0.3	7.1 ± 0.3***
Kidneys (g)	1.97 ± 0.06	1.29 ± 0.10***	2.5 ± 0.1$^{\wedge}$	1.5 ± 0.2***	2.3 ± 0.1	1.9 ± 0.1$^{**;\ \&\&}$
Kidney/BW (mg/g)	7.0 ± 0.1	13.3 ± 0.4***	6.9 ± 0.2	12 ± 1**	6.5 ± 0.2	13.1 ± 0.4***
Liver (g)	10.5 ± 0.6	4.7 ± 0.3***	12.1 ± 0.7	6.9 ± 0.4$^{***;\ \wedge}$	11.7 ± 0.5	7.5 ± 0.4$^{***;\ \&\&\&}$
Liver/BW (mg/g)	37 ± 2	48 ± 2**	33 ± 1	53 ± 2***	33 ± 1	52 ± 1***

Table 2. Anatomical data of control (CON) diabetic (STZ) rats at 4, 8 and 12 weeks after injection of either streptozotocin or vehicle. All data are expressed as mean ± S.E.M. Abbreviations: BW**,** body weight; HW, heart weight. Statistically significant differences between CON and STZ rats of the same age are indicated as **, p<0.01; ***, p<0.001. Statistically significant differences between CON-4 weeks and CON-8 weeks or between STZ-4 weeks and STZ-8 weeks are indicated as $^{\wedge}$, p<0.05; $^{\wedge\wedge\wedge}$, p<0.001. Statistically significant differences between CON-4 weeks and CON-12 weeks or between STZ-4 weeks and STZ-12 weeks are indicated as $^{\&}$, p<0.05; $^{\&\&}$, p<0.01; $^{\&\&\&}$, p<0.001.

	Week 4		Week 8		Week 12	
	Control (n=6)	**STZ (n=7)**	**Control (n=6)**	**STZ (n=8)**	**Control (n=6)**	**STZ (n=10)**
IVSTd (μm)	1156 ± 0.42	1107 ± 72	1565 ± 62$^{\wedge\wedge\wedge}$	1149 ± 47***	1524 ± 53$^{\&\&}$	988 ± 53***
IVSTd/BW (μm/g)	4.1 ± 0.2	13 ± 1***	4.2 ± 0.2	9.5 ± 0.8$^{***;\ \wedge}$	4.3 ± 0.3	7.2 ± 0.3$^{***;\ \&\&\&}$
LVIDd (μm)	9906 ± 329	7185 ± 647**	11461 ± 347	8294 ± 307***	11010 ± 338	8126 ± 280***
LVIDd/BW (μm/g)	35 ± 2	77 ± 5***	31 ± 2	66 ± 5***	31 ± 1	60 ± 3$^{***;\ \&}$
LVPWd (μm)	1778 ± 48	1264 ± 91***	2061 ± 60	1310 ± 49***	2279 ± 184	1656 ± 363**
LVPWd/BW (μm/g)	6.4 ± 0.2	14 ± 1***	5.5 ± 0.2	10.3 ± 0.5***	6.3 ± 0.4	12 ± 2**
IVSTs (μm)	1883 ± 114	1794 ± 53	2624 ± 57$^{\wedge\wedge\wedge}$	1815 ± 123***	2379 ± 74$^{\&}$	1848 ± 85**
IVSTs/BW (μm/g)	6.7 ± 0.5	20 ± 2***	7.1 ± 0.4	14 ± 1$^{***;\ \wedge}$	6.7 ± 0.3	14 ± 1$^{***;\ \&\&}$
LVIDs (μm)	5911 ± 340	3599 ± 532**	6293 ± 258	4697 ± 189***	6261 ± 276	4514 ± 290**
LVIDs/ BW (μm/g)	21 ± 1	38 ± 3**	17 ± 1	37 ± 3***	18 ± 1	33 ± 2**
LVPWs (μm)	2483 ± 117	1807 ± 153**	3122 ± 128$^{\wedge}$	1626 ± 105***	3089 ± 106$^{\&}$	1813 ± 107***
LVPWs/BW (μm/g)	8.9 ± 0.5	20 ± 2***	8.4 ± 0.2	13 ± 1$^{***;\ \wedge\wedge\wedge}$	8.7 ± 0.4	13 ± 1$^{***;\ \&\&\&}$

Table 3. Echocardiography of control (CON) and diabetic (STZ) rats at 4, 8 and 12 weeks after injection of either streptozotocin or vehicle. All data are expressed as mean ± S.E.M. Abbreviations: BW, body weight; IVSTd, telediastolic interventricular septum; LVIDd, diastolic left ventricular intradiameter, LVPWd, telediastolic left ventricular posterior wall; IVSTs, telesystolic interventricular septum; LVIDs, left ventricular systolic intradiameter; LVPWs, systolic left ventricular posterior wall. Statistically significant differences between CON and STZ rats of the same age are indicated as **, $p<0.01$; ***, $p<0.001$. Statistically significant differences between CON-4 weeks and CON-8 weeks or between STZ-4 weeks and STZ-8 weeks are indicated as $^{\wedge}$, $p<0.05$; $^{\wedge\wedge\wedge}$, $p<0.001$. Statistically significant differences between CON-4 weeks and CON-12 weeks or between STZ-4 weeks and STZ-12 weeks are indicated as $^{\&}$, $p<0.05$; $^{\&\&}$, $p<0.01$; $^{\&\&\&}$, $p<0.001$.

Figure 1. Characteristics of the diabetic cardiomyopathy.
(A) Survival rate in control (CON) and diabetic (STZ) rats. The survival curve obtained in both groups were compared using a Log-rank test (Mantel-Cox test) and statistically significant differences between CON and STZ rats are indicated as *, $p<0.05$. (B) Comparison of the fasting glucose levels (mg/dl) in CON (black bars) and diabetic (white bars) rats at 4, 8 and 12 weeks after STZ injection. (C) Cardiac ratio (HW/BW, mg/g) in CON (black bars) and STZ (white bars) rats at 4, 8 and 12 weeks after STZ injection. (D) mRNA expression of ANF normalized to GAPDH measured in CON (black bars) and STZ rats (white bars) at 4, 8 and 12 weeks after STZ or vehicle injection. HW, heart weight; BW, body weight; ANF, atrial natriuretic factor; GAPDH, Glyceraldehyde 3-phosphate dehydrogenase. All data represent the mean ± S.E.M. of the number of rats indicated between brackets above the bars. Statistically significant differences between CON and STZ rats of the same age are indicated as **, $p<0.01$; ***, $p<0.001$. Statistically significant differences between STZ-4 weeks and STZ-8 weeks are indicated as $^{\wedge\wedge\wedge}$, $p<0.001$. Statistically significant differences between STZ-4 weeks and STZ-12 weeks are indicated as $^{\&\&}$, $p<0.01$. Statistically significant differences between STZ-8 weeks and STZ-12 weeks are indicated as $^{\#}$, $p<0.05$.

Figure 2. Cardiac function in control and diabetic rats at 4, 8, and 12 weeks.
Ejection fraction (A), fraction shortening (B), heart rate (C), blood volumes (D) and echocardiography images (E) measured in CON (black bars) and STZ rats (White bars) at 4, 8 and 12 weeks after STZ or vehicle injection. EDV, end diastolic volume; ESV, end systolic volume; SV, stroke volume; EF, ejection fraction; FS, fraction shortening; IVSTd, diastolic interventricular septal thicknesses; LVIDd, Left Ventricular Internal Dimension-Diastole; LVPWd, Left Ventricular Posterior Wall Dimensions. All data represent the mean ± S.E.M. of the number of rats indicated between brackets above the bars. Statistically significant differences between CON and STZ rats of the same age are indicated as *, $p < 0.05$; **, $p<0.01$; ***, $p<0.001$. Statistically significant differences between CON-4 weeks and CON-8 weeks are indicated as $^{\wedge}$, $p<0.05$; $^{\wedge\wedge}$, $p<0.01$.

Figure 3. Representative microphotographs of histological slices of hearts from control and diabetic rats at 4, 8, and 12 weeks. Heart of the control (A, B and C) and diabetic (D, E, F and G) groups at 4, 8, and 12 weeks, stained with hematoxylin and eosin (20 X magnification). Arrows point to representative steatosis at 4 (D) and 8 (F) weeks as well as chronic inflammation at 8 (E) and 12 (G) weeks, respectively. Scale bars indicate 1μm.

Figure 4. Representative microphotographs of histological slices of hearts from control and diabetic rats at 4, 8, and 12 weeks. Heart of control (A, B and C) and diabetic (D-H) groups at 4, 8 and 12 weeks, stained with Masson's trichrome (20 X magnification). Images show the presence of collagen fibers between cardiac myocytes attesting cardiac fibrosis at 4 (D) and 12 weeks (G) as well as representative steatosis at 4 (arrow in D), 8 (arrow in F) and 12 weeks (arrow in H). Scale bars indicate 1μm. (I) Quantitative analysis of fibrotic areas in both control (CON, black bars) and diabetic (STZ, white bars) at 4, 8 and 12 weeks. Fibrosis analysis was performed on 4 non-overlapping randomly chosen fields (40 X magnification) per section per rat using ImageJ software. Two cardiac sections were analyzed per rat and the total fibrotic stained area was

corrected to the total stained area section of the heart tissue. Data represent the mean ± S.E.M. of the number of rats indicated between brackets above the bars. Statistically significant differences between CON and STZ rats of the same age are indicated as ***, $p<0.001$. Statistically significant differences between STZ-8 weeks and STZ-12 weeks are indicated as $^{\#\#}$, $p<0.01$.

Figure 5. mRNA expression of PDE isoforms in hearts from control and diabetic rats at 4, 8, and 12 weeks. Total RNA was extracted from hearts of all control (CON, black bars) and diabetic rats (STZ, white bars) and analyzed by Real-time PCR for PDE1A (A), PDE2A (B), PDE3A (C), PDE4A (D), PDE4B (E), PDE4D (F) and PDE5A (G). mRNA expression of different PDE isoforms was normalized to GAPDH in both STZ and aged-matched CON rats. Data represent the mean ± S.E.M. of the number of rats indicated between brackets above the bars. Statistically significant differences between CON and STZ rats of the same age are indicated as *, $p<0.05$; **, $p<0.01$; ***, $p<0.001$.

Figure 6. Expression of PDE3A and PDE4B proteins in hearts from control and diabetic rats at 4, 8, and 12 weeks. Equal amounts of proteins from hearts isolated from control (CON, black bars) and diabetic rats (STZ, white bars) were separated on SDS/PAGE and revealed with PDE3A and PDE4B specific antibodies. Calsequestrin was used as a loading control. (A) and (C) Shown are representative blots for PDE3A and PDE4B, respectively. Two immunoreactive bands were detected for PDE3A isoform at approximately 125 kDa (Upper band) and 85 kDa (lower band) in both control and diabetic rat hearts. A single band migrating at approximately 78 kDa was detected in rat hearts for PDE4B. (B) and (D) Quantification of all data obtained in several immunoblots from hearts of CON and STZ and represented as mean ± S.E.M. of the number of rats indicated between brackets above the bars. Statistically significant differences between CON and STZ rats of the same age are indicated as *, $p<0.05$; **, $p<0.01$. Statistically significant differences between STZ-4 weeks and STZ-8 weeks are indicated as $^{\wedge\wedge\wedge}$, $p<0.001$.

Methods

Real-time fluorescence quantitative PCR (RT-qPCR).

Table S1. Forward and reverse primers used for quantitative real time PCR.

Gene	*Forward primer (5'-3')*	*Reverse primer (3'-5')*
GAPDH	TGC CAC TCA GAA GAC TGT GG	TTC AGC TCT GGG ATG ACC TT
ANF	ATC TGC CCT CTT GAA AAG CA	AAG CTG TTG CAG CCT AGT CC
MRP4	ATT CTG GGC AGC TCC TAC CT	CGA ACA CGT GGC TAG CTG TA
EPAC1	GAC GTC ACC ACT GCA AAC C	GCT GCC AGC TTG ATG AAC TT
EPAC2	CCA CAC ATT TGG AAG GCA TA	GGG AAC AAA GGC AGA TCT CA
PDE1A	GAA GTT TCG CAG CAT TGT CC	GCA GGA TAT GTC AAA CCA ACC
PDE2A	CTG TGC TGG CTG CAC TCT AC	GAG GAT AGC AAT GGC CTG AG
PDE3A	ACC TCC CTG CCC TGC ATA C	CCT CTC TTG TGG TCC CAT TC
PDE4A	CGT CAG TGC TGC GAC AGT C	CCA GCG TAC TCC GAC ACA CA
PDE4B	GAT GAG CAG ATC AGG GAA CC	GAT GGG ATT TCC ACA TCG TT
PDE4D	GCC AGC CTT CGA ACT GTA AG	ATG GAT GGT TGG TTG CAC AT
PDE5A	GGG AAG AGG TCG TTG GTG T	TTT GTT CTC CAG CAG TGA CG

Histopathology

Harvested organs (lungs and liver) from all CON and STZ rats were fixed in 10 % neutral buffered formalin, dehydrated in 95 % ethanol and then embedded in paraffin as described by Zeeni and her colleagues (1). Briefly, sections were stained with hematoxylin & eosin. All slides were evaluated for pathological changes by an experienced board certified pathologist under a light microscope (Zeiss). Histological lesions (e.g., steatosis, fibrosis, inflammation) were reported as present or not. Lung samples were analyzed for the accumulation of foamy macrophages in the alveoli. Liver samples were analyzed for fibrosis (sinusoidal and portal), steatosis and necro-inflammation.

Results

	Week 4				Week 8				Week 12			
	CON (n=6)		STZ (n=7)		CON (n=6)		STZ (n=8)		CON (n=6)		STZ (n=10)	
	Positive cases (n)	Percent of total (%)	Positive cases (n)	Percent of total (%)	Positives cases (n)	Percent of total (%)	Positives cases (n)	Percent of total (%)	Positive cases (n)	Percent of total (%)	Positives cases (n)	Percent of total (%)
Cardiac steatosis	0	0	6	86	0	0	8	100	0	0	10	100
Cardiac inflammation	0	0	0	0	1	17	3	38	3	50	5	50
Cardiac fibrosis	1	17	2	29	0	0	0	0	1	17	10	100
Lung alveolar foamy macrophages	0	0	5	71	0	0	4	50	2	33	7	70
Liver portal inflammation	0	0	1	14	6	100	7	88	3	50	10	100
Liver necro-inflammation	0	0	2	29	6	100	8	100	6	100	10	100
Liver portal fibrosis	0	0	0	0	0	0	0	0	0	0	3	30
Liver perisinusoidal fibrosis	0	0	0	0	0	0	0	0	0	0	0	0
Liver steatosis	0	0	0	0	0	0	0	0	0	0	0	0

Table S2

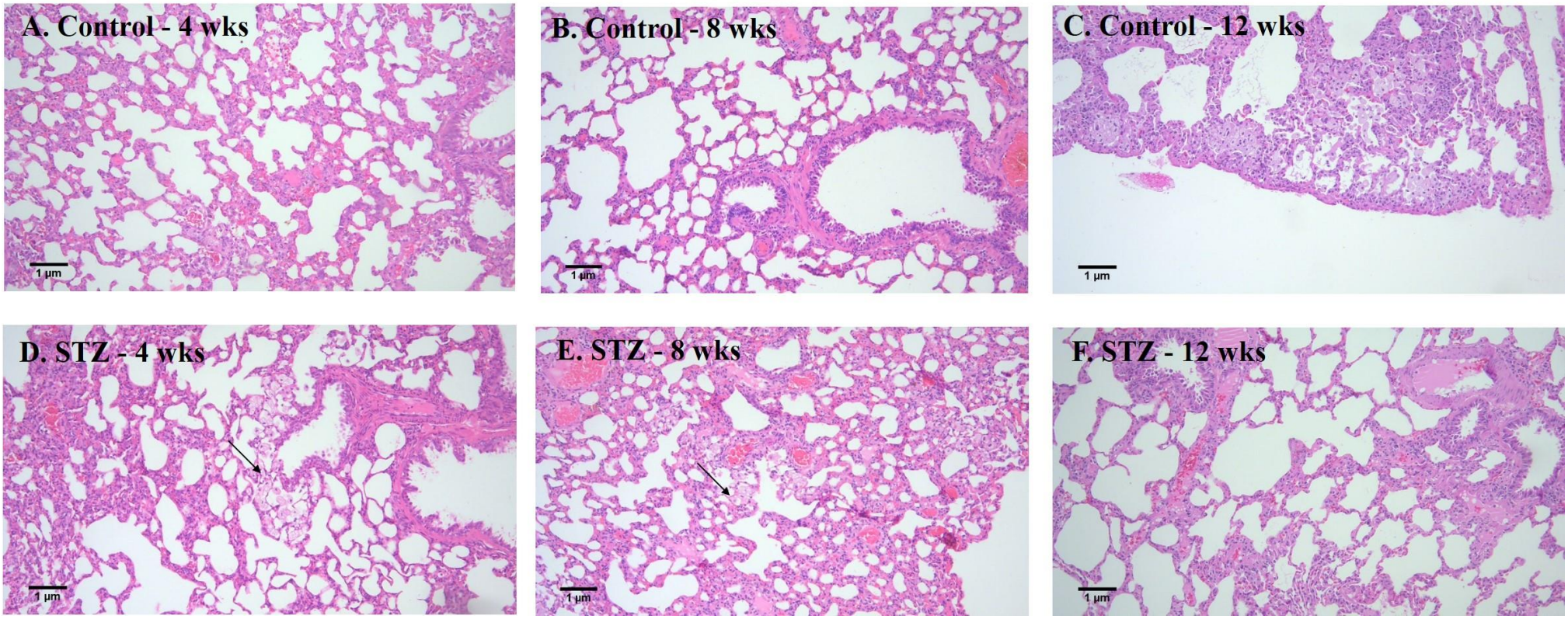
A. Control - 4 wks
B. Control - 8 wks
C. Control - 12 wks
D. STZ - 4 wks
E. STZ - 8 wks
F. STZ - 12 wks
1 µm

Figure S1

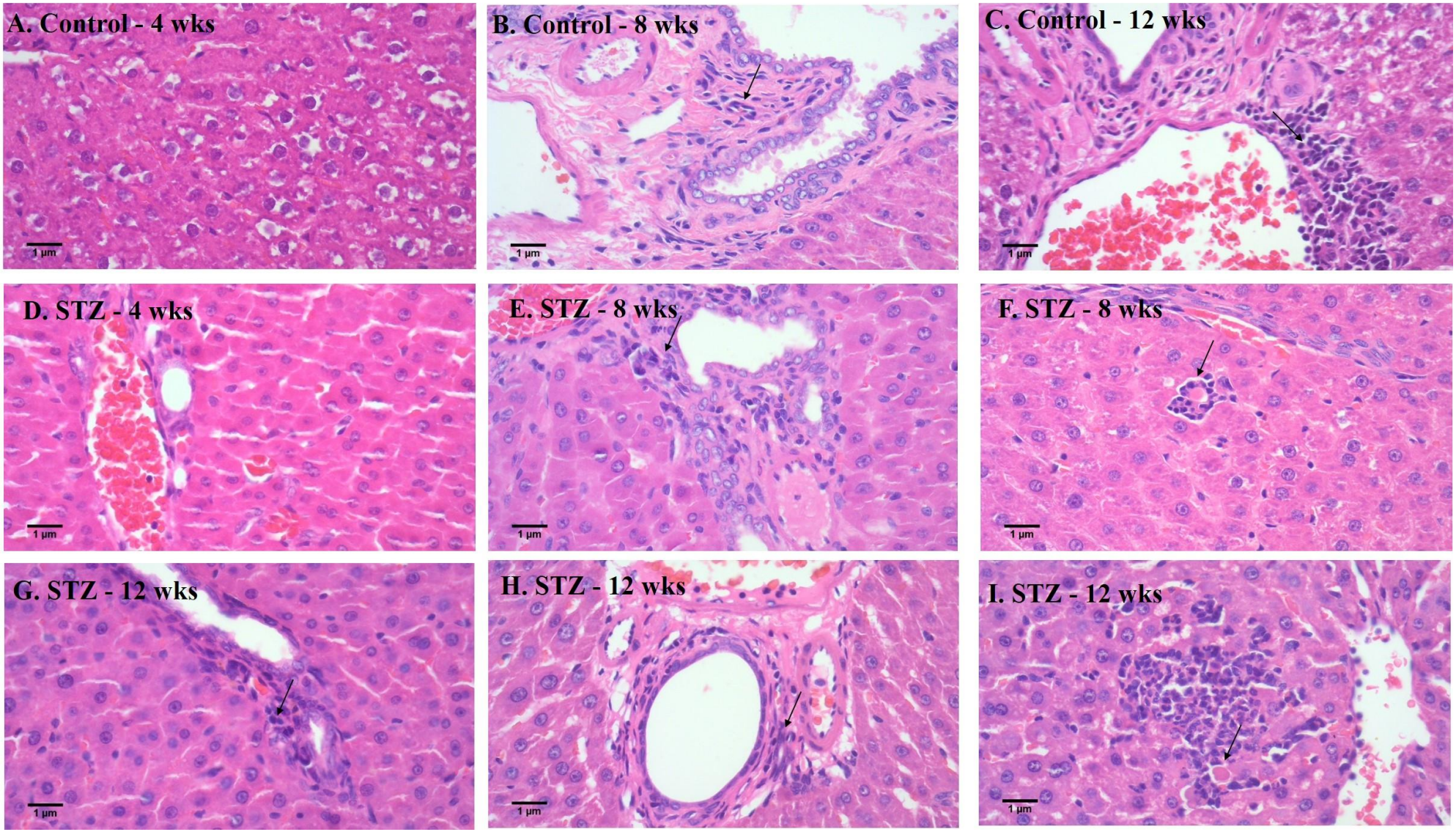
A. Control - 4 wks
B. Control - 8 wks
C. Control - 12 wks
D. STZ - 4 wks
E. STZ - 8 wks
F. STZ - 8 wks
G. STZ - 12 wks
H. STZ - 12 wks
I. STZ - 12 wks
1 µm

Figure S2

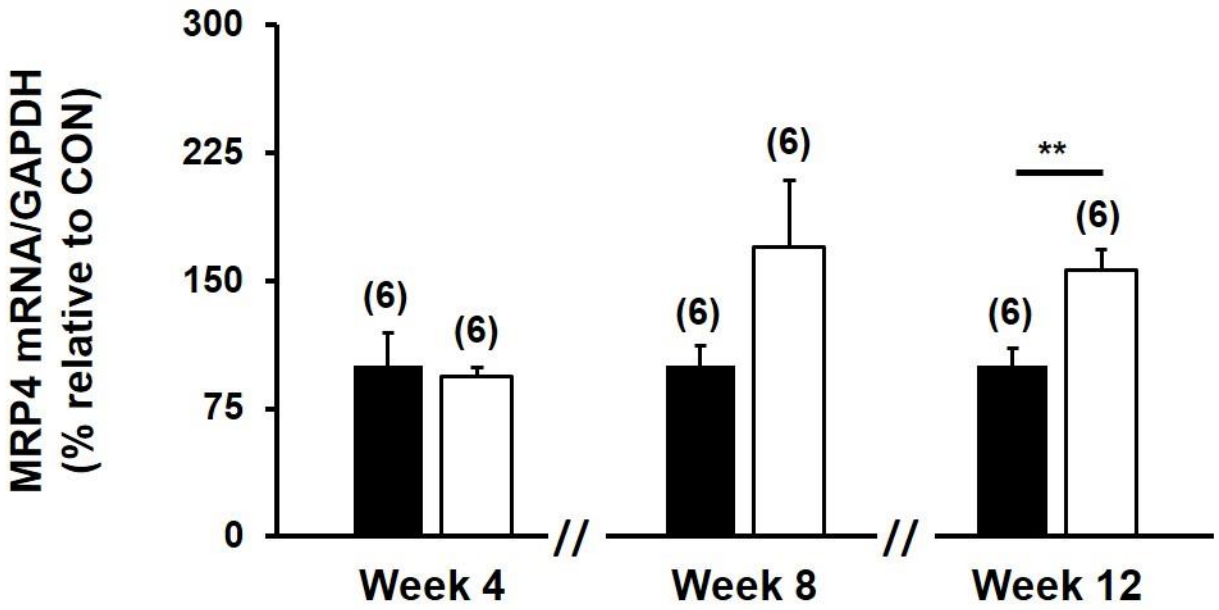
MRP4 mRNA/GAPDH
(% relative to CON)
300
225
150
75
0
(6)
(6)
(6)
(6)
(6)
(6)
**
Week 4
Week 8
Week 12

Figure S3

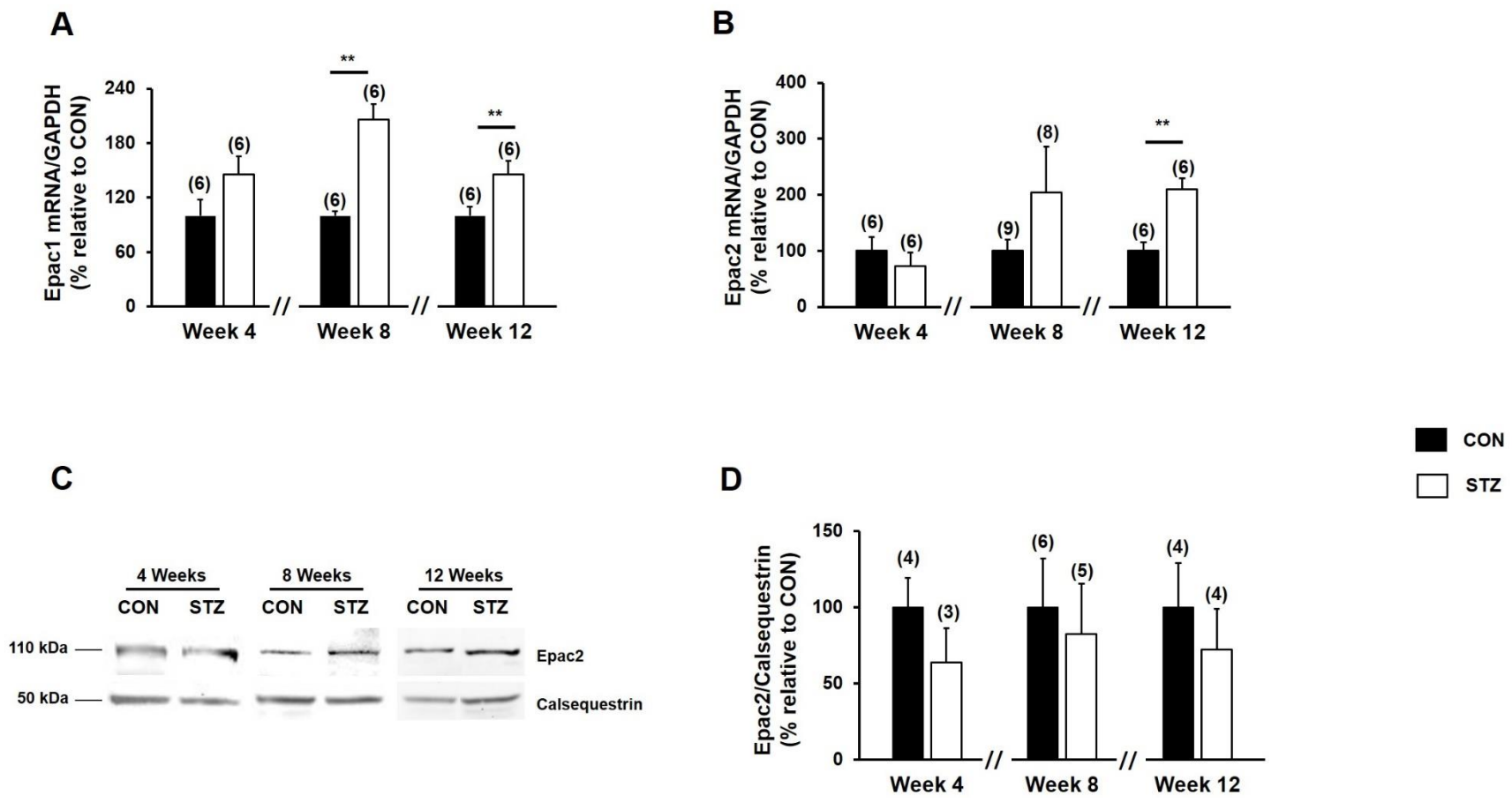
A
Epac1 mRNA/GAPDH
(% relative to CON)
240
180
120
60
0
**
**
(6)
(6)
(6)
(6)
(6)
(6)
Week 4
Week 8
Week 12
B
Epac2 mRNA/GAPDH
(% relative to CON)
400
300
200
100
0
**
(6)
(6)
(9)
(8)
(6)
(6)
Week 4
Week 8
Week 12
CON
STZ
C
4 Weeks
8 Weeks
12 Weeks
CON
STZ
CON
STZ
CON
STZ
110 kDa
50 kDa
Epac2
Calsequestrin
D
Epac2/Calsequestrin
(% relative to CON)
150
100
50
0
(4)
(3)
(6)
(5)
(4)
(4)
Week 4
Week 8
Week 12

Figure S4

Legends

Table S2. Representative of the cardiac, lungs and liver slices histopathology in control (CON) and diabetic (STZ) rats at 4, 8 and 12 weeks after injection of either streptozotocin or vehicle. Data are expressed as % of cases classified as positive for steatosis, inflammation and fibrosis.

Figure S1. Representative microphotographs of histological slices of the lungs from control and diabetic rats at 4, 8 and 12 weeks. Lung of control (A, B, and C) and diabetic rats (D, E, and F) at 4, 8, and 12 weeks, stained with hematoxylin and eosin (10 X magnification). Images show representative accumulation of foamy macrophages in the alveoli (arrows in D and E). Scale bars indicate 1μm.

Figure S2. Representative microphotographs of histological slices of the liver from control and diabetic rats at 4, 8 and 12 weeks. Liver of control (A, B and C) and diabetic (D-I) rats at 4, 8, and 12 weeks, stained hematoxylin and eosin (40 X magnification). Images show representative hepatic portal chronic inflammation (arrows in B, C, E and G), necro-inflammation (F and I), and portal fibrosis (H). Scale bars indicate 1μm.

Figure S3. mRNA expression of MRP4 in hearts from control and diabetic rats at 4, 8 and 12 weeks. Total RNA was extracted from hearts of all control (CON, black bars) and diabetic (STZ, white bars) rats and analyzed by Real-time PCR for MRP4. mRNA expression of MRP4 was normalized to GAPDH in both STZ and aged-matched CON rats. Data represent the mean ± S.E.M. of the number of rats indicated between brackets above the bars. Statistically significant differences between CON and STZ rats of the same age are indicated as **, $p<0.01$.

Figure S4. Expression of Epac1 and Epac2 isoforms in hearts from control and diabetic rats at 4, 8 and 12 weeks. A and **B**: mRNA expression of Epac1 and Epac2 isoforms in hearts from control (CON, black bars) and diabetic (STZ, white bars) rats at 4, 8 and 12 weeks. Total RNA was extracted from hearts of all rats and analyzed by Real-time PCR for Epac1 (A) and Epac2 (B). mRNA expression of Epac1 and Epac2 was normalized to GAPDH in both STZ and aged-matched CON rats. **C** and **D**: Expression of Epac2 proteins in hearts from control (CON, black bars) and diabetic (STZ, white bars) rats at 4, 8 and 12 weeks. Equal amounts of proteins from hearts of all rats were separated on SDS/PAGE and revealed with Epac2 specific antibody. Calsequestrin was used as a loading

control. (C) Shown is a representative blot for Epac2. A single band migrating at approximately 110 kDa was detected in rat hearts for Epac2. (D) Quantification of all data obtained in several immunoblots from hearts of CON and STZ and represented as mean ± S.E.M. of the number of rats indicated between brackets above the bars. Statistically significant differences between CON and STZ rats of the same age are indicated as **, $p<0.01$.

Reference

1. Zeeni N, Dagher-Hamalian C, Dimassi H, Faour WH. Cafeteria diet-fed mice is a pertinent model of obesity-induced organ damage: a potential role of inflammation. Inflamm Res. 2015 Jul;64(7):501-12. PubMed PMID: 25966976. Epub 2015/05/15. eng.

Annex 3

The role of hyperglycemia in the development of diabetic cardiomyopathy

Magali Samia El Hayek*[1], Laura Ernande*[2, 3], Jean-Pierre Bénitah[1], Ana-Maria Gomez[1], Laetitia Pereira[1]

[1]Université Paris-Saclay, Inserm, UMR-S 1180, 92296, Châtenay-Malabry, France.
[2]INSERM U955, Université Paris-Est Créteil (UPEC), Créteil, France.
[3] Department of Cardiology, Institut Mondor de Recherche Biomédicale, Unité INSERM 955-équipe 8, Faculté de médecine de Créteil, Créteil, France.

* The authors contributed equally

Running title: hyperglycemia, a player in diabetic cardiomyopathy

Keywords: Diabetes, Glucose, Cardiomyopathy,

Corresponding Author:

Laboratory of signalling and cardiovascular pathophysiology
UMRS-1180, INSERM
5, Rue Jean-Baptiste Clément
92296 Châtenay-Malabry
FRANCE
Phone : +33 (0)1 46 83 58 07
Fax : (+33) (0)1 46 83 54 75
Email : laetitia.pereira@universite-paris-saclay.fr

Abstract

Diabetes mellitus is a metabolic disorder with a chronic hyperglycemic state. Cardiovascular diseases are the first cause of mortality in diabetic patients. Increasing evidences unraveled the existence of a diabetic cardiomyopathy. Diabetic cardiomyopathy is a cardiac dysfunction with impaired cardiac contraction and relaxation, independently of coronary and/or valvular complications that can lead to

heart failure. Several preclinical and clinical studies aimed to decipher the underlying mechanisms of the diabetic cardiomyopathy. Among all cofactors, hyperglycemia seems to play an important role in this pathology. Hyperglycemia has been shown to alter cardiac metabolism and function through several deleterious mechanisms such as oxidative stress, inflammation, accumulation of advanced glycated end-products and upregulation of the hexosamines biosynthesis pathway. These mechanisms are responsible for the activation of hypertrophic pathways, epigenetics modifications, mitochondrial dysfunction, cell apoptosis, fibrosis and calcium mishandling leading to cardiac stiffness, as well as contractile and relaxation dysfunction. This review aims to describe the hyperglycemic-induced alterations participating in diabetic cardiomyopathy and its correlation with the severity of the disease and patients mortality with an overview on the cardiac outcomes of the glucose lowering therapy.

Introduction

Diabetes mellitus is an increasing health burden affecting about 541 million patients worldwide. Diabetes prevalence is predicted to reach about 693 million cases by 2045, which will rank it as the 7th leading cause of death (1). In diabetic patients, cardiovascular complications represent the main cause of hospitalization and death. The Framingham study showed that the major contributor of morbi-mortality is heart failure (HF), whose risk factor is doubled in diabetic patients compared to non-diabetic ones (2).

Coronary artery diseases and hypertension were often considered as the underlying causes of HF in diabetes. However, in 1972, Rubler *et al*. (3) reported HF associated with left ventricular hypertrophy in diabetic patients with no coronary artery disease or other etiological conditions explaining HF. Therefore, the concept of a specific myocardial dysfunction called diabetic cardiomyopathy was introduced, and was also described by Regan *et al.* (4). Diabetic cardiomyopathy is defined as “a cardiac dysfunction with impaired cardiac contraction and relaxation, leading to heart failure independently of coronary and/or valvular complications, hypertension, congenital cardiomyopathy or other HF known etiologies”. Diabetic cardiomyopathy was later confirmed by several clinical studies (5-9) notably the Strong Heart Study (5, 6). In this population-based cohort, the authors reported a 1.5-fold higher risk of HF in patients with diabetes mellitus after adjustment for multiple cofactors including age, sex, obesity, fat distribution, antihypertensive medications, atrial fibrillation, urinary albumin/creatinine ratio, cholesterol level, Hb1Ac (glycated hemoglobin), smoking, alcohol use, educational level or physical activity. However, our understanding of the underlying mechanisms in diabetic cardiomyopathy remains unclear. Over the last decades, clinical studies have highlighted a correlation between glycemic level and the prevalence of HF in diabetic patients (10-12). Irbarren *et al.* (10) have shown that 1% increase of HbA1c is associated with 8% rise of HF hospitalization in diabetic patients after excluding factors such as age, sex, race/ethnicity, education level, cigarette smoking, alcohol consumption, hypertension, obesity, ACE inhibitors, β-blockers, diabetes type and duration, and interim myocardial infarction (Fig. 1). Since diabetes is

a multifactorial disease, the respective contribution of hyperglycemia, insulin resistance or obesity in cardiac dysfunction is not clear. In order to clarify the contribution of each cofactor in the development of diabetic cardiomyopathy, Montaigne *et al.* (13) aimed to decipher whether obesity, insulin resistance, and diabetes mellitus, respectively impact the cardiac contraction and mitochondrial function in type 2 diabetic patients. They found that *ex vivo* contractile dysfunction of atrial trabeculae is associated to mitochondrial dysfunction and related to HbA1c level regardless of insulin resistance or obesity. Those results support, then, the idea that hyperglycemia is a key component of cardiac dysfunction in type 2 diabetes.

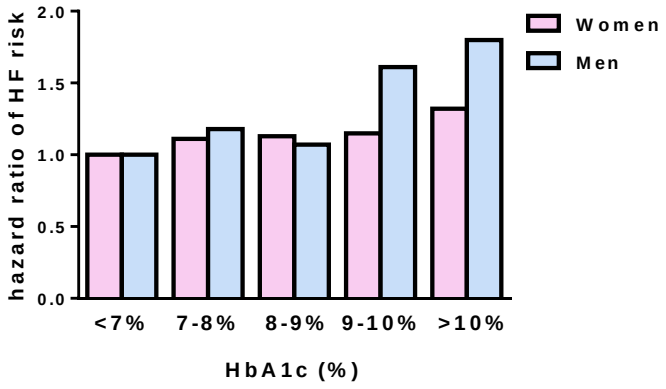

Figure 1: Relationship between glycated hemoglobin (HbA1c) level and risk of HF hospitalization in diabetic patients after adjustment of race/ethnicity, education level, cigarette smoking, alcohol consumption, hypertension, obesity, ACE inhibitors, β-blockers, diabetes type and duration, and interim myocardial infarction. Adapted from Irbarren *et al.* (10).

More recently, preclinical studies have shown that high glucose levels induce intracellular calcium (Ca^{2+}) mishandling, as well as long lasting protein modifications depending on advanced glycated end-products (AGEs) formation and up-regulation of the hexosamine biosynthesis pathway. These alterations have been shown to

participate in cell apoptosis, structural modifications and contractile dysfunction. Among them, proteins O-GlcNAcylation, resulting from the activation of the hexosamine biosynthesis pathway, is emerging as a key player in diabetes. O-GlcNAcylation is a post-translational modification of proteins by the addition of a N-acetylglucosamine moiety to serine and threonine residues changing in protein activity. Uridine-diphospho-N-acetyl-glucosamine, the end-product of the hexosamines biosynthesis pathway is highly dependant on several metabolic pathways in the cell (glucose, fatty acid and amino acid metabolic pathways) thus classifying it as a nutrient sensor in the cell. O-GlcNAcylation is a dynamic and rapid modification, similar to protein phosphorylation, and that often interfere with protein phosphorylation. However, in contrast to phosphorylation that is regulated with hundreds of kinases and phosphatases, O-GlcNAcylation is regulated by only two different enzymes, O-GlcNac transferase (OGT) and O-GlcNAcase (OGA) respectively responsible for the addition or the removal of the N-acetylglucosamine moiety. Contrarely to N- and O-Glycosylation process, that are restricted to some organelles (such as endoplasmic reticulum or Golgi apparatus during protein synthesis process) or secreted proteins outside the cell, O-GlcNAcylation affects nuclear as well as cytosolic and mitochondrial proteins. O-GlcNAcylation plays different roles in cellular signaling and is emerging as a key factor in several pathologies, such as cancer, Alzheimer's disease, glomerular sclerosis, retinopathy, insulin resistance, cardiac diseases and diabetic cardiomyopathy (14). For instance, it has been shown that an increase in the O-GlcNac levels reduces myocardial infarct size in mice model by preserving the mitochondrial potential (15). Furthermore it has been shown that O-GlcNacylation protects the heart from iscyhemia/reperfusion injury in isolated rat heart

(16). However, the role of O-GlcNAcylation in the development of hypertrophy is still unclear. Lowering or increasing O-GlcNAc levels participate in HF development since several players involved in hypertrophic signaling are targets for O-GlcNAcylation, supporting the concept that maintaining O-GlcNAc homeostasis is necessary for normal cardiomyocyte function (17). In diabetic patients and diabetic animal models (18),O-GlcNAcylation is upregulated and the inhibition of this pathway (19, 20) improves cardiac function in type 1 and 2 diabetic mice. In diabetic cardiomyopathy, several proteins undergo O-GlcNAcylation modification which participates in the development of diabetic cardiomyopathy. Those alterations will be further developped in the preclinical section. Additionally, it has been shown that proteins also undergo modification through AGEs formation in diabetes, a non-enzymatic addition of a sugar moiety (fructose or glucose) to a protein, leading to cell damages such as oxidative stress, inflammation, alteration of the excitation contraction coupling (ECC) and cardiac stiffness (21). This review is a translational overview of the hyperglycemia-mediated dysregulation of cardiomyocyte function and their impact on the cardiac function with an overview of the glucose-lowering drugs therapy effect on cardiac outcomes

Clinical evidences of the role of hyperglycemia in the development of diabetic cardiomyopathy

Epidemiological studies support a strong association between diabetes mellitus and HF. In the Framingham study, risk of HF was 2.4 fold increased in diabetic men and 5 fold increased in diabetic women (22). This is associated to an increase risk of hospitalization for HF among diabetic type 2 patients (hazard ratio 1.45; CI95%=1.34-1.57) (23). This relationship between diabetes mellitus and HF is bidirectional. Indeed,

patients with HF have a 4-fold higher prevalence of type 2 diabetes mellitus (25 to 30%) than patients without (4-6%) and this rises up to 40% in hospitalized patients with HF (24).

Prognosis in patients with HF is worst in diabetic than in non-diabetic patients. Study from the 90s' have shown that, 1-year mortality of HF was 30% in patients with diabetes mellitus, corresponding to a 1.5-fold increased as compared to patients without diabetes mellitus (25). In the CHARM (Candesartan in HF: Assessment of Reduction in Mortality and morbidity) trial, after a median follow-up of 37.7 months, diabetes mellitus was associated with an increased risk of mortality or hospitalization for HF with a hazard ratio of 2.0 (IC95%=1.70–2.36) in HFpEF (HF with preserved ejection fraction) and 1.60 (IC95%=1.44–1.77) in HFrEF (HF with reduced ejection fraction) (26). In the I-preserved trial, data confirmed significant higher risk of cardiovascular (CV) death or HF hospitalization in diabetic patients with HFpEF as compared with those without type 2 diabetes mellitus (27). In diabetic patients older than 65 years, a 10-fold higher mortality risk has been reported (28). Finally, in the Everest trial including patients with HFrEF, diabetes mellitus was associated with a higher post-discharge cardiovascular mortality and higher HF hospitalizations compared with patients with no diabetes (HR 1.17; CI95%=1.04-1.31) (29). Diabetes mellitus unfavorably affects left ventricular remodeling in patients with left ventricular pressure or volume overload (30-32).

Diabetes is also an independent risk factor for the development of arrhythmia, notably atrial fibrillation (AF) (33). A large meta-analysis has shown that the patients with diabetes have a nearly 40% greater risk of AF comparing to non-diabetic patients (34). However the relationship between HbA1c levels and AF prevalence are still not clear: in

a population-based case control study, it has been reported that higher HbA1c levels were associated with increased risk of AF, that should however be further investigated in prospective studies (35).

High glucose: epidemiology on HbA1c levels and mortality

Epidemiological data indicates that each 1% increase in HbA1c confers an 8% increased risk of HF (10). However, observational studies and randomized trials have reported controversial evidence of effects of glycemic control with glycated hemoglobin levels (<7.0%) with regard to cardiovascular outcomes (36, 37). In the UKPDS study, a continued reduction in microvascular risk and emergent risk reductions for myocardial infarction and death from any cause were observed during 10 years of post-trial follow-up despite an early loss of glycemic differences (36). Follow-up in the Diabetes Control and Complications (DCCT) trial including patients with type 1 diabetes mellitus reported a beneficial effective intensive glucose treatment on cardiovascular events (38). Finally, in the recent observational study by Rawshani *et al*., a glycated hemoglobin level ≥7% was a strong predictor for all outcomes (death, acute myocardial infarction, stroke, and hospitalization for HF), especially for atherothrombotic events (23). Conversely, follow-up in the Action to Control Cardiovascular Risk in Diabetes (ACCORD) trial (39), in the Action in Diabetes and Vascular disease (ADVANCE) trial (40) and in the Veterans Affairs Diabetes (VADT) trial (41), showed no evidence of cardiovascular beneficit of intensive as compared to standard glycemic control.

Evolution of diabetic cardiomyopathy

Definition consensus

Nowadays, diabetes mellitus is recognized in international guidelines as a specific and direct etiology of HF (ESC heart failure guidelines 2016, AHA HF 2017). Diabetic cardiomyopathy is considered as a distinct form of HF that occurs in diabetic patients in the absence of coronary artery disease, long standing hypertension, valvular or any other etiology of HF. It relies on a diagnosis of exclusion based on the presence of symptomatic cardiomyopathy, a long history of diabetes with many exclusion criteria. However, because of frequent associated comorbidities such as hypertension, obesity, atrial fibrillation or coronary artery diseases (CAD), diagnosis of diabetic cardiomyopathy might be challenging.

Early phenotype of diabetic cardiomyopathy

AHA guidelines (42) classically classify preclinical stages of HF as stage A in patients with HF risk factors and stage B in asymptomatic patients presenting structural and/or function abnormalities whereas stages C and D are symptomatic HF ones. In asymptomatic diabetic patients, early phenotype of diabetic cardiomyopathy corresponding to a stage B HF is observed in one quarter to one third of the patients. This phenotype may include left ventricular concentric remodelling or hypertrophy (6, 43), left ventricular diastolic dysfunction (44, 45) and mildly decreased global longitudinal strain (46-48). Alteration of global longitudinal strain is a sensitive marker of systolic dysfunction in patients with normal ejection fraction and can be the first alteration seen in the early form of diabetic cardiomyopathy (44). Alteration of global

longitudinal strain is associated with left ventricular remodelling (49), and a poorer prognosis as assessed by all-cause mortality after a 10-year follow-up (50). Left ventricular diastolic dysfunction is very common and is reported in about 40 to 50% of the patients (44, 51, 52). Diastolic dysfunction is also associated with a poorer prognosis with an increased risk of overt HF (53). Interestingly, when testing the exercise capacity in those declared asymptomatic patients, the increasing numbers of components of early phenotype of stage B HF (left ventricular concentric remodeling/hypertrophy, diastolic dysfunction and altered strain) is associated with a decreased exercise capacity as assessed by peak Vo2 and compared with healthy subjects (54).

Obesity and hypertension are frequent comorbidities of type 2 diabetes mellitus, In addition to age and sex that might also influence cardiac phenotype. The specific contribution of all these potential causative factors is unclear, as is their synergistic contribution to cardiac dysfunction in patients with type 2 diabetes mellitus. Cluster analysis is an exploratory technique (without prespecified hypothesis) that provides tools to identify unknown subgroups in order to classify individuals with similar characteristics in the same group (or cluster) and individuals with distinct characteristics into different clusters. Using cluster analysis in a large set of asymptomatic diabetic patients, 3 clusters were recently identified in this population: a first cluster with preserved systolic and diastolic function (mainly men) associated with a favorable prognosis; a second cluster of patients with obesity and hypertension with diastolic dysfunction (mostly women); and a third cluster with left ventricular hypertrophy and systolic dysfunction as assessed by strain (mainly men). The latter 2 clusters had a

similar and less favorable prognosis than the 1st one with an increased risk of CV mortality and hospitalization (55).

Despite those data, currently, evidence are not strong enough to support a systematic screening for stage B HF phenotype in asymptomatic diabetic patients (56).

Diabetic cardiomyopathy in type 1 diabetes mellitus

Since type 1 diabetes mellitus is a rare disease, evidence of a specific diabetic cardiomyopathy in patients with type 1 diabetes mellitus is much more challenging than in patients with type 2 diabetes. At the early phase, the thousand and 1 study included 1093 patients with type 1 diabetes mellitus and without known heart disease with a mean age of 49.6±15 years (men=53%, mean duration of diabetes=25.5 years) (57). Among those patients, 15.5% (n=169) of participants had abnormal systolic or diastolic function including 1.7% with left ventricular ejection fraction<45% and 14.4% with diastolic dysfunction (E/e≥12 or E/e= 8 to 12 and left atrial volume >34 ml/m2). The authors reported a decreased global longitudinal strain only in patients with macroalbuminuria (58). Using PET imaging, increased myocardial fatty acid metabolism has been reported in type 1 diabetes mellitus patients (59). In addition, impaired myocardial energetics as assessed by magnetic resonance spectroscopy has been shown in young subjects with uncomplicated type 1 diabetes mellitus irrespective of the duration of diabetes (60).

In a large case-control study based on the Swedish National Diabetes Registry and including patients with type 1 diabetes mellitus, diabetes mellitus was associated with a

a HR 4.69 (CI95%= 3.64-6.04), after adjustment for time-updated age, sex, time-updated diabetes duration, birth in Sweden, educational level, and baseline comorbidities (61). Poor glycaemic control and impaired renal function substantially increased the risk of HF.

Therefore, clinical evidence support the existence of a specific diabetic cardiomyopathy also in patients with type 1 diabetes mellitus. In this patients, dilated phenotype with HFrEF seems more common because of the auto immune process than the restrictive phenotype with HFpEF (62).

Preclinical evidences of the role of hyperglycemia in the development of diabetic cardiomyopathy

Over the years, preclinical studies have shown that glucose toxicity participates in defective cardiac metabolism and cellular cardiac dysfunction *via* oxidative stress, accumulation of AGEs and O-GlcNAcylation pathway leading to hypertrophy, epigenetic modifications, mitochondrial dysfunction, cell apoptosis, fibrosis and intracellular Ca^{2+} mishandling. Altogether, these alterations induce cardiac stiffness and impaired cardiac contraction and relaxation as described below (Fig. 2).

Glucose and structural modification

Structural modification of the left ventricle leading to cardiac stiffness and impaired cardiac function, is a common feature of the diabetic cardiomyopathy (56, 63). Lombarda *et al.* (64) have shown that in patients with type 1 diabetes, myocardial deformation is correlated with HbA1c level. Hyperglycemia–mediated AGEs formation

induces collagen cross-linking molecules responsible for the loss of collagen elasticity with subsequent reduction of myocardial compliance. In addition, AGEs increase the production of reactive oxygen species (ROS), known to promote myocardial fibrosis (65). Even though the underlying fibrotic mechanisms remain unclear in diabetic cardiomyopathy, it has been shown that the fibrogenic agent, TGF-β may be involved in diabetic cardiac fibrosis (for more details see review (66)). Beside fibrosis, high glucose can also induce cardiac hypertrophy, *via* for example the activation of the peroxisome proliferator-activated receptor ɣ (PPARɣ), as described in adult rat cardiomyocytes treated for 48h with high glucose concentration (25mM) (67). The increase of fibronectine production described in streptozotocine type 1 diabetic rats also participates in cardiac hypertrophy and fibrosis as seen in diabetic heart (68).

The glucose memory

Large-scale clinical trials (36, 69, 70) have pointed out the importance of an early tight glucose control in limiting the micro and macro vascular damages in type 1 and 2 diabetic patients.This is related to the glucose-mediated cell damage that persists even after glucose normalization which correlates to the severity of hyperglycemic history.This concept known as “metabolic memory” was first evoked by Engerman *et al.* (71) in 1987. This work showed that an early control of plasmatic glucose level, using insulin, was able, in type 1 diabetic dogs, to prevent retinal damages compared to dogs with long period of hyperglycemia. Although this phenomenon was widely described in retinal or renal cells (72), little is known about its pertinence in cardiomyocytes. Few papers have described some long lasting high glucose effect on cardiac cells related with the “metabolic memory” concept. For instance, streptozotocine-induced type 1

diabetic rats present an increase in cardiac fibronectin mRNA levels, which persist 2 weeks after glucose normalization by insulin (73). Moreover, cardiomyocytes line H9c2 exhibit a decrease of inflammatory interleukin 6 promotor methylation under high 25mM glucose condition for 24h, which leads to a persistent increase of IL-6 expression, despite glucose normalization (74). This mechanism seems related to high glucose-mediated epigenetic alterations (long lasting modification of chromatin structure and gene transcription without modification of gene sequence) known to be involved in metabolic memory development (75, 76). However, studies in other cell types can provide some new insights in our understanding of this metabolic memory. For example, Brownlee *et al.* (77, 78) have postulated that, in aortic endothelial cells and mesangial renal cells, high glucose-mediated mitochondrial superoxide production activates several cellular pathway (e.g the polyol pathway, protein kinase C (PKC) and AGEs) involved in glucotoxicity. All these mechanisms, found in diabetic cardiomyopathy (63), might be activated and paved the way to a better understanding of long-lasting high glucose deleterious effects observed in cardiomyocytes.

Glucose and Metabolic alterations

The heart uses either fatty acid or glucose oxidation to produce ATP, depending on the substrate availability. However, the diabetic heart lacks this substrate flexibility that deeply impacts cardiac metabolic activity. Indeed, the increase of fatty acid oxidation promotes acetyl-CoA and citrate production. These substrates generate nicotinamide adenine dinucleotide (NADH) and flavin adenine dinucleotide (FADH2), through the Krebs cycle, that enter the mitochondrial respiratory chain to produce ATP associated with oxygen consumption. Since these molecules are very rich in electrons,

the increase of their production and thus, flux through the mitochondrial membrane, hyperpolarizes the latter, resulting in the inhibition of the respiratory chain complex leading to ROS generation with less ATP production (79, 80). O-GlcNAcylation pathway can also alter the respiratory mitochondrial complex I, III, and IV complex in neonatal rat cardiomyocytes treated with high glucose. Indeed, high glucose treatment (30 mM) for 48h results in lower ATP production and reduces mitochondrial respiration efficiency (81). Besides altering the mitochondrial respiratory chain, the excess of acetyl-CoA and citrate inhibit the glycolysis in cardiomyocytes and switch the glucose to the pentose pathway promoting ROS formation, AGEs production, and O-GlcNAcylation upregulation. For example, hyperglycemia (30mM) mediates O-GlcNAcylation of the mitochondrial transcriptional factor A (TFAM) (82) in neonatal rat cardiomyocytes, which is essential for mitochondrial DNA transcription and replication. These alterations result in reduced mitochondrial activity with higher ROS and less ATP production and participate to cell death. Indeed, in streptozotocine type 1 diabetic mice and H9c2 cardiomyocytes treated for 48h with high glucose (33mM), the increase in ROS production is associated to cytochrome c release and the activation of the caspase-3 apoptotic pathway leading to cell death (83, 84). The activation of the Na^+/K^+-ATPase protects H9c2 myocardial cells against high glucose-induced cell apoptosis (33mM for 48h) by decreasing ROS level, and alleviating cytosolic Ca^{2+} overload (84). The increase in ROS levels is also associated to high sensitivity to Ca^{2+}-induced mitochondrial permeability transition pore and the activation of the caspase-9 mediated-apoptotic pathway as seen in atrial myoblast from diabetic type 2 patients (79, 85). High glucose (30mM for 72h) also induces nuclear expression of Foxo1, a key transcription

factor in insulin signal transduction, in H9C2 rat cardiomyocytes. Then, Foxo1 promotes GRK2 (β-adrenergic receptor kinase) expression, which increases caspase3-mediated cell apoptosis by promoting ROS production (86). ROS can also promote apoptosis by inhibiting the IGF1–PI3K-Akt survival pathway in H9C2 cardiomyocytes treated by high glucose (33mM) for 36h (87). All these described mechanisms promote ROS production decreasing mitochondrial ATP production and promoting cell death.

Glucose and excitation-contraction coupling

Studies in both type 1 and 2 diabetic animal models have clearly shown that diastolic and systolic dysfunction are associated with defective Ca^{2+} handling (88). In cardiomyocytes, the Ca^{2+} plays a key role in the initiation of contraction through the excitation-contraction coupling (ECC). Indeed, during cardiomyocyte's depolarization, Ca^{2+} enters into the cell through the L-type voltage dependent Ca^{2+} channel (LTCC) activating a massive release of Ca^{2+} from the ryanodine receptor (RyR) of the sarcoplasmic reticulum (SR), which binds to the myofilaments to generate contraction. Then Ca^{2+} returns to diastolic levels by reuptake into the sarcoplasmic reticulum and extrusion out of the cell. The $[Ca^{2+}]_i$ transient is reduced due to a down expression and/or activity of the LTCC Ca^{2+} entry (although still under debate) as well as down-expression of the RyRs (88-90) in animal models of type 1 and type 2 diabetes (88, 89, 91, 92).The aforementioned upregulation of AGEs has been shown to directly alter RyRs activity participating in abnormal diastolic SR Ca^{2+} release decreasing SR Ca^{2+} content necessary for the next contraction (93, 94). In addition, in diabetic models, $[Ca^{2+}]_i$ transient decay time is prolonged due to an impaired SR Ca^{2+} reuptake by the

sarcoplasmic reticulum Ca^{2+}ATP-ase (SERCA) impairing cardiomyocytes relaxation (88, 89). The SERCA dysfunction has been attributed to the modification of phospholamban (PLB) by O-GlcNAcylation. This O-GlcNAcylation of PLB decreases its phosphorylation, thus, promoting its inhibition of SERCA pump activity (95). Moreover, high glucose leads to the O-GlcNAcylation of the transcription factor specificity protein 1 (Sp1), which also downregulates SERCA (19, 96). SERCA is also an AGEs target which reduces its activity and depress cardiac relaxation (94). Taken together, these mechanisms alter SERCA-dependent Ca^{2+} re-uptake into the SR reducing SR Ca^{2+} content and Ca^{2+} release necessary for the generation of cardiomyocytes contraction (88-90, 97). In type 1 diabetic rats myocardial contractile dysfunction has been also attributed to reduced myofilaments sensitivity to Ca^{2+} which results from a shift from *α*-myosin heavy chain (MHC) to the fetal isoform *β*-MHC mRNA (98, 99) and a slower cross bridge cycling (100), slowing the relaxation phase. MHC, myosine light chain and actin are also targets for O-GlcNAcylation, as described in streptozotocine-induced type 1 diabetic rat cardiac muscle fibers (101), participating in the decrease of myofibrils sensitivity to Ca^{2+} (102) and contractile dysfunction. Finally, it is worth to note that the high glucose-mediated alteration of ECC have been shown to increase the cardiac propensity for arrhythmia in animal models. Indeed, Erickson *et al.* (103) have shown that hyperglycemia induces SR abnormal diastolic Ca^{2+} release via O-GlcNAcylation of the Calmoduline kinase II (CaMKII) and exacerbates arrhythmia in diabetic rats under β-adrenergic stimulation. Moreover, other studies in rat ventricular cardiomyocytes have shown that high glucose concentration (25.5 mM for 24 h) prolonged the action potential duration (104) due to a decrease of the outward potassium current amplitude seen in streptozotocine induced

diabetic rats model (105, 106) which promotes cardiac arrhythmia. Furthermore, O-GlcNAcylation of the cardiac voltage-gated sodium channel Nav1.5 in Streptozotocin-induced diabetic type 1 rat decreases its expression and slows its inactivation which further participates in action potential prolongation and ventricular arrhythmia susceptibility under β-adrenergic stimulation (107).

Treatment

The Food and Drug Administration and the European Medicines Agency require evidence of cardiovascular safety for glucose-lowering agents since 2008. Therefore, data regarding the cardiovascular effects of lowering glucose therapies are more and more available. The increased risk of thiazolidinedione on HF has been established (108), effects of DPP4 (dipeptidyl-peptidase-4) inhibitors are controversial. As for, linagliptin, the CARMELINA trial evaluated its effect on cardiovascular outcomes as a noninferior risk of a composite cardiovascular outcome over a median 2.2 year follow-up (109).

GLP-1 receptor agonists

GLP-1 (glucagon like peptide-1) receptor agonists are injectable intestinal-derived incretin peptide that stimulates postprandial insulin secretion and inhibits glucagon release. Recently, a daily oral GLP-1 receptor agonist, semaglutid, have been developed being as efficient as injectable one. The LEADER (Liraglutide Effect and Action in Diabetes: Evaluation of Cardiovascular Outcome Result) randomized trial demonstrated a decreased rate of the first occurrence of death from CV causes, nonfatal myocardial infarction, or nonfatal stroke in the liraglutide group as compared to

the placebo group in type 2 diabetes mellitus patients who presented in majority (82.1%) an established cardiovascular disease (110). The SUSTAIN-6 trial demonstrated the noninferiority in term of CV outcomes (cardiovascular death, nonfatal myocardial infarction, or nonfatal stroke) of semaglutide (111). Altough the LEADER and SUSTAIN-6 trials reported no changes in the rate of hospitalization for HF, only a small proportion of the included patients had HF at baseline. The REWIND TRIAL (112) evaluating a weekly injection of dulaglutide versus placebo demonstrated a favorable effect on the risk of CV outcomes (composite endpoint of non-fatal myocardial infarction, non-fatal stroke, or death from cardiovascular causes or unknown causes) (HR=0.88, CI95%=0.79–0.99, p=0.026). This trial included 2/3 of the patients considered in primary prevention.

The FIGHT (113) and the LIVE (114) smallest randomized trials specifically explored the effects of liraglutide in patients with HFrEF. In the FIGHT trial including patients with and without T2DM, no reduction in the HF hospitalization or CV death was observed. In the LIVE trial, no significant differences were observed between the groups for the primary end-point (increase in left ventricular ejection fraction). But liraglutide treated patients had a higher number of serious cardiac events that might be due to an increased heart rate. Therefore, effects of GLP-1 receptor agonists might differ between patients with type 2 diabetes mellitus and in patients with symptomatic HFrEF.

SGLT-2 inhibitors

Sodium-glucose cotransporter-2 (SGLT-2) inhibitors induce an inhibition of glucose reabsorption in the proximal renal renal tubules by a mechanism independent

of insulin and reduces sodium reabsorption by interaction with and inhibition of sodium-hydrogen exchanger (NHE)-3 resulting in an increased natriuresis (115). SGLT-2 inhibitor use is associated with a reduced rate of HF hospitalizations and, in the case of empagliflozin, markedly reduces cardiovascular death. The EMPA-REG (Empagliflozin Cardiovascular Outcomes and Mortality in Type 2 Diabetes) (116) trial included type 2 diabetes mellitius patients with established cardiovascular disease who presented a reduction of major adverse cardiac events after a median follow-up of 3.1 years in the empagliflozin group compared with placebo (10.5% versus 12.1%, HR=0.86; CI95%=0.74–0.99; P=0.04 for superiority). In addition, the trial demonstrated lower cardiovascular mortality and hospitalization for HF (9.4% versus 14.5%; HR=0.65; CI95%=0.50–0.85) in the empagliflozin groups, a finding that was consistent across all major subgroups, including those with and without baseline HF.

Investigators from the CANVAS (Canagliflozin and Cardiovascular and Renal Events in Type 2 Diabetes) programme included 10,142 patients with either established cardiovascular disease (65%) or a high risk of CV events (35%) and randomly assigned them to canagliflozin (100 mg or 300 mg) or placebo (117). The rate of the primary outcome (nonfatal myocardial infarction or stroke, or CV-related death) was lower in the canagliflozin group than in the placebo group (26.9 versus 31.5 per 1,000 patient-years). Although the reduction in cardiovascular and all-cause death with canagliflozin versus placebo treatment did not reach significance, patients in the canagliflozin treatment group showed a significant 33% risk ratio reduction in HF hospitalization. However, adverse effects occurred more frequently with canagliflozin than with placebo, and most notably lower extremity amputations (117).

The real life study CVD-REAL (Comparative Effectiveness of Cardiovascular Outcomes in New Users of Sodium-Glucose Cotransporter-2 Inhibitors) on 300 000 patients with type 2 diabetes who were newly initiated on SGLT-2 mellitus confirmed the reduced HF hospitalization compared to those who were started on other glucose-lowering medications (118). Although the effect of SGLT-2 inhibitors on HF hospitalization is impressive, both the EMPA-REG outcome and the CANVAS trials enrolled very few patients with established HF. The answer to the potential protector role of SGLT-2 inhibitors against cardiovascular death has been recently evaluated in the EMPEROR and DAPA-HF clinical trials. These two independent trials have respectively demonstrated that empagliflozin and dapagliflozin both reduce the risk of cardiac death and hospitalization for heart failure as well as improve renal outcomes in patients with HFrEF with or without diabetes (119). The mechanism of action through which SGLT-2 inhibitors reduce HF events is unclear and is still under investigations. It is likely that these underling mechanisms are beyond glucose lowering or diuresis *per se*. For instance, the protective cardiovascular effects of SGLT-2 inhibitors might be related to their direct myocardial effects by improving cardiac energy metabolism with increasing ketones oxidation, an extra source of fuel to the failing heart that is associated with icreasing contractile function. Increasing ketones levels participates in the attenuation of the inflammation profile in failing heart observed with SGLT-2 inhibitors although the underlying mechanism is not fully understood. Furthermore, SGLT-2 inhibitors inhibit the cardiac Na^+/H^+ exchanger which can lower myocardial Na^+ and Ca^{2+} levels increased in HF. Besides, SGLT2 inhibitors reduce CaMKII activity and prevent SR Ca^{2+} mishandling observed in HF. However, the effects of SGLT2

inhibitors on the Na^+/H^+ exchanger and CaMKII in protecting the failing heart are not clear to be clinically relevant. Besides their direct action on the cardiomyocyte, the beneficial effect of SGLT2 inhibitors is also related to their renal action. Indeed, SGLT2 inhibitors by increasing natriuresis, reduce renal intraglomerular pressure and subsequent sympathetic system activation and blood pressure indirectly improving cardiac function. Other theories are also proposed such as reduction of ROS, increasing autophagy and provascular cell progenitors that should be further investigated (120).

Conclusion

Several clinical studies have demonstrated an increased risk of HF during diabetes. This is due in part to coronary artery disease and valvulopathy, but also to a specific cardiac dysfunction observed in diabetic patients known as diabetic cardiomyopathy. Hyperglycemia, among several factors, contributes to the development of diabetic cardiomyopathy. Even though the beneficial effect of the HbA1c tight control on the cardiovascular events reduction is still controversial, it is well established that the increase in HbA1c level increases the risk of HF. This is correlated to different cellular disturbances caused by high glucose as metabolic alterations with decrease in energy substrate production and increase in oxidative stress production. The upregulation of the hexosamines pathway and the production of AGEs mediated by high glucose induce structure alteration and participate in intracellular calcium mishandling affecting cardiac compliance, contraction and relaxation. Since cardiac safety is a major challenge in drug development, several studies have decipher the cardiovascular effects of glucose lowering agents. Although thizolidinediones are known to promote HF, studies are still

controversial for DPP4 inhibitors. GLP-1 agonist have demonstrated a non-inferiority effect compared to placebo while the new therapeutic class of SGLT-2 inhibitors seems to be promising in terms of cardiovascular outcomes.

Acknowledgement

This work is funded by a ANR-11-1DEX-0003-02 (group leader grant) to L.P, Inserm and University Paris Sud. M.SH is a fellow from the French Ministry of Research. UMR-S 1180 is member of the Laboratory of Excellence LERMIT.

Disclosure

None

References

1. Cho NH, Shaw JE, Karuranga S, Huang Y, da Rocha Fernandes JD, Ohlrogge AW, et al. IDF Diabetes Atlas: Global estimates of diabetes prevalence for 2017 and projections for 2045. Diabetes Res Clin Pract. 2018;138:271-81.
2. Kannel WB, McGee DL. Diabetes and cardiovascular disease. The Framingham study. Jama. 1979;241(19):2035-8.
3. Rubler S, Dlugash J, Yuceoglu YZ, Kumral T, Branwood AW, Grishman A. New type of cardiomyopathy associated with diabetic glomerulosclerosis. The American journal of cardiology. 1972;30(6):595-602.
4. Regan TJ, Lyons MM, Ahmed SS, Levinson GE, Oldewurtel HA, Ahmad MR, et al. Evidence for cardiomyopathy in familial diabetes mellitus. The Journal of clinical investigation. 1977;60(4):884-99.
5. de Simone G, Devereux RB, Chinali M, Lee ET, Galloway JM, Barac A, et al. Diabetes and incident heart failure in hypertensive and normotensive participants of the Strong Heart Study. J Hypertens. 2010;28(2):353-60.
6. Devereux RB, Roman MJ, Paranicas M, O'Grady MJ, Lee ET, Welty TK, et al. Impact of diabetes on cardiac structure and function: the strong heart study. Circulation. 2000;101(19):2271-6.
7. Garcia MJ, McNamara PM, Gordon T, Kannel WB. Morbidity and mortality in diabetics in the Framingham population. Sixteen year follow-up study. Diabetes. 1974;23(2):105-11.
8. Kannel WB, Hjortland M, Castelli WP. Role of diabetes in congestive heart failure: the Framingham study. The American journal of cardiology. 1974;34(1):29-34.

9. Thrainsdottir IS, Aspelund T, Thorgeirsson G, Gudnason V, Hardarson T, Malmberg K, et al. The association between glucose abnormalities and heart failure in the population-based Reykjavik study. Diabetes Care. 2005;28(3):612-6.
10. Iribarren C, Karter AJ, Go AS, Ferrara A, Liu JY, Sidney S, et al. Glycemic control and heart failure among adult patients with diabetes. Circulation. 2001;103(22):2668-73.
11. Elder DH, Singh JS, Levin D, Donnelly LA, Choy AM, George J, et al. Mean HbA1c and mortality in diabetic individuals with heart failure: a population cohort study. Eur J Heart Fail. 2016;18(1):94-102.
12. Erqou S, Lee CT, Suffoletto M, Echouffo-Tcheugui JB, de Boer RA, van Melle JP, et al. Association between glycated haemoglobin and the risk of congestive heart failure in diabetes mellitus: systematic review and meta-analysis. Eur J Heart Fail. 2013;15(2):185-93.
13. Montaigne D, Marechal X, Coisne A, Debry N, Modine T, Fayad G, et al. Myocardial contractile dysfunction is associated with impaired mitochondrial function and dynamics in type 2 diabetic but not in obese patients. Circulation. 2014;130(7):554-64.
14. Hart GW, Housley MP, Slawson C. Cycling of O-linked beta-N-acetylglucosamine on nucleocytoplasmic proteins. Nature. 2007;446(7139):1017-22.
15. Jones SP, Zachara NE, Ngoh GA, Hill BG, Teshima Y, Bhatnagar A, et al. Cardioprotection by N-acetylglucosamine linkage to cellular proteins. Circulation. 2008;117(9):1172-82.
16. Liu J, Marchase RB, Chatham JC. Increased O-GlcNAc levels during reperfusion lead to improved functional recovery and reduced calpain proteolysis. American journal of physiology Heart and circulatory physiology. 2007;293(3):H1391-9.
17. Mailleux F, Gelinas R, Beauloye C, Horman S, Bertrand L. O-GlcNAcylation, enemy or ally during cardiac hypertrophy development? Biochimica et biophysica acta. 2016;1862(12):2232-43.
18. Qin CX, Sleaby R, Davidoff AJ, Bell JR, De Blasio MJ, Delbridge LM, et al. Insights into the role of maladaptive hexosamine biosynthesis and O-GlcNAcylation in development of diabetic cardiac complications. Pharmacol Res. 2017;116:45-56.
19. Fricovsky ES, Suarez J, Ihm SH, Scott BT, Suarez-Ramirez JA, Banerjee I, et al. Excess protein O-GlcNAcylation and the progression of diabetic cardiomyopathy. American journal of physiology Regulatory, integrative and comparative physiology. 2012;303(7):R689-99.
20. Hu Y, Belke D, Suarez J, Swanson E, Clark R, Hoshijima M, et al. Adenovirus-mediated overexpression of O-GlcNAcase improves contractile function in the diabetic heart. Circ Res. 2005;96(9):1006-13.
21. Bodiga VL, Eda SR, Bodiga S. Advanced glycation end products: role in pathology of diabetic cardiomyopathy. Heart Fail Rev. 2014;19(1):49-63.
22. Leroy J, Richter W, Mika D, Castro LR, Abi-Gerges A, Xie M, et al. Phosphodiesterase 4B in the cardiac L-type Ca(2)(+) channel complex regulates Ca(2)(+) current and protects against ventricular arrhythmias in mice. The Journal of clinical investigation. 2011;121(7):2651-61.
23. Rawshani A, Rawshani A, Franzen S, Sattar N, Eliasson B, Svensson AM, et al. Risk Factors, Mortality, and Cardiovascular Outcomes in Patients with Type 2 Diabetes. N Engl J Med. 2018;379(7):633-44.
24. Mentz RJ, Kelly JP, von Lueder TG, Voors AA, Lam CS, Cowie MR, et al. Noncardiac comorbidities in heart failure with reduced versus preserved ejection fraction. J Am Coll Cardiol. 2014;64(21):2281-93.
25. Gustafsson I, Brendorp B, Seibaek M, Burchardt H, Hildebrandt P, Kober L, et al. Influence of diabetes and diabetes-gender interaction on the risk of death in patients hospitalized with congestive heart failure. J Am Coll Cardiol. 2004;43(5):771-7.
26. MacDonald MR, Petrie MC, Varyani F, Ostergren J, Michelson EL, Young JB, et al. Impact of diabetes on outcomes in patients with low and preserved ejection fraction heart failure: an analysis of the Candesartan in Heart failure: Assessment of Reduction in Mortality and morbidity (CHARM) programme. Eur Heart J. 2008;29(11):1377-85.

27. Kristensen SL, Mogensen UM, Jhund PS, Petrie MC, Preiss D, Win S, et al. Clinical and Echocardiographic Characteristics and Cardiovascular Outcomes According to Diabetes Status in Patients With Heart Failure and Preserved Ejection Fraction: A Report From the I-Preserve Trial (Irbesartan in Heart Failure With Preserved Ejection Fraction). Circulation. 2017;135(8):724-35.
28. Bertoni AG, Hundley WG, Massing MW, Bonds DE, Burke GL, Goff DC, Jr. Heart failure prevalence, incidence, and mortality in the elderly with diabetes. Diabetes Care. 2004;27(3):699-703.
29. Sarma S, Mentz RJ, Kwasny MJ, Fought AJ, Huffman M, Subacius H, et al. Association between diabetes mellitus and post-discharge outcomes in patients hospitalized with heart failure: findings from the EVEREST trial. Eur J Heart Fail. 2013;15(2):194-202.
30. Ernande L, Beaudoin J, Piro V, Meziani S, Scherrer-Crosbie M. Adverse impact of diabetes mellitus on left ventricular remodelling in patients with chronic primary mitral regurgitation. Arch Cardiovasc Dis. 2018;111(8-9):487-96.
31. Raher MJ, Thibault H, Poh KK, Liu R, Halpern EF, Derumeaux G, et al. In vivo characterization of murine myocardial perfusion with myocardial contrast echocardiography: validation and application in nitric oxide synthase 3 deficient mice. Circulation. 2007;116(11):1250-7.
32. Raher MJ, Thibault HB, Buys ES, Kuruppu D, Shimizu N, Brownell AL, et al. A short duration of high-fat diet induces insulin resistance and predisposes to adverse left ventricular remodeling after pressure overload. Am J Physiol Heart Circ Physiol. 2008;295(6):H2495-502.
33. Benjamin EJ, Levy D, Vaziri SM, D'Agostino RB, Belanger AJ, Wolf PA. Independent risk factors for atrial fibrillation in a population-based cohort. The Framingham Heart Study. Jama. 1994;271(11):840-4.
34. Huxley RR, Filion KB, Konety S, Alonso A. Meta-analysis of cohort and case-control studies of type 2 diabetes mellitus and risk of atrial fibrillation. The American journal of cardiology. 2011;108(1):56-62.
35. Qi W, Zhang N, Korantzopoulos P, Letsas KP, Cheng M, Di F, et al. Serum glycated hemoglobin level as a predictor of atrial fibrillation: A systematic review with meta-analysis and meta-regression. PloS one. 2017;12(3):e0170955.
36. Holman RR, Paul SK, Bethel MA, Matthews DR, Neil HA. 10-year follow-up of intensive glucose control in type 2 diabetes. N Engl J Med. 2008;359(15):1577-89.
37. S Marxa AM. Dysfunctional ryanodine receptors in the heart: New insights into complex cardiovascular diseases. Journal of molecular and cellular cardiology. 2013;58:225-31.
38. Armstrong AC, Ambale-Venkatesh B, Turkbey E, Donekal S, Chamera E, Backlund JY, et al. Association of Cardiovascular Risk Factors and Myocardial Fibrosis With Early Cardiac Dysfunction in Type 1 Diabetes: The Diabetes Control and Complications Trial/Epidemiology of Diabetes Interventions and Complications Study. Diabetes Care. 2017;40(3):405-11.
39. Nine-Year Effects of 3.7 Years of Intensive Glycemic Control on Cardiovascular Outcomes. Diabetes care. 2016;39(5):701-8.
40. Zoungas S, Chalmers J, Neal B, Billot L, Li Q, Hirakawa Y, et al. Follow-up of blood-pressure lowering and glucose control in type 2 diabetes. The New England journal of medicine. 2014;371(15):1392-406.
41. Davis SN, Duckworth W, Emanuele N, Hayward RA, Wiitala WL, Thottapurathu L, et al. Effects of Severe Hypoglycemia on Cardiovascular Outcomes and Death in the Veterans Affairs Diabetes Trial. Diabetes Care. 2019;42(1):157-63.
42. Yancy CW, Jessup M, Bozkurt B, Butler J, Casey DE, Jr., Drazner MH, et al. 2013 ACCF/AHA guideline for the management of heart failure: a report of the American College of Cardiology Foundation/American Heart Association Task Force on Practice Guidelines. J Am Coll Cardiol. 2013;62(16):e147-239.
43. Galderisi M, Anderson KM, Wilson PW, Levy D. Echocardiographic evidence for the existence of a distinct diabetic cardiomyopathy (the Framingham Heart Study). Am J Cardiol. 1991;68(1):85-9.

44. Ernande L, Bergerot C, Rietzschel ER, De Buyzere ML, Thibault H, Pignonblanc PG, et al. Diastolic dysfunction in patients with type 2 diabetes mellitus: is it really the first marker of diabetic cardiomyopathy? J Am Soc Echocardiogr. 2011;24(11):1268-75 e1.
45. Poirier P, Bogaty P, Garneau C, Marois L, Dumesnil JG. Diastolic dysfunction in normotensive men with well-controlled type 2 diabetes: importance of maneuvers in echocardiographic screening for preclinical diabetic cardiomyopathy. Diabetes Care. 2001;24(1):5-10.
46. Ernande L, Rietzschel ER, Bergerot C, De Buyzere ML, Schnell F, Groisne L, et al. Impaired myocardial radial function in asymptomatic patients with type 2 diabetes mellitus: a speckle-tracking imaging study. J Am Soc Echocardiogr. 2010;23(12):1266-72.
47. Ernande L, Thibault H, Bergerot C, Moulin P, Wen H, Derumeaux G, et al. Systolic myocardial dysfunction in patients with type 2 diabetes mellitus: identification at MR imaging with cine displacement encoding with stimulated echoes. Radiology. 2012;265(2):402-9.
48. Fang ZY, Najos-Valencia O, Leano R, Marwick TH. Patients with early diabetic heart disease demonstrate a normal myocardial response to dobutamine. J Am Coll Cardiol. 2003;42(3):446-53.
49. Ernande L, Bergerot C, Girerd N, Thibault H, Davidsen ES, Gautier Pignon-Blanc P, et al. Longitudinal myocardial strain alteration is associated with left ventricular remodeling in asymptomatic patients with type 2 diabetes mellitus. J Am Soc Echocardiogr. 2014;27(5):479-88.
50. Holland DJ, Marwick TH, Haluska BA, Leano R, Hordern MD, Hare JL, et al. Subclinical LV dysfunction and 10-year outcomes in type 2 diabetes mellitus. Heart. 2015;101(13):1061-6.
51. Boyer JK, Thanigaraj S, Schechtman KB, Perez JE. Prevalence of ventricular diastolic dysfunction in asymptomatic, normotensive patients with diabetes mellitus. Am J Cardiol. 2004;93(7):870-5.
52. Nagueh SF, Smiseth OA, Appleton CP, Byrd BF, 3rd, Dokainish H, Edvardsen T, et al. Recommendations for the Evaluation of Left Ventricular Diastolic Function by Echocardiography: An Update from the American Society of Echocardiography and the European Association of Cardiovascular Imaging. Eur Heart J Cardiovasc Imaging. 2016;17(12):1321-60.
53. From AM, Scott CG, Chen HH. The development of heart failure in patients with diabetes mellitus and pre-clinical diastolic dysfunction a population-based study. J Am Coll Cardiol. 2010;55(4):300-5.
54. Kosmala W, Jellis CL, Marwick TH. Exercise limitation associated with asymptomatic left ventricular impairment: analogy with stage B heart failure. J Am Coll Cardiol. 2015;65(3):257-66.
55. Ernande L, Audureau E, Jellis CL, Bergerot C, Henegar C, Sawaki D, et al. Clinical Implications of Echocardiographic Phenotypes of Patients With Diabetes Mellitus. J Am Coll Cardiol. 2017;70(14):1704-16.
56. Marwick TH, Ritchie R, Shaw JE, Kaye D. Implications of Underlying Mechanisms for the Recognition and Management of Diabetic Cardiomyopathy. J Am Coll Cardiol. 2018;71(3):339-51.
57. Jensen MT, Sogaard P, Andersen HU, Bech J, Hansen TF, Galatius S, et al. Prevalence of systolic and diastolic dysfunction in patients with type 1 diabetes without known heart disease: the Thousand & 1 Study. Diabetologia. 2014;57(4):672-80.
58. Jensen MT, Sogaard P, Andersen HU, Bech J, Fritz Hansen T, Biering-Sorensen T, et al. Global longitudinal strain is not impaired in type 1 diabetes patients without albuminuria: the Thousand & 1 study. JACC Cardiovasc Imaging. 2015;8(4):400-10.
59. Herrero P, Peterson LR, McGill JB, Matthew S, Lesniak D, Dence C, et al. Increased myocardial fatty acid metabolism in patients with type 1 diabetes mellitus. J Am Coll Cardiol. 2006;47(3):598-604.
60. Shivu GN, Phan TT, Abozguia K, Ahmed I, Wagenmakers A, Henning A, et al. Relationship between coronary microvascular dysfunction and cardiac energetics impairment in type 1 diabetes mellitus. Circulation. 2010;121(10):1209-15.

61. Rosengren A, Vestberg D, Svensson AM, Kosiborod M, Clements M, Rawshani A, et al. Long-term excess risk of heart failure in people with type 1 diabetes: a prospective case-control study. Lancet Diabetes Endocrinol. 2015;3(11):876-85.
62. Seferovic PM, Paulus WJ. Clinical diabetic cardiomyopathy: a two-faced disease with restrictive and dilated phenotypes. Eur Heart J. 2015;36(27):1718-27, 27a-27c.
63. Bugger H, Abel ED. Molecular mechanisms of diabetic cardiomyopathy. Diabetologia. 2014;57(4):660-71.
64. Labombarda F, Leport M, Morello R, Ribault V, Kauffman D, Brouard J, et al. Longitudinal left ventricular strain impairment in type 1 diabetes children and adolescents: a 2D speckle strain imaging study. Diabetes Metab. 2014;40(4):292-8.
65. Aronson D. Cross-linking of glycated collagen in the pathogenesis of arterial and myocardial stiffening of aging and diabetes. J Hypertens. 2003;21(1):3-12.
66. Yue Y, Meng K, Pu Y, Zhang X. Transforming growth factor beta (TGF-beta) mediates cardiac fibrosis and induces diabetic cardiomyopathy. Diabetes Res Clin Pract. 2017;133:124-30.
67. Aloud BM, Raj P, O'Hara K, Shao Z, Yu L, Anderson HD, et al. Conjugated linoleic acid prevents high glucose-induced hypertrophy and contractile dysfunction in adult rat cardiomyocytes. Nutr Res. 2016;36(2):134-42.
68. Chiu J, Farhangkhoee H, Xu BY, Chen S, George B, Chakrabarti S. PARP mediates structural alterations in diabetic cardiomyopathy. Journal of molecular and cellular cardiology. 2008;45(3):385-93.
69. Nathan DM, Cleary PA, Backlund JY, Genuth SM, Lachin JM, Orchard TJ, et al. Intensive diabetes treatment and cardiovascular disease in patients with type 1 diabetes. N Engl J Med. 2005;353(25):2643-53.
70. Nathan DM, Genuth S, Lachin J, Cleary P, Crofford O, Davis M, et al. The effect of intensive treatment of diabetes on the development and progression of long-term complications in insulin-dependent diabetes mellitus. N Engl J Med. 1993;329(14):977-86.
71. Engerman RL, Kern TS. Progression of incipient diabetic retinopathy during good glycemic control. Diabetes. 1987;36(7):808-12.
72. Berezin A. Metabolic memory phenomenon in diabetes mellitus: Achieving and perspectives. Diabetes Metab Syndr. 2016;10(2 Suppl 1):S176-83.
73. Roy S, Sala R, Cagliero E, Lorenzi M. Overexpression of fibronectin induced by diabetes or high glucose: phenomenon with a memory. Proceedings of the National Academy of Sciences of the United States of America. 1990;87(1):404-8.
74. Yu XY, Geng YJ, Liang JL, Zhang S, Lei HP, Zhong SL, et al. High levels of glucose induce "metabolic memory" in cardiomyocyte via epigenetic histone H3 lysine 9 methylation. Mol Biol Rep. 2012;39(9):8891-8.
75. Cooper ME, El-Osta A. Epigenetics: mechanisms and implications for diabetic complications. Circulation research. 2010;107(12):1403-13.
76. Villeneuve LM, Natarajan R. The role of epigenetics in the pathology of diabetic complications. Am J Physiol Renal Physiol. 2010;299(1):F14-25.
77. Nishikawa T, Edelstein D, Du XL, Yamagishi S, Matsumura T, Kaneda Y, et al. Normalizing mitochondrial superoxide production blocks three pathways of hyperglycaemic damage. Nature. 2000;404(6779):787-90.
78. Brownlee M. The pathobiology of diabetic complications: a unifying mechanism. Diabetes. 2005;54(6):1615-25.
79. Bugger H, Abel ED. Molecular mechanisms for myocardial mitochondrial dysfunction in the metabolic syndrome. Clin Sci (Lond). 2008;114(3):195-210.
80. Teshima Y, Takahashi N, Nishio S, Saito S, Kondo H, Fukui A, et al. Production of reactive oxygen species in the diabetic heart. Roles of mitochondria and NADPH oxidase. Circ J. 2014;78(2):300-6.

81. Hu Y, Suarez J, Fricovsky E, Wang H, Scott BT, Trauger SA, et al. Increased enzymatic O-GlcNAcylation of mitochondrial proteins impairs mitochondrial function in cardiac myocytes exposed to high glucose. The Journal of biological chemistry. 2009;284(1):547-55.
82. Suarez J, Hu Y, Makino A, Fricovsky E, Wang H, Dillmann WH. Alterations in mitochondrial function and cytosolic calcium induced by hyperglycemia are restored by mitochondrial transcription factor A in cardiomyocytes. Am J Physiol Cell Physiol. 2008;295(6):C1561-8.
83. Cai L, Li W, Wang G, Guo L, Jiang Y, Kang YJ. Hyperglycemia-induced apoptosis in mouse myocardium: mitochondrial cytochrome C-mediated caspase-3 activation pathway. Diabetes. 2002;51(6):1938-48.
84. Yan X, Xun M, Li J, Wu L, Dou X, Zheng J. Activation of Na+/K+-ATPase attenuates high glucose-induced H9c2 cell apoptosis via suppressing ROS accumulation and MAPKs activities by DRm217. Acta Biochim Biophys Sin (Shanghai). 2016;48(10):883-93.
85. Anderson EJ, Rodriguez E, Anderson CA, Thayne K, Chitwood WR, Kypson AP. Increased propensity for cell death in diabetic human heart is mediated by mitochondrial-dependent pathways. American journal of physiology Heart and circulatory physiology. 2011;300(1):H118-24.
86. Yang M, Lin Y, Wang Y, Wang Y. High-glucose induces cardiac myocytes apoptosis through Foxo1 /GRK2 signaling pathway. Biochem Biophys Res Commun. 2019;513(1):154-8.
87. Huang YT, Liu CH, Yang YC, Aneja R, Wen SY, Huang CY, et al. ROS- and HIF1alpha-dependent IGFBP3 upregulation blocks IGF1 survival signaling and thereby mediates high-glucose-induced cardiomyocyte apoptosis. J Cell Physiol. 2019;234(8):13557-70.
88. Pereira L, Matthes J, Schuster I, Valdivia HH, Herzig S, Richard S, et al. Mechanisms of [Ca2+]i transient decrease in cardiomyopathy of db/db type 2 diabetic mice. Diabetes. 2006;55(3):608-15.
89. Choi KM, Zhong Y, Hoit BD, Grupp IL, Hahn H, Dilly KW, et al. Defective intracellular Ca(2+) signaling contributes to cardiomyopathy in Type 1 diabetic rats. American journal of physiology Heart and circulatory physiology. 2002;283(4):H1398-408.
90. Yaras N, Ugur M, Ozdemir S, Gurdal H, Purali N, Lacampagne A, et al. Effects of diabetes on ryanodine receptor Ca release channel (RyR2) and Ca2+ homeostasis in rat heart. Diabetes. 2005;54(11):3082-8.
91. Lee SL, Ostadalova I, Kolar F, Dhalla NS. Alterations in Ca(2+)-channels during the development of diabetic cardiomyopathy. Molecular and cellular biochemistry. 1992;109(2):173-9.
92. Lu Z, Jiang YP, Xu XH, Ballou LM, Cohen IS, Lin RZ. Decreased L-type Ca2+ current in cardiac myocytes of type 1 diabetic Akita mice due to reduced phosphatidylinositol 3-kinase signaling. Diabetes. 2007;56(11):2780-9.
93. Shao CH, Tian C, Ouyang S, Moore CJ, Alomar F, Nemet I, et al. Carbonylation induces heterogeneity in cardiac ryanodine receptor function in diabetes mellitus. Molecular pharmacology. 2012;82(3):383-99.
94. Tian C, Alomar F, Moore CJ, Shao CH, Kutty S, Singh J, et al. Reactive carbonyl species and their roles in sarcoplasmic reticulum Ca2+ cycling defect in the diabetic heart. Heart Fail Rev. 2014;19(1):101-12.
95. Yokoe S, Asahi M, Takeda T, Otsu K, Taniguchi N, Miyoshi E, et al. Inhibition of phospholamban phosphorylation by O-GlcNAcylation: implications for diabetic cardiomyopathy. Glycobiology. 2010;20(10):1217-26.
96. Clark RJ, McDonough PM, Swanson E, Trost SU, Suzuki M, Fukuda M, et al. Diabetes and the accompanying hyperglycemia impairs cardiomyocyte calcium cycling through increased nuclear O-GlcNAcylation. The Journal of biological chemistry. 2003;278(45):44230-7.
97. Pereira L, Ruiz-Hurtado G, Rueda A, Mercadier JJ, Benitah JP, Gomez AM. Calcium signaling in diabetic cardiomyocytes. Cell Calcium. 2014;56(5):372-80.

98. Depre C, Young ME, Ying J, Ahuja HS, Han Q, Garza N, et al. Streptozotocin-induced changes in cardiac gene expression in the absence of severe contractile dysfunction. J Mol Cell Cardiol. 2000;32(6):985-96.
99. Hofmann PA, Menon V, Gannaway KF. Effects of diabetes on isometric tension as a function of [Ca2+] and pH in rat skinned cardiac myocytes. Am J Physiol. 1995;269(5 Pt 2):H1656-63.
100. Ishikawa T, Kajiwara H, Kurihara S. Alterations in contractile properties and Ca2+ handling in streptozotocin-induced diabetic rat myocardium. Am J Physiol. 1999;277(6):H2185-94.
101. Ramirez-Correa GA, Jin W, Wang Z, Zhong X, Gao WD, Dias WB, et al. O-linked GlcNAc modification of cardiac myofilament proteins: a novel regulator of myocardial contractile function. Circulation research. 2008;103(12):1354-8.
102. Ramirez-Correa GA, Ma J, Slawson C, Zeidan Q, Lugo-Fagundo NS, Xu M, et al. Removal of Abnormal Myofilament O-GlcNAcylation Restores Ca2+ Sensitivity in Diabetic Cardiac Muscle. Diabetes. 2015;64(10):3573-87.
103. Erickson JR, Pereira L, Wang L, Han G, Ferguson A, Dao K, et al. Diabetic hyperglycaemia activates CaMKII and arrhythmias by O-linked glycosylation. Nature. 2013;502(7471):372-6.
104. Ren J, Gintant GA, Miller RE, Davidoff AJ. High extracellular glucose impairs cardiac E-C coupling in a glycosylation-dependent manner. Am J Physiol. 1997;273(6 Pt 2):H2876-83.
105. Jourdon P, Feuvray D. Calcium and potassium currents in ventricular myocytes isolated from diabetic rats. The Journal of physiology. 1993;470:411-29.
106. Shimoni Y, Firek L, Severson D, Giles W. Short-term diabetes alters K+ currents in rat ventricular myocytes. Circulation research. 1994;74(4):620-8.
107. Yu P, Hu L, Xie J, Chen S, Huang L, Xu Z, et al. O-GlcNAcylation of cardiac Nav1.5 contributes to the development of arrhythmias in diabetic hearts. Int J Cardiol. 2018;260:74-81.
108. Nassif M, Kosiborod M. Effect of glucose-lowering therapies on heart failure. Nat Rev Cardiol. 2018;15(5):282-91.
109. Rosenstock J, Allison D, Birkenfeld AL, Blicher TM, Deenadayalan S, Jacobsen JB, et al. Effect of Additional Oral Semaglutide vs Sitagliptin on Glycated Hemoglobin in Adults With Type 2 Diabetes Uncontrolled With Metformin Alone or With Sulfonylurea: The PIONEER 3 Randomized Clinical Trial. JAMA. 2019.
110. Marso SP, Daniels GH, Brown-Frandsen K, Kristensen P, Mann JF, Nauck MA, et al. Liraglutide and Cardiovascular Outcomes in Type 2 Diabetes. The New England journal of medicine. 2016;375(4):311-22.
111. Marso SP, Bain SC, Consoli A, Eliaschewitz FG, Jodar E, Leiter LA, et al. Semaglutide and Cardiovascular Outcomes in Patients with Type 2 Diabetes. N Engl J Med. 2016;375(19):1834-44.
112. Gerstein HC, Colhoun HM, Dagenais GR, Diaz R, Lakshmanan M, Pais P, et al. Dulaglutide and cardiovascular outcomes in type 2 diabetes (REWIND): a double-blind, randomised placebo-controlled trial. Lancet. 2019;394(10193):121-30.
113. Margulies KB, McNulty SE, Cappola TP. Lack of Benefit for Liraglutide in Heart Failure-Reply. JAMA. 2016;316(22):2429-30.
114. Jorsal A, Kistorp C, Holmager P, Tougaard RS, Nielsen R, Hanselmann A, et al. Effect of liraglutide, a glucagon-like peptide-1 analogue, on left ventricular function in stable chronic heart failure patients with and without diabetes (LIVE)-a multicentre, double-blind, randomised, placebo-controlled trial. Eur J Heart Fail. 2017;19(1):69-77.
115. Vijayakumar S, Vaduganathan M, Butler J. Glucose-Lowering Therapies and Heart Failure in Type 2 Diabetes Mellitus: Mechanistic Links, Clinical Data, and Future Directions. Circulation. 2018;137(10):1060-73.
116. Zinman B, Wanner C, Lachin JM, Fitchett D, Bluhmki E, Hantel S, et al. Empagliflozin, Cardiovascular Outcomes, and Mortality in Type 2 Diabetes. N Engl J Med. 2015;373(22):2117-28.

117. Neal B, Perkovic V, Matthews DR. Canagliflozin and Cardiovascular and Renal Events in Type 2 Diabetes. N Engl J Med. 2017;377(21):2099.
118. Kosiborod M, Cavender MA, Fu AZ, Wilding JP, Khunti K, Holl RW, et al. Lower Risk of Heart Failure and Death in Patients Initiated on Sodium-Glucose Cotransporter-2 Inhibitors Versus Other Glucose-Lowering Drugs: The CVD-REAL Study (Comparative Effectiveness of Cardiovascular Outcomes in New Users of Sodium-Glucose Cotransporter-2 Inhibitors). Circulation. 2017;136(3):249-59.
119. Zannad F, Ferreira JP, Pocock SJ, Anker SD, Butler J, Filippatos G, et al. SGLT2 inhibitors in patients with heart failure with reduced ejection fraction: a meta-analysis of the EMPEROR-Reduced and DAPA-HF trials. Lancet (London, England). 2020;396(10254):819-29.
120. Lopaschuk GD, Verma S. Mechanisms of Cardiovascular Benefits of Sodium Glucose Co-Transporter 2 (SGLT2) Inhibitors: A State-of-the-Art Review. JACC Basic to translational science. 2020;5(6):632-44.

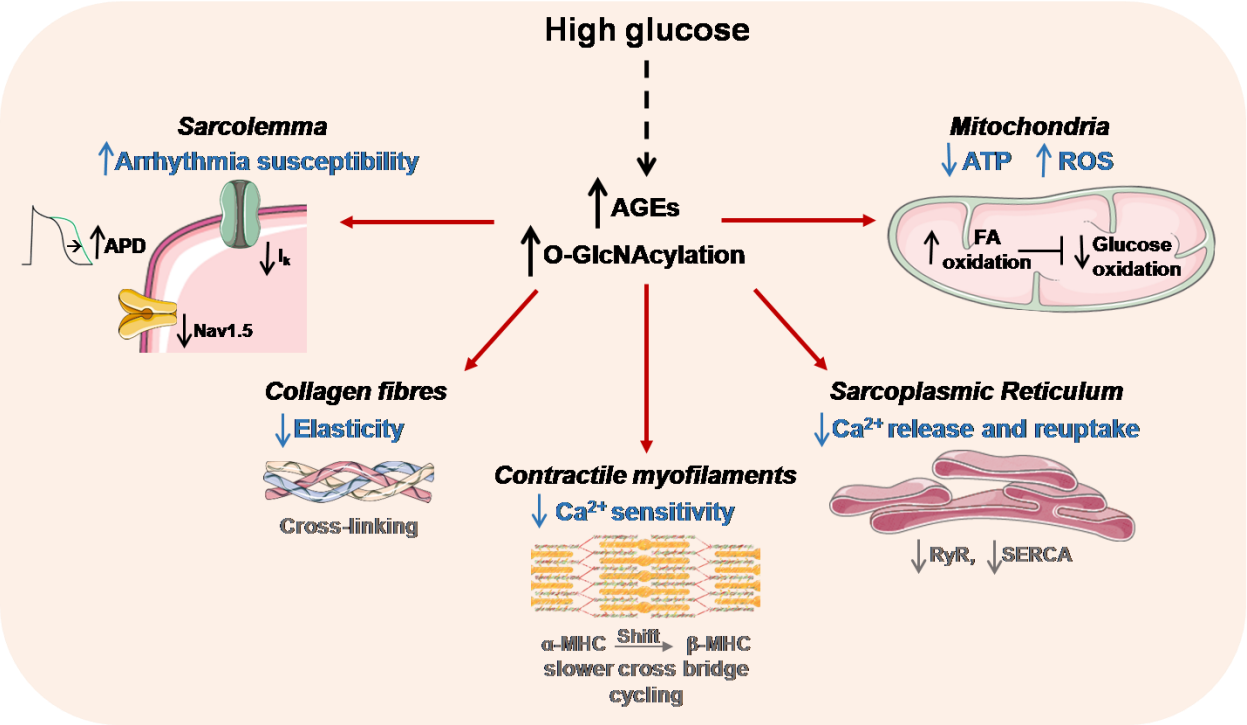

Figurure 2: High glucose-mediated cellular dysfunction involved in diabetic cardiomyopathy development. High glucose induces both AGEs formation and upregulation of protein O-GlcNAcylation that mediate several molecular alterations: 1) Increase of the arrhythmia susceptibility related to the action potential duration (APD) prolongation due to a decrease in potassium outward current (I_k) and voltage-gated sodium channel (Nav1.5) function by O-GlcNAcylation; 2) Reduced cardiac elasticity caused by AGEs-mediated collagen cross-linking molecules; 3) Decrease of contractile myofilaments Ca^{2+} sensitivity due to the shift from *α*-myosin heavy chain (MHC) to the fetal isoform *β*-MHC as well as myosine light chain and actin O-GlcNAcylation which slow cross bridge cycling; 4) Decrease of Ca^{2+} release and reuptake at the sarcoplasmic reticulum related to AGEs-mediated alteration of the ryanodine receptor (RyR) and sarco-endoplasmic reticulum Ca^{2+} ATP-ase (SERCA) underlying cardiac contraction and relaxation; 5) Decrease of ATP and increase of reactive oxygen species (ROS) production in the mitochondria as a result of fatty acid (FA) oxidation enhancement which inhibits glucose oxidation.

université PARIS-SACLAY

ECOLE DOCTORALE N°569
Innovation thérapeutique, du fondamental à l'applique (ITFA)

Titre : Rôle de l'Epac2 dans l'altération de la signalisation calcique cardiaque induite par les fortes concentrations de glucose

Mots clés : Epac2, calcium, glucose, récepteur à la ryanodine, O-GlcNacylation, cardiomyocyte.

Résumé : Epac2 (protéine d'échange directement activée par l'AMPc) est un acteur essentiel dans l'altération de la signalisation Ca^{2+} observée dans les cardiomyopathies, telles que l'insuffisance cardiaque et l'arythmie, également décrites dans le diabète. Récemment, nous avons découvert que l'hyperglycémie diabétique entraînait une fuite Ca^{2+} du réticulum sarcoplasmique (RS) mettant en jeu la CaMKII, molécule effectrice d'Epac2. Cependant, le rôle d'Epac2 dans l'altération de la signalisation calcique cardiaque induite par les fortes concentrations de glucose est inconnu. Mes travaux de thèse, montrent que les cardiomyocytes adultes de souris exposés à des concentrations élevées aigües de glucose présentent une augmentation de la fuite Ca^{2+} diastolique du RS, qui est pro-arythmogène, sans altérer la libération Ca^{2+} globale nécessaire à la contraction cellulaire. Cette fuite Ca^{2+} est réduite par l'inhibition pharmacologique ou génétique de l'Epac2, et est reliée à une augmentation de la probabilité d'ouverture du récepteur à la ryanodine (RyR), qui elle aussi est prévenue par l'inhibition d'Epac2. De façon intéressante, l'inhibition de l'O-GlcNacylation prévient aussi l'hyperactivation du RyR. L'O-GlcNacylation est une modification post-traductionnelle des protéines modifiant leur activité qui est hyperactivée en hyperglycémie. Nous avons mis en évidence pour la première fois l'activation d'Epac par O-GlcNAcylation sous concentrations hyperglycémiques. A l'instar des cellules de souris nous n'observons aucune diminution de la libération Ca^{2+} en fortes concentrations aigües de glucose. Cependant une exposition chronique de 7 jours à des concentrations hyperglycémiques diminue la libération calcique nécessaire pour la contraction, qui est prévenue par l'inhibition pharmacologique d'Epac2. Pour conclure, Epac2 est activée par O-GlcNacylation sous fortes concentrations de glucose, induisant une fuite calcique anormale du RS. A long terme, cette fuite calcique peut participer à la diminution de la libération calcique nécessaire pour la contraction, pouvant jouer un rôle dans les altérations cardiaques observées dans le diabète.

Title : Role of Epac2 in high glucose-mediated cardiac calcium mishandling

Keywords : Epac2, calcium, glucose, ryanodine receptor, O-GlcNacylation, cardiomyocyte.

Abstract : Epac2 (Exchange Protein directly Activated by cAMP) has emerged as a critical player in cardiomyopathies, such as heart failure and arrhythmia, also seen in diabetes. Recently, we found that diabetic hyperglycemia leads to CaMKII-dependent sarcoplasmic reticulum (SR) Ca^{2+} leak, a downstream effector of Epac2. However, the role of Epac2 in hyperglycemia-mediated SR Ca^{2+} leak is still unknown. My thesis work shows that adult mouse cardiomyocytes exposed to high glucose concentrations exhibit an increase of diastolic SR Ca^{2+} leak, which is pro-arrhythmogenic, without altering the Ca^{2+} released needed for cell contraction. This SR Ca^{2+} leak is reduced by pharmacological or genetic inhibition of Epac2. This Ca^{2+} leak is related to an increase of the open probability of the ryanodine receptor (RyR), which is prevented by Epac2 inhibition. Interestingly, the rise in RyR activity by high glucose concentrations is also prevented by O-GlcNacylation inhibition. O-GlcNacylation is a post-translational modification on the serine and threonine residues of proteins modifying their activities, which is upregulated by high glucose concentrations. Since Epac2 is a multidomain protein with several serine and threonine residues that can potentially be O-GlcNacylated, we demonstrated for the first time the activation of Epac by O-GlcNAcylation under hyperglycemic concentrations. In line with the murine model, we didn't find any alteration of the Ca^{2+} transient in acutely treated human induced pluripotent stem cells derived into cardiomyocytes (h-iPSC-CM). However a chronic treatment of high glucose reduces the Ca^{2+} transient amplitude in h-iPSC-CM in an Epac2-dependent manner. To conclude, our work suggest that hyperglycemia activates Epac2 by O-GlcNAcylation to mediate SR Ca^{2+} leak and arrhythmia that lead to the reduction of the systolic Ca^{2+} release over long term exposure that may play a role in the cardiac alterations seen in diabetic-associated cardiomyopathy.

Université Paris-Saclay
Espace Technologique / Immeuble Discovery
Route de l'Orme aux Merisiers RD 128 / 91190 Saint-Aubin, France